Melatonin MT_2 receptors in the descending antinociceptive pathway and reward: the role of the opioid system

Luca Posa, BSc, PharmD

Department of Psychiatry, Faculty of Medicine

McGill University, Montreal, Quebec, Canada

Dissertation

Submitted to Graduate and Postdoctoral Studies Office McGill University in Partial Fulfillment of the Requirements for the Degree of

Doctor of Philosophy (Ph.D.) in Psychiatry

Copyright © By Luca Posa 2020

Table of contents

« Science never solves a problem without creating ten more »

(George Bernard Shaw)

« Dans les champs de l'observation le hasard ne favorise que les esprits préparés »

(Louis Pasteur)

Acknowledgments

I would like to start by thanking my parents and brother, Mario, Antonietta and Mirko, who supported and allowed me to begin and complete this incredible adventure in Canada. Their enthusiastic encouragement and unconditional support have been instrumental during my doctoral studies and has given me the strength to pursue my goals. I would like to thank my supervisor Dr. Gabriella Gobbi for her support during the conceptualization and realization of my dissertation. Her academic excellence has contributed to my intellectual development and growth throughout my doctoral studies. She encouraged me to excel, provided ample academic opportunities and research experiences which has allowed me to disseminate my findings all around the world, and to grow as a scientist from many different perspectives.

I would like to express great admiration and appreciation to my committee members and several other faculty members who have played instrumental roles during my studies. They include my co-supervisor Dr. Brigitte Kieffer whose invaluable contributions made this study a success and who made me passionate about the “opioid world”. Dr. Laura Stone and Dr. Luda Diatchenko spent countless hours sharing their expertise and teaching me about the “pain world”. These amazing female scientists provided guidance, personal support, critical viewpoints and stimulating new ideas which contributed greatly to enrich my research.

A special thanks to the several institutions and granting agencies for their financial support. This research was supported by doctoral fellowships from the (1) Fonds de recherche du Quebec (2 and the Alan Edwards Centre for the Research on Pain. I am deeply indebted to all members, faculties, trainees, collaborators of the AECRP; an amazing micro-world inside McGill University which fed my intellectual and scientific curiosity during these past five years. A special thanks also to all

the members of the Program in Psychiatry: Dr Mechawar, Cindy and Danielle, who provided inestimable help during these years.

I would also like to thank several of my peers for contributing to this study including Dr. Stefano Comai who first introduced me to the Gobbi lab. I must thank my brilliant and amazing labmates: Dr. Danilo De Gregorio, Dr. Martha Canul Lopez, Dr. Nicolas Nunez, Ms. Rita Zakarian, and Mr. Antonio Farina for numerous stimulating conversations on several scientific topics which assisted me in my research. I could not have asked for a better work environment and I will never forget those amazing days and nights spent in the lab together. To all the students I had the privilege to coach: Sam, Alexandra, Matthew, I also have learnt a lot from you. To Justine and Elena, two great collaborators and smart promising scientists. To my collaborators from Italy: Drs Romualdi, Candeletti, and Caputi, Laura and Serena, for having welcomed me back to their lab and taught me all about gene expression.

I am grateful to my terrific friends at McGill University. Daniel (my step-bro in mind), Kelly, Laura-Joy, Hussein, Maria, Noosha. I want to thank all my friends, particularly those I had the chance to meet here, who became part of my "Montreal family". We spent great moments during these years, providing me with the energy to continue on!

Finally, the most special thanks go to my compañero Marco, who has enriched my life with happiness, friendship, kindness, joy, love and above all has given me the strength to pursue my goals in this overseas adventure and supported, stood, encouraged, and inspired me with his presence.

Abstract

Pain is a feeling characterized by uncomfortable sensations in the body. It involves the activation of the central and peripheral nervous systems and it may be short lasting or chronic (an ongoing sensation lasting for more than three months). Although pain is a physiological hallmark of the health conditions of our body and generally has an adaptive function, chronic pain is often debilitating with a serious impact on quality of life and an important economic burden. Melatonin (MLT) is a neurohormone implicated in the regulation of many different physiological responses, including pain. MLT acts mostly through the activation of two G-protein coupled receptors, MT_1 and MT_2, whose differential roles in pain conditions remain to be unequivocally defined. Analgesic supraspinal acting drugs such as opioids and MLT modulate pain transmission via the brainstem descending pathway which includes the periaqueductal gray (vlPAG) and its projections to the rostral ventromedial medulla (RVM). Two types of neurons have been characterized in the RVM: ON cells which are pronociceptive and OFF cells which are antinociceptive.

The aim of this thesis is first to characterize the role of each MLT receptor subtype in nociception and later to investigate the putative relationship of the melatonergic system with the opioid system, which is responsible for, among other functions, pain control and reward in the brain. We have therefore explored the nociceptive responses of mice with genetic inactivation of melatonin MT_1 ($MT_1^{-/-}$), or MT_2 ($MT_2^{-/-}$), or both MT_1/MT_2 ($MT_1^{-/-}$/$MT_2^{-/-}$) receptor subtypes in the supraspinal integrated response using the hot plate test (HPT), and in tonic/inflammatory nociception using the formalin test (FT). Compared to wild type (WT) controls, mice lacking MT_2, but not MT_1, receptors displayed a reduced nociceptive response in the HPT and in the second phase of the FT. In agreement, the systemic administration of the MLT MT_2 partial agonist, UCM924, produced

analgesic effects in controls and $MT_1^{-/-}$, but not in $MT_2^{-/-}$ or $MT_1^{-/-}/MT_2^{-/-}$, mice. Intriguingly, the non-selective competitive opioid antagonist, naloxone, reduced the basal nociceptive threshold only in $MT_2^{-/-}$ mice, that also exhibited an increased expression of the endogenous opioid proenkephalin *Penk* in the RVM, suggesting that the inactivation of the MT_2 receptor leads to a constitutive upregulation of the opioid system.

In a chronic neuropathic pain model, the antiallodynic effects of UCM924 were prevented by the pharmacological or genetic blockage of mu (MOR), but not delta (DOR), opioid receptors. In congruence, the modulatory effect on ON and OFF cells of the RVM by microinjection of the UCM924 in the vlPAG were blocked by non-selective and selective MOR, but not DOR, antagonists. These findings identified a crucial role of MOR in the MT_2-induced antiallodynia. Immunohistochemical labeling revealed that MT_2 receptors are localized in both excitatory and inhibitory interneurons in the vlPAG, but not in the RVM, while MOR is expressed in both these regions. Co-labelling of MT_2-MOR in the vlPAG was sparse. Moreover, while the UCM924 antiallodynic effect and its modulatory responses on the ON-OFF cells involved the G protein-gated inwardly rectifying potassium 1/4 (GIRK) channel, morphine did not. Repeated administration of UCM924 reduced the antiallodynic effects and its modulatory responses on the ON-OFF cells (tolerance), similar to the effects of morphine. Interestingly, while UCM924 lost its antiallodynic and ON-OFF cells modulatory effects in neuropathic morphine-tolerant rats (cross-tolerance), morphine still showed antiallodynic and ON-OFF cell modulatory properties in neuropathic rats tolerant to UCM924. Preliminary data showed that UCM924 administration increased the *Penk* mRNA level in the PAG of neuropathic mice. Altogether, these findings demonstrated the distinct localization, the specific pathway of the MOR and MT_2 receptor, and the MT_2 upstream position in the descending pathway compared to MOR and a possible involvement

of the enkephalin in MT_2-induced antiallodynia. Finally, in contrast to the effects of opioids, UCM924 did not result in behavioural reinforcing properties or alter dopamine neuron firing in the ventral tegmental area (VTA). These findings suggest a safe profile for MT_2 partial agonists regarding their potential abuse liability.

Together, these results demonstrated the critical role of the opioid system, and particularly of MOR, in the MT_2-induced analgesia, which does not involve rewarding properties.

Résumé

La douleur est une sensation caractérisée par des perceptions inconfortables dans le corps. Elle implique l'activation des systèmes nerveux central et périphérique et peut être aiguë (de courte durée) ou chronique (une sensation persistante pendant plus de trois mois). Bien que la douleur soit une caractéristique physiologique des conditions de santé de notre corps et qu'elle ait généralement une fonction d'adaptation, la douleur chronique est souvent débilitante, a un impact sérieux sur la qualité de vie et engendre un fardeau économique important. La mélatonine (MLT) est une neurohormone impliquée dans la régulation de nombreuses réponses physiologiques différentes, y compris la douleur. La MLT agit principalement à la suite de l'activation de deux récepteurs couplés aux protéines G, MT_1 et MT_2, dont les rôles différentiels dans les conditions de douleur restent à définir précisément. Les médicaments analgésiques qui agissent au niveau supraspinal, tels que les opioïdes et la MLT, modulent la transmission de la douleur via la voie descendante du tronc cérébral, qui comprend la substance grise périaqueducale (vlPAG) et ses projections vers la moelle ventromédiale rostrale (RVM). Deux types de neurones ont été caractérisés dans la RVM: les cellules ON qui sont pronociceptives et les cellules OFF qui sont antinociceptives.

Le but de cette thèse est, d'abord, de caractériser le rôle de chaque sous-type de récepteur de la MLT dans la nociception et, ensuite, d'étudier la relation putative du système mélatonergique avec le système opioïde, qui est responsable, entre autres fonctions, du contrôle de la douleur et de la récompense dans le cerveau. La caractérisation des souris knockout (invalidées, KO) pour les récepteurs MT_1 ($MT_1^{-/-}$), MT_2 ($MT_2^{-/-}$) ou les deux ($MT_1^{-/-}$ / $MT_2^{-/-}$) a permis d'évaluer la réponse intégrée supraspinale (test de la plaque chaude, HPT) et celle tonique / inflammatoire (test de la

formaldéhyde, FT). Par rapport aux groupe de de contrôle (WT) et $MT_1^{-/-}$, les souris KO pour le récepteur $MT_2^{-/-}$ ont présenté un une réponse nociceptive réduite dans le HPT et dans la deuxième phase du FT. En accord, l'administration systémique de l'agoniste partiel pour le récepteur MT_2, UCM924, a produit des effets analgésiques chez les control et $MT_1^{-/-}$, mais pas chez les souris $MT_2^{-/-}$ ou $MT_1^{-/-}$ / $MT_2^{-/-}$. Curieusement, l'antagoniste opioïde compétitif non sélectif, naloxone, a réduit le seuil nociceptif basal uniquement chez les souris $MT_2^{-/-}$, qui présentaient également une expression accrue du gène pour l'opioïde endogène proenképhaline, *Penk*, dans le RVM, suggérant que l'inactivation du récepteur MT_2 mène à une régulation positive constitutive du système opioïde.

Dans un modèle de douleur chronique neuropathique, les effets antiallodyniques de l'UCM924 ont été antagonisées par le blocage pharmacologique ou génétique des récepteurs opioïdes mu (MOR), mais pas delta (DOR). En congruence, l'effet modulateur sur les cellules ON et OFF du RVM à la suite de la microinjection de l'UCM924 dans le vlPAG a été bloqué par des antagonistes non sélectifs et sélectifs pour le MOR, mais pas pour le DOR. Ces résultats ont mis en évidence le rôle crucial de MOR dans les effets antiallodyniques produits par l'activation du récepteur MT_2. Le marquage immunohistochimique a révélé que les récepteurs MT_2 sont localisés dans les interneurones excitateurs et aussi dans les inhibiteurs dans le vlPAG, mais pas dans le RVM, tandis que le MOR est exprimé dans ces deux régions du cerveau. Le co-marquage MT_2-MOR dans le vlPAG a montré un faible niveau de colocalization. De plus, l'effet antiallodynique UCM924 et ses réponses modulatrices sur les neurones ON et OFF ont été antagonisés par le bloqueur de courant potassique rectifiant activé par les protéines G (GIRK),Tertiapin-Q (T-Q). Au contraire, la T-Q n'a pas modifié l'effet de l'agoniste MOR, morphine, sur la modulation des neurones ON et OFF. L'administration répétée d'UCM924 a montré une diminution des effets antiallodyniques

et modulateurs sur les cellules ON-OFF (tolérance), de manière similaire à la morphine. Cependant, lorsque les effets antiallodyniques et modulateurs sur les neurones ON et OFF de l'UCM924 chez les rats neuropathiques tolérants à la morphine ont été supprimés (tolérance croisée), les effets antiallodyniques et modulateurs sur les neurones ON et OFF de la morphine chez les rats neuropathiques tolérants à l'UCM924 sont restés inchangés. De plus, les données préliminaires ont montré que l'administration d'UCM924 a augmenté le niveau d'ARNm de la *Penk* dans le PAG des souris neuropathiques. Dans l'ensemble, ces résultats démontrent que les récepteurs MT2 et MOR ont une expression dans des régions distinctes du cerveau, qu'ils utilisent des voies de signalisation spécifiques, que le récepteur MT_2 est en amont par rapport à MOR dans la voie antinociceptive descendante, et, finalement, une probable implication des enképhalines dans l'effet antiallodynique provoqué par la stimulation du récepteur MT_2.

De plus, contrairement aux effets des opioïdes, l'UCM924 n'a pas montré l'effet récompensant ni celui d'altération des caractéristiques électrophysiologiques des neurones dopaminergiques dans la zone tegmentale ventrale (ATV). Ces résultats suggèrent une faible probabilité pour les agonistes partiels du récepteur MT_2 en ce qui concerne leur implication d'abus potentiel. Ensemble, ces résultats démontrent le rôle critique du système opioïde, et en particulier du MOR, dans l'analgésie induite par le récepteur MT_2, sans montrer des propriétés récompensant.

Contribution of Authors

Chapter I: Luca Posa wrote the general introduction under the supervision of Dr. Gabriella Gobbi and Dr. Brigitte Kieffer.

Chapter II: Luca Posa contributed to the experimental design, performed behavioural and molecular experiments, analyzed the data, created the figures, and wrote the first draft of the manuscript. Dr. Martha Lopez-Canul performed behavioural experiments and analyzed preliminary data. Laura Rullo performed molecular experiments and analyzed preliminary data. Dr. Danilo De Gregorio contributed to the experimental design and revised the manuscript. Dr. Sergio Dominguez-Lopez performed behavioural experiments and analyzed preliminary data. Matthew Kaba Aboud assisted with the behavioural experiments. Dr. Francesca Felicia Caputi, Dr. Sanzio Candeletti, and Dr. Patrizia Romualdi contributed to the experimental design and to the data analysis and revised the manuscript. Dr. Gabriella Gobbi conceived and supervised the study and contributed to the manuscript writing.

Chapter III: Luca Posa designed the study, performed behavioural, electrophysiological, immunohistological and molecular experiments, analyzed the data, created the figures, and wrote the first draft of the manuscript. Dr. Danilo De Gregorio performed preliminary electrophysiological experiments and helped with the data analysis and figure creation. Dr. Aliou Badara Gueye performed self-administration experiments, analyzed the data and contributed to the manuscript writing. He Qianzi and Dr. Emmanuel Darcq and Dr. Livio Luongo assisted in immunohistochemical experiments. Dr. Martha Lopez-Canul assisted in the behavioural experiments. Tania Sasson and Ali Nasr performed electrophysiological recordings in the VTA. Dr. Anne-Nöel Samaha assisted in the design of the reward experiments and contributed to the

manuscript writing. Dr. Brigitte Kieffer supervised the project, assisted in the experimental design, and contributed to the manuscript writing. Dr. Gabriella Gobbi supervised the project, designed the experiments, and contributed to write the manuscript.

Chapter IV: Luca Posa wrote the general discussion under the supervision of Dr. Gabriella Gobbi and Dr. Brigitte Kieffer.

Contributions to Original Knowledge

Prior to the studies in the present manuscript-based PhD thesis dissertation, studies on the analgesic properties of melatonin focused on (i) the clinical application of this neurohormone, (ii) the identification of the melatonin receptor subtypes involved in analgesia and (iii) suggested a role for the opioid system in melatonin-induced analgesia.

In Chapter I, the background literature regarding melatonin, including its receptors and signaling, were reviewed. Next, the antinociceptive pathway was presented, with a focus on the supraspinal mechanisms of the descending pathway in chronic pain conditions and the preclinical gold standard models of chronic pain. The role of the opioid system in pain was also discussed in this chapter. Finally, the preclinical and clinical literature regarding the melatonergic system, and particularly the melatonin MT_2 receptor, was discussed, with regards to its analgesic properties and mechanism of action in the descending pathway.

In Chapter II, the role of each melatonin receptor subtype (MT_1 and MT_2) was characterized using a model for supraspinal nociception (hot plate test) and a tonic/inflammatory pain model (formalin test) both in the light and dark phase. By employing transgenic mice lacking MT_1 and/or MT_2 receptors, we determined that the disruption of the MT_2 receptor altered the nociceptive threshold. Moreover, we identified a plausible explanation by showing that mice lacking MT_2 receptors had a tonic opioid activation which was pharmacologically suppressed by the opioid antagonist, naloxone. This first manuscript is now published in the *Journal of Pineal Research* (Impact factor: 15.22; DOI: 10.1111/jpi.12671).

In Chapter III, I assessed, for the first time, the interaction between the melatonin MT_2 receptor and the opioid receptors. Previous work showed that melatonin analgesia was blocked by naloxone

(Golombek et al. 1991; Lakin et al. 1981). Here, the critical role of the mu opioid receptor (MOR) was identified in the descending antinociceptive pathway in a chronic neuropathic pain model in rodents. By using behavioural, *in vivo* electrophysiological, immunohistochemical and molecular methods, I have also demonstrated that MT_2 receptors are upstream in this pathway and that while the MT_2 agonism provokes antiallodynia, it does not produce reward in animals. This second manuscript is in preparation for submission to the journal, PAIN (Impact factor: 5.48).

Finally, in Chapter IV, I integrated the results from my thesis as a whole, discussed important limitations, and proposed future lines of research.

Table of Figures and Tables

Abbreviations

[^{125}I]Mel	2-iodo-melatonin
4P-PDOT	4-phenyl-2-propionamidotetralin
5-HT	Serotonin (5-hydroxytryptamine)
5-HT2A	Serotonin 2A subtype receptor
5-HT2C	Serotonin 2C subtype receptor
5-HT3	Serotonin 3 subtype receptor
5-HT7	Serotonin 7 subtype receptor
AC	Adenylate cyclase
AP	Antero-posterior
ATP	Adenosine triphosphate
AUC	Area under the curve
CA2	Cornu Ammonis subfield 2
CA3	Cornu Ammonis subfield 3
CAMKIIα	Calcium/calmodulin-dependent protein kinase type II subunit alpha
cAMP	Cyclic adenosine monophosphate
CCI	Chronic constriction injury
cm	Centimeter
CNS	Central nervous system
DA	Dopamine neurotransmitter
DOR	Delta Opioid receptor
DOR$^{-/-}$	Delta Opioid receptor knock-out
fmol	Femtomol
FT	Formalin test
g	Grams
GABA	Gamma-aminobutyric acid neurotransmitter
GABAA	Gamma-aminobutyric acid receptor subtype A
GABAB	Gamma-aminobutyric acid receptor subtype B
GAD65	Glutamic acid decarboxylase 65
GAD67	Glutamic acid decarboxylase 67
GAPDH	Glyceraldehyde-3-phosphate dehydrogenase
GIRK (or Kir3)	G protein-coupled inward rectifier K^+
GPCR	G protein-couple receptors
GPR50	G protein-coupled receptor 50
h	Hour
HDAC4	Histone deacetylase 4
HTP	Hot plate test
Hz	Hertz, cycles per second
IASP	International Association for the Study of Pain
i.p (ip)	Intraperitoneal (or intraperitoneally)
i.v (iv)	Intravenous (or intravenously)
i.t. (it)	Intrathecal (or intrathecally)
K-185	(N-Butanoyl 2-(5,6,7-trihydro-11-methoxybenzo[c]cyclohept[2,1-a]indol-13-yl)ethanamine)
kg	Kilogram

KOR	Kappa Opioid receptor
LC	Locus coeruleus
M	Molar
MAPK	Mitogen-activated protein kinase
mg	Milligrams
min	Minutes
ml	Millilitre
MLT	Melatonin *(*N-acetyl-5-methoxytryptamine)
mm	Millimetre
MOR	Mu Opioid receptor
$MOR^{-/-}$	Mu Opioid receptor knock-out
mRNA	Messenger Ribonucleic acid
ms	Milliseconds
MT_1	Melatonin receptor subtype 1
$MT_1^{-/-}$ / $MT_2^{-/-}$	Melatonin receptor subtypes 1 and 2 knock-out
$MT_1^{-/-}$	Melatonin receptor subtype 1 knock-out
MT_2	Melatonin receptor subtype 2
$MT_2^{-/-}$	Melatonin receptor subtype 2 knock-out
MT_3	Melatonin receptor subtype 3
NAc	Nucleus Accumbens
NE	Noradrenaline neurotransmitter
ng	Nanograms
nM	Nanomolar
nm	Nanometre
NMDA	N-Methyl-D-aspartate
NREMS	Non-rapid eye movement sleep
(vl)PAG	(ventrolateral)Periaqueductal gray matter
PB	Phosphate buffer
PBS	Phosphate buffered saline
PDYN	Prodynorphin
PENK	Proenkephalin
PFA	Paraformaldehyde
PFC	Prefrontal cortex
pg	Picograms
pKi	Log dissociation constant
PKC	Protein kinase C
POMC	Pro-opiomelanocortin
PV	Parvalbumin
REMS	Rapid eye movement sleep
RT-PCR	Reverse transcription-polymerase chain reaction
RVM	Rostral ventromedial medulla
S22153	N-[2-(5-ethyl-1-benzothiophen-3-yl)ethyl]acetamide
s	Seconds
SCN	Suprachiasmatic nucleus
shRNA	Short hairpin Ribonucleic acid
SNI	Spared nerve injury
SNL	Spinal Nerve Ligation
SP	Substance P
SSRI	Serotonin-specific reuptake inhibitor

STZ	Streptozotocin
T-Q	Tertiapin-Q
UCM765	N-{2-[(3-methoxyphenyl)phenylamino]ethyl}acetamide
UCM924	N-{2-[(3-bromophenyl)(4-fluorophenyl)amino]ethyl}acetamide
VP	Ventral pallidum
VTA	Ventral tegmental area
WT	Wild type
µA	Microampere
µg	Microgram
µl	Microliter
µm	Micrometre
µM	Micromolar

Chapter I - Introduction and Objectives

1.1. Melatonin

Melatonin (MLT, N-acetyl-5-methoxytryptamine) is a natural compound which has been isolated in a large number of organisms, including bacteria (Jiao et al. 2016), plants, animals, and humans (Zhao et al. 2019). In animals, MLT plays a role in different physiological functions such as circadian rhythms, sleep, mood regulation, appetite, anxiety, immune responses, cardiac functions and pain modulation (Reiter, Tan, and Fuentes-Broto 2010). In humans, the major source of MLT is the pineal gland, a neuro-endocrine gland, where MLT is synthesized by the pinealocytes. Although the pineal gland is embryologically part of the brain, it is situated outside the blood brain barrier, receiving only sympathetic projections as its main source of innervation (Cipolla-Neto and Amaral 2018). The first precursor is L-tryptophan, which is then hydroxylated into 5-hydroxytryptophan and then into serotonin (5-HT). 5-HT is then acetylated by aryl alkylamine N-acetyltransferase and then converted into MLT by hydroxyindole O-methyltransferase (Zhao et al. 2019; Cardinali and Pévet 1998). The synthesis of MLT is controlled by the suprachiasmatic nucleus (SCN) and is regulated by the photoperiod and neurotransmitters including noradrenaline and GABA (Recio et al. 1996). Importantly, MLT secretion by the pineal gland follows a specific circadian pattern. Darkness stimulates the pineal gland to secrete MLT, whereas exposure to light inhibits its release into the bloodstream (Cipolla-Neto and Amaral 2018). Later, it crosses the blood-brain barrier and enters the central nervous system (CNS) (Longatti et al. 2007). Once in the bloodstream, MLT has a short half-life of 2–20 minutes in rats (Gibbs and Vriend 1981), while in humans, the half-life of endogenous MLT is approximately one hour (Fourtillan et al. 2001; Fourtillan et al. 2000). The level of MLT in the body is lower during the day (light phase) and

reaches maximal levels during the night (dark phase) in both diurnal and nocturnal species. In humans, plasma levels of MLT rise about 2 hours before habitual bedtime and remain elevated during the night. For example, the average levels of circulating MLT in humans during daytime and nighttime is approximately 10 and 60 pg/mL, respectively (Arendt 1988). MLT is mainly metabolized by the liver where it is first hydroxylated into 6-hydroxymelatonin and then conjugated with sulfate or glucuronic acid to finally be excreted (Kopin et al. 1961; Semak et al. 2008).

1.2. Melatonin receptors: distribution and signaling

MLT binds to two high-affinity (Ki ≅ 0.1 nM) receptors named MT_1 (or Mel1A or *MTNR1A*) and MT_2 (or Mel1B or *MTNR1B*) (Dubocovich et al. 2010), belonging to the seven transmembrane G protein-coupled receptor (GPCR) family. In addition to these MLT receptors, another low-affinity MLT binding site, termed MT_3, has been characterized as an MLT-sensitive form of the human enzyme quinone reductase 2 (Nosjean et al. 2000), though it is not included in the IUPHAR classification as a GPCR subtype for MLT (Mailliet et al. 2005). MLT receptors are broadly expressed throughout the central nervous system and are also localized in many peripheral tissues of mammals. The first studies addressing the localization of MLT receptors were done by in-vitro quantitative autoradiography using the non-selective high-affinity radioligand 2-[^{125}I]Mel (Dubocovich and Takahashi 1987; Weaver, Rivkees, and Reppert 1989) or using real-time quantitative reverse transcription-polymerase chain reaction (RT-PCR) (Mazzucchelli et al. 1996; Sallinen et al. 2005). In rodents, MLT binding sites have been found in the median eminence, pituitary, suprachiasmatic nucleus (SCN), anteroventral thalamic nucleus, and paraventricular thalamic nucleus, and, less densely, in other brain areas such as the hippocampus, cerebellum,

parietal cortex, lateral habenula, amygdala, and striatum (Weaver, Rivkees, and Reppert 1989; Weaver et al. 1993). In rodents, for instance, RT-PCR has detected MT_1 and MT_2 receptor mRNAs in the hippocampus, hypothalamus, vestibular nuclei, retina and pineal gland (Musshoff et al. 2002; Sallinen et al. 2005; Yerer, Delgado, and Aydogan 2010; Ahn et al. 2012). In humans, both RT-PCR and autoradiography with [^{125}I]Mel have detected the expression of MT_1 and MT_2 receptors in the cerebellum, hypothalamus, thalamus, cortex and hippocampus (Mazzucchelli et al. 1996; Al-Ghoul, Herman, and Dubocovich 1998). Interestingly, MLT receptors have been reported in regions implicated in pain regulation, such as the dorsal horn of the spinal cord, the spinal trigeminal tract, and the trigeminal nucleus (Wan and Pang 1994; Zahn et al. 2003), particularly in the lamina I-V and X of the spinal cord. Moreover, both MT_1 and MT_2 have been found in the peripheral nervous system particularly in the dorsal root ganglions (DRGs) (Oliveira-Abreu et al. 2018; Lin et al. 2017). Studies suggest that MT_1 and MT_2 receptors are distributed in specific regions of the brain, which is in line with their distinct neurobiological effects (Klosen et al. 2019; Ochoa-Sanchez et al. 2011; Lacoste et al. 2015). Using polyclonal antibodies (Lacoste et al. 2015), we have identified in rats the presence of MT_1 and MT_2 receptors in different brain regions. While MT_2 receptors are widely expressed in the reticular thalamus, substantia nigra (pars reticulata), supraoptic nucleus, the glutamatergic neurons of the ventral lateral periaqueductal grey matter (vlPAG) (Lopez-Canul, Palazzo, et al. 2015), and the CA2 and CA3 areas of the hippocampus (Ochoa-Sanchez et al. 2011), MT_1 receptors have been found in the retrosplenial cortex, in the basal forebrain, medial habenula and SCN of the hypothalamus (Lacoste et al. 2015). Moreover, using a "knock-in" strategy replacing MT_1 or MT_2 coding sequences with a LacZ reporter, Klosen and colleagues (Klosen et al. 2019) confirmed that MT_1 and MT_2 mRNAs are mostly located in non-overlapping areas of the brain.

As mentioned above, MLT effects in the brain are mainly mediated by the activation of two GPCRs, MT_1 and MT_2 (Reppert et al. 1995; Reppert, Weaver, and Ebisawa 1994). The activation of these receptors promotes dissociation of G proteins into α and βγ dimer, which interact with various molecules involved in the transmission of cell signaling. Using recombinant human receptors, Reppert and colleagues confirmed that adenylate cyclase inhibition and the production of cAMP via pertussis toxin (PTX) -sensitive G proteins is a signaling mechanism for both MT_1 and MT_2 melatonin receptor types (Reppert et al. 1995). Notably, PTX sensitivity indicates the involvement of G proteins in the Gi/Go family, which downstream in the pathway activates inward-rectifier potassium channels (GIRKs). Indeed, MT_1 stimulation opens inward-rectifier potassium (Kir3 or GIRK) channels through a PTX-sensitive mechanism that may involve βγ subunits of Gi (Nelson, Marino, and Allen 1996). Using recombinant human receptors, adenylate cyclase (AC) inhibition has been confirmed as a signaling mechanism for both MT_1 and MT_2 melatonin receptor types (Reppert et al. 1995). Moreover, the MT_1 receptor is coupled to different G-proteins that mediate the AC inhibition by a PTX-insensitive G-protein (Gq/11) and phospholipase C beta activation (Brydon et al. 1999; Reppert et al. 1995), and the MT_2 receptor additionally inhibits the soluble guanylyl cyclase (GC) pathway (Petit et al. 1999). While the MT_1 receptor activates protein kinase C (PKC) in the rat SCN (McArthur, Hunt, and Gillette 1997), the MT_2 receptor stimulates the activity of the human myometrial smooth muscle cells through the PKC (Sharkey et al. 2009); these findings suggest an interaction of both MT_1 and MT_2 receptors with the phospholipase C/diacylglycerol signaling pathway.

In sum, MT_1 and MT_2 receptors seem to induce multiple and specific cellular responses which, downstream, modulate unique physiological actions of MLT (Witt-Enderby et al. 2003), leading to complementary or opposite effects (Doolen et al. 1998; Wan et al. 1999). For example,

MT_1, but not MT_2, receptors regulate rapid eye movement (REM) sleep and its activation decreases non-rapid eye movement (NREM) sleep, while MT_2 activation increases it (Comai, Ochoa-Sanchez, and Gobbi 2013; Ochoa-Sanchez et al. 2011); MT_1 receptor activation induces vasoconstriction whereas MT_2 receptor stimulation induces vasodilatation (Doolen et al. 1998); in rats, MT_1 increases the body temperature, while MT_2 decreases it during the dark phase (Lopez-Canul et al. 2019). Moreover, these receptors are independently involved in mood and anxiety disorders: the MT_1 receptor is implicated in anhedonia/depression (Comai et al. 2015), whereas MT_2 is implicated in anxiety (Comai et al. 2020; Ochoa-Sanchez et al. 2012).

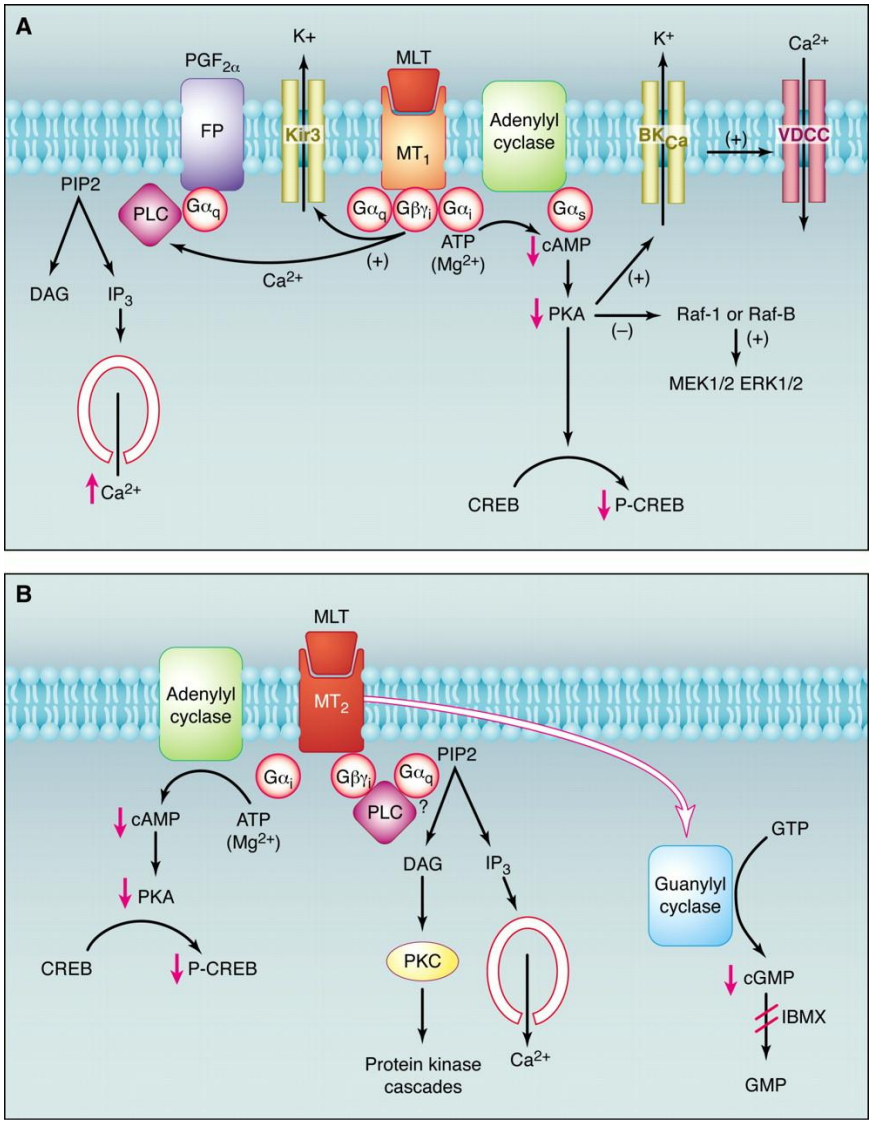

Chapter I - Figure 1. Signaling pathways activated by MT_1 and MT_2 melatonin receptors. (**A**) Multiple signaling pathways for MT_1 melatonin receptors coupled to Gαi and Gαq/11. (**B**) Signaling pathways coupled to MT_2 melatonin receptor activation. PIP2, phosphatidylinositol 4,5-bisphosphate; PLC, phospholipase C; DAG, diacylglycerol; PKA, protein kinase A; CREB, cAMP-responsive element binding protein; ER, endoplasmic reticulum; VDCC, voltage-dependent Ca^{2+} channel; BKCa, calcium activated potassium channel; FP, receptor for prostaglandin F2α; PGF2α, prostaglandin F2α; IBMX, isobutylmethylxantine; ATP, adenosine triphosphate; MLT, melatonin; GTP, guanosine triphosphate; GMP, guanosine monophosphate. From Masana and Dubocovich (2001). Reprinted with permission from AAAS.

	MT_1 receptor activation	**MT_2 receptor activation**
REM sleep	Increase duration	No effects
NREM sleep	Not investigated	Increase duration
Circadian Rhythm	deceleration of re-entrainment; * phase advance when administered at subjective dusk *	Not investigated
Pain	Not investigated	Analgesia
Vascular level	Vasoconstriction	Vasodilatation
Body temperature	Increase	Decrease

Chapter I - Table 1. Distinct pharmacological effects obtained following the selective activation of MT_1 or MT_2 receptors.

* pharmacological effect shown *in vivo* by MT_1 selective inverse agonists.

Not investigated: findings are yet too preliminary.

1.3. **The opioid system**

In the early 1970s, the three classical opioid receptors, mu (*Oprm1*/MOR), delta (*Oprd1*/DOR) and kappa (*Oprk1*/KOR) (Pert, Pasternak, and Snyder 1973; Pert and Snyder 1973; Simon, Hiller, and Edelman 1973), were identified. Later, the three families of endogenous peptides derived from either proopiomelanocortin (POMC), proenkephalin (PENK) or prodynorphin (PDYN) were also identified and cloned (Goldstein et al. 1979; Comb et al. 1982; Nakanishi et al. 1979). These three gene families encode for precursors which in turn generate several active peptides including β-endorphin (from POMC), met- and leu-enkephalin (from PENK), dynorphins and neo-endorphins (from PDYN) (Kieffer and Gavériaux-Ruff 2002). Notably, the endogenous opioid ligands exhibit different affinities for each opioid receptor. The opioid receptors, similar to the MLT MT_1 and MT_2 receptors, belong to the GPCR with 7 α-helices transmembrane domains (Befort et al. 1996) and the opioid peptides all contain the amino-terminal sequence, Tyr-Gly-Gly-Phe, called the "opioid motif" (Akil et al. 1998).

Autoradiographic and genetic studies have revealed that opioid receptors are broadly expressed throughout the central nervous system (CNS) and in many peripheral mammalian tissues (Kitchen et al. 1997; Wittert, Hope, and Pyle 1996). Generally, the mRNA expression of opioid receptors substantially overlaps with the protein expression. However, in some brain regions such as the olfactory bulb, cortex, and hippocampus, the mRNA is expressed but the protein is not (Mansour et al. 1994). This finding suggests that presynaptic receptors are likely transported to projection structures. The opioid peptide immunoreactivity distribution shows that endogenous opioids are also largely expressed in the brain. However, conversely to the opioid receptors, a substantial discrepancy between peptide immunoreactivity and cell body localization has been found, suggesting that a significant amount of peptides are released by projection neurons

(Le Merrer et al. 2009). While the anatomical distribution of POMC-producing cells is relatively limited within the CNS, peptides from prodynorphin and proenkephalin are distributed widely throughout the CNS and are frequently found together (Le Merrer et al. 2009). Of note, proenkephalin peptides are present in the areas of the CNS that are presumed to be related to the perception of pain (i.e., laminae I and II of the spinal cord, the spinal trigeminal nucleus, and the periaqueductal gray), and to the modulation of affective behaviors (e.g., amygdala, hippocampus, locus coeruleus and the frontal cerebral cortex) (Le Merrer et al. 2009; Akil et al. 1998; Bagley and Ingram 2020; Fricker et al. 2020).

1.3.1. The Mu opioid receptor (MOR)

Mu opioid receptors (MORs) are the most studied opioid receptors and numerous ligands have been synthetized for therapeutic, research, or recreational purposes. Morphine is the most commonly used clinical MOR agonist, prescribed for the treatment of moderate to severe pain as capsules, syrup or injectable solution (Spetea et al. 2013). This alkaloid is extracted from *Papaver somniferum* and its analgesic effect is due to the activation of MOR for which it has a good affinity (Ki= 1.17 nM) (Volpe et al. 2011). Because of the appearance of a strong physical dependence, abuse liability and tolerance during treatment with morphine, synthetic or hemi-synthetic alkaloids were synthesized to obtain effective molecules in the treatment of pain with fewer side effects. However, outcomes are generally unsuccessful as heroin has an even stronger addictive effects, codeine can only be used for mild pain, and finally, oxycodone, a hemi-synthetic opiate which initially seemed to be very promising, has triggered a new wave of opioid epidemics in North America during the last decade (Control and Prevention 2011).

MOR anatomical localization

MORs are expressed throughout the central and peripheral nervous systems. In the brain, MOR density is variable depending on brain structures (Le Merrer et al. 2009; Mansour et al. 1994). Of note, MORs are abundantly expressed in all the supraspinal areas of the pain circuit including insular cortex, amygdala, hypothalamus, PAG, RVM and dorsal horns of the spinal cord (Mansour et al. 1994; Mansour et al. 1988; Arvidsson et al. 1995) and are expressed in the dopaminergic mesocorticolimbic circuitry (Kitchen et al. 1997) which is composed of neurons of the ventral tegmental area (VTA) projecting to forebrain structures including the amygdala, nucleus accumbens and frontal cortex (Nieh et al. 2013).

MOR pharmacology and signaling

As mentioned above, MORs belong to the superfamily of GPCRs, and are generally coupled to a monomeric subunit αi/o and a dimeric Gβγ complex. When an agonist binds to the opioid receptor, it causes a change in conformation that causes the dissociation of the Gα subunit from the Gβγ dimer. At this point, Gα and Gβγ interact with different effectors, regulating the cell activity. The αi/o activation inhibits the effector adenylyl cyclase (AC), resulting in inhibition of cAMP production (Bernstein and Welch 1998). Downstream, the stimulation of MORs reduces the presynaptic depolarization-dependent release of neurotransmitters through the inhibition of the N-type Ca^{2+} channels. The stimulation of MOR postsynaptic receptors produces hyperpolarization by the activation of K^+ channels and inhibition of L-type Ca^{2+} channels, through the release of the Gβγ dimer leading to the production of IP3, which releases intracellular Ca^{2+}, and diacylglycerol (DAG), which activates PKC (Williams, Christie, and Manzoni 2001). In this way, opioids promote the inhibition of neuronal transmission and therefore, the transmission impulses generated by noxious stimuli (Vaughan and Christie 1997; Chieng and Christie 1994a). Moreover, the Gβγ

complex (after its uncoupling from the Gα unit) plays a crucial role in the diversification of the signal transduction activated by opioids, as well as for other GPCRs. The G protein-coupled inwardly-rectifying potassium (GIRK or Kir3) channels are activated from direct interaction with Gβγ dimers after stimulation of GPCRs (Wickman et al. 1994; Raveh, Riven, and Reuveny 2009). This event is considered part of the inhibiting mechanism of opioid nociceptive transmission, since missense mutations (Patil et al. 1995) or null mice (Mitrovic et al. 2003) of GIRK2 or GIRK3 (Marker et al. 2002) prevent morphine's ability to prolong avoidance behavior in the hot plate test, a response that involves supraspinal integration. The thalamus and limbic cortex are likely the nuclei of supraspinal GIRK-mediated analgesia, since both of them express GIRK2-3 subunits (Del Burgo et al. 2008; Fernández-Alacid et al. 2011) as well as opioid receptors (Le Merrer et al. 2009). On the contrary, the midbrain PAG seems less involved because in this area, opioid receptors act mostly at presynaptic levels, decreasing neurotransmitter release via phospholipase A2, arachidonic acid and 12-lipoxygenase activation, which in turn modulate voltage-dependent potassium channels (Vaughan and Christie 1997; Vaughan et al. 1997). In addition, knock out mice for GIRK1 or GIRK2 subunits (Marker, Stoffel, and Wickman 2004) or GIRK blocker tertiapin-Q pretreatment (Marker et al. 2005) reduced the responses to intrathecal administration of opioid agonists in the tail flick test. These findings are in keeping with an immunohistological study from the same group which identified the colocalization of GIRK1 or GIRK2 subunits with MORs in interneurons of lamina II of the spinal cord (Marker et al. 2006). Conversely, GIRK3 seems to not be involved in spinal mechanisms of opioid analgesia (Marker, Stoffel, and Wickman 2004), in agreement with immunostaining results showing expression in the dorsal horn of spinal cord (Marker, Stoffel, and Wickman 2004).

For many years, it was considered that the opioid receptors were exclusively coupled to the inhibitory pertussis toxin (PTX) - sensitive Gα i/o proteins. Indeed, MOR, DOR and KOR can couple to five different isoforms of Gαi/o (αi1-3 and αoA-B), thereby regulating a signal transduction with different effectors such as adenylate cyclase (AC 1, 5, 6, 8), ion channels and the protein kinase mitogen-activated (MAP) kinase pathway (Williams, Christie, and Manzoni 2001). However, it was also demonstrated that DOR (Allouche, Polastron, and Jauzac 1996) and MOR/DOR dimer (Fan et al. 2005) may transduce the inhibitory signal through PTX-insensitive G protein, like Gαz protein, which is the only type of the Gαi insensitive to PTX because of the missing residue of cysteine in the carboxy-terminal portion, which is the site for the ADP-ribosylation catalyzed by PTX. Gαz is expressed in nervous tissue and it is co-expressed with the opioid receptors in neuronal cell lines; it is also coupled with the MOR in the PAG where it mediates supraspinal analgesia.

Although it is still controversial, it has also been suggested that opioids may modulate some events such as tolerance and dependence via the Gαs subunit. Some recent findings showed that a subset of MOR co-immunoprecipitated with Gαs enhanced by morphine exposure in Chinese hamster ovary (CHO) cell culture and *ex vivo* (Chakrabarti, Regec, and Gintzler 2005; Chakrabarti and Gintzler 2007).

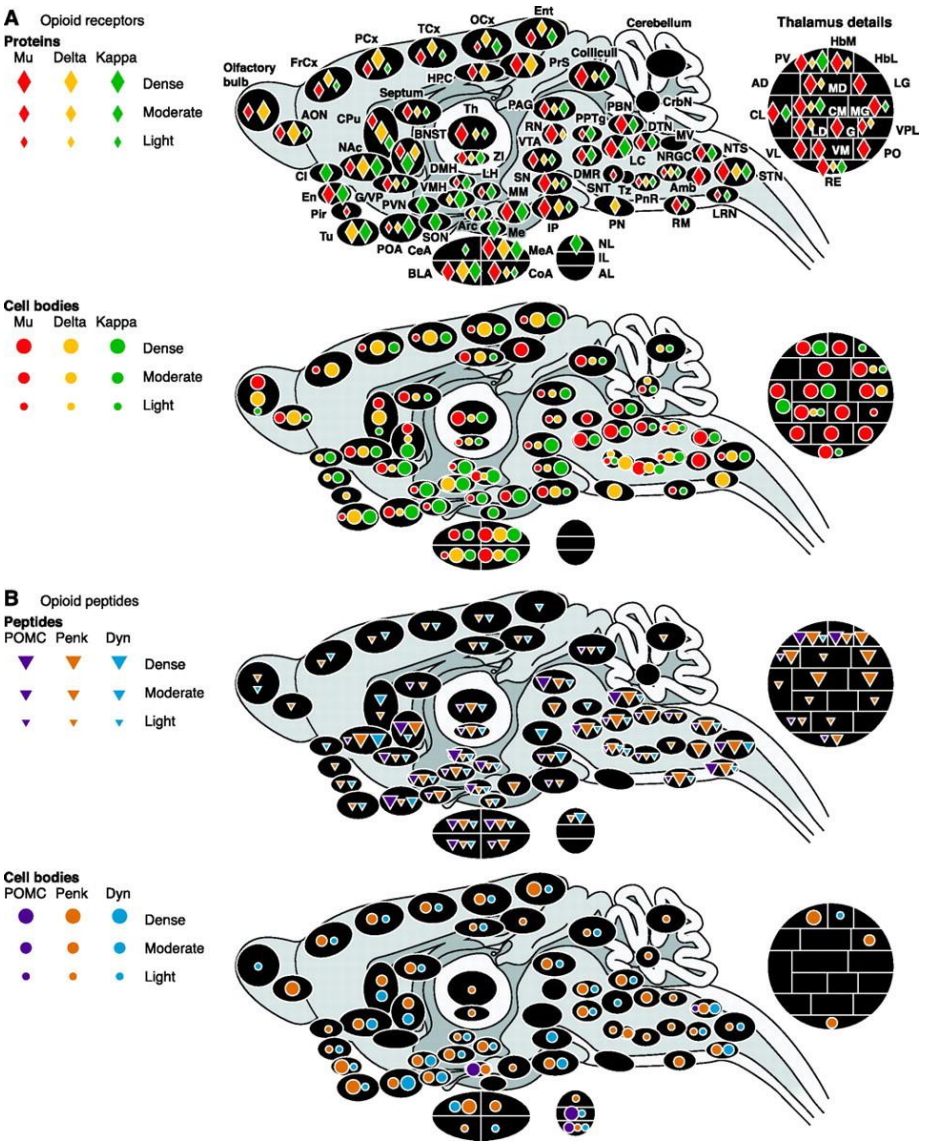

Chapter I - Figure 2. Anatomical distribution of opioid receptors (A) and peptides (B) in the rodent brain.

Amb, nucleus ambiguus; AD, anterodorsal thalamus; AL, anterior lobe, pituitary; AON, anterior olfactory nucleus; Arc, arcuate nucleus, hypothalamus; BLA, basolateral nucleus, amygdala; BNST, bed nucleus of the stria terminalis; CeA, central nucleus, amygdala; Cl, claustrum; CL, centrolateral thalamus; CM, centromedial thalamus; CoA, cortical nucleus, amygdala; CPu, caudate putamen; CrbN, cerebellar nuclei; DMH, dorsomedial hypothalamus; DMR, dorsal and medial raphe; DTN, dorsal tegmental nucleus; En, endopiriform cortex; Ent, entorhinal cortex; FrCx, frontal cortex; G, nucleus gelatinosus, thalamus; G/VP, globus

pallidus/ventral pallidum; HbL, lateral habenula; HbM, medial habenula; HPC, hippocampus; IL, intermediate lobe, pituitary; IP, interpeduncular nucleus; LC, locus coeruleus; LD, laterodorsal thalamus; LG, lateral geniculate, thalamus; LH, lateral hypothalamus; LRN, lateral reticular nucleus; MD, mediodorsal thalamus; Me, median eminence; MEA, median nucleus, amygdala; MG, medial geniculate; MM, medial mammillary nucleus; MV, medial vestibular nucleus; NAc, nucleus accumbens; NL, neuronal lobe, pituitary; NRGC, nucleus reticularis gigantocellularis; NTS, nucleus tractus solitarius; OCx, occipital cortex; PAG, periaqueductal gray; PCx, parietal cortex; Pir, piriform cortex; PN, pontine nucleus; PnR, pontine reticular; PO, posterior thalamus; POA, preoptic area; PPTg, pedunculopontine nucleus; PrS, presubiculum; PV, paraventricular thalamus; PVN, paraventricular hypothalamus; RE, reuniens thalamus; RN, red nucleus; RM, raphe magnus; SON, supraoptic nucleus; SN, substancia nigra; SNT, sensory trigeminal nucleus; STN, spinal trigeminal nucleus; TCx, temporal cortex; Th, thalamus; Tu, olfactory tubercle; Tz, trapezoid nucleus; VL, ventrolateral thalamus; VM, ventromedial thalamus; VMH, ventromedial hypothalamus; VPL, ventroposterolateral thalamus; VTA, ventral tegmental area; ZI, zona incerta. From *Le Merrer et al. (2009)*. Reprinted with permission.

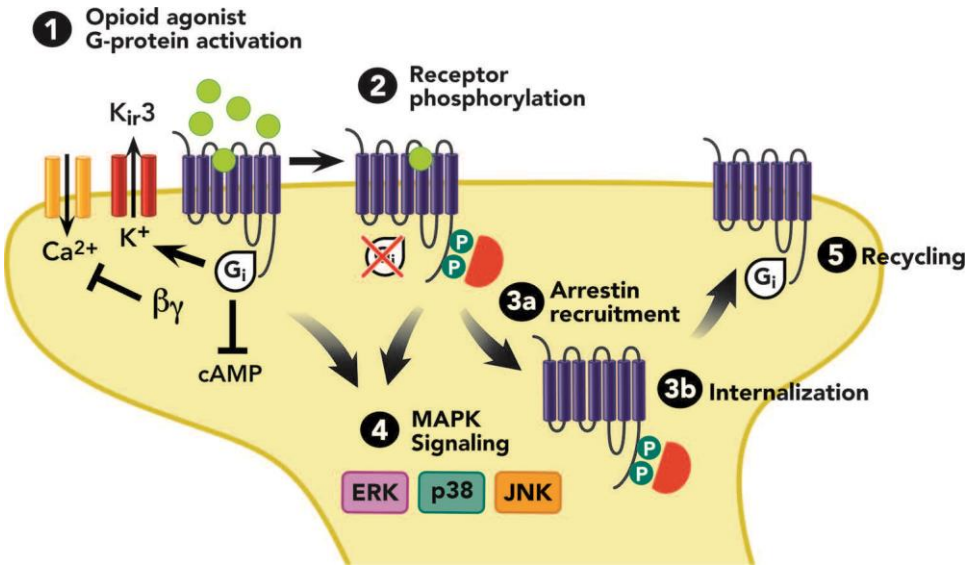

Chapter I - Figure 3. Signal transduction induced by mu opioid receptor (MOR) activation.

Generally, all three opioid receptor subtypes (MOR, DOR, KOR) can activate these pathways. Specific ligands can direct opioid receptors signaling or trafficking to one or more of these events (biased agonism or ligand-directed signaling). βγ = G protein β-γ subunit; cAMP = cyclic adenosine monophosphate; ERK = extracellular signal-regulated kinase; JNK = c-jun N-terminal kinase; MAPK = mitogen-activated protein kinases; P = phosphorylation. From *Al-Hasani and Bruchas (2011)*. Reprinted with permission.

1.4. **Pain and its circuits**

In 2020, the International Association for the Study of Pain (IASP) proposed a new definition of pain. Pain is: “An unpleasant sensory and emotional experience associated with, or resembling that associated with, actual or potential tissue damage” (Raja et al. 2020). Pain is essential to the proper functioning of the body and it has a protective role in warning body to prevent tissue damage. If tissue damage is unavoidable, a set of excitability changes in the peripheral and central nervous system establish a profound but reversible pain hypersensitivity in the inflamed and surrounding tissue. Although it is convenient to frame pain in anatomical, physiological and pharmacological terms, it should be noted that many other factors are involved and a multi-factorial approach is required to achieve analgesia.

1.4.1. The Nociceptive Ascending Pathways

From a physiological point of view, the integration of painful stimuli in the body takes place in several steps. At the peripheral level, primary afferent nociceptors (mechanoreceptor, thermoreceptor, chemoreceptor) detect the intense, potentially harmful stimuli and transmit the pain message through two types of fibers: myelinated Aδ and unmyelinated C fibers (for a review see: Meyer et al. 2006). Aδ fibers transmit the primary hyperalgesia, which is intense, localized, and proportional to the application and quickly stopped by reflexes (for example, withdrawal of the affected area in case of burns). Aδ fibers differ from Aβ fibers since the latter have a larger diameter, a fast stimulus conduction and respond to innocuous mechanical stimulation such as a light touch. Small diameter C fibers transmit the secondary hyperalgesia that lasts longer, has a slower integration and is poorly localized. Nociceptive afferent fibers project to specific areas (called “laminae”) of the dorsal horn of the spinal cord in an organized manner. Myelinated Aδ fibers project to lamina I and deeper lamina V, low-threshold Aβ fibers project to laminae III-V

and unmyelinated C fibers synapse onto superficial laminae I-II. Projecting neuronal axons within dorsal horn laminae contact the supraspinal centers through the ascending nociceptive pathways: the spinothalamic and the spinoreticularthalamic tracts (Basbaum et al. 2009). The former transmits the stimulus to the somatosensory cortex via the thalamus and is involved in the sensory-discriminative aspect of pain such as location and intensity. The spinoreticularthalamic tract projects to the reticular formation in the medulla and pons, to the thalamic nuclei, and then to the somatosensory cortex and is relevant to less localized pain. Recently, a third pathway of the ascending pathway involving the projections form the parabrachial nucleus of the dorsolateral pons was investigated. This tract connects the brainstem to the cingulate and the insular cortex through the amygdala, a critical region for the affective component of the pain experience (Janak and Tye 2015; Corder et al. 2019).

1.4.2. The Nociceptive Descending pathway

Alongside with the ascending circuits, the descending control of nociception also plays a pivotal role in determining the transmission and the experience of both acute and chronic pain. This "top-down" modulatory pathway involves multiple brain regions such as the hypothalamus, the amygdala, the anterior cingulate cortex, the midbrain PAG, the midline nucleus raphe magnum and the medulla (Heinricher and Fields 2013). These areas mediate both inhibitory and facilitatory control of pain which means they can reduce or enhance the nociceptive sensation of pain (Heinricher and Fields 2013). The descending pathway is the pharmacological target of many analgesic drugs, including opiates, cannabinoids, nonsteroidal anti-inflammatory drugs (NSAIDs) and serotonin/noradrenergic reuptake blockers. The more studied site of this central is the PAG-RVM system. The PAG receives inputs from the hypothalamus, the limbic area of the amygdala, and spinomesecephalic areas. In turn, the PAG projects to the RVM which sends its axons to the

dorsal horn of the spinal cord through the dorsal lateral funiculus (DLF) (Fields, Barbaro, and Heinricher 1988; Fields, Malick, and Burstein 1995). Using electrophysiological studies coupled to a noxious stimulation (tail-flick), Fields and colleagues identified three different neuronal subpopulations in the RVM: ON cells, OFF cells and Neutral cells (Fields et al. 1983). While the ON cells increase their firing rate just before the tail-flick, the OFF cells are tonically active and silence their firing prior to the initiation of the noxious stimulus. Neutral cells were not modulated by the noxious stimulation (Fields et al. 1983). Both ON and OFF cells project to the spinal cord and this opposite effect is consistent with the bidirectional facilitatory/inhibitory role of the descending system (Fields, Malick, and Burstein 1995; Vanegas, Barbaro, and Fields 1984).

1.4.3. ON, OFF and Neutral cells in the RVM

ON and OFF cells have also been studied from a pharmacological point of view. When opioids are systemically or locally administrated into the PAG or the RVM, the activity of the OFF cells is increased, leading to analgesia (Jensen and Yaksh 1989; Fang et al. 1989; Cheng, Fields, and Heinricher 1986; Heinricher, Cheng, and Fields 1987). Conversely, opioids micro-injected into these areas reduce the ON activity (Cheng, Fields, and Heinricher 1986; Jensen and Yaksh 1989). Moreover, *in vivo* electrophysiological evidence showed that opioids produce analgesia through the disinhibition of OFF cells (Heinricher et al. 1994), suggesting that MOR is localized at the presynaptic level. Of note, the $GABA_A$ selective antagonist bicuculline also leads to similar antinociceptive effects, suggesting that MOR is presynaptically expressed on GABA-releasing inputs (Heinricher and Tortorici 1994). In contrast, the ON cell subpopulation is directly inhibited by opioids, indicating that MOR is expressed at the somatodendritic level (Pan, Williams, and Osborne 1990; Heinricher, Morgan, and Fields 1992). Subsequent *in vitro* patch clamp studies confirmed that opioids can modulate the PAG-RVM descending pathway by both post- and

presynaptic cellular mechanism. The former occurs through a direct disinhibition of GABA interneurons via postsynaptic MOR in PAG and RVM, producing an increase in inwardly rectifying K^+ conductance (Pan, Williams, and Osborne 1990; Vaughan et al. 2003; Chieng and Christie 1994a). In the latter, the activation of GABAergic presynaptic MOR in PAG and RVM disinhibits PAG-RVM outputs (Vaughan and Christie 1997; Chieng and Christie 1994b), likely through a voltage-dependent K^+ channel modulation linked to a phospholipase A2/arachidonic acid cascade (Vaughan et al. 1997). Some studies pointed out that the presynaptic inhibition of glutamatergic excitatory inputs to ON cells might contribute to the opioid analgesic effect both in PAG (Connor et al. 1999) and RVM (Finnegan et al. 2004). However, compelling evidence supports the hypothesis that MOR agonists produce analgesia thought the disinhibition of OFF cells in these brain structures (Heinricher, Morgan, and Fields 1992; Heinricher and Tortorici 1994; Heinricher et al. 1994; Vaughan and Christie 1997; Vaughan et al. 1997; Vaughan et al. 2003). Eventually, a large amount of OFF and neutral cells (but also ON cells, although with less magnitude) have been found positive to GAD67 immunoreactivity (Winkler et al. 2006), a marker for inhibitory GABAergic neurons.

Based on early studies (Yeung, Yaksh, and Rudy 1977; Behbehani and Fields 1979; Wiklund et al. 1988), Basbaum and Fields proposed the "GABA disinhibition" hypothesis of analgesia (Basbaum and Fields 1984). According to it, tonically active GABAergic interneurons are localized within the PAG and RVM, release the neurotransmitter GABA, which activate $GABA_A$ receptors to inhibit spinally projecting output neurons. Importantly, the 'lateral inhibition' model presumes that outputs from the PAG to the RVM are solely excitatory glutamatergic projections (Basbaum and Fields 1984). Opioids (and cannabinoids) in PAG and RVM produce antinociception removing the inhibitory control of local GABAergic interneurons in the

descending pathway. Later, *in vivo* neuropharmacological studies indirectly confirmed this hypothesis (Moreau and Fields 1986; Heinricher, Morgan, and Fields 1992; Heinricher et al. 1994; Tortorici and Morgan 2002). More direct observations using transgenic mice and electrophysiological recordings support the GABA disinhibition hypothesis. MOR agonists directly inhibit GABAergic neurons in vlPAG (Vaughan et al. 2003), but not descending projection neurons (Osborne et al. 1996), suggesting that MOR sensitive neurons do not project to the RVM, and are therefore likely to be GABAergic interneurons. A recent study using GAD67-GFP retrogradely labelled transgenic mice in PAG-RVM confirmed opioid antinociception is due to MOR-mediated inhibition of fast-spiking, GABAergic interneurons in vlPAG (Park et al. 2010). Although the 'lateral inhibition' is the predominant model to explain supraspinal opioid analgesia, some evidence suggest that inhibitory and excitatory neurons constitute two distinct and parallel pathways. Using immunohistochemistry and anterograde/retrograde labelling of PAG and spinal cord to RVM, it has been demonstrated that a large part of PAG fibers projecting to GAD67-immunoreactive reticulospinal neurons in the RVM were also GAD67-immunoreactive (Morgan et al. 2008), suggesting that outputs from PAG to RVM are not only excitatory but also inhibitory. Moreover, *in vivo* electrophysiological studies support the "parallel inhibition-excitation" hypothesis. In a first study, Cleary, Neubert, and Heinricher (2008) compared the onset of the ON and OFF cell firing changes before the nociceptive tail-flick response and they found that the pause of OFF cell firing precedes the increase in firing (burst) of ON cells. This finding is directly in contrast with the "lateral inhibition" model, in which ON cells are presumed to be GABAergic interneurons which tonically inhibit OFF cells. Therefore, ON cell bursts should occur immediately prior to the pause in OFF cell firing. Further studies showed that the activation of ON cells can promote nociception without requiring inhibition of OFF cell activity (Heinricher and

McGaraughty 1998; Neubert, Kincaid, and Heinricher 2004) and other studies demonstrated that both ON and OFF cells distinctly project to the dorsal horn of the spinal cord (Fields, Malick, and Burstein 1995). Altogether, these findings suggest that the descending analgesic pathway is more complex than previously supposed. Future work will need to address these issues by using more direct approaches.

ON and OFF cell populations are also activated by the neuropeptide cholecystokinin (CCK) through CCK2 receptors (Heinricher, Morgan, and Fields 1992; Heinricher et al. 1994). Interestingly, Zhang and colleagues demonstrated that 80% of RVM neurons co-express MOR and CCK2, facilitate pain and might correspond to ON cells (Zhang et al. 2009).

The possible role of neutral cells is still debated. This cellular population do not respond during nocifensor withdrawal or acute inflammation (Xu et al. 2007) and their firing rate is not altered after local microinjection of opioids, cannabinoids, or CCK at doses that affect ON and OFF cell activity (Meng et al. 1998; Heinricher, McGaraughty, and Tortorici 2001). Despite the evidence of a lack of responsiveness of neutral cells in the nociception descending control, it has been speculated that neural cells can become ON or OFF cells in chronic pain conditions, since an increase in ON- and OFF-like cells and a decrease in neutral-like cells has been reported in a chronic inflammatory pain model, compared to naïve animals (Miki et al. 2002). Furthermore, a subpopulation of neutral cells is serotoninergic (Potrebic, Fields, and Mason 1994), whereas neither ON nor OFF cells are 5-HT positive (Gao and Mason 2000, 2001; Winkler et al. 2006).

1.4.4. Serotonergic and noradrenergic system in the descending pain pathway

Although the contribution of serotonin (5-HT) in the brainstem control of nociception transmission is still debated, a considerable number of studies demonstrated that the 5-HT neurons of the RVM are part of a pathway that is functionally distinct but anatomically interactive with the opioid-mediated pain modulatory circuit. Stimulation of the PAG promotes the release of 5-HT in the spinal cord (Cui et al. 1999), intrathecal injection of 5-HT agonists produce antinociception (Yaksh and Wilson 1979; Alhaider, Lei, and Wilcox 1991), while 5-HT antagonist injections block the stimulation-induced antinociception from the RVM (Jensen and Yaksh 1984). Also, the spinal dorsal horns receive serotonergic projections from the nucleus raphe magnus a region located between the PAG and the RVM (Kwiat and Basbaum 1992). In adult rats, around 20% of RVM neurons express 5-HT (Potrebic, Fields, and Mason 1994; Moore 1981), although 5-HT was found only in neural cells which are not affected by opioids. Conversely, in young rats, spinally-projecting serotonergic RVM neurons showed postsynaptic inhibition by both MOR and KOR selective agonists (Marinelli et al. 2002). Using selective ablation of 5-HT neurons in the RVM, Wei and colleagues showed that the descending 5-HT projections from the RVM are an important contributor to pain facilitation in inflammatory or neuropathic pain states, but they are not involved in opioid-induced descending inhibition in acute pain (Wei et al. 2010). These findings suggest that the role of the 5-HT system in the descending pain transmission might depend on neural development and the pain chronicization. 5-HT has dual effects since it can have both excitatory and inhibitory actions on dorsal horn neurons (Mason 2001) and this depends on the 5-HT receptor subtype activated. It has been demonstrated that while 5-HT_7 receptors are inhibitory, 5-HT_3 receptors are facilitatory in the descending pain pathway (Dogrul, Ossipov, and Porreca 2009). Indeed, the 5-HT_7 receptor is expressed in the dorsal root ganglion and on primary afferent fibers and on GABAergic interneurons in the dorsal horn of the spinal cord (Doly et al. 2005). These

findings are in agreement with the capability of a 5-HT_7 receptor antagonist at the spinal level to nullify the antinociceptive effect of morphine administered into the RVM (Dogrul, Ossipov, and Porreca 2009). Yet, while 5-HT_7 antagonists induced mechanical hypersensitivity in capsaicin-induced hyperalgesia in mice, 5-HT_7 agonists blocked it (Brenchat et al. 2009). When 5-HT_3 is pharmacologically antagonized, the hyperalgesia induced by CCK microinjected into the RVM is blocked (Dogrul, Ossipov, and Porreca 2009).

Emerging preclinical evidence suggests the contribution of the noradrenergic system, more than the serotonergic one, to the antinociceptive descending pathway (Pertovaara 2006; Wigdor and Wilcox 1987). The electrical stimulation of both the PAG and RVM increased the norepinephrine neurotransmitter (NE) and the analgesia induced by electrical stimulation was blocked by adrenergic antagonists (Cui et al. 1999; Barbaro, Hammond, and Fields 1985). Neither the PAG nor RVM contain noradrenergic neurons, but they form synapses with some noradrenergic structures involved in pain modulation, including the locus coeruleus (LC) and A7 nucleus (Bajic and Proudfit 1999; Yeomans and Proudfit 1990; Holden and Proudfit 1998; Cameron et al. 1995), which in turn project to the spinal cord (Heinricher and Fields 2013). Local intra-PAG iontophoresis of the selective α2-adrenergic agonist clonidine reduced noxious responses in the dorsal horn neurons (Budai, Harasawa, and Fields 1998), and α2-adrenergic activation suppressed nociceptive transmission in the spinal cord through presynaptic mechanism, inhibiting the excitatory neurotransmission from primary afferences, as well as through postsynaptic sites (Pan, Li, and Pan 2002; Kawasaki et al. 2003). In comparison, the function of the α1-adrenergic role in pain transmission is less clear. While α1-adrenergic receptors enhance responses of dorsal horn neurons to noxious inputs (Budai, Harasawa, and Fields 1998), its spinal stimulation can also induce behavioural antinociception (Howe, Wang, and Yaksh 1983), likely through postsynaptic

depolarization of GABAergic dorsal horn neurons (Gassner, Ruscheweyh, and Sandkühler 2009). A recent study, using an optogenetic approach combined with *in vivo* electrophysiology, revealed a basolateral amygdala (BLA)-prefrontal cortex (PFC)-periaqueductal gray (PAG)-spinal cord circuit which determines the development of mechanical and thermal allodynia in neuropathy by decreasing the serotoninergic and noradrenergic modulation of spinal signals (Huang et al. 2019).

1.5. **Descending pathway and chronic pain**

A large body of preclinical literature shows that descending facilitation is increased in chronic pain and putative pain facilitatory cells play an important role in this state. However, why this mechanism co-occurs with the clinical aspects of pain chronicization remains unclear. During inflammation and nerve injury conditions, the balance of ON and OFF cells shifts to marked preponderance of ON cells (Palazzo et al. 2011; Kincaid et al. 2006; Gonçalves, Almeida, and Pertovaara 2007). However, some intriguing differences in ON-OFF cell equilibrium and physiological characterization have been found among the different models of chronic pain.

In chronic inflammation arthritis, both ON- and OFF-cell spontaneous activity was modestly increased and, while no change in the threshold for withdrawal to noxious heat was displayed, the responses of both ON- and OFF-cells to noxious pinch were decreased (Pinto-Ribeiro et al. 2008). Furthermore, in a model of monoarthritic ankle, innocuous stimulation produced early increases in *c-fos* expression in the RVM, but not at the spinal level, whereas *c-fos* expression was increased in RVM neurons after a noxious pinch, and associated with decreased expression at the level of the dorsal horn (Pinto, Lima, and Tavares 2007). This *c-fos* neuronal activation at the supraspinal level (RVM) is in line with the ongoing activity of both ON- and OFF-cells in chronic inflammation (Pinto-Ribeiro et al. 2008). Interestingly, descending modulation undergoes time-

dependent changes after complete Freund's adjuvant (CFA) injection in the rat hind paw, with an initial decrease and a subsequent increase in the neuronal excitability in the RVM (Terayama et al. 2000). This enhanced descending facilitation seems to be mediated by an upregulation of excitatory N-Methyl-d-aspartate (NMDA) receptors (Terayama et al. 2000).

Descending facilitation has an important role also in chronic neuropathic pain. Indeed, both ON and OFF cells developed responses to non-noxious mechanical stimuli (mechanical allodynia), and increased responses to noxious heat and mechanical stimulation (thermal and mechanical hyperalgesia) at an ipsilateral-injured paw (Gonçalves, Almeida, and Pertovaara 2007; Carlson et al. 2007). In a spared-nerve injury (SNI) model, an increase of the pinch-induced burst activity of the ON cells and of the pause duration of OFF cells was observed (Palazzo et al. 2011). Moreover, naloxone-precipitated opioid withdrawal has been found to be associated with enhancement of ON cell activity and hyperalgesia (Bederson, Fields, and Barbaro 1990; Kim, Fields, and Barbaro 1990); the latter is suppressed by RVM microinjection of lidocaine (Kaplan and Fields 1991). These outcomes suggest that supraspinal sites can contribute to either development or maintenance of chronic pain states (for a review see Urban and Gebhart 1999).

Porreca and colleagues (2001; Burgess et al. 2002) proposed an elegant experiment to demonstrate the importance of ON cell activity to neuropathic pain. Using the MOR agonist, dermorphin, conjugated to the cytotoxin ribosome-inactivating protein saporin, they selectively destroyed the RVM ON cells which express MOR at somatodendritic level (Pan, Williams, and Osborne 1990; Heinricher, Morgan, and Fields 1992). In this group of rats, both behavioural and biochemical neuropathy responses, but not normal nociceptive ones, were suppressed. Similar results were obtained after the selective ablation of CCK2-positive neurons in the RVM (Zhang et al. 2009). Also, microinjection of CCK into the RVM increased the behavioural responses (Kovelowski et

al. 2000; Xie et al. 2005), enhanced the ON cell activity (Heinricher and Neubert 2004) and the nociceptive effect was reversed by the lesion of the DLF (Kovelowski et al. 2000; Xie et al. 2005). Intra-RVM injection of a CCK antagonist blocked both the tactile allodynia and thermal hyperalgesia in L5-L6 spinal nerve spinal nerve ligated (SNL) animals (Kovelowski et al. 2000). The role of the DLF in maintaining neuropathy has also been demonstrated. When this fiber tract is ipsilaterally lesioned with respect to the injured nerve, the thermal hyperalgesia and tactile hypersensitivity were suppressed without modifying the physiological nociceptive response in sham-operated rats (Burgess et al. 2002; Ossipov et al. 2000). Moreover, intra-RVM injection of lidocaine reversed the increased pain behaviors in neuropathic rats (Burgess et al. 2002; Kovelowski et al. 2000; Pertovaara, Wei, and Hämäläinen 1996). Interestingly, microinjection of lidocaine in the RVM evoked reward in two nerve-injured pain models (both SNI and SNL), showing the contribution of the descending facilitation to tonic-aversive aspects of pain (King et al. 2009).

Several studies showed that (pro)nociceptive alterations in the spinal cord are linked to the activation of descending facilitation in neuropathy. After capsaicin injection peripheral nerve injury models, an increase of the release of calcitonin gene-related peptide (CGRP), a neuropeptide involved in pain, was observed as well as upregulation of the dynorphin in spinal cord (Burgess et al. 2002; Gardell et al. 2004; Gardell et al. 2003). Other findings suggest that pronociceptive spinal dynorphin is upregulated in neuropathy and is required for the maintenance, but not initiation, of chronic neuropathic pain (Wang et al. 2001; Xu et al. 2004). In agreement with what is detailed above, dynorphin upregulation and increased CGRP release are abolished after DLF lesion or dermorphin-saporin injection into RVM, confirming the pivotal role of descending facilitation in chronic neuropathic pain (Burgess et al. 2002; Gardell et al. 2004; Gardell et al. 2003). Recently,

Lai and colleagues (2006) showed that spinal dynorphin activates bradykinin receptors, increasing intracellular calcium and that the blockade of the spinal bradykinin receptor also reverses persistent neuropathic pain only when dynorphin is upregulated, as in neuropathic conditions.

Altogether, these findings suggest that multiple changes at the supraspinal pain control centers promote the imbalance between inhibition and facilitation during chronic pain. This neuronal plasticity at medullary sites appears to be specific for inflammation compared to nerve injury and it likely occurs to reorganize the pain system as an ongoing chronic pain state.

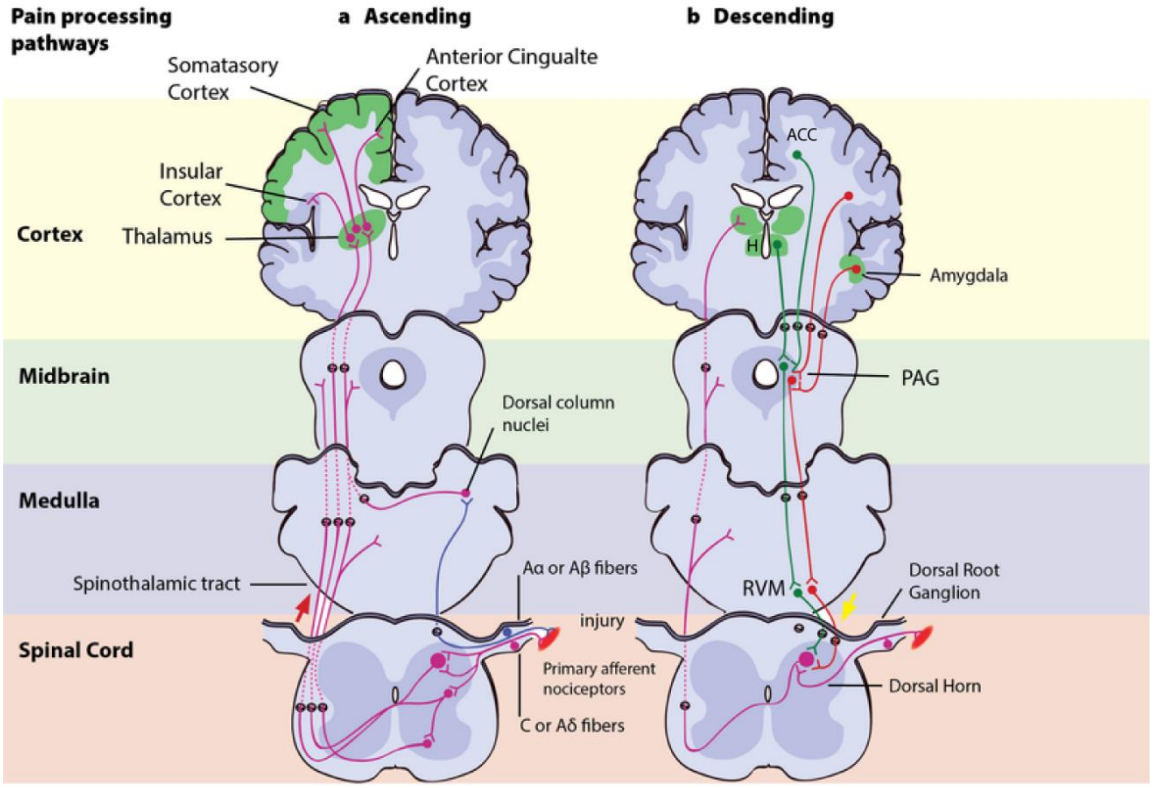

Chapter I - Figure 4. Pain processing pathways.

A: Ascending pathway. Noxious stimuli are signaled simultaneously via fast-conducting Aβ-fibres and slow-conducting primary afferent nociceptors (Aδ- and C-fibres, PAN). PAN terminals contact second order neurons in specific laminae of the dorsal horn of the spinal cord.

The second order neurons then cross over to contralateral side, forming the ascending spinothalamic tract which terminate in the medulla and midbrain up to the thalamus. The thalamus transmits the information to the insular and somatosensory cortex, as well as other cortical regions (i.e. cingulate cortex) involved in different aspects of the pain experience including the affective component. B: Descending pathway. This top–down pathway can be activated by both environmental stimuli and certain motivational states. Several areas in the limbic forebrain including the anterior cingulate (ACC) and insular cortex, the central nucleus of the amygdala and the hypothalamus (H), project to the periaqueductal grey (PAG). In turn, the PAG projects into the rostral ventromedial medulla (RVM) in the brainstem, modulating ON and OFF cells to exert either inhibitory (green) or facilitatory (red) control of nociceptive signals at the spinal dorsal horn. A separate pathway involving serotonergic neurons in the RVM (yellow) can also modulate pain in a state-dependent manner. From *Fields (2004)*. Adapted with permission from Springer *Nature Reviews Neuroscience*.

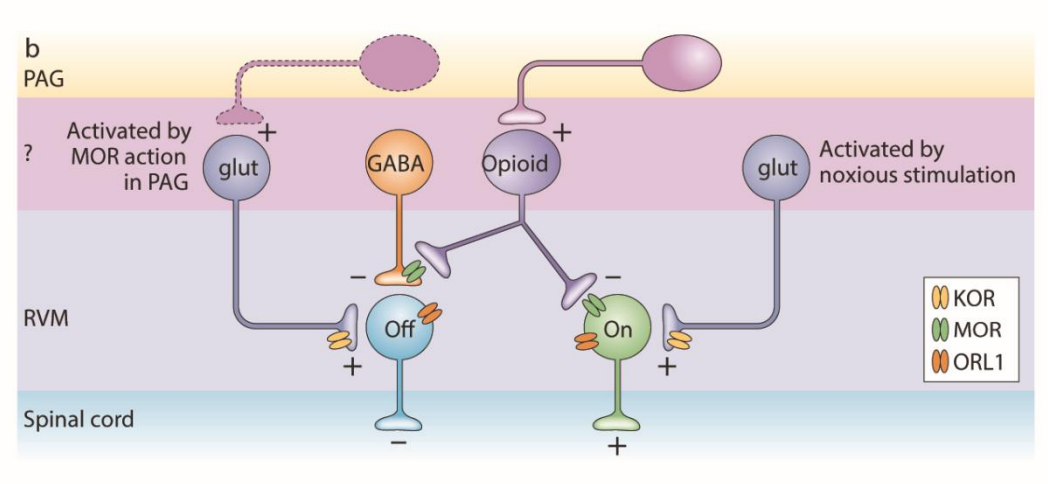

Chapter I - Figure 5. Opioid receptor contribution in the PAG-RVM pathway.

Mu opioid receptors (MOR) are located on γ-aminobutyric acid (GABA) presynaptic terminals at OFF cells and the somadendritic postsynaptic region of ON cells. Both cell classes are excited by glutamatergic terminals (glut) that arise from different input neurons. MOR agonists (e.g. morphine) produce anti-nociceptive effects by inhibiting ON cells and disinhibiting OFF cells. PAG, periaqueductal grey. From *Fields (2004)*. Adapted with permission from Springer *Nature Reviews Neuroscience*.

1.6. Overview of gold standard models to study pain in preclinical research

Different experimental paradigms have been employed to investigate the analgesic effect in animals. However, challenges and limitations in their applications have been observed due to the complexity of the phenomenon of pain (Mogil 2009). Nociceptive pain is assessed by both spontaneous and evoked behaviours. Acute pain (lasting seconds to hours) is more readily measured by spontaneous behaviours (nocifensive actions including licking and flinching), or by injured paw stimulation. Chronic pain (lasting from weeks to months) is instead most easily measured by evoked stimulation (thermal, mechanical, or chemical).

The most used and validated *acute pain* tests include the hot plate (Hunskaar, Berge, and Hole 1986), tail flick, and von Frey (Bennett 2001; Lopez-Canul, Comai, et al. 2015). They are used to measure stimulus-evoked pain in both animals with chronic pain and controls. The hot plate evokes spinally integrated behaviours (Hunskaar, Berge, and Hole 1986; Posa et al. 2015), while the tail-flick withdrawal is both spinally and supraspinally modulated (Bennett 2001). The von Fey test measures the mechano-tactile sensitivity to touch in the hind paw using filaments of increasing thickness (Bennett 2001).

1.6.1. Preclinical model of inflammatory and neuropathic pain

Inflammatory pain: a localized inflammatory reaction is induced in these models in response to a noxious chemical that elicits tissues irritation, as described below.

Formalin injection. The cross-linking agent formalin activates transient receptor potential cation channel A1 (TRPA1) (McNamara et al. 2007). A 2.5% to 5% formalin injection in the hind paw dose-dependently produces lifting, licking, favouring, and flinching/shaking of the injured paw. Two distinct periods of high licking activity have been observed in this short-term inflammatory pain model: the early phase lasting 5-10 min, resulting from direct chemical activation of

nociceptive primary afferents and in which inflammatory processes are not relevant; the late phase lasting from 20 to 30 min after formalin injection which is correlated to an authentic inflammatory response which can therefore be inhibited by anti-inflammatory drugs (Hunskaar and Hole 1987; Lopez-Canul, Comai, et al. 2015; Sufka et al. 1998).

Capsaicin injection. Capsaicin activates transient receptor potential vanilloid 1 (TRPV1) and in a dose-dependent fashion, producing mechanical allodynia, heat hyperalgesia and neurogenic inflammation (Gilchrist, Allard, and Simone 1996; Palazzo et al. 2010).

Carrageenan intraplantar injection. A 1% to 2% carrageenan produces a unilateral inflammation in the injected hind paw that starts a few hours after the administration and lasts for 10 days or more. In this condition, the T-cell mediated immune response is altered, decreasing the latency of the response to a thermal or mechanical stimulus, resulting in hyperalgesia and allodynia conditions (Kirchhoff et al. 1990).

Complete Freund's adjuvant (CFA). CFA is a suspension of heat-killed *Mycobacterium* that generates a unilateral inflammatory condition in the injected hind paw which lasts for days or weeks, producing thermal hyperalgesia and mechanical allodynia. CFA injection produces robust infiltration of immune cells in the tissue which dose-dependently elicits extensive damage to toe and ankle joints, resulting in a pronounced oedema (Stein, Millan, and Herz 1988).

Chronic neuropathic pain is ongoing and can be caused by damage or disease affecting any part of the nervous system which involves the somatosensory system. It can be measured as spontaneous pain (not dependent on peripheral stimuli) or peripherally-evoked pain.

Chronic constriction injury (CCI). This model of peripheral mononeuropathy is associated with behavioural signs of spontaneous pain including excessive licking, limping of the injured side paw, autotomy, and avoidance of placing weight on the ipsilateral paw. Tactile and heat hyperalgesia,

chemical hyper-reactivity, and cold allodynia develop within a week and persist for at least 7 weeks after the surgery (Bennett and Xie 1988; Dowdall, Robinson, and Meert 2005).

L5/L6 spinal nerve ligation (SNL). This model is induced by unilateral ligation of the L5 and L6 branches of the spinal nerves. Stable mechanical allodynia, as assessed by manual von Frey filaments, is observed from week 1 up to week 7 post-surgery (Kim and Chung 1992; Lopez-Canul, Palazzo, et al. 2015).

Spared nerve injury (SNI). In the SNI model of peripheral neuropathy a partial denervation of the sciatic nerve occurs by lesioning the tibial and common peroneal nerve branches, leaving the sural nerve intact. SNI produces a robust, reliable and long-lasting (months) neuropathic pain-like behaviour (mechanical and cold allodynia, and thermal hyperalgesia) as well as the possibility of studying both injured and non-injured neuronal populations in the same spinal ganglion (Decosterd and Woolf 2000; Lopez-Canul, Palazzo, et al. 2015).

Streptozotocin (STZ)-induced diabetes. This model is commonly employed to study mechanisms of painful diabetic neuropathy and to assess potential therapies. A low dose STZ is known to induce experimental diabetes mellitus in rats through a preferential toxicity for pancreatic β cells. Different behaviours reflective of neuropathic pain are exhibited in this animal model, including tactile allodynia and thermal hyperalgesia (Courteix, Eschalier, and Lavarenne 1993).

Oxaliplatin (OXA)-induced neuropathy. Chronic exposure to the anticancer drug oxaliplatin produces acute but reversible neurotoxicity particularly in peripheral sensory nerves in humans. Neuropathy can be induced in animals by multiple doses of oxaliplatin for more than four consecutive weeks (Ghirardi et al. 2005; Ling, Authier, et al. 2007; Mannelli et al. 2012) or with a single injection of oxaliplatin with different doses, inducing varying levels of mechanical and cold allodynia and tactile and thermal hyperalgesia (Ling, Coudoré-Civiale, et al. 2007).

Formalin-induced neuropathy. A subcutaneous injection of formalin (1.25 %) in the dorsal surface of the hind paw of mice produces a significant decrease in both mechanical and thermal thresholds in the injected and contralateral paw that persists for 3 and 7 days, respectively, after formalin administration (Luongo et al. 2013). Similarly, different concentrations of formalin (1-5%) have been shown to induce long-lasting hypersensitivity in rats (Ambriz-Tututi et al. 2011; Fu, Light, and Maixner 2001; Fu et al. 1999). In particular, a single hind-paw injection of 5% formalin induces microglial activation in the spinal cord (Fu et al. 1999), which is responsible for the maintenance of chronic pain (Clark et al. 2007). Moreover, 2% (Braz and Basbaum 2010) and 5% (Tsujino et al. 2000) formalin were also found to enhance the activating transcription factor 3 (ATF3), a marker of nerve injury, in neurons of the dorsal root ganglia and spinal cord. Recently, Salinas-Abarca et al. (2017) observed that 2% and 5%, but not 1%, formalin injections produce long-lasting hypersensitivity with a pharmacological and molecular pattern that resembles neuropathic pain induced by L5/L6 SNL.

1.7. **Melatonin and its receptors in the neurobiology of pain**

At the beginning of the 1970s, some experimental evidence showed that MLT was able to reduce the nociceptive response to noxious stimuli. During the dark phase, when plasma levels of MLT are higher, mice were less susceptible to nociceptive stimuli (Morris and Lutsch 1969; Lutsch and Morris 1971). Ablation of the pineal gland abolished differential nociceptive thresholds dependent on the phase of the day (Lakin et al. 1981). Later studies demonstrated that intraperitoneal (i.p.), intracerebroventricular (i.c.v.) and intravenous (i.v.) injections of exogenous MLT produced dose-dependent antinociception in several supra-spinal (Lakin et al. 1981; Ying and Huang 1990; Xu et al. 1996) and spinal (Yu et al. 2000; Wang et al. 2006; Xu et al. 1996; Naguib et al. 2003) acute pain models. Noseda et al. (2004), reported that intrathecally (i.t.) MLT could depress synaptic potentiation (wind-up) in the spinal cord, likely through hyperpolarization of dorsal horn neurons directly induced by melatonin stimulation, and/or via intracellular interaction with an NMDA receptor-dependent nitric oxide pathway (Laurido et al. 2002).

Of note, the antinociceptive effects of MLT are blocked by the competitive and non-selective MT_1/MT_2 receptor antagonist luzindole (Yu et al. 2000; Wang et al. 2006; Noseda et al. 2004), but also by the opioid receptor antagonist naloxone (Lakin et al. 1981; Yu et al. 2000; Wang et al. 2006), suggesting the involvement of the opioid system in MLT-induced analgesia. In agreement with this hypothesis, Kasap and Can (2016) recently showed that agomelatine, a non-selective MT_1/MT_2 receptor agonist and a serotonin 5-HT_{2C} antagonist, was effective in reducing the response to mechanical, thermal, and chemical nociceptive stimuli. These effects were also prevented by pretreatment with the MOR antagonist naloxonazine, the DOR antagonist naltrindole, and the KOR antagonist nor-binaltorphimine (Kasap and Can 2016). Some other evidence showed that MLT and endogenous opioids modulate one another. MLT induces the

release of beta-endorphine in mouse pituitary cell cultures (Shavali et al. 2005), gamma-endorphine increases the plasmatic level of MLT (Geffard et al. 1981), and morphine induces MLT release from the pineal gland (Esposti et al. 1988). Altogether, this evidence suggests a cross-talk between the melatonergic and opioid systems which can occur at intracellular and/or extracellular levels. Further studies are thus needed to clarify this interaction.

Recently, it has been demonstrated that a single dose of agomelatine dose-dependently reduced mechanical hypersensitivity in STZ and CCI chronic pain models (Chenaf et al. 2016); agomelatine also displayed a marked anti-hypersensitivity effect in the OXA model after daily administration for two weeks. These findings suggest that the anti-hypersensitivity effect of agomelatine involved 5-HT_{2C} and the melatonergic system, since its effects were markedly reduced by the MT_1/MT_2 receptor antagonist, S22153 (Chenaf et al. 2016). They also proposed that the downstream signalling or other indirect mechanisms involving α_2-adrenergic receptors might be involved, given that the effects of agomelatine were inhibited by intrathecal injection of the selective α2- receptor antagonist, idazoxan (Chenaf et al. 2016). Furthermore, another group reported that MLT attenuated repetitive morphine-induced hyperalgesia and tolerance by PKC/NMDA activities in the spinal cord (Song, Wu, and Zuo 2015).

Few studies have indicated the involvement of the GABAergic system in MLT-induced antinociception. Golombek et al. (1991) demonstrated that MLT's antinociceptive effects were blocked by the $GABA_A$ receptor antagonist, flumazenil. Moreover, six day pretreatment with MLT prevented the tolerance to analgesia induced by the KOR agonist U50-488H in mice, and this effect was abolished by flumazenil (Dhanaraj, Nemmani, and Ramarao 2004).

Some other evidence suggests that MLT is also effective in reducing acute and chronic inflammatory pain. MLT reduced paw oedema and inflammatory mediators such as oxyradicals,

nitric oxide (NO) and peroxynitrite in a rat model of acute local inflammation (Costantino et al. 1998). MLT also exerted anti-inflammatory and antinociceptive properties after carrageenan injection, reducing NO and malondialdehyde (Bilici, Akpinar, and Kiziltunc 2002; Hernández-Pacheco et al. 2008), the inducible isoform of NO synthase (Cuzzocrea et al. 1997), and the release of prostaglandins (Cuzzocrea et al. 1999). Furthermore, acute administration of MLT reduced the pathological NO increase in the brain and spinal cord tissues in a postherpetic neuralgic paradigm, probably through the modulation of the L-arginine-NO-cGMP pathway (Deng et al. 2015). The authors also claimed that the analgesic effect of MLT involved both MT_2 and opioid receptors, but further studies are needed to validate this hypothesis.

MLT demonstrated antiallodynic and anti-hyperalgesic effects in the capsaicin-induced secondary allodynia and lipopolysaccharide-induced secondary hyperalgesia models. In the first model, MLT dose-dependently inhibited the nociceptive response (Mantovani et al. 2003) and limited both the intensity and duration of secondary mechanical allodynia (Tu, Sun, and Willis 2004). Of note, naloxone abolished MLT's antinociceptive effect (Mantovani et al. 2003). In the second model, intra-plantar MLT injection reduced hyperalgesia and blocked the inflammatory response (Raghavendra, Agrewala, and Kulkarni 2000). In the formalin test, MLT decreased the licking response particularly in the second phase of the test which involves prostaglandins recruitment (Hernández-Pacheco et al. 2008; Lopez-Canul, Comai, et al. 2015; Ray et al. 2004). Acute administration of MLT decreased the mechanical and thermal hyperalgesia induced by CFA injection in the orofacial pain model, and modified the secretion of specific tissue neuroimmunomodulators associated with pain and inflammation such as the brain-derived neurotrophic factor (BDNF), nerve growth factor (NGF), and interleukin 6 (Scarabelot et al. 2016).

Furthermore, MLT has been shown to reverse hyperalgesia induced by repeated morphine exposure in the neonatal period in the medium- and long-term in rats (Rozisky et al. 2016).

Eventually, several studies reported analgesic effects of MLT in different neuropathic pain models including the CCI nerve injury (Zeng et al. 2008), the SNI (Lopez-Canul, Palazzo, et al. 2015), the partial ligation of the sciatic nerve (Ulugol et al. 2006), L5-L6 ligation (Ambriz-Tututi and Granados-Soto 2007; Lopez-Canul, Palazzo, et al. 2015), and the STZ-induced hyperalgesia and allodynia (Arreola-Espino et al. 2007).

1.7.1. Clinical investigations of analgesic effects of melatonin

A large body of clinical literature has demonstrated the therapeutic efficacy of MLT in functional pain disorders including chronic back pain (Kurganova and Danilov 2016), fibromyalgia (Citera et al. 2000; Hussain et al. 2011; de Zanette et al. 2014), irritable bowel syndrome (IBS) (Song et al. 2005; Lu et al. 2005; Saha et al. 2007; Chojnacki et al. 2013), headaches (Gagnier 2001; Peres et al. 2006; Miano et al. 2008; Bougea et al. 2016), and postoperative pain (Seet et al. 2015; Marseglia et al. 2015).

MLT has been shown to improve the analgesic efficacy in combination with either Artra (a combination of 500 mg of glucosamine hydrochloride and 500 mg of chondroitin sulfate), diclofenac, or Artra plus diclofenac in the treatment of low back pain by reducing pain intensity both at movement and in the resting state (Kurganova and Danilov 2016).

A potential involvement of MLT in the physiopathology of fibromyalgia is debated, since clinical results are not consistent concerning its therapeutic efficacy. While some studies reported no significant differences in serum MLT levels between females affected by fibromyalgia and healthy volunteers (Klerman et al. 2001), Wikner et al. (1998) found lower MLT levels in the serum of women with fibromyalgia during the dark phase. According to an open randomized study, 3 mg

MLT improved sleep quality and decreased the number of painful trigger points during the day in patients affected with fibromyalgia (Citera et al. 2000). The effect of MLT in combination with antidepressants has been investigated in fibromyalgia patients. In a double-blinded placebo-controlled study, Hussain et al. (2011) reported that the combination of 20 mg/day of the selective serotonin reuptake inhibitor (SSRI), fluoxetine, with 3 or 5 mg/day of MLT for 4 weeks decreased anxiety, pain, stiffness, and depressive symptoms compared to fluoxetine or MLT alone. In a second randomized double-dummy controlled study, 63 female patients suffering from fibromyalgia were randomized into three groups, treated with either 10 mg MLT, 25 mg amitriptyline, or a combination of the two (25 mg amitriptyline plus 10 mg MLT) before sleep for 6 weeks. The results indicated that MLT alone or associated with amitriptyline was more effective than amitriptyline alone in improving pain symptoms (de Zanette et al. 2014). Recently, a clinical study showed a reduction of MLT synthesis in female participants with fibromyalgia and a positive correlation between increased 6-sulfatoxymelatonin secretion and fibromyalgia clinical symptoms (Caumo et al. 2019), suggesting a link between disruption in MLT secretion and pain syndrome.

Besides the pineal gland, MLT is synthesized in other peripheral tissues such as the gastro intestinal (GI) tract, in which it exerts both excitatory and inhibitory effects on gut motility (Harlow and Weekley 1986; Bubenik and Dhanvantari 1989). Although the exact mechanism by which MLT regulates GI motility remains unclear, research suggests that it may be related to an interaction between MLT and Ca^{2+}-dependent K^{+}-channels (Storr, Schusdziarra, and Allescher 2000) or to MLT-induced blockade of nicotinic channels (Barajas-López et al. 1996). In randomized double-blind clinical trials, MLT at the dose of 3 mg for two weeks (Song et al. 2005; Lu et al. 2005; Saha et al. 2007) and at the dose of 3 to 5 mg for six months (Chojnacki et al. 2013), significantly decreased abdominal pain and extra bowel symptoms in IBS patients.

The pathophysiological role of MLT in migraine and headache and its potential therapeutic benefits have also been investigated (for a review see: Peres et al. 2006). Some evidence supports the hypothesis that headaches, migraines, and cluster headaches are, at least in part, related to circadian rhythm disorders since MLT administration decreases the frequency and intensity of headache episodes as well as normalizes the circadian rhythms often impaired in these conditions (Peres 2005; Peres et al. 2006; Vogler et al. 2006). The anatomical localization of MLT receptors in the trigeminal ganglion and the trigeminal nucleus of mammals may support this hypothesis (Weaver, Rivkees, and Reppert 1989). While 3 mg (Peres et al. 2004; Miano et al. 2008) and 4 mg (Bougea et al. 2016) MLT administered before bedtime prevented migraines and chronic tension-type headaches, 2 mg MLT (as slow-release formulation) failed to replicate these results (Alstadhaug et al. 2010). In keeping with this, agomelatine showed to decrease the frequency and the duration of migraine attacks (Tabeeva, Sergeev, and Gromova 2011).

MLT's efficacy in the management of post-surgical pain and related anxiety is still debated. In randomized double-blinded studies, MLT was ineffective in the treatment of intraoperative and postoperative pain in laparoscopic cholecystectomy (Andersen et al. 2014) and cataract surgery (Khezri, Oladi, and Atlasbaf 2013), and did not improve postoperative sleep or pain after total knee arthroplasty compared to placebo (Kirksey et al. 2015). Conversely, other studies indicated that preoperative MLT administration (6 mg) decreased anxiety levels before abdominal surgery (Radwan et al. 2010) and cataract surgery (Khezri, Oladi, and Atlasbaf 2013) compared to gabapentin and placebo. Furthermore, MLT significantly reduced both anxiety and pain levels compared to placebo during blood withdrawal in children (Marseglia et al. 2015). Interestingly, in a randomized controlled trial, MLT did not significantly improve pain and anxiety compared to placebo following the extraction of wisdom teeth, but it showed a positive analgesic and anxiolytic

effect in female patients, suggesting a possible sexual dimorphism (Seet et al. 2015). Indeed, Schwertner et al. (2013) reported efficacy for MLT in the treatment of endometriosis-associated chronic pain in a double-blind trial. Stefani et al. (2013) demonstrated that sublingual administration of MLT dose-dependently induces an analgesic effect on the thermal and pressure pain threshold in healthy volunteers. However, in a double-blind, placebo-controlled, three-arm crossover study, 10 or 100 mg i.v. of MLT failed to provide any analgesic, anti-hyperalgesic, or skin-related anti-inflammatory effects compared to placebo (Andersen et al. 2015).

Summarizing, the efficacy of MLT's analgesic effects was tested in different acute and chronic pain conditions using distinct criteria, drug doses, protocols of administration, and in populations differing in sex and age. Albeit the sample size in some of these studies was small (less than 20 individuals per group), MLT was able to improve or relieve pain conditions in most of them. For all of these reasons, large and randomized double-blind studies are warranted to clarify the potential analgesic use of MLT in acute and chronic pain conditions.

1.7.2. Role of the melatonin MT_2 receptor in pain states

A considerable number of studies support the hypothesis that the analgesic effects of MLT are mostly mediated by MT_2 (for a review see: Ambriz-Tututi et al. 2009; Posa et al. 2018). Yu et al. (2000) were the first to suggest that the analgesic properties of MLT were mediated by MT_2 receptors. They found that MLT dose-dependently increased the pain threshold in the hot water tail-flick test, which was reversed by i.c.v. injection of luzindole. However, luzindole is a relatively non-selective MT_1 and MT_2 antagonist, since its affinity for MT_2 compared MT_1 receptors is only 16 to 26-fold greater (Dubocovich et al. 1997).

Further studies using different pain paradigms and full selective MT_2 antagonists such 4P-PDOT and K-185 have clarified the involvement of MT_2 receptors in pain (Ambriz-Tututi and Granados-

Soto 2007; Deng et al. 2015; Huang et al. 2020; Lin et al. 2016; Lopez-Canul, Comai, et al. 2015; Lopez-Canul, Palazzo, et al. 2015; Tu, Sun, and Willis 2004).

In a capsaicin-induced hyperalgesia rat model, 4P-PDOT co-administered with either MLT or the non-selective MT_1/MT_2 agonist 6-chloromelatonin blocked a decrease in tactile allodynia (Tu, Sun, and Willis 2004). 4P-PDOT also prevented MLT's dose-dependent reduction of flinching behaviour induced by the injection of 5% formalin into the hind paw (Yoon et al. 2008).

In 2007, two papers by Granados-Soto's group reported mechanical antiallodynic effects of MLT that were blocked by the selective MT_2 receptors antagonists, 4P-PDOT (Ambriz-Tututi and Granados-Soto 2007)and K-185 (Arreola-Espino et al. 2007). Oral administration of MLT reduced allodynia in a rodent model of neuropathic pain induced by L5-L6 spinal nerve ligation, and this effect was blocked by either i.t. injection or oral administration of 4P-PDOT, the first suggesting a spinal involvement of MT_2 receptors. In addition, the authors showed that the non-selective opioid antagonist naltrexone blocked the antiallodynic effect of MLT, and intriguingly, that the co-administration of sub-effective doses of both 4P-PDOT and naltrexone were also able to reduce MLT-induced spinal antiallodynia (Ambriz-Tututi and Granados-Soto 2007). In neuropathic diabetic rats, pre-treatment with K-185 attenuated the flinching response during phase 1 and 2 of the formalin test and the tactile antiallodynic effect induced by MLT (Arreola-Espino et al. 2007). Moreover, naltrexone and naltrindole, but not 5′-guanidinonaltrindole (a selective KOR antagonist), also blocked MLT antiallodynic effects (Arreola-Espino et al. 2007). These findings support the hypothesis that the antinociceptive effects of MLT are likely mediated by MT_2 and opioid receptor activation, though the neurobiological interaction between MT_2 and opioid receptors has not yet been elucidated. Moreover, it has been shown that MLT administration not only has an analgesic effect, but it also increases the RNA expression of DORs and MT_2 receptors

at the level of the hippocampus, the spinal cord, and the hypothalamus in a model of post-herpetic neuralgia (Deng et al. 2015). These antinociceptive effects were blocked by pretreatment with 4P-PDOT (Deng et al. 2015).

A recent study investigated the contribution of MLT-associated epigenetic modifications in an SNL model in rats (Lin et al. 2016). Together with the induction of tactile allodynia, neuropathy decreased the expression of the phosphatase 2A (PP2Ac) subunit and enhanced histone deacetylase 4 (HDAC4) phosphorylation and its cytoplasmic accumulation, leading to the suppression of *hmgb1* gene transcription, which in turn resulted in a selectively increased expression of high-mobility group protein B1 in the ipsilateral dorsal horn. MLT reversed this process, increasing PP2Ac expression, HDAC4 dephosphorylation and its nuclear accumulation, restoring HDAC4-mediated *hmgb1* suppression, and thus inducing antinociception. Pre-treatment with 4P-PDOT prevented all these behavioural and molecular effects (Lin et al. 2016). MLT treatment prevents the development of neuropathic pain in a lysophosphatidylcholine (LPC)-induced median nerve demyelination neuropathy model via the suppression of glial mitogen-activated protein kinases (MAPKs) activation and the production of pro-inflammatory cytokines. Notably, all these effects were blocked by pre-treatment with 4P-PDOT, but not S26131 (a selective MT_1 antagonist) or prazosin (a selective MT_3 antagonist) (Huang et al. 2020).

With the recent availability of selective MT_2 receptor partial agonists (UCM765 and UCM924) (Rivara et al. 2007), our laboratory has investigated the possible analgesic properties of these novel compounds in paradigms of neuropathic, acute and inflammatory pain (Lopez-Canul, Comai, et al. 2015; Lopez-Canul, Palazzo, et al. 2015). These compounds have an optimal hydrophilic–lipophilic balance (LogP of 2.64) (Ochoa-Sanchez et al. 2011), leading to a high brain penetrance. Our data indicated that acute subcutaneous injections (s.c.) of both UCM765 and UCM924 dose-

dependently increased the temperature of the first hind paw lick in the hot-plate test, and their antinociceptive effects at 20 mg/kg were comparable to that of acetaminophen (M. Lopez-Canul et al., 2015). These two compounds also decreased the total time spent licking the hind paw injected with formalin during both phase 1 and 2 of the formalin test in a dose-dependent manner, and their effect at 20 mg/kg was comparable to that of ketorolac (Lopez-Canul, Comai, et al. 2015). Importantly, the antinociceptive effects of UCM765 and UCM924 in both the hot plate and the formalin test were prevented by pre-treatment with 4P-PDOT (Lopez-Canul, Comai, et al. 2015). We also investigated UCM924 in two neuropathic pain models (the L5-L6 spinal nerve ligation and the spared nerve injury) in rats (Lopez-Canul, Palazzo, et al. 2015). We found that s.c. injection of UCM924 dose-dependently produced a prolonged (7 hours) antiallodynic effect. Moreover, 20 mg/kg UCM924 induced an antiallodynic effect comparable with that of 100 mg/kg gabapentin, but unlike gabapentin, without producing any motor coordination impairment in the rotarod test (Lopez-Canul, Palazzo, et al. 2015). Investigating the possible analgesic mechanism of action of MT_2 partial agonists in the descending antinociceptive pathways, we found that MT_2 receptors were expressed in glutamatergic neurons of the vlPAG (Lopez-Canul, Palazzo, et al. 2015). *In vivo* electrophysiology recordings combined with the tail flick test showed that intra-vlPAG microinjection of UCM924 dose-dependently inhibited the firing activity of pronociceptive ON cells and enhanced the firing rate of antinociceptive OFF cells in the RVM. These electrophysiological effects were blocked by pre-injection of 4P-PDOT into vlPAG (Lopez-Canul, Palazzo, et al. 2015). It is important to note that MOR and DOR are also expressed in the vlPAG and RVM (Le Merrer et al. 2009; Commons, Van Bockstaele, and Pfaff 1999), suggesting a possible interaction between opioid and MT_2 receptors that requires further investigation. Thus, the expression of both receptors in these crucial regions modulating the descending pain

transmission may explain the previous finding demonstrating that the analgesic effects of MLT are blocked by both MT_2 and opioid receptors antagonists (Ambriz-Tututi and Granados-Soto 2007; Arreola-Espino et al. 2007; Lakin et al. 1981; Wang et al. 2006; Yu et al. 2000). Taken together, these preclinical findings demonstrate that MT_2 receptors play an important role in the pathophysiology of pain and confirmed that the analgesic properties of MLT are more likely mediated by MT_2 receptors. No human studies have yet been conducted using selective MT_2 receptor agonists.

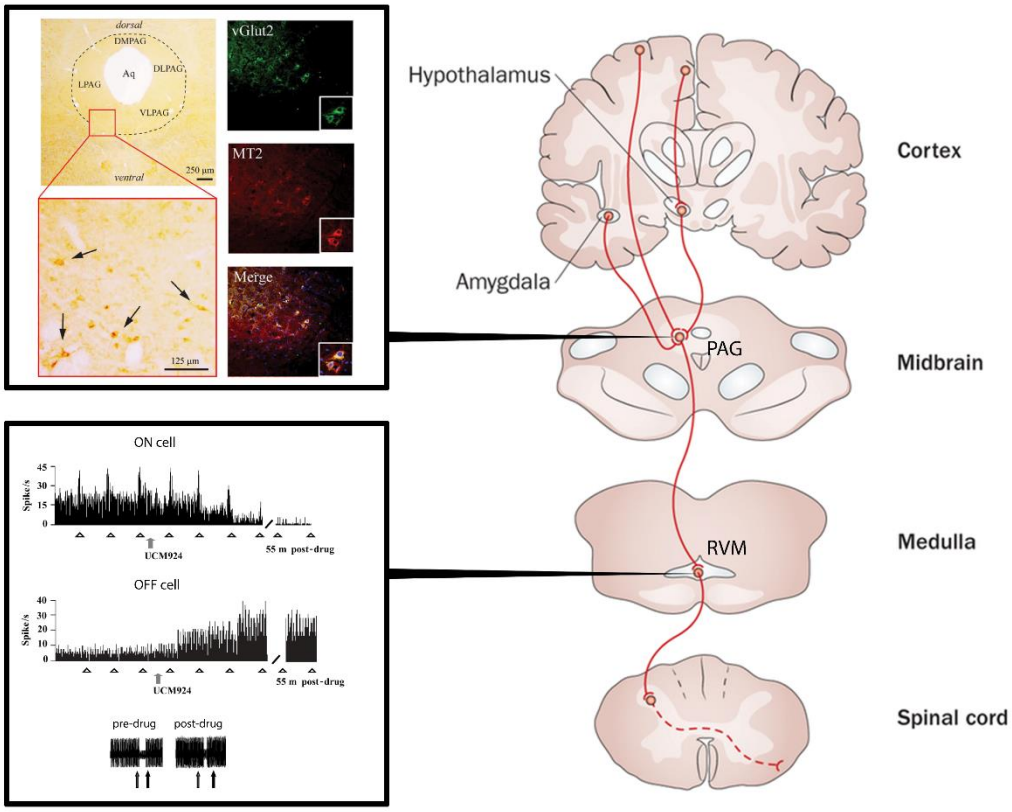

Chapter I - Figure 6. Schematic illustration of the nociceptive descending pathway and the analgesic mechanism resulting from activation of MT_2 receptors.

Top-left box: MT_2 receptors are expressed in glutamatergic neurons of the ventrolateral periaqueductal grey (vlPAG). Bottom-left box: Pharmacological activation of MT_2 receptors by selective partial agonist UCM924 activates OFF cells and inhibits ON cells of the RVM, leading to analgesia. PAG, periaqueductal grey; RVM, rostral ventromedial medulla. From *Posa et al. (2018)*. Adapted with permission.

1.8. Objectives and hypotheses

The overall goal of my thesis is to investigate the role of the MLT receptors in the pain transmission with a particular focus on supra-spinal pathways.

Chapter II constitutes the first manuscript of the dissertation and it explores the distinct role of each melatonin receptor subtype in acute and tonic/inflammatory conditions. A first objective was to determine whether the genetic deletion of the MT_1, MT_2 or both MT_1/MT_2 receptors alters the nociception threshold of WT and mutant mice. Moreover, we aimed to identify if the nociceptive threshold was also modulated across the light/dark cycle in WT and $MT_2^{-/-}$ mice. Additionally, we tested whether the genetic inactivation of MT_2, but not MT_1, receptors prevent the antinociceptive properties of the MT_2 partial agonist, UCM924. Eventually, we tested whether the inactivation of MT_2 receptors modulates the endogenous opioid activity in two brain structures of the descending antinociceptive pathway. Overall, it was hypothesized that the lack of MT_2, but not MT_1, receptors would exhibit a decreased response to thermal and chemical noxious stimuli during the light phase. Furthermore, the genetic inactivation of MT_2 receptors would lead to a positive modulation of the endogenous opioid system in brain areas involved in pain transmission.

The second goal was to investigate the interaction between the MT_2 receptor and the opioid system in chronic neuropathic pain condition, in order to elucidate the role of the opioid receptors in MLT MT_2-induced antiallodynia. The third chapter (second manuscript) of this dissertation will focus on this aspect. Therefore, we assessed whether the blockage or the genetic deletion of MOR or DOR blocks the mechanical antiallodynic effect of the MT_2 partial agonist, UCM924. We also characterized, for the first time, the specific role of MOR and DOR in the PAG in preventing the modulation of ON and OFF cell in the RVM. It was predicted that MOR blockage would abolish two effects of UCM924, antiallodynia and ON-OFF cell modulation. Moreover, we tested whether MT_2 receptor blockage would abolish the effects of MOR. Therefore, we evaluated the

development of tolerance to the antiallodynic effects induced either by UCM924 and morphine and the eventual cross-tolerance between these two agonists. Also, we determined the expression of MT_2 receptors in excitatory and inhibitory neurons of the PAG and RVM and their possible co-localization with MOR in the PAG. These experiments allowed the up-stream determination of MT_2 receptors compared to MORs in the PAG-RVM descending pathway. Finally, we aimed to rule out the reward properties of UCM924 and compared them to those induced by morphine.

Given the capability of MLT to induce endogenous opioid release in *in vitro* pinealocyte culture (Shavali et al. 2005), in the chapter III, we sought to measure the effect of UCM924 treatment in the mRNA expression of the endogenous opioid enkephalin (*Penk*) in the PAG and RVM of neuropathic mice. In Annex to chapter III, for the first time, we studied the modulatory effects of acute administration of UCM924 on dopaminergic neuronal firing and burst activity in the VTA.

Chapter II

Running Head: MT_1 and MT_2 receptors in pain

Nociceptive responses in MT_2 receptor knockout mice compared to MT_1 and double MT_1/MT_2 receptor knockout mice

Luca Posa[1,2*], Martha Lopez-Canul[1*], Laura Rullo[3], Danilo De Gregorio[1], Sergio Dominguez-Lopez[1#], Matthew Kaba Aboud[1], Francesca Felicia Caputi[3], Sanzio Candeletti[3], Patrizia Romualdi[3], Gabriella Gobbi[1,2]

Journal of Pineal Research. 2020; 69(3):e12671. doi: 10.1111/jpi.12671

[1] Neurobiological Psychiatry Unit, Department of Psychiatry, McGill University Health Center, McGill University, Montreal, QC, Canada.

[2] Alan Edwards Centre for Research on Pain, McGill University, Montreal, QC, Canada.

[3] Department of Pharmacy and Biotechnology, Alma Mater Studiorum-University of Bologna, Bologna, Italy.

[*]These authors contributed equally to this work.

Correspondence to be directed to:
Gabriella Gobbi, MD, PhD
Neurobiological Psychiatry Unit
Dept. of Psychiatry
McGill University
1033 Pine Avenue West
Montreal, Q.C. Canada H3A 1A1
Email: gabriella.gobbi@mcgill.ca
Phone: 514-398-1290
Fax: 514-398-4866

Abstract: 181 words
Introduction: 261 words
Material&Methods: 851
Results: 983
Discussion: 1288 words
Figures: 5
Number of references: 7

2.1 Abstract

Melatonin, a neurohormone that binds to two G-protein coupled receptors MT_1 and MT_2, is involved in pain regulation, but the distinct role of each receptor has yet to be defined. We characterized the nociceptive responses of mice with genetic inactivation of MT_1 ($MT_1^{-/-}$), or MT_2 ($MT_2^{-/-}$), or both MT_1/MT_2 ($MT_1^{-/-}$/$MT_2^{-/-}$) receptors in the hot plate test (HPT), and the formalin test (FT). In HPT and FT, $MT_1^{-/-}$ display no differences compared to their wildtype littermates (CTL), whereas both $MT_2^{-/-}$ and $MT_1^{-/-}$/$MT_2^{-/-}$ mice showed a reduced thermal sensitivity as well as a decreased tonic nocifensive behavior during phase 2 of the FT in the light phase. The MT_2 partial agonist UCM924 induced an antinociceptive effect in $MT_1^{-/-}$ but not in $MT_2^{-/-}$ and $MT_1^{-/-}$ /$MT_2^{-/-}$ mice. Also, the competitive opioid antagonist naloxone had no effects in CTL, whereas it induced a decrease of nociceptive thresholds in $MT_2^{-/-}$ mice. Our results show that the genetic inactivation of MT_2, but not MT_1 receptors, produces a distinct effect on nociceptive threshold, suggesting that the MT_2 melatonin receptor subtype is selectively involved in the regulation of pain responses.

Keywords

Pain, melatonin, MT_1 receptor, MT_2 receptor, knockout mice

2.2 Introduction

Melatonin (MLT) is a neurohormone synthesized by the pineal gland during the dark period of the circadian light/dark cycle. It acts mostly through two G protein-coupled receptors, MT_1 and MT_2, showing a high affinity for both receptors (Ki ≈ 0.1 nM). MLT plays a role at both central and peripheral levels, affecting circadian rhythms, sleep[3], mood[4-6], cardiovascular and immune systems[7,8], and pain sensation[9]. Several animal studies have suggested that MLT may have analgesic properties[10]. In patients, MLT alleviates pain conditions including migraine[11,12], fibromyalgia[13-15], and irritable bowel syndrome[16-18]. Despite this evidence, it is still unknown how the two primary receptors of MLT regulate this analgesic effect.

Recent studies suggested an antinociceptive role of MT_2 receptors in response to acute/inflammatory[19,20] and chronic pain conditions[21-24] since the analgesic properties of MLT were blocked by the MT_2 selective antagonist 4P-PDOT[19,21,23-26]. These results were corroborated by the observation that the MT_2 selective partial agonists N-2-[(3-meth-oxyphenyl)phenylamino]ethylacetamide (UCM765)[27] and its analogue N-2-[(3-bromophenyl)-(4-fluorophenyl)amino]ethylacetamide (UCM924)[27] produce analgesia in acute and tonic/inflammatory pain models[19], as well as in chronic neuropathic pain conditions, through the modulation of the brainstem descending antinociceptive pathways[21].

However, MLT's analgesic mechanism of action also involved the activation of $GABA_A$[28,29], dopamine D_2[29], 5-HT_{2A} [29], alpha$_2$-adrenoceptors[28,29], and opioid[9,22,26] receptors. Here, we examined the response to the thermal and chemical nocifensive stimuli in wild type (CTL), and in three different mutant mice $MT_1^{-/-}$, $MT_2^{-/-}$ and $MT_1^{-/-}/MT_2^{-/-}$, attempting to better understand the role of each MLT receptor subtype in the regulation of nociception. In addition, we investigated the possible involvement of the endogenous opioid system in $MT_2^{-/-}$ mice nociceptive responses.

2.3 Materials and methods

Experimental procedures were approved by the Animal Care Committee of McGill University, QC, Canada (protocol#7181) and were conducted following the Canadian Council guidelines on Animal Care as well as the Ethical Guidelines for Investigation of Experimental Pain in Conscious Animals of the International Association for the Study of Pain.

Animals

Adult male mice (PND 60-120, 25-32 g) with C3H/HeN genetic background and with a functional mutation for MT_1 receptors ($MT_1^{-/-}$), or MT_2 receptors ($MT_2^{-/-}$), or both MT_1 and MT_2 receptors ($MT_1^{-/-}$/ $MT_2^{-/-}$) and their wild-type littermates (CTL) were used in our study. Mutant mice were generated as previously described[30,31]. The colonies were initially kindly provided by Dr. Weaver (Univ. of Massachusetts, USA) and latter a novel colony was purchased from Jackson Laboratory (Bar Harbor, Maine, US; stock #010488) generated through cryo-recovery of embryos containing the *Mtnr1b*^{tm1Drw} mutations (donating investigator Dr. Weaver). Upon arrival, mice were fully backcrossed onto the C3H/HeN background (Charles River, QC, Canada) in order to generate dominant ($MT_2^{+/+}$) and recessive ($MT_2^{-/-}$) homozygotes mice. Experiments were conducted using $MT_2^{-/-}$ mice and their wild type littermate (CLT) at the 3-4 generation. Animals were housed in groups of 2-5 per cage, in temperature (21±2°C) and humidity (~55%) controlled rooms, and a 12 h light/dark cycle (light on: 7:00; light off: 19:00) with free access to food and water. Experiments were conducted during the light phase between 12:00h and 17:00h (light phase) or 0:00h and 5:00h (dark phase). All experiments were conducted by experimenters who were blind to drug treatments and genotypes.

Hot plate test

The HPT was performed using an electronically controlled hot-plate (Ugo Basile, Italy)[32]. The initial temperature was set at 37 °C with a near linear increase in temperature of 3 °C per min. The temperature causing a fast-hind paw lick was recorded as the nociceptive endpoint. Typically, animals had their first hind paw lick occurring at a temperature lower than 52°C; this temperature was then set as the experiment endpoint[32]. After each session, the plate was cleaned with a wet cloth, and a fan was then used to cool the plate rapidly. No habituation to the test apparatus was done in order to avoid any learning effects[33,34].

Formalin test

The FT was conducted as previously described[35]. Mice were placed in the experimental chamber 30 min before the experiment for habituation. Then, animals were gently restrained while the dorsum of the hind paw was subcutaneously injected with 50 μl of 1% formalin with a 30-G needle. Mice were immediately returned to the experimental chambers and nociceptive behaviour was observed for 60 min. Mirrors were placed behind the chamber to enable unhindered observation. Nociceptive behaviour was quantified as the cumulative time the animal spent licking, flinching, or shaking the injected hind paw[36]. As previously reported[35,36], formalin-induced licking behaviour was biphasic: the initial acute phase (0–10 min) was followed by a relatively short quiescent period, which was then followed by a prolonged tonic response (15–60 min).

Gene expression

Total RNA was extracted as previously described[37]. Briefly, periaqueductal gray (PAG; −3.6 to −4.9 mm from Bregma) and rostral ventromedial medulla (RVM; −5.8 to −6.0 mm from Bregma)

were punched from freshly dissected brain slices according to Paxinos mouse atlas[38], immediately frozen on dry ice and stored at −80 °C. RNA integrity was checked by 1% agarose gel electrophoresis, and the concentrations were measured by using the Nanodrop 1000 system spectrophotometer (Thermo Fisher Scientific). RNA samples with OD260/OD280 ratio > 1.8 and < 2.0 were subsequently subjected to DNAse treatment and reverse transcribed with the GeneAmp RNA PCR kit (Life Technologies). The relative abundance of each mRNA of interest was assessed by real-time qRT-PCR using the Syber Green gene expression Master Mix (Life Technologies) in a Step One Real-Time PCR System (Life Technologies). All data were normalized to glyceraldehyde-3-phosphate dehydrogenase (GAPDH) as the endogenous reference gene. Relative expression of different gene transcripts was calculated by the Delta-Delta Ct (DDCt) method and converted to relative expression ratio (2^{-DDCt}) for statistical analysis[39]. The following primers were used (5'–3'): *Gapdh* forward TGCGACTTCAACAGCAACTC and reverse CTTGCTCAGTGTCCTTGCTG; *Penk* forward TTCAGCAGATCGGAGGAGTTG and reverse GAAGCGAACGGAGGAGAGAT. Results are presented as fold changes in mRNA levels.

Drugs

N-2-[(3-bromophenyl)-(4-fluorophenyl)amino]ethylacetamide (UCM924; MT_1 receptor: pKi= 6.76; MT_2 receptor: pKi= 9.27; 20 mg/kg)[19,27] , and naloxone (2 mg/kg) (Sigma-Aldrich, Oakville, ON, Canada) were all dissolved in a vehicle (veh) composed of 70% dimethylsulfoxide (MP Biochemicals, Solon, OH, USA) and 30% saline. The dose of UCM924 was chosen according to our recent study[19]. Drugs were injected subcutaneously (s.c.-in 0.2 ml volume) 30 min before behavioural tests.

Statistical analyses

Statistical analysis was carried out using GraphPad Prism (version 8.0.1; Inc., San Diego, CA). Data were expressed as mean ± S.E.M. After testing for assumptions of normality distribution and homogeneity of variance, one-way ANOVA was used to compare the nociceptive threshold of the 4 genotypes. Student's t-test was used to analyze the UCM924 analgesic effect and to compare the relative *Penk* gene expression. To compare the effect of naloxone two-way ANOVA was used. When appropriate, the Tukey test for *post-hoc* comparison was performed. Statistical values reaching $P<0.05$ were considered significant.

2.4 Results

Inactivation of MT_2 receptor decreases acute thermal nociception in the HPT

We first determined whether the $MT_1^{-/-}$, $MT_2^{-/-}$ and $MT_1^{-/-}/MT_2^{-/-}$ mice had different baseline responses in the HPT. One-way ANOVA of the temperature inducing the first hind paw lick indicated a significant effect of genotype ($F_{3,113}=10.89$, $P<0.001$) (Fig. 1A). $MT_2^{-/-}$ and $MT_1^{-/-}/MT_2^{-/-}$ mice showed an increased threshold temperature compared to CLT ($P<0.001$ and $P=0.0035$, respectively). The threshold temperature was also higher in $MT_2^{-/-}$ compared to $MT_1^{-/-}$ mice ($P=0.0012$). $MT_1^{-/-}$ mice did not display any significant difference in the threshold temperature compared to CTL mice ($P=0.4707$).

Inactivation of MT_2 receptor decreases tonic nociception in the FT

The time course of the nociceptive response of the four genotypes to formalin injection is reported in Figure 1B. The area under the curve (AUC), quantified from the two distinct phases of the FT (Phase 1 and Phase 2), were analyzed separately. In the Phase 1 (corresponding to 0–10 min, also called *nociceptive phase*), no differences were observed in the AUC responses of the four

genotypes ($F_{3, 32}$=0.085, P=0.967) (Fig. 1C). Differently, in the AUC of the Phase 2 (corresponding to the 15–60 min, also called *tonic phase*) we observed a significant effect of the genotype ($F_{3,36}$=15.94, P<0.001) (Fig. 1D). While $MT_1^{-/-}$ mice did not display any significant difference in the total time spent licking the hind paw compared to CTL (P=0.935), both $MT_2^{-/-}$ and $MT_1^{-/-}/MT_2^{-/-}$ mice showed a decrease in the total time spent in licking behaviour in comparison with CTL and $MT_1^{-/-}$ (P<0.001 for both genotypes) animals.

$MT_2^{-/-}$ mice nociceptive response across the light/dark cycle

Several studies reported that pain sensitivity varies during the light/dark cycle following the circadian rhythm of melatonin[9,28,40]. We thus performed the experiments during the light/inactive and dark/active phase. In the HPT, the pain sensitivity (express as AUC) was significantly different during the dark/active phase (genotype: $F_{1,39}$ = 13.44, P=0.0007; phase: $F_{1,39}$ = 4.897, P=0.0328; interaction: $F_{1,39}$ = 4.897, P=0.0328). At night, the pain threshold was increased compared to the light phase in CTL (P=0.0008), but not in $MT_2^{-/-}$ mice (P= 0.7448) (Fig.2A). In phase 1 of the FT, the two-way ANOVA showed a main effect of the circadian phase (P=0.0077). Moreover, Student's t-test confirmed a decrease of the nociceptive behaviour only in CTL mice (t_{16}=3.757, P= 0.0017), suggesting that the light/dark pattern for this behavioural response was lost in their $MT_2^{-/-}$ littermates (Fig. 2B-C).

During phase 2 of the FT the $MT_2^{-/-}$ mice displayed a significant increase of the AUC during the night compared to the light phase (genotype: $F_{1,31}$ = 11.71, P=0.0018; interaction genotype x phase: $F_{1,31}$=17.36, P=0.0002), confirmed by post-hoc comparation (P <0.001) (Fig. 2B and D).

Deletion of MT2 receptors prevents the antinociceptive properties of the MT2 partial agonist UCM924

Hot Plate test

Next, to confirm that the MT_2 receptor modulates nociceptive responses, we administered the MT_2 selective partial agonist UCM924 (20 mg/kg, s.c.) 30 minutes, 1 hour and 4 hours before the HPT (Figure 3A-D). Since we observed a different baseline in the hot plate test, each genotype group was analyzed separately.

As we previously reported[19], treatment with UCM924 produced an analgesic effect in CTL animals ($F_{1,57}$= 35.43, P<0.001; Fig. 3A), as well as in $MT_1^{-/-}$ mice ($F_{1,41}$=32.66, P<0.001) (Fig.3B). UCM924 treatment had no effect in $MT_2^{-/-}$ and $MT_1^{-/-}/MT_2^{-/-}$ mice (P=0.643 and P=0.814, respectively) (Fig 3C-D). Notably, we did not observe differences in the nociceptive responses to vehicle administration in any genotypes across time (see Fig.2).

Formalin test

We also tested whether the effects of UCM924 administration in the formalin test are modified by the genetic availability of MT_2 receptors (Fig.4A-D-G-J). We administered UCM924 (20 mg/kg, s.c.) 30 minutes before injecting formalin in the hind paw of the mice. UCM924 decreased the AUC responses of phase 1 (t_{19}=3.622, P=0.0018, Fig.4B) and phase 2 (t_{19}=6.55, P<0.0001, Fig. 4C) in CTL and in $MT_1^{-/-}$ mice (phase 1: t_{13}=2.40, P=0.0323; phase 2: t_{12}=4.225, P=0.0012, Fig. 4E-F), but not in $MT_2^{-/-}$ (phase 1: t_{17}=0.265, P=0.794; phase 2: t_{16}=0.959, P=0.351, Fig. 4H-I) and $MT_1^{-/-}/MT_2^{-/-}$ mice (phase 1: t_{17}=0.435, P=0.671; phase 2: t_{14}=0.796, P= 0.796, Fig. 4K-L).

MT_2 inactivation increases endogenous opioid tonic activity

Based on the data shown above, we hypothesized that the decreased response to nociceptive stimuli in the mice lacking the MT_2 receptor could be related to hyper-activation of the opioid system. Thus, we hypothesized that naloxone would increase the nociceptive response in $MT_2^{-/-}$ mice by suppressing tonic opioid activation. In the HPT, while no change was observed in the threshold temperature in CTL after the injection of 2 mg/kg of naloxone, in $MT_2^{-/-}$ mice, naloxone treatment decreases the temperature of the first hind paw lick (treatment: $F_{1,42}$=36.07, P<0.001; interaction treatment x genotype: $F_{1,42}$=14.13, P<0.001). However, naloxone was able to decrease the nociceptive thermal threshold in $MT_2^{-/-}$ (P<0.001), but not in CTL mice (Fig. 5A).

In the FT naloxone treatment uncovered similar results, and the experiment time course is shown in Figure 5B. No differences were found in phase 1 due to genotype or treatment (Fig 5C). On the contrary, in phase 2, the overall time spent licking the formalin-injected hind paw was increased in $MT_2^{-/-}$ mice treated with naloxone compared to veh. However, naloxone treatment did not modify licking behavior in CTL mice (genotype: $F_{1,32}$ = 48.75, P<0.001; treatment: $F_{1,32}$ = 18.86, P<0.001; interaction: $F_{1,32}$= 13.87, P<0.001). *Post hoc* comparisons confirmed that naloxone increased the total AUC in $MT_2^{-/-}$ (P<0.001) (Fig. 5D).

Based on these findings, we then hypothesized that $MT_2^{-/-}$ mice have an increased opioid tone. We thus investigated the relative gene expression of the endogenous opioid enkephalin (*Penk*) in periaqueductal grey (PAG) and rostral ventromedial medulla (RVM), two crucial regions of the descending antinociceptive pathway. A significant increase of the *Penk* mRNA levels was found in the RVM (t_8=2.586, P=0.0323) of $MT_2^{-/-}$ mice compared to CTL but not in PAG (t_8=0.9411, P=0.374), as shown in Figure 5E-F.

2.5 Discussion

Here we reported for the first time the nociceptive behavioral response of mice lacking MLT MT_1, MT_2 and both MT_1/MT_2 receptors, using two well established paradigms of acute (HPT) and tonic (FT) pain. Our data show that $MT_2^{-/-}$ and $MT_1^{-/-}$/$MT_2^{-/-}$, but not $MT_1^{-/-}$, mice exhibited an increased thermal threshold in the HPT and a decrease in the nociceptive overall time in the tonic phase of the FT, thus suggesting that the MT_2 receptor plays a significant role in pain modulation, especially during the light/inactive phase. Moreover, this increased pain threshold in $MT_2^{-/-}$ mice was reversed after treatment with a low dose (2 mg/kg) of the non-selective opioid antagonist naloxone. A considerable number of studies have characterized the antinociceptive properties of exogenous and endogenous MLT in several spinal[26,41,42] and supra-spinal[9,28,40,41] acute pain models. Previous studies from our laboratory have investigated the pharmacological effects of melatonin MT_2 ligands in pain conditions[19,21]. We found that the selective MT_2 partial agonists UCM765 and UCM924 produce a dose-dependent anti-nociceptive effect in both behavioural paradigms described above. Importantly, these effects were completely blocked by the selective MLT MT_2 receptor antagonist 4P-PDOT, suggesting a modulatory role of MT_2 receptors in acute and chronic pain. MT_2 receptors are expressed in the periaqueductal grey (PAG)[21,43], an area of the brainstem descending antinociceptive pathways. Intra-PAG injection of MT_2 partial agonists, as well as MLT, silences the pronociceptive ON neurons and activates the anti-nociceptive OFF neurons of the rostroventral medulla (RVM)[21], similarly to other classes of analgesic drugs[44-46]. The HPT measures the integrated response to an acute nociceptive stimulus where the scored behavioral responses are supraspinally organized[20]. In keeping with a previous study about MLT and MT_2 partial agonists analgesic properties[19], here we confirmed that MT_2 partial agonists decrease the central thermal sensitivity. Furthermore, we found that the genetic inactivation of the MT_2 receptor leads to an increased thermal threshold. One may ask why the MT_2 inactivation produces the same

effects as pharmacological doses of a non-selective (MLT) or selective MT_2 partial agonists. It cannot be ruled out that the $MT_2^{-/-}$ mice have a neurodevelopmental adaptive response to pain, as confirmed by the elevated opioid tonic activation, observed here with the naloxone challenge and with the increase of the enkephalin precursor *Penk* mRNA (see below).

The injection of formalin in the paw causes an immediate and intense increase in the spontaneous activity of C afferent fibers (phase 1, 0-10 min) and evokes a distinct quantifiable pain behavior [35,36,47,48]. On the other hand, the 2nd late phase (15-60 min) of the FT describes a tonic response that combines an increased excitability (wind up) of neurons in the dorsal horns of the spinal cord (sensitization)[49-51] and an inflammatory reaction (prostaglandin synthesis) in the peripheral tissue[35,36,48].

The FT in transgenic mice shows that the role of the MT_2 receptor might be less relevant in phase 1, since no differences were found in this phase among the four genotypes. However, the selective MT_2 partial agonist UCM924 (20 mg/kg) decreased the licking behavior in the early phase of the FT, confirming our previous results[13] about the antinociceptive effect of the MT_2 agonists.

In phase 2 only $MT_2^{-/-}$ and $MT_1^{-/-}/MT_2^{-/-}$ mice showed a decreased pain sensitivity. It is known that the tonic noxious stimulation is produced by an increase in the excitability of spinal cord neurons (wind up)[50]. Like the HPT, the opioid tonic activation in the RVM of $MT_2^{-/-}$ mice might explain this phenotype. In fact, the spinal cord receives afferents from the RVM[52] and the overexpression of the enkephalin precursor *Penk* mRNA may reduce the sensitivity to pain in the late phase of the FT. Nevertheless, the anti-inflammatory role of MLT may play a role in this phase[53]. MLT reduces edema and inflammatory mediator levels, such as peroxynitrite[54], the inducible isoform of NO synthase[55,56], and the release of prostaglandins[56], likely through the activation of NO-cGMP-protein kinase G–K^+ channels pathway[57]. UCM924 (20 mg/kg) decreased licking behavior in CTL

and $MT_1^{-/-}$ mice in the late phase of the FT. Again, this confirms our previous results in rats [13], and the anti-inflammatory properties may also contribute to the analgesia produced by MT_2 agonists in the phase 2 of the FT.

A reduced response to the noxious stimulus was detected during the night in CTL mice in HPT and the early phase of FT; this light/dark pattern was absent in $MT_2^{-/-}$ mice. These results are in agreement with previous studies[9,28,40], reporting that wild type mice exhibited an increased pain threshold in the HPT during the night, when the endogenous MLT level are higher (0-2)[45].

Still, during the second phase of the FT, $MT_2^{-/-}$ mice displayed a reduced nociceptive response compared to CTL during the light/inactive, but a normalization of this response occurred during the dark phase.

In agreement with previous literature[58-60], our data show that in CTL animals, a low dose of naloxone alone did not modify the pain threshold either in the HP or the FT. However, naloxone can block the analgesic effect of morphine in the HPT and in phase 1 and 2 of the FT[48,60], confirming its competitive and selective antagonism properties. In $MT_2^{-/-}$ mice, naloxone decreased the pain sensitivity in HPT and phase 2 of FT, suggesting that the lack of MT_2 receptors induces a tonic activation of the opioidergic system in the CNS which is blocked by naloxone injection. We hypothesized that this opioid tonic activation could be linked to an overexpression of endogenous opioid ligands in some brain areas involved in the modulation of pain[44,61]. Recently, Minett and colleagues[62] demonstrated that mice lacking sodium channel Nav1.7 displayed a congenital insensitivity to pain and upregulation of *Penk* mRNA in sensory neurons, which were reversed by naloxone. Indeed, we confirmed that the enkephalin precursor *Penk* mRNA is upregulated in RVM, a key structure of the brainstem antinociceptive pathway. These findings support the hypothesis that the genetic deletion of MT_2 receptors (a target for antinociception), but

not MT_1, may be counterbalanced by an increased opioidergic tonic activity due to an overexpression of the endogenous opioid enkephalin in RVM.

A few studies have suggested the involvement of the opioid system in MLT-induced analgesia[9,10,22,24,28,63,64]. In particular, the mu and delta opioid receptors (MOR and DOR respectively) are highly expressed in the RVM[61,65], and the activation of these receptors modulates ON and OFF cells of the RVM [45,66,67], similarly to MLT and the UCM924. Interestingly, Takada and colleagues[68] demonstrated that the expression of MOR mRNA follows a circadian pattern, where MOR is more expressed during the late light phase (14-20) and less during the dark phase (2-8). Thus, the increased sensitivity during the night in $MT_2^{-/-}$ mice might be related to the scarce availability of MOR in these areas of the descending antinociceptive pathway.

Our study affirms the distinct and unique function of each MLT receptor, as previously demonstrated in sleep[69,70], circadian rhythms[71], anxiety[5,72], depression[4], and vascular activity[73,74]. These findings corroborate the hypothesis that the MT_2 receptor, but not MT_1, plays a specific role in nociception, thus representing a potential target for therapeutics to treat pain conditions, particularly during the inactive phase (day), when MT_2 receptors are more abundant in the brain[75]. Altogether, our data indicate that the lack of functional MT_2 receptors leads to decreased pain sensitivity in an acute (HPT) and a tonic (FT) model of pain during the light phase, which was reversed by a low dose of competitive opioid antagonist naloxone. We proposed that in the $MT_2^{-/-}$ conventional knockout mice, the lack of the MT_2 endogenous tone might activate neuronal compensatory mechanism through an increased *Penk* mRNA levels in RVM, leading to an upregulation of endogenous opioid enkephalin at the central level. Future research into the potentially regulatory and interactive mechanism between MT_2 receptors and opioid transmission in nociception is warranted.

Acknowledgements

This study was supported by grants from CIHR, MEIE, CQDM and Brain Canada (to GG) and from RFO (to PR/SC) University of Bologna. LP received a fellowship from the Alan Edward Pain Centre, FRQS and POND; MLC from CONACYT and PBEEE; SDL from CONACYT, and DDG from FRQS and CIHR. Authors thank Mr Robin Lorne Dick for proofreading the manuscript.

Author contribution

LP, ML-C, SD-L and LR performed experiments. MKA assisted the experiments. ML-C and SD-L analyzed preliminary data. LP, LR, and FFC analyzed data. LP, ML-C, SD-L, DDG, FFC, SC and PR contributed to experimental design and revised the manuscript. LP wrote the manuscript. GG conceived, supervised the study and wrote the manuscript.

2.6 References

1. Cajochen C, Kräuchi K, Wirz-Justice A. Role of melatonin in the regulation of human circadian rhythms and sleep. *Journal of neuroendocrinology.* 2003;15(4):432-437.
2. Dubocovich ML. Melatonin receptors: role on sleep and circadian rhythm regulation. *Sleep medicine.* 2007;8:34-42.
3. Mauriz JL, Collado PS, Veneroso C, Reiter RJ, González-Gallego J. A review of the molecular aspects of melatonin's anti-inflammatory actions: recent insights and new perspectives. *Journal of pineal research.* 2013;54(1):1-14.
4. Comai S, Ochoa-Sanchez R, Dominguez-Lopez S, Bambico FR, Gobbi G. Melancholic-like behaviors and circadian neurobiological abnormalities in melatonin MT1 receptor knockout mice. *International Journal of Neuropsychopharmacology.* 2015;18(3).
5. Comai S, De Gregorio D, Posa L, Ochoa-Sanchez R, Bedini A, Gobbi G. Dysfunction of serotonergic activity and emotional responses across the light-dark cycle in mice lacking MT2 receptors. *Journal of Pineal Research.* 2020.
6. Comai S, Gobbi G. Unveiling the role of melatonin MT2 receptors in sleep, anxiety and other neuropsychiatric diseases: a novel target in psychopharmacology. *Journal of psychiatry & neuroscience: JPN.* 2014;39(1):6.
7. Tengattini S, Reiter RJ, Tan DX, Terron MP, Rodella LF, Rezzani R. Cardiovascular diseases: protective effects of melatonin. *Journal of pineal research.* 2008;44(1):16-25.
8. Carrillo-Vico A, Lardone PJ, Álvarez-Sánchez N, Rodríguez-Rodríguez A, Guerrero JM. Melatonin: buffering the immune system. *International journal of molecular sciences.* 2013;14(4):8638-8683.
9. Lakin M, Miller C, Stott M, Winters W. Involvement of the pineal gland and melatonin in murine analgesia. *Life Sci.* 1981;29(24):2543-2551.
10. Posa L, De Gregorio D, Gobbi G, Comai S. Targeting melatonin MT2 receptors: A novel pharmacological avenue for inflammatory and neuropathic pain. *Current medicinal chemistry.* 2018;25(32):3866-3882.
11. Peres MFP, Zukerman E, da Cunha Tanuri F, Moreira FR, Cipolla-Neto J. Melatonin, 3 mg, is effective for migraine prevention. *Neurology.* 2004;63(4):757.
12. Miano S, Parisi P, Pelliccia A, Luchetti A, Paolino MC, Villa MP. Melatonin to prevent migraine or tension-type headache in children. *Neurological sciences.* 2008;29(4):285-287.
13. Citera G, Arias M, Maldonado-Cocco J, et al. The effect of melatonin in patients with fibromyalgia: a pilot study. *Clinical rheumatology.* 2000;19(1):9-13.
14. Hussain SAR, Al-Khalifa II, Jasim NA, Gorial FI. Adjuvant use of melatonin for treatment of fibromyalgia. *Journal of pineal research.* 2011;50(3):267-271.
15. de Zanette SA, Vercelino R, Laste G, et al. Melatonin analgesia is associated with improvement of the descending endogenous pain-modulating system in fibromyalgia: a phase II, randomized, double-dummy, controlled trial. *BMC Pharmacology and Toxicology.* 2014;15(1):1.
16. Song GH, Leng PH, Gwee KA, Moochhala SM, Ho KY. Melatonin improves abdominal pain in irritable bowel syndrome patients who have sleep disturbances: a randomised, double blind, placebo controlled study. *Gut.* 2005;54(10):1402-1407.
17. Lu W, Gwee K, Moochhalla S, Ho K. Melatonin improves bowel symptoms in female patients with irritable bowel syndrome: a double-blind placebo-controlled study. *Alimentary pharmacology & therapeutics.* 2005;22(10):927-934.

18. Saha L, Malhotra S, Rana S, Bhasin D, Pandhi P. A preliminary study of melatonin in irritable bowel syndrome. *Journal of clinical gastroenterology.* 2007;41(1):29-32.
19. Lopez-Canul M, Comai S, Domínguez-López S, Granados-Soto V, Gobbi G. Antinociceptive properties of selective MT2 melatonin receptor partial agonists. *European journal of pharmacology.* 2015;764:424-432.
20. Yoon MH, Park HC, Kim WM, Lee HG, Kim YO, Huang LJ. Evaluation for the interaction between intrathecal melatonin and clonidine or neostigmine on formalin-induced nociception. *Life sciences.* 2008;83(25):845-850.
21. Lopez-Canul M, Palazzo E, Dominguez-Lopez S, et al. Selective melatonin MT2 receptor ligands relieve neuropathic pain through modulation of brainstem descending antinociceptive pathways. *Pain.* 2015;156(2):305-317.
22. Arreola-Espino R, Urquiza-Marín H, Ambriz-Tututi M, et al. Melatonin reduces formalin-induced nociception and tactile allodynia in diabetic rats. *European journal of pharmacology.* 2007;577(1-3):203-210.
23. Lin TB, Hsieh MC, Lai CY, et al. Melatonin relieves neuropathic allodynia through spinal MT 2-enhanced PP 2Ac and downstream HDAC 4 shuttling-dependent epigenetic modification of hmgb1 transcription. *Journal of pineal research.* 2016;60(3):263-276.
24. Ambriz-Tututi M, Granados-Soto V. Oral and spinal melatonin reduces tactile allodynia in rats via activation of MT2 and opioid receptors. *Pain.* 2007;132(3):273-280.
25. Tu Y, Sun R-Q, Willis WD. Effects of intrathecal injections of melatonin analogs on capsaicin-induced secondary mechanical allodynia and hyperalgesia in rats. *Pain.* 2004;109(3):340-350.
26. Yu C-X, Zhu C-B, Xu S-F, Cao X-D, Wu G-C. Selective MT2 melatonin receptor antagonist blocks melatonin-induced antinociception in rats. *Neuroscience letters.* 2000;282(3):161-164.
27. Rivara S, Lodola A, Mor M, et al. N-(substituted-anilinoethyl) amides: design, synthesis, and pharmacological characterization of a new class of melatonin receptor ligands. *Journal of medicinal chemistry.* 2007;50(26):6618-6626.
28. Golombek DA, Escolar E, Burin LJ, Sánchez MGDB, Cardinali DP. Time-dependent melatonin analgesia in mice: inhibition by opiate or benzodiazepine antagonism. *European journal of pharmacology.* 1991;194(1):25-30.
29. Mantovani M, Pértile R, Calixto JB, Santos AR, Rodrigues ALS. Melatonin exerts an antidepressant-like effect in the tail suspension test in mice: evidence for involvement of N-methyl-D-aspartate receptors and the L-arginine-nitric oxide pathway. *Neuroscience letters.* 2003;343(1):1-4.
30. Jin X, Von Gall C, Pieschl RL, et al. Targeted disruption of the mouse Mel1b melatonin receptor. *Molecular cellular biology.* 2003;23(3):1054-1060.
31. Liu C, Weaver DR, Jin X, et al. Molecular dissection of two distinct actions of melatonin on the suprachiasmatic circadian clock. *Neuron.* 1997;19(1):91-102.
32. Hunskaar S, Berge O-G, Hole K. A modified hot-plate test sensitivie to mild analgesics. *Behavioural Brain Research.* 1986;21(2):101-108.
33. Bardo MT, Hughes RA. Exposure to a nonfunctional hot plate as a factor in the assessment of morphine-induced analgesia and analgesic tolerance in rats. *Pharmacology Biochemistry and Behavior.* 1979;10(4):481-485.

34. Gamble G, Milne R. Repeated exposure to sham testing procedures reduces reflex withdrawal and hot-plate latencies: attenuation of tonic descending inhibition? *Neuroscience letters.* 1989;96(3):312-317.
35. Hunskaar S, Hole K. The formalin test in mice: dissociation between inflammatory and non-inflammatory pain. *Pain.* 1987;30(1):103-114.
36. Wheeler-Aceto H, Porreca F, Cowan A. The rat paw formalin test: comparison of noxious agents. *Pain.* 1990;40(2):229-238.
37. Caputi FF, Palmisano M, Carboni L, Candeletti S, Romualdi P. Opioid gene expression changes and post-translational histone modifications at promoter regions in the rat nucleus accumbens after acute and repeated 3, 4-methylenedioxy-methamphetamine (MDMA) exposure. *Pharmacological research.* 2016;114:209-218.
38. Paxinos G, Franklin K. The Mouse Brain in Stereotaxic Coordinates, Compact 3rd Edition. Academic Press; 2008.
39. Livak KJ, Schmittgen TD. Analysis of relative gene expression data using real-time quantitative PCR and the $2^{-\Delta\Delta CT}$ method. *Methods.* 2001;25(4):402-408.
40. Konecka AM, Sroczynska IJGPTVS. Circadian rhythm of pain in male mice. 1998;31(5):809-810.
41. Xu S, Wei W, Shen Y, Hao J, Ding C. Studies on the antiinflammatory, immunoregulatory, and analgesic actions of melatonin. *Drug development research.* 1996;39(2):167-173.
42. Naguib M, Hammond D, Schmid III P, et al. Pharmacological effects of intravenous melatonin: comparative studies with thiopental and propofol. *British journal of anaesthesia.* 2003;90(4):504-507.
43. Lacoste B, Angeloni D, Dominguez-Lopez S, et al. Anatomical and cellular localization of melatonin MT1 and MT2 receptors in the adult rat brain. *Journal of pineal research.* 2015;58(4):397-417.
44. Fields H, Barbaro NM, Heinricher M. Brain stem neuronal circuitry underlying the antinociceptive action of opiates. *Progress in brain research.* 1988;77:245-257.
45. Heinricher MM, Morgan MM, Tortorici V, Fields HL. Disinhibition of off-cells and antinociception produced by an opioid action within the rostral ventromedial medulla. *Neuroscience.* 1994;63(1):279-288.
46. Meng ID, Manning BH, Martin WJ, Fields HL. An analgesia circuit activated by cannabinoids. *Nature.* 1998;395(6700):381-383.
47. Dubuisson D, Dennis SGJP. The formalin test: a quantitative study of the analgesic effects of morphine, meperidine, and brain stem stimulation in rats and cats. 1977;4:161-174.
48. Malmberg AB, Yaksh TL. Pharmacology of the spinal action of ketorolac, morphine, ST-91, U50488H, and L-PIA on the formalin test and an isobolographic analysis of the NSAID interaction. *Anesthesiology.* 1993;79(2):270-281.
49. Coderre TJ, Katz J, Vaccarino AL, Melzack R. Contribution of central neuroplasticity to pathological pain: review of clinical and experimental evidence. *Pain.* 1993;52(3):259-285.
50. Coderre TJ, Melzack R. The role of NMDA receptor-operated calcium channels in persistent nociception after formalin-induced tissue injury. *Journal of Neuroscience.* 1992;12(9):3671-3675.
51. Raboisson P, Dallel R, Clavelou P, Sessle BJ, Woda A. Effects of subcutaneous formalin on the activity of trigeminal brain stem nociceptive neurones in the rat. *Journal of neurophysiology.* 1995;73(2):496-505.

52. Fields H, Malick A, Burstein R. Dorsal horn projection targets of ON and OFF cells in the rostral ventromedial medulla. *Journal of neurophysiology.* 1995;74(4):1742-1759.
53. Reiter RJ, Calvo JR, Karbownik M, Qi W, Tan DX. Melatonin and its relation to the immune system and inflammation. *Annals of the New York Academy of Sciences.* 2000;917(1):376-386.
54. Costantino G, Cuzzocrea S, Mazzon E, Caputi AP. Protective effects of melatonin in zymosan-activated plasma-induced paw inflammation. *European journal of pharmacology.* 1998;363(1):57-63.
55. Cuzzocrea S, Zingarelli B, Gilad E, Hake P, Salzman AL, Szabo C. Protective effect of melatonin in carrageenan-induced models of local inflammation: relationship to its inhibitory effect on nitric oxide production and its peroxynitrite scavenging activity. *Journal of pineal research.* 1997;23(2):106-116.
56. Cuzzocrea S, Costantino G, Mazzon E, Caputi AP. Regulation of prostaglandin production in carrageenan-induced pleurisy melatonin. *Journal of pineal research.* 1999;27(1):9-14.
57. Hernández-Pacheco A, Araiza-Saldaña CI, Granados-Soto V, Mixcoatl-Zecuatl T. Possible participation of the nitric oxide-cyclic GMP-protein kinase GK+ channels pathway in the peripheral antinociception of melatonin. *European journal of pharmacology.* 2008;596(1):70-76.
58. Noble F, Fournié-Zaluski M-C, Roques B. Paradoxical analgesia induced by low doses of naloxone is not potentiated by complete inhibition of enkephalin degradation. *Neuropharmacology.* 1994;33(1):135-140.
59. Kocher L. Systemic naloxone does not affect pain-related behaviour in the formalin test in rat. *Physiology behavior.* 1988;43(3):265-268.
60. Pini LA, Vitale G, Ottani A, Sandrini M. Naloxone-reversible antinociception by paracetamol in the rat. *Journal of Pharmacology Experimental Therapeutics.* 1997;280(2):934-940.
61. Le Merrer J, Becker JA, Befort K, Kieffer BL. Reward processing by the opioid system in the brain. *Physiological reviews.* 2009;89(4):1379-1412.
62. Minett MS, Pereira V, Sikandar S, et al. Endogenous opioids contribute to insensitivity to pain in humans and mice lacking sodium channel Na v 1.7. *Nature communications.* 2015;6:8967.
63. Wang T, Li S-r, Dai X, Peng Y-l, Chen Q, Wang R. Effects of melatonin on orphanin FQ/nociceptin-induced hyperalgesia in mice. *Brain research.* 2006;1085(1):43-48.
64. Kasap M, Can ÖD. Opioid System Mediated Anti-Nociceptive Effect of Agomelatine in Mice. *Life Sciences.* 2016.
65. Erbs E, Faget L, Scherrer G, et al. A mu–delta opioid receptor brain atlas reveals neuronal co-occurrence in subcortical networks. *Brain Structure and Function.* 2015;220(2):677-702.
66. Roychowdhury S, Fields H. Endogenous opioids acting at a medullary μ-opioid receptor contribute to the behavioral antinociception produced by GABA antagonism in the midbrain periaqueductal gray. *Neuroscience.* 1996;74(3):863-872.
67. Kalyuzhny AE, Arvidsson U, Wu W, Wessendorf MW. μ-Opioid and δ-opioid receptors are expressed in brainstem antinociceptive circuits: studies using immunocytochemistry and retrograde tract-tracing. *Journal of Neuroscience.* 1996;16(20):6490-6503.
68. Takada T, Yamashita A, Date A, et al. Changes in the circadian rhythm of mRNA expression for μ-opioid receptors in the periaqueductal gray under a neuropathic pain-like state. *Synapse.* 2013;67(5):216-223.

69. Comai S, Ochoa-Sanchez R, Gobbi G. Sleep–wake characterization of double MT1/MT2 receptor knockout mice and comparison with MT1 and MT2 receptor knockout mice. *Behavioural brain research.* 2013;243:231-238.
70. Ochoa-Sanchez R, Comai S, Lacoste B, et al. Promotion of non-rapid eye movement sleep and activation of reticular thalamic neurons by a novel MT2 melatonin receptor ligand. *The Journal of Neuroscience.* 2011;31(50):18439-18452.
71. Pévet P. Melatonin receptors as therapeutic targets in the suprachiasmatic nucleus. *Expert opinion on therapeutic targets.* 2016;20(10):1209-1218.
72. Ochoa-Sanchez R, Rainer Q, Comai S, et al. Anxiolytic effects of the melatonin MT 2 receptor partial agonist UCM765: Comparison with melatonin and diazepam. *Progress in Neuro-Psychopharmacology and Biological Psychiatry.* 2012;39(2):318-325.
73. Masana MI, Doolen S, Ersahin C, et al. MT2 melatonin receptors are present and functional in rat caudal artery. *Journal of Pharmacology and Experimental Therapeutics.* 2002;302(3):1295-1302.
74. Doolen S, Krause DN, Dubocovich ML, Duckles SP. Melatonin mediates two distinct responses in vascular smooth muscle. *European journal of pharmacology.* 1998;345(1):67-69.
75. Pinato L, Ramos D, Hataka A, et al. Day/night expression of MT1 and MT2 receptors in hypothalamic nuclei of the primate Sapajus apella. *Journal of chemical neuroanatomy.* 2017;81:10-17.

2.7 Figures

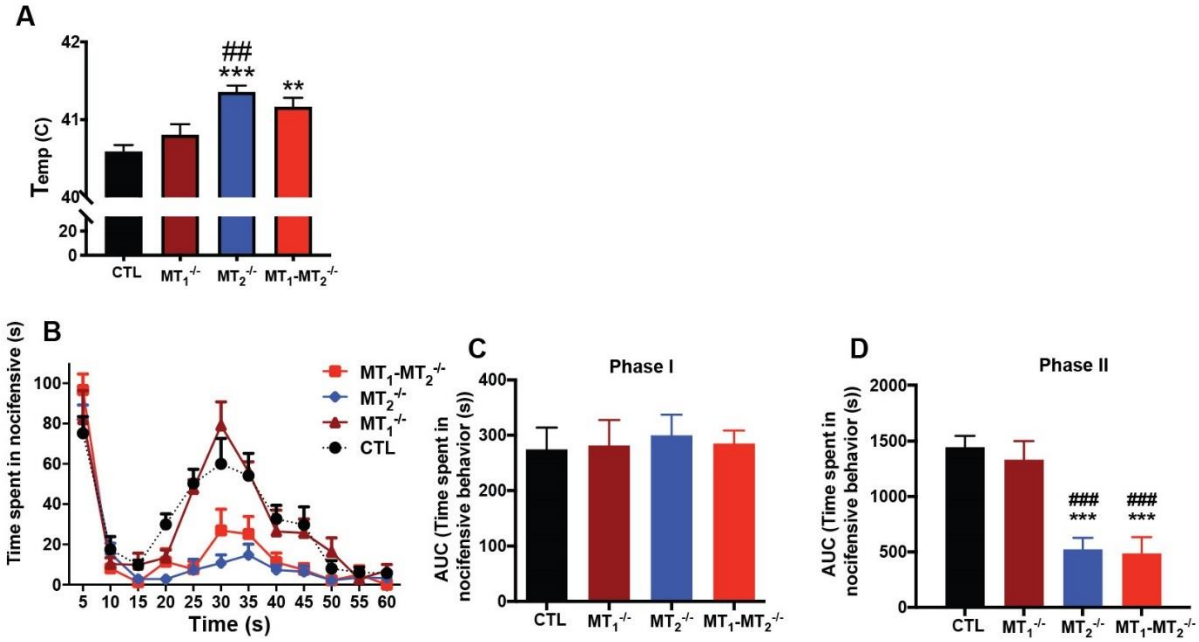

Chapter II - Figure 1. $MT_2^{-/-}$ and $MT_1^{-/-}/MT_2^{-/-}$ mice responses to the thermal and chemical nociceptive stimuli compared to CTL and $MT_1^{-/-}$ mice.

(A) $MT_2^{-/-}$ and $MT_1^{-/-}/MT_2^{-/-}$ showed an increased threshold to thermal stimulus compared to CTL and $MT_1^{-/-}$ mice in the HPT. Data are expressed as mean ± SEM (n= 25-30 each group). **P < 0.01, ***P < 0.001 vs. CTL; ## P < 0.01 vs $MT_1^{-/-}$. One-way ANOVA followed by Tukey *post-hoc* test. (B) Time course of formalin test in CTL, $MT_1^{-/-}$, $MT_2^{-/-}$, and $MT_1^{-/-}/MT_2^{-/-}$ mice (n = 11-7 each group). Data are expressed as mean ± SEM (n= 10-7 each group). (C-D) $MT_2^{-/-}$ and $MT1^{-/-}/MT2^{-/-}$ showed a reduced cumulative time spending licking/flinching in phase 2, but not in phase 1, of the FT compared to CTL and $MT_1^{-/-}$ mice. Data are expressed as mean ± SEM (n= 10-7 each group). ***P < 0.001 vs. CTL; ### P < 0.001 vs $MT_1^{-/-}$. One-way ANOVA followed by Tukey *post-hoc* test.

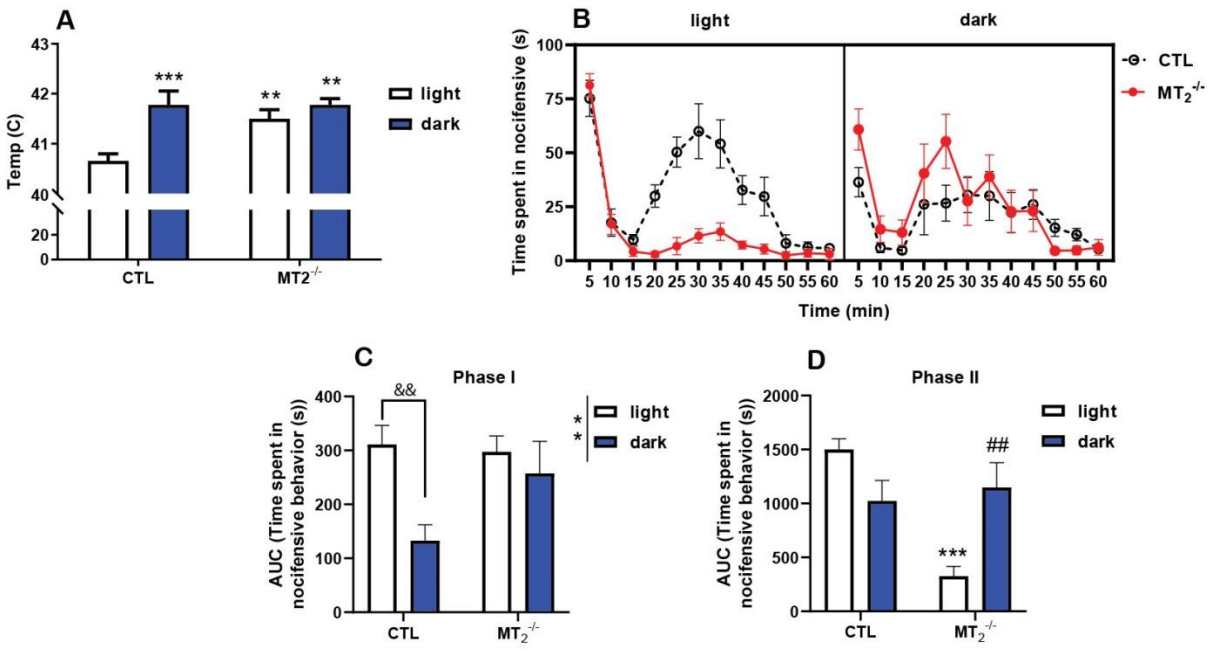

Chapter II - Figure 2. Circadian rhythmicity of nociceptive response in $MT_2^{-/-}$ mice.

(A) During the dark phase (7 pm – 7 am) CTL mice, but not $MT_2^{-/-}$, displayed a decreased response to thermal noxious stimulus (n = 13-8 each group). **(B)** Time course of formalin test in CTL and $MT_2^{-/-}$ mice (n = 11-7 each group). **(C)** CTL, but not $MT_2^{-/-}$, mice showed a reduced cumulative time spending licking/flinching in phase 1 of the FT at night. **(D)** The sensitivity during the phase 2 of the FT was decreased in CTL mice at night (trend), while $MT_2^{-/-}$ exhibited an increased response to the chemical pain stimulus during the dark phase. All data are expressed as mean ± SEM. *P < 0.05, **P < 0.01, ***P < 0.001 vs. CTL light; ### P < 0.001 vs $MT_2^{-/-}$ light; two-way ANOVA followed by Tukey *post-hoc* test. && P < 0.01 light vs dark after Student's t-test.

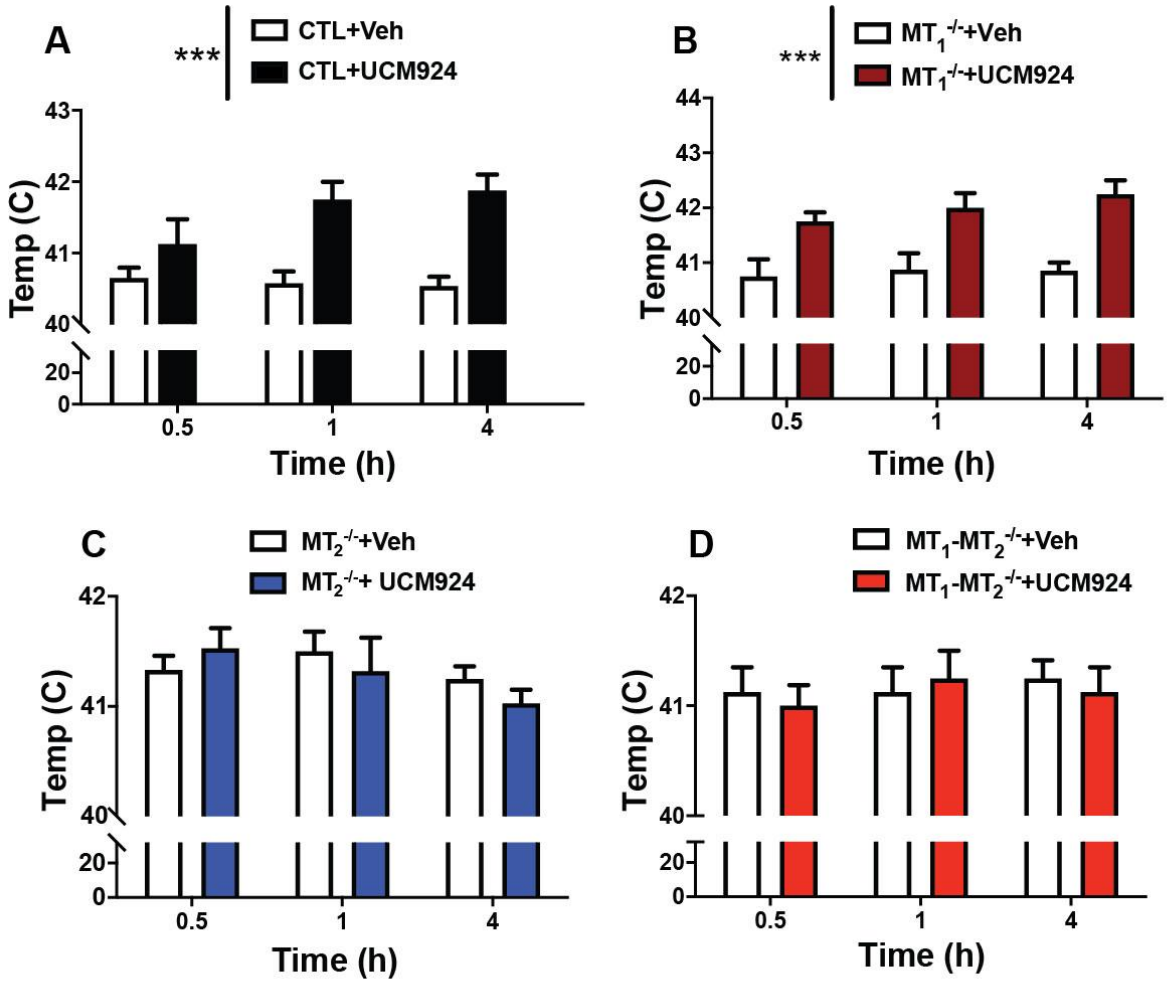

Chapter II - Figure 3. Antinociceptive effect of UCM924 in the Hot Plate Test.

UCM924 (20mg/kg, s.c.) increased the latency to the first nociceptive response in CTL (A) and $MT_1^{-/-}$ (B), but not in $MT_2^{-/-}$ (C) and $MT_1^{-/-}/MT_2^{-/-}$ (D) mice. Data are expressed as mean ± SEM (n = 13-8 each group). ***P < 0.001 main effect of the treatment. Two-way ANOVA.

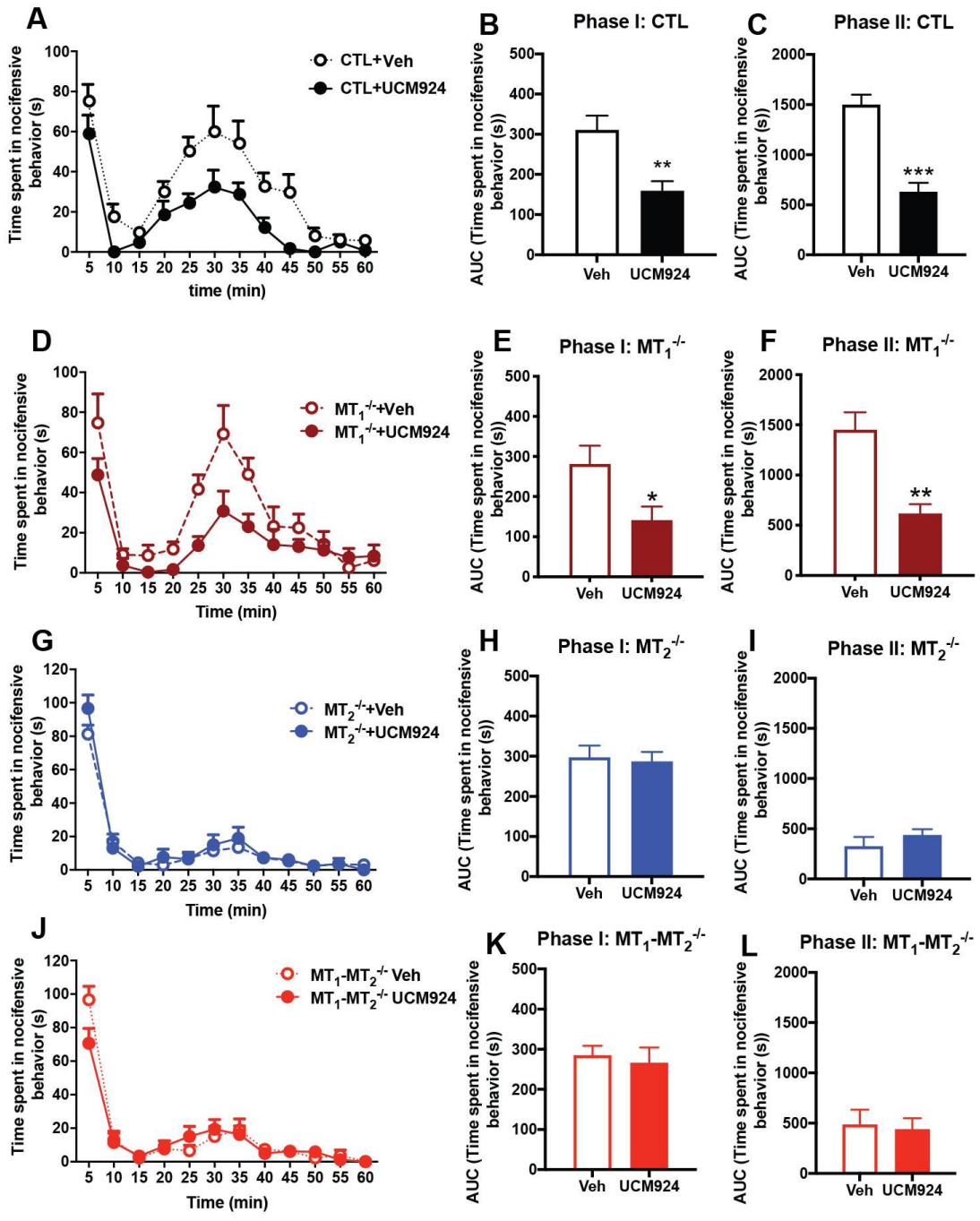

Chapter II - Figure 4. Antinociceptive effect of UCM924 in the Formalin Test.

UCM924 (20mg/kg, s.c.) decreased the cumulative nociceptive response in phase 1 and 2 in CTL **(A-C)** and $MT_1^{-/-}$ **(D-F)**, but not in $MT_2^{-/-}$ **(G-I)** and $MT_1^{-/-}/MT_2^{-/-}$ **(J-L)** mice. Data are expressed as mean ± SEM (n= 12-7 each group). *P< 0.05, **P< 0.01, ***P< 0.001 vs vehicle. Student's t-test.

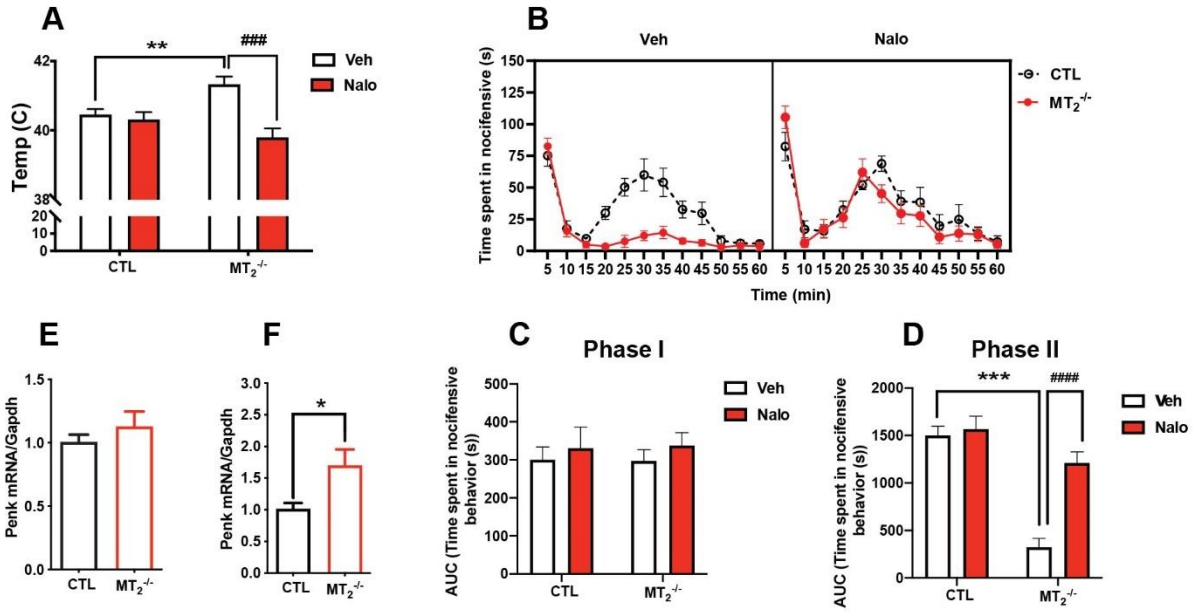

Chapter II - Figure 5. Opioidergic involvement in the reduced nociceptive sensitivity of the $MT_2^{-/-}$ mice.

Systemic naloxone (2 mg/kg, s.c.) reduced thermal and chemical pain thresholds of $MT_2^{-/-}$ mice but has no effect in CTL. **(A)** Naloxone decreased the latency to the first nociceptive response in $MT_2^{-/-}$, but not in CTL mice in the HPT. Data are expressed as mean ± SEM (n= 15-8 each group). **P<0.01 vs CTL veh; ###P<0.001 vs $MT_2^{-/-}$ veh. Two-way ANOVA followed by Tukey post-hoc test. **(B-D**) Naloxone increased the cumulative time spending licking/flinching in phase 2 of the FT in $MT_2^{-/-}$, but not in CTL mice. Data are expressed as mean ± SEM (n= 10-7 each group). ***P<0.001 vs CTL veh; ###P< 0.001 vs $MT_2^{-/-}$ veh. Two-way ANOVA followed by Tukey *post-hoc* test.

Reverse transcriptase–PCR (RT–PCR) analysis of *Penk* mRNA expression in PAG and RVM relative to *Gapdh* mRNA levels in CTL and $MT_2^{-/-}$ mice. (E-F) Increased expression of *Penk* mRNA was observed in $MT_2^{-/-}$ mice compared to CTL in RVM, but not in PAG. Data are expressed as mean ± SEM (n= 5 each group). *P< 0.05 vs CTL. Student's t-test.

Connecting Statement to Chapter III

In Chapter II we established that the genetic inactivation of the MT_2 receptor leads to a reduced nociceptive sensitivity and that this phenomenon was linked to increased tonic activation of the opioid system at the supraspinal level.

Intriguingly, some evidence suggests a possible interaction between opioid and MT_2 receptors. Both MT_2 and opioid receptors are expressed in periaqueductal gray (PAG), a crucial area of the antinociceptive descending pathway. Also, microinjection into the PAG of MT_2 and opioid receptor agonists produce antiallodynia. and both MT_2 and opioid agonists modulate the ON and OFF cells of the rostral-ventromedial-medulla (RVM), a downstream area of the antinociceptive descending pathway which receives axonal projections from the PAG.

Thus, the experiments described in Chapter III sought to determine whether the mu (MOR) or delta (DOR) opioid receptors have a functional role in the inhibitory and facilitatory modulation at the supraspinal level, induced by MT_2 agonism.

Although other studies have demonstrated an involvement of the opioid system in melatonin analgesia, this was the first study to characterize the interaction between the MT_2 receptors and MOR and MOR endogenous ligand in the neuronal circuit of the descending pathway and to suggest an eventual mechanism of action by which MT_2 agonism induces its antiallodynic effects. Moreover, we sought to investigate the rewarding properties of MT_2 partial agonist.

Chapter III

Running Head: MT_2 and mu opioid receptors in neuropathic pain

Melatonin MT_2 receptor agonism alleviates pain via mu opioid receptors without inducing reinforcement

Luca Posa[1,2], Danilo De Gregorio[1], Aliou Badara Gueye[3], Laura Rullo[4], He Qianzi[1], Martha Lopez-Canul[1], Emmanuel Darcq[5], Francesca Felicia Caputi[4], Livio Luongo[6], Sanzio Candeletti[4], Patrizia Romualdi[4], Anne-Nöel Samaha[3], Brigitte Lina Kieffer[5], Gabriella Gobbi[1,2]

(in preparation for submission to the journal, PAIN)

[1] Neurobiological Psychiatry Unit, Department of Psychiatry, McGill University Health Center, McGill University, Montreal, QC, Canada.

[2] Alan Edwards Centre for Research on Pain, McGill University, Montreal, QC, Canada.

[3] Department of Pharmacology and Physiology, Faculty of Medicine, Université de Montréal, Montréal, Canada

[4] Department of Pharmacy and Biotechnology, Alma Mater Studiorum-University of Bologna, Bologna, Italy

[5] Department of Psychiatry, School of Medicine, Douglas Hospital Research Center, McGill University, Montreal, QC, Canada

[6] Department of Experimental Medicine, University of Campania "Luigi Vanvitelli", Naples, Italy

Correspondence to be directed to:
Gabriella Gobbi, MD, PhD
Neurobiological Psychiatry Unit
Dept. of Psychiatry
McGill University
1033 Pine Avenue West
Montreal, Q.C. Canada H3A 1A1
Email: gabriella.gobbi@mcgill.ca
Phone: 514-398-1290
Fax: 514-398-4866

Abstract: 185 words
Introduction: 450 words
Material and methods: 3810 words
Results: 2814 words
Discussion: 1193 words
Figures: 8
Number of references: 84

3.1 Abstract

The research on novel analgesics that stimulates the opioid system without addiction liability remains a priority. In neuropathic rodents, the selective melatonin MT_2 agonist UCM924 (20 mg/kg, subcutaneously) produced antiallodynia, which was nullified by the pharmacological or genetic blockade of the mu opioid receptor (MOR), but not the delta opioid receptor (DOR). Electrophysiological recordings in the rostral-ventromedial medulla (RVM) revealed that the typical reduction of the firing activity of pronociceptive ON cells, and the enhancement of the firing of the antinociceptive OFF cells induced by the microinjection of UCM924 into the ventrolateral periaqueductal gray (vlPAG) were blocked by MORs antagonism. Interestingly, MORs and MT_2 receptors are differentially expressed in the neurons of the brainstem descending antinociceptive pathway and the stimulation of these two GPCRs differently involves the signaling pathway of G protein coupled inwardly rectifying potassium (GIRK) channels. Moreover, the systemic administration of UCM924 increased the proenkephalin (PENK) mRNA level in the PAG of neuropathic animals. Finally, the intravenous self-administration test demonstrated that UCM924, unlike morphine, did not produce reinforcement. The melatonin MT_2 receptor agonists may represent a novel class of opioid-modulators without abuse liability.

3.2 Introduction

Neuropathic pain is a chronic condition affecting 7-10% of population representing a major health problem[75]. The available therapeutics to treat pain have moderate efficacy and present several side effects limiting their long-term use. Particularly, opioids, whose long-term use can induce physical dependence, abuse, and overdose are the cause of the so-called "opioid crisis" in North-America[31; 35] leading to the death of 100 people a day in the US alone[11]. Consequently, drug-discovery aimed at finding alternative analgesic drugs with reduced side effects is a priority for medical research. While several studies have attempted to synthesize and characterize novel opioid-derived drugs without tolerance and addiction potential[48] or biased opioid agonists[56], little has been done in exploring the potential effects of G protein coupled receptors (GPCRs) ligands[81] which could indirectly stimulate opioid receptors.

Melatonin is a neurohormone that binds two GPCRs, MT_1 and MT_2, widely expressed in mammalian brains. Clinical studies have shown that melatonin displays analgesic properties in chronic conditions such as low back pain, fibromyalgia and migraine[79].. Moreover, a plethora of animal studies has demonstrated that the effect of melatonin in chronic neuropathic and inflammatory conditions[60] is likely mediated by the MT_2 receptor[2; 43; 46; 47], as its analgesic effects are prevented by the pretreatment with selective MT_2 antagonist 4P-PDOT[43; 47; 74]. The MT_2 receptors are expressed in the ventro-lateral periaqueductal gray (vlPAG)[39; 47], an area of the brainstem descending antinociceptive pathways, projecting to the rostral-ventromedial medulla (RVM), which in turn projects to the dorsal horns of the spinal cord[27], a network involved in chronic pain states and in opioid-induced analgesia[27; 57]. The selective melatonin MT_2 partial agonist N-{2-([3-bromophenyl]-4-fluorophenylamino)ethyl}acetamide UCM924 shows antiallodynic properties in neuropathic pain models by modulating the ON and OFF neurons of

the RVM[47], similarly to other classes of analgesic drugs acting at the central level, including opiates like morphine[34] and cannabinoids[52]. Although some studies suggest that melatonin's analgesic effects can be blocked by naloxone[1; 40], it is still unknown whether the analgesic mechanism of the MT_2 receptor agonists is directly or indirectly mediated by opioids. In this study we investigate 1) the pharmacological interaction between the MT_2 and mu (MOR) or delta (DOR) opioid receptors; 2) the interaction between MOR and MT_2 receptors in the ON and OFF neurons in the antinociceptive PAG-RVM pathway and their specific downstream effect on K^+ channels using *in vivo* electrophysiology; 3) the cellular localization of MORs and MT_2 receptors at the level of PAG-RVM pathway; 4) the potential cross-tolerance between the MT_2 receptor agonist UCM924 and morphine; 5) the effect of the administration of UCM924 on the endogenous opioid gene expression in the PAG-RVM circuit; 6) the potential abuse liability of the UCM924 compared to that of morphine using intravenous self-administration.

3.3 Materials and methods

3.3.1 Animals and animal care

Male Sprague Dawley rats (Charles River, Quebec, Canada) weighting 140-160 g at the beginning of the experiments were used for pain behavioural studies and for electrophysiological recordings coupled to mechanical paw pinch response. Male mice lacking mu $MOR^{-/-}$ [51], or delta opioid $DOR^{-/-}$ [30] receptors (20-25 g, PND 5-8 weeks) and the corresponding mice with the same genetic background (WT) were generated by homologous recombination as previously described. Male MOR-mCherry knock-in mice (20-25 g, PND 5-8 weeks) expressing the mu opioid receptor fused at its C-terminus to the red protein mCherry were generated by homologous recombination[22], as well as male CaMKIIα-[21; 75] and GAD65-tdTomato[5] knock-in mice (20-25 g, PND 5-8

weeks) expressing the red fluorescent tdTomato protein. All these transgenic mice were used for confocal immunohistochemistry. All animals (except those used for self-administration experiments) were housed in standardized animal facilities under a 12-hour light/dark cycle (lights were on at 7 AM) with ad libitum access to food and water. All the experiments (except those used for self-administration experiments) were conducted between 9:00 and 18:00 hours.

For self-administration experiments, thirty-eight male Sprague Dawley rats (225-250 g; Charles River Laboratories, St Constant, Qc) were individually housed in a climate-controlled colony room under a 12-h reverse light/dark cycle (lights off at 8:30 am). Experiment 1 included 18 rats; experiment 2 included 20 rats. Starting 3 days after their arrival, the rats were restricted to 25 g/day of standard laboratory chow. This moderate food restriction regimen is commonly used in rodent drug self-administration studies and it achieves 80-85% of free-feeding body weight[7; 25; 29; 52]. All rats gained weight over days. Self-administration sessions occurred during the dark phase of the animal circadian cycle.

All surgeries and experimental procedures were performed during the light phase. Experimental protocols were approved by the Animal Ethics Committees of McGill University (protocol #7181) and the Université de Montréal (CDEA 17-095) and followed ethical guidelines of IASP for investigation of experimental pain in conscious animals and the Canadian Institutes of Health Research guidelines for animal care and scientific use. Animals were randomized into treatment groups before any behavioral assessment was performed. All experiments, except self-administration studies, were conducted by experimenters who were blind to drug treatments.

3.3.2 Pain Animal models

Spared nerve injury was performed according to the method of Decosterd and Woolf[17]. Animals were anesthetized with 3% isoflurane/100% O2 inhalation and maintained on 2% isoflurane/100% O2. The sciatic nerve was exposed at mid-thigh level distal to the trifurcation and the 3 peripheral branches (sural, common peroneal, and tibial nerves) of the sciatic nerve were exposed. Both tibial and common peroneal nerves were ligated and transected together. Incisions were closed using vicryl sutures, and animals were allowed to recover for 14 days at the time point of maximal mechanical/thermal allodynia. Animals exhibiting motor deficiency or health issues were excluded from testing (less than 5%). Mechanical and cold allodynia were absent in healthy (pre-surgery) animals, and the mechanical or thermal withdrawal threshold in rodents before SNI (pre-surgery) was very close to the set cut-offs.

Mechanical allodynia

On day 15 after surgery, animals were placed in a test chamber (elevated mesh platform in an enclosure) separated by opaque grey dividers and allowed to acclimatize for 30 to 40 minutes (rats) or 60 to 90 min (mice). Von Frey filaments (Stoelting, Wood Dale, IL) were used to measure the 50% paw withdrawal threshold using the up-and-down method reported by Chaplan et al. [13]. A series of calibrated filaments, for rats [Stoelting, Wood Dale, IL, ranging from 3.61 (0.407 g) to 5.18 (15 g) bending force] and mice [Stoelting, ranging from 2.83 (0.07 g) to 4.31 (2 g) bending force] were applied to the midplantar surface (sural portion) of the hind paw. Lifting of the paw indicated a positive response and prompted the use of the next weaker filament, whereas absence of paw withdrawal after 5 seconds indicated a negative response and prompted the next filament of increased weight. This paradigm continued for 4 more measurements after the initial change of the behavioral response or until 5 consecutive negative or 4 consecutive positive responses.

Cutoffs were set at 15 g (for rats) and 2 g (for mice). 50% paw withdrawal threshold were calculated using the formula proposed by Dixon et al.[20]. Animals without allodynia were excluded. After the determination of the basal response, allodynia was assessed at 0.5, 1, 2, 3, 4, 5, 6, 7, and 8 hours (for rats) and 1, 2, 3, 4, 5, 6, 7 (for mice) post-administration for each treatment described below.

Cold plantar essay

Cold allodynia was assed as previously described by Brenner et al[8]. Briefly, ¼″ thick pyrex borosilicate glass (Corning Inc., NY) was used. Mice were acclimated on the glass plate in transparent plastic test chamber separated by separated by opaque grey dividers for 60 to 90 min. In order to prepare the cold probe, fresh dry ice was crushed into a fine powder using a hammer and stored at −80°C. To shape the probe, a blade was used to cut the top off a 3 mL BD syringe (Franklin Lakes, NJ), and a BD needle tip was used to make 3 holes on each side of the syringe to prevent gas buildup inside the syringe body. The powdered dry ice was packed into the modified syringe and the open end of the syringe was held against a flat surface while pressure was applied to the plunger to compress the dry ice into a flattened, dense pellet 1 cm in diameter. Awake mice were tested by extending the shaped dry ice pellet and pressing it to the glass underneath the hindpaw using a consistent pressure applied to the syringe plunger. The mid plantar portion of the injured paw was targeted ensuring that the paw was accurately touching the glass surface. A stopwatch was used to measure the withdrawal latency. Withdrawal was defined as any vertical or horizontal movement of the paw away from the cold glass. An interval of at least 3 minutes was allowed between trials on any single paw. These intervals were chosen to allow enough time for the average mouse to return to a resting state after stimulation. A least 2 measurements were made per timepoint and the average of the measurements were calculated. Cutoff was set at 20 seconds

to avoid any tissue damage. Trials where the animal did not withdraw in under 20 seconds were repeated.

3.3.3 Drug administration

For subcutaneous (s.c.) and intra-vlPAG single administrations, MT_2 partial agonist N-{2-([3-bromophenyl]-4-fluorophenylamino)ethyl}acetamide UCM924[64] was dissolved in a vehicle (Veh) as previously described[48]. Naloxone, naltrindole, CTOP, TQ (Cederlane, Burlington, ON) and morphine (Sigma-Aldrich, Dorset, UK) were dissolved in vehicle solution. A final volume of 0.4 mL in rats and 0.2 mL in mice was injected for s.c. administration and 1 µL was injected for intra-vlPAG administration. All the antagonists were administrated 10 min before UCM924, except for experiment described at section 3.7 where naloxone or Veh was s.c. injected 2.5 h post UCM924 administration. For tolerance experiments, rats were injected once a day with UCM924 (or Veh) or twice a day with morphine (or Veh) for 8 days. For gene expression experiments, UMC924 was injected subcutaneously (s.c. in 0.2 ml volume) 3 hours before mice were euthanized. For i.v. self-administration rats received UCM924 (0.01-1 mg/kg/infusion), morphine (0.5 mg/kg/infusion) or Veh.

3.3.4 Intra-vlPAG cannulation and microinjection

Neuropathic rats received ventrolateral periaqueductal grey guide cannulation and intra-vlPAG microinjections. Animals were anesthetized using 3% isoflurane/100% O2 inhalation and maintained on 2% isoflurane/100% O2 and mounted into a stereotaxic apparatus. The skull was exposed and stainless steel guide cannula (4 mm below pedestral; 20 gauge; Plastics One, Roanoke, VA, USA) directed toward the vlPAG using coordinates from the atlas of Paxinos and Watson 65 (A: 7.8 mm and L: 0.5 mm from bregma and V: 4.5 mm below the dura). The cannula was secured to the skull with dental cement to a stainless-steel screw). A paired dummy cannula

was inserted into the guide cannula to prevent contamination. Animals recovered on a heating pad and carprofen (10 mg/kg, s.c.) was administrated immediately post-cannulation and every 24 h post-surgery for 2 days. Cannulations were performed 7 days post to SNI. Microinjections were performed using a 25-gauge needle (Plastics One) that extended 2 mm beyond the paired guide cannula into the vlPAG. Drugs or Veh were administered using a 5 µl Hamilton syringe in an automated syringe pump (Braintree Scientific, Inc., Baintree, MA, US) over a period of 60 seconds. The total microinjection volume was 1 µl. The injection cannula was left in position for 2 min. All cannulae were double-checked after microinjection of 0.2 µl of pontamine sky blue dye through the cannula. Rats with microinjection site outside of the vlPAG were excluded from the study.

3.3.5 In vivo electrophysiology

In-vivo electrophysiology coupled to mechanical pinch

The guide cannula implantation into the vlPAG was performed as described above except for the anesthesia. Rats were instead anesthetized with ethyl-urethane 1.2 g/kg i.p., placed in a stereotaxic apparatus (David Kopf Instruments, Tujunga, CA), and a hole was drilled through the skull according to the coordinates from rat brain atlas of Paxinos and Watson [60] (2.8-3.3 mm caudal and 0.4-0.9 mm lateral to lambda and 8.9-10.7 mm depth from the surface of the brain). Anesthesia was confirmed by the absence of nociceptive reflex reaction to a tail or paw pinch and of an eye blink response to pressure. In order to maintain a full anesthetic state during the experiments, supplemental doses of ethyl-urethane (10% of the initial dose, i.p.) were administered if required. Body temperature was maintained at 35 to 36.5°C using a thermal pad (Yellow Springs Instrument Co, Yellow Springs, OH).

In the RVM, ON cells were identified based on their burst of activity, and OFF cells were identified by the firing pause when a nociceptive mechanical stimulation (hind-paw pinch) was applied. Anesthesia was adjusted so that hind paw flicks were elicited with a constant latency of <6 seconds. The mechanical stimulation was delivered by a nociceptive pinch on the rat's injured paw for approximately 5 seconds. Pinches were elicited every 5 minutes for at least 15 minutes before the microinjection of the drugs or Veh into the vlPAG.

Extracellular single-unit recordings were performed using single-barreled glass micropipettes pulled from 2-mm Stoelting (Wood Dale, IL) capillary glass on a Narashige (Tokyo, Japan) PE-21 pipette puller. The micropipettes were preloaded with fiberglass strands to promote capillary filling with 2% pontamine sky blue dye in 3 M NaCl. The micropipette tips were broken down to diameters of 1 to 3 μm to reach an electrode impedance of 2 to 5 MΩ. Single-unit activity was recorded as large-amplitude action potentials captured by a software window discriminator, amplified by an AC Differential MDA-3 amplifier (BAK Electronics, Inc., FL), post amplified and band-pass filtered by a Realistic 10 band frequency equalizer, digitized by a CED 1401 interface system (Cambridge Electronic Design, Cambridge, United Kingdom), processed online, and analyzed off-line using Spike2 software version 5.20 for Windows PC. The first 30 seconds immediately after detecting the neuron was not recorded to eliminate mechanical artifacts due to electrode displacement.

Recording of RVM ON and OFF neurons

Once a neuron was identified from its background activity, we optimized spike size before the treatments and included only those neurons with a constant spike configuration and which could clearly be discriminated from activity in the background throughout the experiment.

The spontaneous single-spike activity of the neuron was then recorded for at least 5 minutes before Veh injection. The neuronal responses before and after intra-vlPAG drug or Veh microinjections were measured and expressed as spikes per second (Hz). The RVM neural activity was expressed as mean ± SEM of the spikes/s by averaging the ongoing cell firing recorded 50 seconds before hind paw flick trials (which were performed every 15 minutes). ON cells included in the data analysis were those with spontaneous activity. Paw flick–related ON cell burst was calculated as mean ± SEM of the spikes in the 10 s interval starting from the beginning of the increase in cell frequency (which was at least the double of its spontaneous activity). Finally, the duration of the OFF cell pause was expressed as mean ± SEM of the time elapsing between the pause onset and the first spike after the hind paw flick. Once the recordings were terminated, pontamine sky blue dye was injected iontophoretically by passing a constant positive current of 20 μA for 5 minutes through the recording pipette to mark the recording site. Then, rats were decapitated and their brains were extracted and frozen at −20°C. Subsequent localization of the labeled site was made by cutting 20-μm-thick brain sections using a microtome (Leica CM 3050 S), and the electrode placement was identified with a microscope (Olympus U-TVO.5 × C-3).

3.3.6 Immunohistochemistry

Tissue preparation and immunohistochemistry

Mice were anesthetized with sodium pentobarbital (100 mg/kg, i.p.) and perfused intracardiacally with 50 ml of freshly prepared, ice-cold 4% paraformaldehyde in 0.1 M phosphate buffer (PB) pH 7.4 for 15 minutes at 10mL/min using a peristaltic pump. Brains were dissected and post-fixed for 24 h at 4 °C in 4 % PFA solution, cryoprotected at 4 °C in a 30 % sucrose, PB 0.1 M pH 7.4 solution, embedded in OCT (Optimal Cutting Temperature medium, Thermo Scientific), frozen and kept at −80 °C. 30-μm thick brain coronal sections containing the PAG and RVM were

collected using a cryostat (CM3050, Leica) and kept floating in PB 0.1 M pH 7.4. 30-µm thick sections were incubated in blocking solution (PB 0.1 M pH 7.4, 0.5 % Triton X100 (Sigma, St. Louis, MO, USA) (PBST), 10% donkey serum (Abcam, ab7475) for 2 h at room temperature (RT). Sections were then incubated for 48 hours at 4 °C in the blocking solution with appropriate primary antibodies: rabbit polyclonal anti MT_2 (Alomone, AMR-032, dilution 1:250), rat monoclonal anti m-cherry (Invitrogen, M11217, dilution 1:1000), mouse monoclonal anti-parvalbumin (PV) (Millipore, MAB1572, dilution 1: 10,000). After 3 washes with PB 0.1 M pH 7.4, 0.5 % Triton X100 buffer, sections were incubated for 2 hours at RT with appropriate donkey AlexaFluor-conjugated secondary antibodies: anti-rabbit Alexa 488 (Invitrogen, A-21206, dilution 1:800), anti-rat Alexa 594 (Invitrogen, A-21209, dilution 1:800, and anti-mouse Alexa 647 (Invitrogen, A-31571, dilution 1:800). Sections were washed three times with PB 0.1 M pH 7.4, 0.5 % Triton X100 and incubated with Neurotrace 435/455 blue Nissl (molecular probes N214791, dilution 1:100) for 30 minutes. After three washes, slices were mounted on gelatin-coated slides and coverslips added with mounting medium (DPX Mountant, Sigma #06522).

Image acquisition

Images of PAG and RVM were collected with a confocal microscope (Carl Zeiss, LSM 710). Acquisitions were performed using X20; 0.80 NA dry objective and zoom values ranging from 0.6 to 1.2 were used for high magnification and images were acquired with the LCS (Leica) software. Confocal acquisitions in the sequential mode (single excitation beams: 405, 488, 594 and 647 nm) to avoid potential crosstalk between the different fluorescence emissions were also used to validate double and triple colocalization. Neurons (cells positive for the specific neuronal marker Neurotrace blue Nissl) expressing a given fluorescent marker were counted using Fiji ImageJ software cell counter plugin. Colocalization between the green fluorescence expression (MT2), the

red MOR-mCherry, or calcium/calmodulin-dependent protein kinaseIIα red fluorescent protein-labelled (CaMKIIα-tdTomato) or glutamic acid decarboxylase red fluorescent protein-labelled (GAD65-tdTomato)or blue fluorescence (PV) associated with expression of the neuronal marker was determined manually and blindly for each slice using Fiji ImageJ software. Counting was performed in the well-described area of the vlPAG (Bregma: −4.60 mm to −4.72 mm). At least 3 slices from 4 animals were counted.

3.3.7 Gene expression

Total RNA was extracted as described elsewhere[10]. Briefly, periaqueductal gray (PAG; −3.6 to −4.9 mm from Bregma) was punched from freshly dissected brain slices according to Paxinos & Franklin mouse atlas[59], immediately frozen on dry ice and stored at −80 °C. RNA integrity was checked by gel electrophoresis, and the concentrations were measured by using the Nanodrop 1000 system spectrophotometer (Thermo Fisher Scientific). RNA samples with OD260/OD280 ratio > 1.8 and < 2.0 were subsequently subjected to DNAse treatment and reverse transcribed with the GeneAmp RNA PCR kit (Life Technologies). The relative abundance of each mRNA of interest was assessed by real-time qRT-PCR using the Syber Green gene expression Master Mix (Life Technologies) in a Step One Real-Time PCR System (Life Technologies). All data were normalized to glyceraldehyde-3-phosphate dehydrogenase (GAPDH) as the endogenous reference gene. Relative expression of different gene transcripts was calculated using the Delta-Delta Ct (DDCt) method and converted to relative expression ratio (2−DDCt) for statistical analysis[46]. The following primers were used (5'–3'): Gapdh forward TGCGACTTCAACAGCAACTC and reverse CTTGCTCAGTGTCCTTGCTG; PENK forward TTCAGCAGATCGGAGGAGTTG and reverse GAAGCGAACGGAGGAGAGAT; POMC forward GAACAGCCCCTGACTGAAAA

and reverse ACGTTGGGGTACACCTTCAC. Results are presented as fold changes in mRNA levels.

3.3.8 Intravenous Self-administration

Self-administration Apparatus

Self-administration occurred in standard operant chambers (Med Associates, St Albans, VT) following our standard protocol[68]. At the start of each session, the house light was turned on and both levers were inserted into the cage. Pressing the inactive lever had no programmed consequences. Pressing the active lever delivered food (a 45-mg, banana flavoured, grain-based food pellet; VWR, Montreal, QC), intravenous UCM924 (0.001-1 mg/kg/infusion), intravenous morphine (0.5 mg/kg/infusion), or intravenous vehicle [a 70% dimethylsulfoxide (DMSO) and 30% saline solution], when schedule requirements were met. The dose of morphine was chosen according to the literature[78], and that of UCM924 was chosen according to its pharmacokinetics; indeed, UCM924 20 mg/kg s.c. corresponds to ca 100 ng/ml in the plasma (see Fig. S8). Upon reward delivery and during the ensuing 20-s timeout-period (see below), both levers were retracted and the light above the active lever was illuminated. This stimulus served as the discrete drug (or food)-associated cue. After the timeout-period, the levers were reinserted into the cage to signal reward availability. Four infrared photocells aligned horizontally at the bottom of each cage measured locomotor activity during sessions. 3.33-RPM syringe pump motors delivered intravenous solutions over 5 s at a rate of 30.26 µl/s.

Surgery and acquisition of food self-administration behaviour

Rats were implanted with a homemade catheter into the jugular vein, as in Samaha et al[68]. Briefly, an indwelling catheter was implanted into the jugular vein of rats anaesthetized with isoflurane (5% for induction and 2-3% for maintenance; CDMV, Saint-Hyacinthe, QC, Canada).

The other end of the catheter was set to exit between the scapulae. At the time of surgery, rats received a subcutaneous injection of 5 mg/kg carprofen (Rimadyl; 50 mg/mL; CDMV) and an intramuscular injection of 0.02 mL of a penicillin solution (Procillin; 300 000 IU/mL; CDMV). Catheters were flushed on alternate days with either 0.1 mL physiological saline or a solution containing 0.2 mg/mL Heparin (Sigma-Aldrich, Oakville, ON, Canada) and 2 mg/mL of the antibiotic Baytril (CDMV). Rats recovered in their home cages for 7 days prior to further manipulation. Thereafter, all rats were trained to lever-press for food pellets under a fixed ratio 3 (FR3) schedule of reinforcement. Once rats took ≥ 20 pellets/session for two consecutive sessions they were assigned to self-administer intravenous vehicle, UCM924, or morphine, as described below.

UCM924 and morphine self-administration

In Experiment 1, we determined whether UCM924 had reinforcing effects. To this end, rats were assigned to self-administer vehicle (n = 4), or UCM924 [0.01 (n = 4), 0.1 (n = 5) or 1 (n = 5) mg/kg/infusion) during daily, 1-h sessions. The rats first self-administered under FR3 for 10 sessions. During each session, each infusion was delivered over 5 s and was followed by a 20-s timeout period. Because we observed no reliable self-administration behaviour under these conditions (i.e., no difference from vehicle), we gave the rats 5 more sessions where they could now self-administer UCM924 under a less effortful schedule of reinforcement, FR1. In Experiment 2, we compared the reinforcing efficacy of UCM924 to that of morphine. Rats were assigned to self-administer UCM924 (0.1 mg/kg/infusion) or morphine (0.5 mg/kg) during daily 2-h sessions under FR3, for 10 sessions. In Experiment 2, we also compared incentive motivation for UCM924 versus morphine. To this end, 1 day after the last FR3 session, we allowed the rats to respond for UCM924 (0.1 mg/kg) or morphine (0.5 mg/kg) under a progressive ratio schedule of reinforcement

(PR) during a single session. Under PR, response requirements increased according to the following formula (5 $e^{(\text{injection number} \times 0.2)}$)−5, yielding the following ratio progression 1, 2, 4, 6, 9, 12, 15, 20, 25, 32, 40, 50, 62, etc. 68. Drugs were injected over 5 s. Sessions ended when 1 h elapsed since the last infusion or after 5 h. The total number of infusions self-administered prior to this point was used as a measure of incentive motivation for drug.

3.3.9 Pharmacokinetics study

Three SD rats were s.c. injected with 20 mg/kg of UCM924 (diluted in 70% DMSO and 30% saline) and blood was collected after 0.5, 1, 2, 4 and 8 hours after injection. For plasma samples an aliquot of 30 µL sample was protein precipitated with 300 µL IS, the mixture was vortex-mixed for 1 min and centrifuged at 4000 rpm for 20 min, 4°C. 80 µL supernatant was then mixed with 160 µL water with 0.1% FA, vortex-mixed 10 min and centrifuged for 10 min at 4000 rpm, 4°C. 1 µL sample was injected for LC-MS/MS analysis (LC-MS/MS-AJ, Triple Quad 5500). Calibration curve: 1-3000ng/mL for UCM924 in male SD rat plasma. Internal standards: 100 ng/mL labetalol & 100 ng/mL liclofenac & 100 ng/mL tolbutamide in CAN. Data were analyzed using Phoenix WinNonlin 6.3.

3.3.10 Statistical Analysis

Mechanical allodynia time-course and electrophysiological recordings were analyzed by repeated measures or mixed-model two-way ANOVA (after testing for normality distribution and sphericity) followed by the Tuckey post hoc comparison. Areas under the curve (AUC) were analyzed by one-way ANOVA. Welch's correction was used, when required. Student's t-test was used to analyze the UCM924 effect on the relative *POMC* and *Penk* gene expression. Group differences in lever-pressing behaviour during FR3 and FR1 sessions were analyzed using three-way ANOVA (group x gession x lever type; session and sever type as within-subjects variables).

Repeated measures two-way ANOVA followed by the Tuckey post hoc comparison was used to analyze group differences in either the number of self-administered infusions during FR3 and FR1 (group x session; session as a within-subjects variable) or locomotor activity over time during each session (group x time; time as a within-subjects variable). Group differences in responding to drug under PR were assessed using a two-tailed unpaired t-test. All data are expressed as mean ± S.E.M. Statistical values reaching $P<0.05$ were considered significant. Statistical analyses were performed using Graphpad Prism v8.3.1 (GraphPad Software, San Diego, CA, US) or SPSS v24 (IBM Corp, Armonk, NY, US). Tuckey or Dunnett post hoc comparisons was used for pair-wise comparisons when interaction was significant. Detailed results of statistical tests are reported in the supplementary table.

3.4 Results

3.4.1 MT_2-mediated antiallodynic effect is nullified by MOR, but not by DOR, blockage

We first determined the contribution of the opioid system to the MT_2-mediated antiallodynic effect in SNI rats. We tested UCM924 that is a selective MT_2 partial agonist belonging to the class of N-(substituted-anilinoethyl)amides[65] with no affinity for opioid receptors[47]. The subcutaneous administration of UCM924, at the dose of 20 mg/kg, reversed the tactile allodynia in neuropathic animals (Fig.1A-B), as previously demonstrated[48]. We therefore tested whether the non-selective opioid antagonist naloxone, the selective MOR antagonist CTOP and the DOR antagonist naltrindole counteracted UCM924's effect. Systemic administration of naloxone (1mg/kg) prior to UCM924 nullified the UCM924-induced antiallodynic effect in SNI rats across 8 hours (interaction: $F_{27,207}=12.36$, $P<0.001$; naloxone+UCM924 vs UCM924 $P<0.05$ Fig. 1A). The area under the curve (AUC) analysis confirmed that the overall UCM924 effect was prevented by

naloxone pre-treatment ($F_{3,23}$=28.28; P<0.001; naloxone+UCM924 vs UCM924 P<0.001, Fig.1B). Importantly, low dose of naloxone (1 mg/kg) alone did not affect the paw withdrawal threshold baseline, as previously reported [38; 62] (Fig.1A-B). To explore the selective effect of UCM924 in the PAG, UCM924 (10μg) was injected intra-vlPAG where it showed an antiallodynic effect (Fig.1C-H). This across-time effect was nullified in animals pretreated with naloxone (interaction: $F_{15,90}$=8.36, P<0.001; naloxone+UCM924 vs UCM924 at 1h P<0.01; AUC: $F_{3,18}$=12.36, P<0.01; naloxone+UCM924 vs UCM924 P<0.001; Fig.1C-D), with CTOP (interaction: $F_{15,95}$=9.09, P<0.001; CTOP+UCM924 vs UCM924 at 1h P<0.01; AUC: $F_{3,19}$=9.03, P<0.001; CTOP+UCM924 vs UCM924 P<0.01; Fig.1E-F), but not with naltrindole (interaction: $F_{15,105}$=5.55, P<0.001; naltrindole+UCM924 vs UCM924 at 1h P=0.36; AUC: $F_{3,24}$=9.06, P<0.001; naltrindole+UCM924 vs UCM924 P=0.07; Fig.1G-H). Moreover, the analysis comparing the AUC of the three antagonists naloxone, CTOP and naltrindole together confirmed it (Fig.S1).

3.4.2 MT_2-mediated antiallodynic effect is nullified in $MOR^{-/-}$, but not in $DOR^{-/-}$ mice

In order to better clarify the role of DOR in MT_2-mediated antiallodynia, we treated SNI $MOR^{-/-}$ and $DOR^{-/-}$ mice with the MT2 agonist UCM924. We found that UCM924 produced a significant mechanical antiallodynic effect in WT (time x treatment $F_{7, 112}$= 13.40, P<0.001; UCM924 vs Veh at 2-5h P<0.001, Fig.2A) and $DOR^{-/-}$ (time x treatment $F_{7, 98}$ = 31.78, P<0.001; UCM924 vs Veh at 2-5h P<0.001, Fig. 2B), but not in $MOR^{-/-}$ (time x treatment $F_{7, 98}$ = 0.802, P=0.588; Fig. 2C) mice across time. These results were confirmed when comparing all the three strains in the AUC (treatment x genotype $F_{2,45}$=97.26, P<0.001; WT UCM924 vs MOR UCM924 P<0.001; Fig. 2D). Interestingly, a similar outcome was found in the cold allodynia test[8]. Indeed, UCM924 significantly reduced the SNI-induced cold allodynia, measured as thermal response threshold

increase, in WT (time x treatment $F_{7, 98}$ = 48.06, P<0.001; UCM924 vs Veh at 2-5h P<0.001, Supplementary Fig. S2A) and $DOR^{-/-}$ mice (time x treatment $F_{7,84}$ = 44.75, P<0.001; UCM924 vs Veh at 2-5h P<0.001, Fig. S2B), but not in $MOR^{-/-}$ mice (time x treatment $F_{7,112}$ =2.07, P=0.052) (Fig. S2C). These results were confirmed when comparing all the three strains in the AUC (treatment x genotype $F_{2, 42}$ = 86.39, P<0.001; WT UCM924 vs MOR UCM924 P<0.001; Fig. S2D).

3.4.3 Naloxone and CTOP block the activation of ON and OFF neurons induced by the MT_2 partial agonist UCM924

We next explored the relationship between MORs and MT_2 receptors in the modulation of the ON and OFF cells[26; 27], the two main populations of neurons in the PAG-RVM circuit implicated in pain modulation. ON cells increase their firing just prior the occurrence of reflexes induced by noxious stimulation, playing a pronociceptive role. OFF cells undergo a characteristic pause just before the nocifensive reflex, and their activation promotes antinociception[28; 35]. UCM924 microinjection into the vlPAG (Fig.3A) decreases the firing rate of the pronociceptive ON cells (Fig.3B top left -C-E-G) and enhances that of the antinociceptive OFF cells (Fig.3B top right-D-F-H) as previously determined[48]. Intra-vlPAG naloxone pre-treatments abolished the UCM924-induced decrease in the frequency of the spontaneous activity (interaction $F_{36,117}$=3.72 P<0.001; naloxone+UCM924 vs UCM924 at 30-60 min P<0.001; Fig. 3C) and in the mechanical pinch burst of firing (Fig.S3A) in the ON cells. CTOP pretreatment also abolished the effects of UCM924 (interaction $F_{36,117}$=3.87, P<0.001; CTOP+UCM924 vs UCM924 at 30-60 min P<0.001; Fig.3E) and in the mechanical pinch burst (Fig.S2C) in the ON cells. Together, naloxone and CTOP prevented the enhanced firing of the OFF cells (naloxone+UCM924 vs UCM924 interaction: $F_{36,117}$= 3.10, P<0.001; CTOP+UCM924 vs UCM924, interaction: $F_{36,117}$= 4.67, P<0.001; Fig.3D,

F, respectively) and the reduction of the OFF cell pause duration (Fig.S3 B-D) promoted by UCM924. In agreement with the behavioural data, the naltrindole neither altered the modulation of the firing activity induced by UCM924 (naltrindole+UCM924 vs UCM924 at 0-60 min, P=n.s., Fig.3G-H), nor the burst and pause of ON and OFF cells (Fig.S3E-F, respectively).

3.4.4 MT_2 receptors and MORs are expressed in different areas and neurons of the PAG-RVM descending pathway

To explore the neurobiological mechanisms underlying the antinociceptive effects in the PAG-RVM circuit, we investigated the localization of MT_2 receptors using SNI transgenic MOR-mCherry[23], calcium/calmodulin-dependent protein kinaseIIα red fluorescent protein-labelled (CaMKIIα-tdTomato)[75], glutamic acid decarboxylase red fluorescent protein-labelled (GAD65-tdTomato) mouse[5] and the GABAergic-associated calcium-binding protein, parvalbumin (PV)[3; 12; 32].

Our previous immunohistochemical results showed that the MT_2 receptor[40; 48] and MOR-mCherry[22] are both expressed in the vlPAG. MT_2 receptors have been found in GAD65-tdTomato$^+$ cells of the vlPAG (Fig. 4A), and specifically this co-localization was observed in PV inhibitory interneurons (Fig. 4A,C). Using knock-in transgenic mice lines CaMKIIα-td tomato, we also confirmed that MT_2 receptors co-localize with CaMKIIα, an excitatory neuronal promoter in the adult forebrain[21; 75] (Fig. 4B). Moreover, while MOR-mCherry signal was revealed in PV$^+$-inhibitory neuronal cell bodies in the RVM, MT_2 receptor immunoreactivity was instead absent (Fig.4C-D).

We then quantified the percentage of neurons positive for somatic MT_2 and MOR-mCherry. While we counted 2.16±0.32% of MT_2 receptors in the total neural cell body population of the vlPAG (17/768), 1.19±0.18% of MOR were quantified over the total vlPAG neural population (9/768)

(Fig.4C). The co-localization MT_2^+/MOR-mCherry$^+$ neurons were only 0.20±0.02 % of the total vlPAG neurons (2/768) (Fig.3C). Specifically, among the population of MOR-mCherry$^+$ in the vlPAG 17.14±2.62% co-labeled with MT_2^+ expressing neurons (2/9), and among the MT_2^+ neurons 9.44±4.24% co-labeled with MOR-mCherry$^+$ in the vlPAG (2/16) (Fig.4C).

Altogether, these data suggest that MT_2 and MOR are differentially expressed in distinct neuronal populations of the PAG and in distinct brain areas.

3.4.5 UCM924-, but not morphine-induced antiallodynia and ON-OFF cell modulation involve postsynaptic G protein-coupled inwardly-rectifying potassium channels (GIRKs) in vlPAG

Next, we investigated whether MT_2 receptors and MORs modulate the G protein-coupled inwardly-rectifying potassium channels GIRK1/4 channel, which is coupled to the inhibitory Gi/o family. We tested the effects of the GIRK1/4 blocker tertiapin-Q (T-Q) in behavioral and electrophysiological experiments in the vlPAG. Intra-vlPAG 1µM pre-administration of T-Q antagonized the antiallodynic effect of UCM924 across time (interaction: $F_{15,120}$=9.89, P<0.001; T-Q+UCM924 vs UCM924 P<0.01; AUC: $F_{3,24}$=11.62, P<0.001; T-Q+UCM924 vs UCM924 P<0.001, Fig.5A-B respectively). Notably, a similar dose of T-Q was showed to have no effect in decreasing the pain threshold in neuropathic animals when injected i.c.v.[73]. Furthermore, T-Q administration prior to UCM924 abolished the UCM924-induced decrease in both spontaneous activity (interaction: $F_{36,130}$=2.98, P<0.001; TQ+UCM924 vs UCM924 at 25-60 min, P<0.01; Fig.5C) and pinch-induced burst (Fig.S4A) in the ON cells. T-Q also blocked the increase in the firing activity of the OFF cells (interaction: $F_{36,132}$=3.95, P<0.001; TQ+UCM924 vs UCM924 at 15-60 min P<0.001 Fig.5D) and the reduction in the OFF cell pause (Fig.S4B) promoted by UCM924. Conversely, intra-PAG T-Q did not block the effects of 5µg MOR agonist morphine on

firing of ON neurons[14] (interaction: $F_{36,132}$=6.77, P<0.001; T-Q+morphine vs morphine, P=n.s, Fig.5E) and burst (Fig.S4C) nor was the firing of OFF cells[14] (interaction: $F_{36,72}$=9.09, P<0.001; T-Q+morphine vs morphine, P=n.s; Fig.5F) and the pause (Fig.S4D) when T-Q was injected prior to morphine. These latter findings confirmed previous results[37; 55]. Taken together, these data show that MOR and MT_2 activate different signaling pathways and GIRK1/4 channels contribute to the electrophysiological and behavioral effects of MT_2 receptor.

3.4.6 Cross tolerance between MT_2 receptor and MOR agonists

Acute morphine administration has antiallodynic effects after repeated administration of UCM924

One of the main side-effects of opioids is the induction of tolerance to their analgesic effects[24; 50]. To test whether repeated administration of UCM924 induces tolerance and if a cross-tolerance between UCM924 and morphine occurs, we administered UCM924 (20mg/kg, s.c., once a day for 9 days) or Veh to SNI rats and tested at day (D) D1, D3, D5, D7 and D9. The antiallodynic effects of UCM924 were attenuated over time (interaction: $F_{40,376}$=6.24, P<0.001; D1 vs D9 P<0.01at 3-6 h; AUC: $F_{5,20.23}$=20.09, P<0.001; D1 vs D7, P=0.018 and D1 vs D9, P=0.001; Fig.6A-B), as expected for GPCR agonists; however, at D9, UCM924 still produced a significant antiallodynic effect compared to vehicle (Veh vs D9 P=0.025, Fig.6B). Intriguingly, morphine (5mg/kg) at day 10 (D10) in D9-UCM924-tolerant rats had an antiallodynic effect comparable to that reached in rats treated with Veh for 9 days (interaction: $F_{12,96}$=38.97, P<0.001; D9-UCM924+Morph vs D9-Veh+ Veh at 30-180 min P<0.001; AUC: $F_{2,7.86}$=217.9, P<0.001; D9-UCM924+Morph vs D9-Veh+Veh P<0.001, Fig.6C-D). In agreement with these behavioral findings, electrophysiological recording showed that a single dose of morphine (5µg), but not UCM924 (10µg), injected into the vlPAG was effective in reducing the ON cells firing across time in D9-UCM924-tolerant rats compared to Veh (interaction: $F_{24,84}$=5.67, P<0.001; D9-UCM924+Morph vs D9-UCM924+Veh

P<0.05 and D9-UCM924+UCM924 vs D9-UCM924+Veh P= n.s.; Fig.6E) and their burst magnitude (Fig.S5A). Similarly, morphine, but not UCM924, microinjected in the vlPAG increased the OFF cells' firing (interaction: $F_{24,91}$=1.68, P=0.043; Fig.6F), and decreased the OFF cells' pause (Fig.S5B) compared to Veh.

Acute UCM924 administration does not produce antiallodynic effects after repeated administration of morphine

Chronic morphine administration leads not only to the development of tolerance to their analgesic effects[24], but also disrupts the physiological modulation of ON and OFF cells in the RVM[74], which become unresponsive. To better elucidate the reciprocal interaction and cross-tolerance between the MT_2 receptor and MOR in a neuropathic pain condition, we administered UCM924 or Veh in rats treated with repeated morphine (5mg/kg, twice a day, s.c.,) or vehicle injections for 9 days, and tested at D1, D3, D5, D7 and D9. After a 9 day treatment with morphine SNI rats developed a complete tolerance[56] to its antiallodynic effect (interaction: $F_{30,234}$=14.43, P<0.001; D1 vs D9 P<0.01 at 30-120 min; AUC: $F_{5,19.25}$=102.6, P<0.001; D1 vs D9 P<0.001, Fig. 6G-H). Also, UCM924 (20mg/kg) administrated at D10 in morphine-tolerant rats lost its antiallodynic effect compared to D9-Veh treated rats (interaction: $F_{16,120}$=10.34; P<0.001; D9-Morph+UCM924 vs D9-Veh+UCM924 at 1-6h P<0.01; AUC: $F_{2,16}$=157.3, P<0.001; D9-Morph+UCM924 vs D9-Veh+UCM924 P<0.001, but D9-Morph+UCM924 vs D9-Veh P<0.05 Fig.6I-J). Electrophysiological recordings showed that UCM924 microinjected into the vlPAG at D10 did not reduce the ON cells' firing activity in morphine-tolerant animals (interaction: $F_{24,84}$=0.89, P=0.608; Fig.6K) and burst magnitude (Fig.S5C), nor modulate the firing of OFF cells (interaction: $F_{24,117}$=0.145, P=n.s.; Fig. 6L) and decrease the OFF cell pause (Fig.S5D).

These data suggest that a normal functioning of the MORs is necessary for the MT_2 agonism to provide antiallodynic properties and confirm their upstream position in the descending pathway compared to MORs.

3.4.7 PENK mRNA expression after MT_2 partial agonist UCM924 administration

Based on the above findings and previous work suggesting that melatonin increases the release of endogenous opioids[4; 71], we questioned whether MT_2-induced anti-allodynia is mediated by opioid endogenous ligands and whether the MT_2 activation by UCM924 increases the synthesis of β-endorphin precursor pro-opiomelanocortin (POMC) and/or the enkephalin precursor proenkephalin (PENK). Systemic administration of naloxone (1mg/kg) 2.5 h post UCM924 administration reversed the UCM924-induced antiallodynic effect in SNI animals (interaction: $F_{16, 112} = 20.27$, $P<0.001$; UCM924 + Veh vs. UCM924 + Nalo $P<0.01$ at 3h Fig. 7A). The AUC analysis confirmed that the overall UCM924 effect was antagonized by naloxone post-treatment ($F_{2,15} = 41.51$, $P<0.001$; UCM924+veh vs. UCM924+Nalo $P<0.001$, Fig.7B).

Next, we measured the relative gene expression of the POMC and PENK mRNA in the PAG. While a significant increase of the PENK mRNA levels was found in SNI animals treated with 20 mg/kg of UCM924 compared to veh ($t_7=3.80$, $P= 0.0067$), no change in POMC mRNA level was detected ($t_8=0.25$, $P=0.8110$) in the PAG. Interestingly, in the PAG of SNI mice the PENK mRNA level was increased compared to sham animal ($t_6=2.65$, $P= 0.038$), confirming previous findings in a chronic inflammatory pain model[82]. Together, these data show that the MT_2 receptor activation stimulates the PENK transcription in the PAG and that endogenous opioid ligands play a crucial role in MT_2-induced anti-allodynia.

3.4.8 Lack of reliable intravenous self-administration induced by MT_2 receptor agonist UCM924

Opioids, including morphine, have rewarding effects [19; 39]. It was thus important to investigate this side effect for the MT_2 receptor partial agonists. To determine whether UCM924 has intrinsic reinforcing efficacy, in Experiment 1 we allowed rats to press a test lever to self-administer vehicle or different doses of UCM924 (0.01, 0.1 or 1mg/kg/infusion). These doses were chosen based on the pharmacokinetics showed in Fig S5. Rats first lever-pressed for UCM924 (or Veh) under FR3 and then FR1. Fig.5 illustrates the average number of active lever presses (Fig.5A), inactive lever presses (Fig.5B) and self-administered injections (Fig.5C) during these sessions. Across UCM924 doses and schedules of reinforcement, lever-pressing behaviour was similar in the UCM924 and vehicle groups (Figs.5A-B; Group x Lever type x Session: FR3 sessions, $F_{27,126}$=0.67, P=0.88; FR1 sessions, $F_{12,56}$=1.15, P= 0.34). In addition, neither the UCM924 nor vehicle groups discriminated between the active and inactive levers (Figs.5A-B; Lever type x Group: FR3 sessions, $F_{3,1}$=2.08, P=0.15; FR1 sessions, $F_{3,14}$=0.73, P=0.54). Finally, across UCM924 doses and schedules of reinforcement, the number of self-administered infusions was similar to vehicle (Fig.5C; main effect of Group: FR3 sessions, $F_{3,14}$=1.80, P=0.19; FR1 sessions, $F_{3,14}$=0.96, P=0.43; Session x Group effect: FR3 sessions, $F_{27,126}$=0.66, P=0.89; FR1 sessions, $F_{12,56}$=1.08, P=0.39). Locomotor activity during the self-administration sessions was also similar in the UCM924 and vehicle groups in session 1 (Fig.5D; Group x Time interaction effect: FR3 session, $F_{33,154}$=1.11, P=0.33), suggesting no locomotor effects induced by UCM924. Post-hoc analyses are in Supplementary table. Thus, when tested under a range of doses and across two different fixed ratio schedules of reinforcement, the rats did not self-administer UCM924 more than a vehicle solution, and UCM924 did not influence locomotor activity. Altogether, these findings indicate that at the doses tested, UCM924 has no motor effects or intrinsic reinforcing properties in rats.

3.4.9 Reliable intravenous self-administration induced by morphine, but not MT_2 receptor agonist UCM924

In Experiment 2, we compared UCM924 (0.1mg/kg) and morphine (0.5mg/kg) self-administration behavior, first under FR3 (10 daily 2-h sessions) and then under progressive ratio (PR; one session). Fig.5 shows lever-pressing behavior and self-administered infusions in morphine (Fig.5G) and UCM924 rats (Fig.5H). The morphine rats pressed significantly more on the active versus inactive lever ($F_{1,18}$=73.52, P<0.001), indicating that the rats reliably discriminated between a lever that produced morphine injections and a lever that did not. The UCM924 rats pressed just as often on the active than on the inactive lever ($F_{1,18}$=1.12, P=0.30). Moreover, the morphine rats pressed more often on the active lever than the UCM924 rats did (P<0.001). The morphine rats also earned more infusions than the UCM924 rats did (session x group effect: $F_{9,162}$=3.82, P<0.001). We also measured locomotor activity during each self-administration session. Figs. 5I-K show average locomotor counts in the morphine and UCM924 groups on the first, 5th and 10th self-administration session, respectively. During each of these sessions, the morphine rats showed more locomotor activity compared to UCM924 rats (Main effects of Group; All P's<0.05). The morphine rats also showed more locomotor activity on the 10th than on the 1st self-administration session (P<0.05). Post-hoc analyses are in Supplementary table.

This finding indicates that these rats developed psychomotor sensitization. In contrast, the UCM924 rats maintained low and unchanging levels of locomotion throughout the 10 self-administration sessions.

The absence of discrimination between the active and inactive levers in the UCM924 group also reproduced the effect seen in Experiment 1, where a different cohort of rats also failed to show lever discrimination when allowed to lever press for 0.1 mg/kg/infusion UCM924. The data in Experiment 2 further shows that morphine self-administration evokes psychomotor sensitization.

Psychomotor sensitization is thought to reflect neuroplasticity underlying the increased drug-wanting characteristic of addiction[66]. Thus, while rats reliably self-administered morphine and developed robust psychomotor sensitization, rats did not self-administer UCM924. This indicates that compared to morphine, UCM924 does not have reinforcing effects in rats.

3.4.10 Incentive motivation for morphine is higher than for UCM924

Fig.5 shows the number of self-administered UCM924 versus morphine infusions under a PR schedule of drug reinforcement. The morphine rats took more infusions than the UCM924 rats did (Fig.5L; t_{18}=-3.46, P<0.01) and pressed more on the active lever than the UCM924 rats did (Group x Lever: $F_{1,18}$=7.69, P<0.05; Figs.5M-N) during the PR test. In other words, the rats were willing to work much harder to obtain 0.5mg/kg/infusion morphine than 0.1mg/kg/infusion UCM924. Thus, rats showed significantly greater incentive motivation for morphine than for UCM924.

3.5 Discussion

The results presented here showed that the antiallodynic effects of the melatonin MT_2 agonist UCM924 are mediated by the opioid system, specifically MOR, but unlike morphine, it is not self-reinforcing, which suggests no abuse liability. The antiallodynic effects of MT_2 agonist are blocked by the MOR, but not DOR, antagonist CTOP; similarly, CTOP blocks the ability of UCM924 to decrease pronociceptive ON cells firing and increase antinociceptive OFF cells firing. Immunohistochemical data suggest that the MT_2 receptor is upstream of the MOR, and are mostly localized in the glutamatergic and GABAergic neurons of the PAG, while the MOR is modestly present in the neuronal soma in the vlPAG and are also expressed in the RVM. The fact that in morphine tolerant animals the UCM924 no longer showed its antiallodynic properties, but not

vice-versa, confirms the upstream position of the MT_2 receptor and that MT_2 receptor agonists need functional MOR for their therapeutic effects.

Despite considerable drug-discovery efforts[54], therapeutics for chronic neuropathic pain remain scant, and novel effective therapies without addiction liability are needed to manage untreatable pain. Previous studies have shown that exogenous and endogenous melatonin provides analgesic effects with the involvement of the opioid systems. Notably, melatonin increases the release of beta-endorphin[4; 71], and the naloxone blocks the melatonin-induced analgesia in the hot plate[34; 41] and tail-flick tests[80]. In addition, the opioid antagonist naltrexone blocks the melatonin-induced mechano-allodynia in a spinal nerve ligation model[1]. Here, we showed that non-selective naloxone and MOR-selective CTOP antagonists blocked both the antiallodynic effect and the central modulation of ON and OFF cells in the PAG-RVM descending antinociceptive circuit. In agreement with a previous study[2], we also found that naltrindole has a limited effectiveness in blocking the effect of UCM924. Of note, at the dose used in this study (1µg intra-PAG), naltrindole is a selective DOR antagonist *in vivo*[9]. Indeed, this finding was confirmed by electrophysiological recordings with 1µg naltrindole and the allodynic tests in $DOR^{-/-}$ mice. Although DORs have a great potential for the treatment of chronic pain[33; 63], the MT_2-induced antiallodynic effect at supraspinal level seems to be more linked to the MOR.

We confirmed that the MT_2 receptor is expressed in neurons of the vlPAG[40; 48], but not in the RVM. We found that MT_2 receptors are expressed in both excitatory and inhibitory neuronal cell bodies in the vlPAG (~2.16%), while 1.19% of MORs have been found in somatodendritic neuronal population. On the other hand, our findings confirmed that MORs are expressed in the PAG and RVM[15; 23; 42; 84], corroborating our hypothesis that MT_2 receptors are localized upstream of MORs. UCM924's, but not morphine's, antiallodynic effect and its capability to

modulate ON and OFF cells are antagonized by T-Q, suggesting the involvement of GIRK1/4 to promote MT_2 antiallodynia at supraspinal level. These findings are in line with previous results, showing that supraspinal morphine analgesia was not directly mediated by GIRK in chronic pain conditions[37; 73]. It has been shown that the $GABA_BR$ agonist baclofen induces a post-synaptic inhibition through GIRK in the vlPAG[45], leading to analgesia[6; 43]. This effect can stimulate excitatory synapses activating antinociceptive OFF cells. In parallel, the MT_2-induced inhibition of glutamatergic cells activated by noxious stimuli directly contributes to the decrease of pronociceptive ON cell firing. Although inhibition of glutamatergic neuronal activity or activation of GABAergic neuronal activity potentiates nociception[70], previous studies suggested that presynaptic inhibition of glutamatergic transmission onto ON cells in PAG can contribute to analgesia[16]; MT_2 receptor activation on glutamatergic neurons may play this role.

Nevertheless, GABA-disinhibition has been proposed as a mechanism underlying opioid analgesia[27; 67]. Opioids activate the PAG–RVM descending pathway by indirectly removing the inhibitory control of local GABAergic interneurons. The results presented here showed that naloxone treatment after UCM924 reversed the MT_2-induced antiallodynia. This effect is likely due to the displacement of the MOR endogenous ligand enkephalin produced by competitive antagonism naloxone (Ki = 1.5 nM)[79] for the MOR, since the enkephalin precursor PENK mRNA levels are increased after the administration of UCM924 in the PAG of SNI mice. Based on this evidence, the GABA-disinhibition promoted by MT_2 activation in the vlPAG may stimulate the release of the endogenous opioid enkephalins at a downstream level in the RVM, as observed with melatonin[4; 71]. Similarly, the expression of the enkephalin precursor *PENK* gene is increased in the RVM of MT_2 knock-out mice[62]. Here, MT_2 receptors may induce a double effect, activating MORs, which are presynaptically expressed on GABA inhibitory interneurons,

thus promoting the disinhibition of antinociceptive OFF cells; and/or, in parallel, activating enkephalins, stimulating postsynaptic MORs localized on the ON cells, thus inhibiting the pronociceptive ON firing[26].

Opioid side effects include tolerance to analgesia and abuse liability, both limiting their long-term use. After 9 days of morphine, the rats became tolerant to the antiallodynic effects of morphine and its capacity to modulate ON and OFF neurons. On the other hand, after 9 days of repeated UCM924 treatment, UCM924 showed attenuated, but still significant antiallodynic effects over time (AUC) compared to control. Moreover, whereas 9 day-morphine-treated rats did not respond to UCM924 antiallodynic effect and to ON and OFF cell modulation (cross-tolerance), 9 day-UCM924-treated rats responded to the morphine, suggesting that the MT_2 agonism needs functional MOR to be effective. This evidence suggests also that the MOR acts downstream of MT_2 in the PAG-RVM pathway, pointing out the crucial engagement of MOR in the MT_2-induced supraspinal analgesia. Moreover, single microinjection of UCM924 or morphine failed to modulate ON and OFF cells after repeated treatment with UCM924 or morphine respectively, suggesting a decreased responsiveness in these two populations of neurons due to repeated drug administration[74].

While rats given the opportunity to self-administer UCM924 did not voluntarily take the drug, they self-inject morphine. This result provides the first evidence that UCM924, unlike morphine, has no robust reinforcing properties, suggesting no abuse potential. Drugs of abuse produce reinforcing effects in large part by activating the mesolimbic dopamine system, which also underlies the reinforcing properties of non-drug rewards[18]. The mesolimbic system consists of dopaminergic neurons in the ventral tegmental area and their axonal projections to terminal fields in the nucleus accumbens and the prefrontal cortex. First, the lack of MT_2 receptors in the mesolimbic

dopaminergic pathways, including the VTA and prefrontal cortex[40] could explain the lack of rewarding effects of UCM924. Second, MT_2 receptors are scarcely co-localized with the MOR receptors at the cellular level, thus not directly activating the intracellular cascade that is responsible for opioid side effects[49].

The lack of UCM924 reinforcement could be explained by its longer half-life (Fig.S7) and its slow indirect stimulation of MORs through the MT_2-induced release of enkephalins. In support of this hypothesis, a recent study showed that morphine and synthetic opioids, but not endogenous opioids, activate opioid receptors inside cells at Golgi apparatus level and much more quickly than endogenous opioids[72]. This time difference could be important in the development of addiction, because typically drugs that act faster have an enhanced propensity to addiction[69].

Even if many questions are still open, the stimulation of the MT_2 receptor by agonists may represent a novel avenue to treat neuropathic pain conditions by activating opioid receptors, all the while presenting low abuse liability.

Acknowledgements

The research was sponsored by the CIHR (Canadian Institutes for Health Research), Brain Canada and the CQDM (Quebec Consortium for Drug Discovery) to G.G and RFO University of Bologna (to PR/SC). L.P. is recipient of the The Louise and Alan Edwards Foundation, FRQS (Fond Recherche Québec-Santé) doctoral scholarship, and POND. D.D.G. is recipient of FRQS and CIHR postdoctoral fellowships. M.L.C is recipient of the McGill University, Faculty of Medicine/Ferring post-doctoral fellowship.

Author Contribution

L.P. designed the study, performed experiments, analyzed data and wrote the first draft of the manuscript. D.D.G. performed preliminary electrophysiological experiments and helped in data analysis. A.B.G. performed self-administration experiments and analyzed data. H.Q., E.D. and L.L assisted in immunohistochemical experiments. L.R. and F.F.C. assisted in gene expression experiments and analysis. M.L.C. assisted in behavioural experiments. S.C., P.R., A.N.S and B.L.K assisted in experimental design and contributed to write the manuscript. G.G. supervised the project, designed experiments and contributed to write the manuscript. Authors thank Drs Arkady Khoutorsky and Alfredo Ribeiro-da-Silva for providing CaMKIIα- and GAD65-tdTomato mice.

Conflict of interest statement

G.G. is an inventor of patents in selective melatonin MT_2 ligands. The remaining authors declare no conflict of interest.

3.6 References

[1] Ambriz-Tututi M, Granados-Soto V. Oral and spinal melatonin reduces tactile allodynia in rats via activation of MT2 and opioid receptors. Pain 2007;132(3):273-280.

[2] Arreola-Espino R, Urquiza-Marín H, Ambriz-Tututi M, Araiza-Saldaña CI, Caram-Salas NL, Rocha-González HI, Mixcoatl-Zecuatl T, Granados-Soto V. Melatonin reduces formalin-induced nociception and tactile allodynia in diabetic rats. European journal of pharmacology 2007;577(1-3):203-210.

[3] Barbaresi P, Mensà E, Lariccia V, Pugnaloni A, Amoroso S, Fabri M. Differential distribution of parvalbumin-and calbindin-D28K-immunoreactive neurons in the rat periaqueductal gray matter and their colocalization with enzymes producing nitric oxide. Brain Research Bulletin 2013;99:48-62.

[4] Barrett T, Kent S, Voudouris N. Does melatonin modulate beta-endorphin, corticosterone, and pain threshold? Life sciences 2000;66(6):467-476.

[5] Besser S, Sicker M, Marx G, Winkler U, Eulenburg V, Hülsmann S, Hirrlinger JJPo. A transgenic mouse line expressing the red fluorescent protein tdTomato in GABAergic neurons. PLoS One 2015;10(6):e0129934.

[6] Bonanno G, Fassio A, Sala R, Schmid G, Raiteri M. GABAB receptors as potential targets for drugs able to prevent excessive excitatory amino acid transmission in the spinal cord. European journal of pharmacology 1998;362(2-3):143-148.

[7] Bongiovanni M, See RE. A comparison of the effects of different operant training experiences and dietary restriction on the reinstatement of cocaine-seeking in rats. Pharmacology Biochemistry and Behavior 2008;89(2):227-233.

[8] Brenner DS, Golden JP, Gereau IV RW. A novel behavioral assay for measuring cold sensation in mice. PloS one 2012;7(6):e39765.

[9] Calcagnetti DJ, Holtzman SG. Delta opioid antagonist, naltrindole, selectively blocks analgesia induced by DPDPE but not DAGO or morphine. Pharmacology Biochemistry and Behavior 1991;38(1):185-190.

[10] Caputi FF, Palmisano M, Carboni L, Candeletti S, Romualdi P. Opioid gene expression changes and post-translational histone modifications at promoter regions in the rat nucleus accumbens after acute and repeated 3, 4-methylenedioxy-methamphetamine (MDMA) exposure. Pharmacological research 2016;114:209-218.

[11] CDC/NCHS. National Vital Statistics System, Mortality. In: C US Department of Health and Human Services editor. Atlanta, GA: CDC WONDER, 2018.

[12] Celio M. Calbindin D-28k and parvalbumin in the rat nervous system. Neuroscience 1990;35(2):375-475.

[13] Chaplan S, Bach F, Pogrel J, Chung J, Yaksh T. Quantitative assessment of tactile allodynia in the rat paw. Journal of neuroscience methods 1994;53(1):55-63.

[14] Cheng Z-F, Fields HL, Heinricher MM. Morphine microinjected into the periaqueductal gray has differential effects on 3 classes of medullary neurons. Brain research 1986;375(1):57-65.

[15] Commons KG, Van Bockstaele EJ, Pfaff DW. Frequent colocalization of mu opioid and NMDA-type glutamate receptors at postsynaptic sites in periaqueductal gray neurons. Journal of Comparative Neurology 1999;408(4):549-559.

[16] Connor M, Schuller A, Pintar JE, Christie MJ. μ-opioid receptor modulation of calcium channel current in periaqueductal grey neurons from C57B16/J mice and mutant mice lacking MOR-1. British journal of pharmacology 1999;126(7):1553-1558.
[17] Decosterd I, Woolf CJ. Spared nerve injury: an animal model of persistent peripheral neuropathic pain. Pain 2000;87(2):149-158.
[18] Di Chiara G, Bassareo V. Reward system and addiction: what dopamine does and doesn't do. Current opinion in pharmacology 2007;7(1):69-76.
[19] Di Chiara G, Imperato A. Drugs abused by humans preferentially increase synaptic dopamine concentrations in the mesolimbic system of freely moving rats. Proceedings of the National Academy of Sciences 1988;85(14):5274-5278.
[20] Dixon WJ. Efficient analysis of experimental observations. Annual review of pharmacology and toxicology 1980;20(1):441-462.
[21] Dragatsis I, Zeitlin S. CaMKIIα-cre transgene expression and recombination patterns in the mouse brain. Genesis 2000;26(2):133-135.
[22] Erbs E, Faget L, Scherrer G, Matifas A, Filliol D, Vonesch J-L, Koch M, Kessler P, Hentsch D, Birling M-C. A mu–delta opioid receptor brain atlas reveals neuronal co-occurrence in subcortical networks. Brain Structure and Function 2015;220(2):677-702.
[23] Erbs E, Faget L, Veinante P, Kieffer BL, Massotte D. In vivo neuronal co-expression of mu and delta opioid receptors uncovers new therapeutic perspectives. Receptors & clinical investigation 2014;1(5):210.
[24] Fairbanks CA, Wilcox GL. Acute tolerance to spinally administered morphine compares mechanistically with chronically induced morphine tolerance. Journal of Pharmacology and Experimental Therapeutics 1997;282(3):1408-1417.
[25] Ferrario CR, Gorny G, Crombag HS, Li Y, Kolb B, Robinson TE. Neural and behavioral plasticity associated with the transition from controlled to escalated cocaine use. Biological psychiatry 2005;58(9):751-759.
[26] Fields H. State-dependent opioid control of pain. Nature Reviews Neuroscience 2004;5(7):565-575.
[27] Fields H, Barbaro NM, Heinricher M. Brain stem neuronal circuitry underlying the antinociceptive action of opiates. Progress in brain research 1988;77:245-257.
[28] Fields HL, Heinricher MM, Mason P. Neurotransmitters in nociceptive modulatory circuits. Annual review of neuroscience 1991;14(1):219-245.
[29] Figueroa-Guzman Y, Mueller C, Vranjkovic O, Wisniewski S, Yang Z, Li S-J, Bohr C, Graf EN, Baker DA, Mantsch JR. Oral administration of levo-tetrahydropalmatine attenuates reinstatement of extinguished cocaine seeking by cocaine, stress or drug-associated cues in rats. Drug and alcohol dependence 2011;116(1-3):72-79.
[30] Filliol D, Ghozland S, Chluba J, Martin M, Matthes HW, Simonin F, Befort K, Gavériaux-Ruff C, Dierich A, LeMeur M. Mice deficient for δ-and μ-opioid receptors exhibit opposing alterations of emotional responses. Nature genetics 2000;25(2):195-200.
[31] Fischer B, Pang M, Tyndall M. The opioid death crisis in Canada: crucial lessons for public health. The Lancet Public Health 2019;4(2):e81-e82.
[32] Fukuda T, Heizmann CW, Kosaka T. Quantitative analysis of GAD65 and GAD67 immunoreactivities in somata of GABAergic neurons in the mouse hippocampus proper (CA1 and CA3 regions), with special reference to parvalbumin-containing neurons. Brain research 1997;764(1-2):237-243.

[33] Gavériaux-Ruff C, Kieffer BL. Delta opioid receptor analgesia: recent contributions from pharmacology and molecular approaches. Behavioural pharmacology 2011;22(5-6):405.
[34] Golombek DA, Escolar E, Burin LJ, Sánchez MGDB, Cardinali DP. Time-dependent melatonin analgesia in mice: inhibition by opiate or benzodiazepine antagonism. European journal of pharmacology 1991;194(1):25-30.
[35] Heinricher MM, Morgan MM, Tortorici V, Fields HL. Disinhibition of off-cells and antinociception produced by an opioid action within the rostral ventromedial medulla. Neuroscience 1994;63(1):279-288.
[36] Hoots BE, Xu L, Kariisa M, Wilson NO, Rudd RA, Scholl L, Schieber L, Seth P. 2018 Annual surveillance report of drug-related risks and outcomes - United States. 2018.
[37] Kanbara T, Nakamura A, Shibasaki M, Mori T, Suzuki T, Sakaguchi G, Kanemasa T. Morphine and oxycodone, but not fentanyl, exhibit antinociceptive effects mediated by G-protein inwardly rectifying potassium (GIRK) channels in an oxaliplatin-induced neuropathy rat model. Neuroscience letters 2014;580:119-124.
[38] Kocher L. Systemic naloxone does not affect pain-related behaviour in the formalin test in rat. Physiology & behavior 1988;43(3):265-268.
[39] Kreek MJ, LaForge KS, Butelman E. Pharmacotherapy of addictions. Nature reviews Drug discovery 2002;1(9):710-726.
[40] Lacoste B, Angeloni D, Dominguez-Lopez S, Calderoni S, Mauro A, Fraschini F, Descarries L, Gobbi G. Anatomical and cellular localization of melatonin MT1 and MT2 receptors in the adult rat brain. Journal of pineal research 2015;58(4):397-417.
[41] Lakin M, Miller C, Stott M, Winters W. Involvement of the pineal gland and melatonin in murine analgesia. Life Sciences 1981;29(24):2543-2551.
[42] Le Merrer J, Becker JA, Befort K, Kieffer BL. Reward processing by the opioid system in the brain. Physiological reviews 2009;89(4):1379-1412.
[43] Levy RA, Proudfit HK. Analgesia produced by microinjection of baclofen and morphine at brain stem sites. European journal of pharmacology 1979;57(1):43-55.
[44] Lin TB, Hsieh MC, Lai CY, Cheng JK, Wang HH, Chau YP, Chen GD, Peng HY. Melatonin relieves neuropathic allodynia through spinal MT 2-enhanced PP 2Ac and downstream HDAC 4 shuttling-dependent epigenetic modification of hmgb1 transcription. Journal of pineal research 2016;60(3):263-276.
[45] Liu Z-L, Ma H, Xu R-X, Dai Y-W, Zhang H-T, Yao X-Q, Yang K. Potassium channels underlie postsynaptic but not presynaptic GABAB receptor-mediated inhibition on ventrolateral periaqueductal gray neurons. Brain research bulletin 2012;88(5):529-533.
[46] Livak KJ, Schmittgen TD. Analysis of relative gene expression data using real-time quantitative PCR and the $2^{-\Delta\Delta CT}$ method. Methods 2001;25(4):402-408.
[47] Lopez-Canul M, Comai S, Domínguez-López S, Granados-Soto V, Gobbi G. Antinociceptive properties of selective MT2 melatonin receptor partial agonists. European journal of pharmacology 2015;764:424-432.
[48] Lopez-Canul M, Palazzo E, Dominguez-Lopez S, Luongo L, Lacoste B, Comai S, Angeloni D, Fraschini F, Boccella S, Spadoni G. Selective melatonin MT2 receptor ligands relieve neuropathic pain through modulation of brainstem descending antinociceptive pathways. Pain 2015;156(2):305-317.
[49] Manglik A, Lin H, Aryal DK, McCorvy JD, Dengler D, Corder G, Levit A, Kling RC, Bernat V, Hübner H. Structure-based discovery of opioid analgesics with reduced side effects. Nature 2016;537(7619):185-190.

[50] Marcus DJ, Zee M, Hughes A, Yuill MB, Hohmann AG, Mackie K, Guindon J, Morgan DJ. Tolerance to the antinociceptive effects of chronic morphine requires c-Jun N-terminal kinase. Molecular Pain 2015;11(34):1-15.
[51] Matthes HW, Maldonado R, Simonin F, Valverde O. Loss of morphine-induced analgesia, reward effect and withdrawal symptoms in mice lacking the mu-opioid-receptor gene. Nature 1996;383(6603):819.
[52] McFarland K, Lapish CC, Kalivas PW. Prefrontal glutamate release into the core of the nucleus accumbens mediates cocaine-induced reinstatement of drug-seeking behavior. Journal of neuroscience 2003;23(8):3531-3537.
[53] Meng ID, Manning BH, Martin WJ, Fields HL. An analgesia circuit activated by cannabinoids. Nature 1998;395(6700):381-383.
[54] Moulin D, Boulanger A, Clark A, Clarke H, Dao T, Finley G, Furlan A, Gilron I, Gordon A, Morley-Forster PK. Pharmacological management of chronic neuropathic pain: revised consensus statement from the Canadian Pain Society. Pain Research and Management 2014;19(6):328-335.
[55] Nakamura A, Fujita M, Ono H, Hongo Y, Kanbara T, Ogawa K, Morioka Y, Nishiyori A, Shibasaki M, Mori T. G protein-gated inwardly rectifying potassium (KIR 3) channels play a primary role in the antinociceptive effect of oxycodone, but not morphine, at supraspinal sites. British Journal of Pharmacology 2014;171(1):253-264.
[56] Narita M, Nakamura A, Ozaki M, Imai S, Miyoshi K, Suzuki M, Suzuki T. Comparative pharmacological profiles of morphine and oxycodone under a neuropathic pain-like state in mice: evidence for less sensitivity to morphine. Neuropsychopharmacology 2008;33(5):1097-1112.
[57] Negus SS, Freeman KB. Abuse potential of biased mu opioid receptor agonists. Trends in pharmacological sciences 2018;39(11):916-919.
[58] Ossipov MH, Morimura K, Porreca F. Descending pain modulation and chronification of pain. Current opinion in supportive and palliative care 2014;8(2):143-151.
[59] Paxinos G, Franklin K. The Mouse Brain in Stereotaxic Coordinates, Compact 3rd Edition: Academic Press, 2008.
[60] Paxinos G, Watson C. The Rat Brain in stereotaxic coordinates 7th Edition. New York: Academic Press, 2013.
[61] Posa L, De Gregorio D, Gobbi G, Comai S. Targeting melatonin MT2 receptors: A novel pharmacological avenue for inflammatory and neuropathic pain. Current medicinal chemistry 2018;25(32):3866-3882.
[62] Posa L, Lopez-Canul M, Rullo L, De Gregorio D, Dominguez-Lopez S, Aboud MK, Felicia Caputi F, Candeletti S, Romualdi P, Gobbi G. Nociceptive responses in MT2 receptor knockout mice compared to MT1 and double MT1/MT2 receptor knockout mice. Journal of Pineal Research 2020;69:e12671.
[63] Quirion B, Bergeron F, Blais V, Gendron L. The Delta-Opioid Receptor; a Target for the Treatment of Pain. Frontiers in Molecular Neuroscience 2020;13.
[64] Rivara S, Lodola A, Mor M, Bedini A, Spadoni G, Lucini V, Pannacci M, Fraschini F, Scaglione F, Sanchez RO. N-(substituted-anilinoethyl) amides: design, synthesis, and pharmacological characterization of a new class of melatonin receptor ligands. Journal of medicinal chemistry 2007;50(26):6618-6626.
[65] Rivara S, Vacondio F, Fioni A, Silva C, Carmi C, Mor M, Lucini V, Pannacci M, Caronno A, Scaglione F. N-(Anilinoethyl) amides: Design and Synthesis of Metabolically Stable,

Selective Melatonin Receptor Ligands. ChemMedChem: Chemistry Enabling Drug Discovery 2009;4(10):1746-1755.
[66] Robinson TE, Berridge KC. The neural basis of drug craving: an incentive-sensitization theory of addiction. Brain research reviews 1993;18(3):247-291.
[67] Roychowdhury S, Fields H. Endogenous opioids acting at a medullary μ-opioid receptor contribute to the behavioral antinociception produced by GABA antagonism in the midbrain periaqueductal gray. Neuroscience 1996;74(3):863-872.
[68] Samaha A-N, Minogianis E-A, Nachar W. Cues paired with either rapid or slower self-administered cocaine injections acquire similar conditioned rewarding properties. PloS one 2011;6(10):e2648.
[69] Samaha A-N, Robinson TE. Why does the rapid delivery of drugs to the brain promote addiction? Trends in pharmacological sciences 2005;26(2):82-87.
[70] Samineni VK, Grajales-Reyes JG, Copits BA, O'Brien DE, Trigg SL, Gomez AM, Bruchas MR, Gereau IV RW. Divergent modulation of nociception by glutamatergic and GABAergic neuronal subpopulations in the periaqueductal gray. eNeuro 2017;4(2):e0129-0116.2017.
[71] Shavali S, Ho B, Govitrapong P, Sawlom S, Ajjimaporn A, Klongpanichapak S, Ebadi M. Melatonin exerts its analgesic actions not by binding to opioid receptor subtypes but by increasing the release of β-endorphin an endogenous opioid. Brain research bulletin 2005;64(6):471-479.
[72] Stoeber M, Jullié D, Lobingier BT, Laeremans T, Steyaert J, Schiller PW, Manglik A, von Zastrow M. A genetically encoded biosensor reveals location bias of opioid drug action. Neuron 2018;98(5):963-976. e965.
[73] Takasu K, Ogawa K, Nakamura A, Kanbara T, Ono H, Tomii T, Morioka Y, Hasegawa M, Shibasaki M, Mori T. Enhanced GABA ergic synaptic transmission at VLPAG neurons and potent modulation by oxycodone in a bone cancer pain model. British journal of pharmacology 2015;172(8):2148-2164.
[74] Tortorici Vc, Morgan MM, Vanegas H. Tolerance to repeated microinjection of morphine into the periaqueductal gray is associated with changes in the behavior of off-and on-cells in the rostral ventromedial medulla of rats. J Pain 2001;89(2-3):237-244.
[75] Tsien JZ, Chen DF, Gerber D, Tom C, Mercer EH, Anderson DJ, Mayford M, Kandel ER, Tonegawa SJC. Subregion-and cell type–restricted gene knockout in mouse brain. 1996;87(7):1317-1326.
[76] Tu Y, Sun R-Q, Willis WD. Effects of intrathecal injections of melatonin analogs on capsaicin-induced secondary mechanical allodynia and hyperalgesia in rats. Pain 2004;109(3):340-350.
[77] Van Hecke O, Austin SK, Khan RA, Smith B, Torrance N. Neuropathic pain in the general population: a systematic review of epidemiological studies. PAIN 2014;155(4):654-662.
[78] Van Ree JM, Slangen JL, de Wied D. Intravenous self-administration of drugs in rats. Journal of Pharmacology and Experimental Therapeutics 1978;204(3):547-557.
[79] Volpe DA, Tobin GAM, Mellon RD, Katki AG, Parker RJ, Colatsky T, Kropp TJ, Verbois SL. Uniform assessment and ranking of opioid mu receptor binding constants for selected opioid drugs. Regulatory Toxicology and Pharmacology 2011;59(3):385-390.
[80] Wang T, Li S-r, Dai X, Peng Y-l, Chen Q, Wang R. Effects of melatonin on orphanin FQ/nociceptin-induced hyperalgesia in mice. Brain research 2006;1085(1):43-48.

[81] Wilhelmsen M, Amirian I, Reiter RJ, Rosenberg J, Gögenur I. Analgesic effects of melatonin: a review of current evidence from experimental and clinical studies. Journal of pineal research 2011;51(3):270-277.
[82] Williams FG, Mullet MA, Beitz AJ. Basal release of Met-enkephalin and neurotensin in the ventrolateral periaqueductal gray matter of the rat: a microdialysis study of antinociceptive circuits. Brain research 1995;690(2):207-216.
[83] Yosten GL, Harada CM, Haddock C, Giancotti LA, Kolar GR, Patel R, Guo C, Chen Z, Zhang J, Doyle TM. GPR160 de-orphanization reveals critical roles in neuropathic pain in rodents. The Journal of Clinical Investigation 2020;130(5):2587-2592.
[84] Zhang W, Gardell S, Zhang D, Xie JY, Agnes RS, Badghisi H, Hruby VJ, Rance N, Ossipov MH, Vanderah TW. Neuropathic pain is maintained by brainstem neurons co-expressing opioid and cholecystokinin receptors. Brain 2009;132(3):778-787.

3.7 Figures

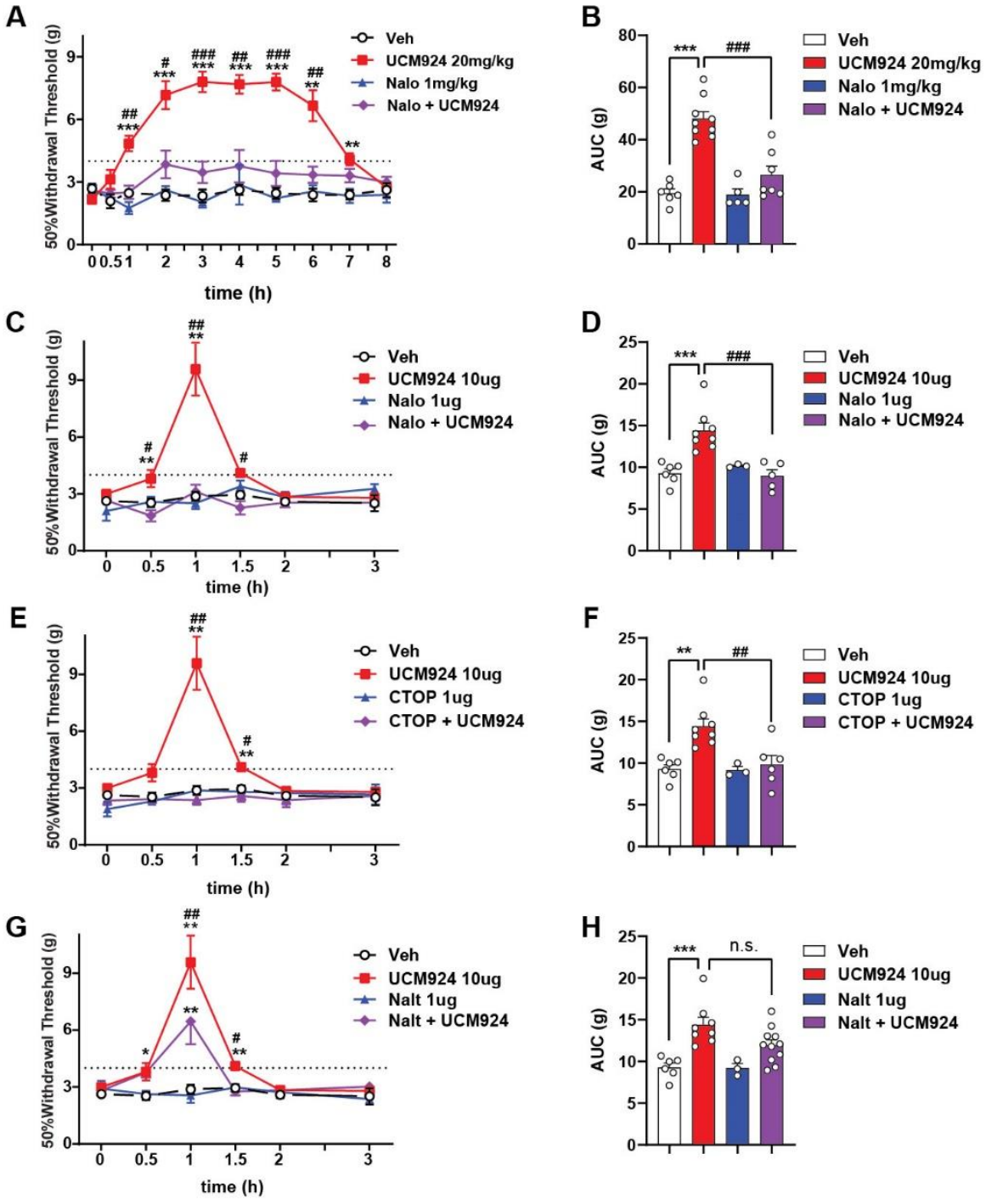

Chapter III - Figure 1. The antiallodynic effect of the MT_2 agonist UCM924 is nullified by the non-selective naloxone and selective MOR antagonist CTOP.

(A) Time course. UCM924 (20 mg/kg, s.c.) increases the paw withdrawal threshold in neuropathic rats. Pretreatment with the non-selective opioid antagonist naloxone (1 mg/kg, s.c.), but not Veh, blocks the UCM924 antiallodynic effect across time. **(B)** Area under the curve (AUC). UCM924 (20 mg/kg, s.c.) produces a significant antiallodynic effect for 7 hours. Pretreatment with naloxone (1 mg/kg, s.c.) reduces the overall UCM924 antiallodynic effect across time. **(C** and **E)** Time course. UCM924 (10 μg, intra-vlPAG) increases the paw withdrawal threshold in neuropathic rats. Pretreatment with naloxone or MOR selective CTOP (1 μg, intra-vlPAG, both), but not Veh, completely blocks the UCM924 antiallodynic effect. **(D** and **F)** AUC. Pretreatment with naloxone or CTOP (1 μg, intra-vlPAG, both) reduces the overall UCM924 antiallodynic effect. **(G)** Time course. Pretreatment with the selective DOR antagonist naltrindole (1 μg, intra-vlPAG), but not Veh, partially blocks the UCM924 antiallodynic effect at 1 hour. **(H)** Area under the curve (AUC). Pretreatment with naltrindole (1 μg, intra-vlPAG) reduces the overall UCM924 antiallodynic effect. Intermittent line on the bottom of **A**, **C**, **E** and **G** represents the threshold cutoff (4 g) for allodynia in SNI rats. Values above this line are considered an antiallodynic effect. Data are expressed as mean ± SEM (n= 8-5 each group). *P < 0.05, **P < 0.01, and ***P < 0.001 vs Veh; #P < 0.05, ##P < 0.01, and ###P < 0.001 vs naloxone/CTOP/naltrindole + UCM924. Data are analyzed using two-way ANOVA (time course) or one-way ANOVA (AUC) followed by Tukey post-hoc test. Detailed data and post hoc analysis are available in Supplementary Table.

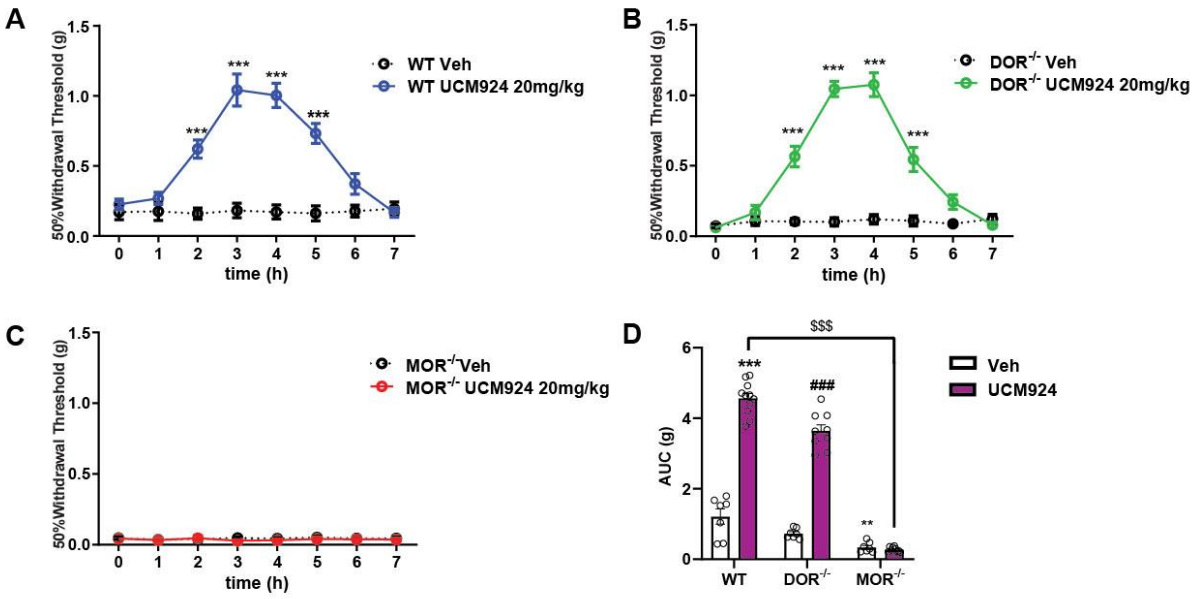

Chapter III - Figure 2. The MT_2 agonist UCM924 does not have anti-allodynic effect in MOR knockout mice.

UCM924 (20 mg/kg, s.c.) increases the paw withdrawal threshold across time in WT (**A**) and $DOR^{-/-}$ (**B**), but not in $MOR^{-/-}$ (**C**) neuropathic mice. (**D**) AUC. UCM924 (20 mg/kg, s.c.) produces an overall antiallodynic effect in WT and $DOR^{-/-}$, but not in $MOR^{-/-}$ neuropathic mice. Data are expressed as mean ± SEM (n= 11-7 each group). **P < 0.01, and ***P < 0.001 vs WT Veh (**A, D**) or $DOR^{-/-}$ Veh (**B**); ###P < 0.001 vs $DOR^{-/-}$ Veh (**D**), $$$ < 0.001 vs WT UCM924 (**D**). Data are analyzed using two-way ANOVA followed by Tukey post-hoc test. Detailed data and post hoc analysis are available in Supplementary Table.

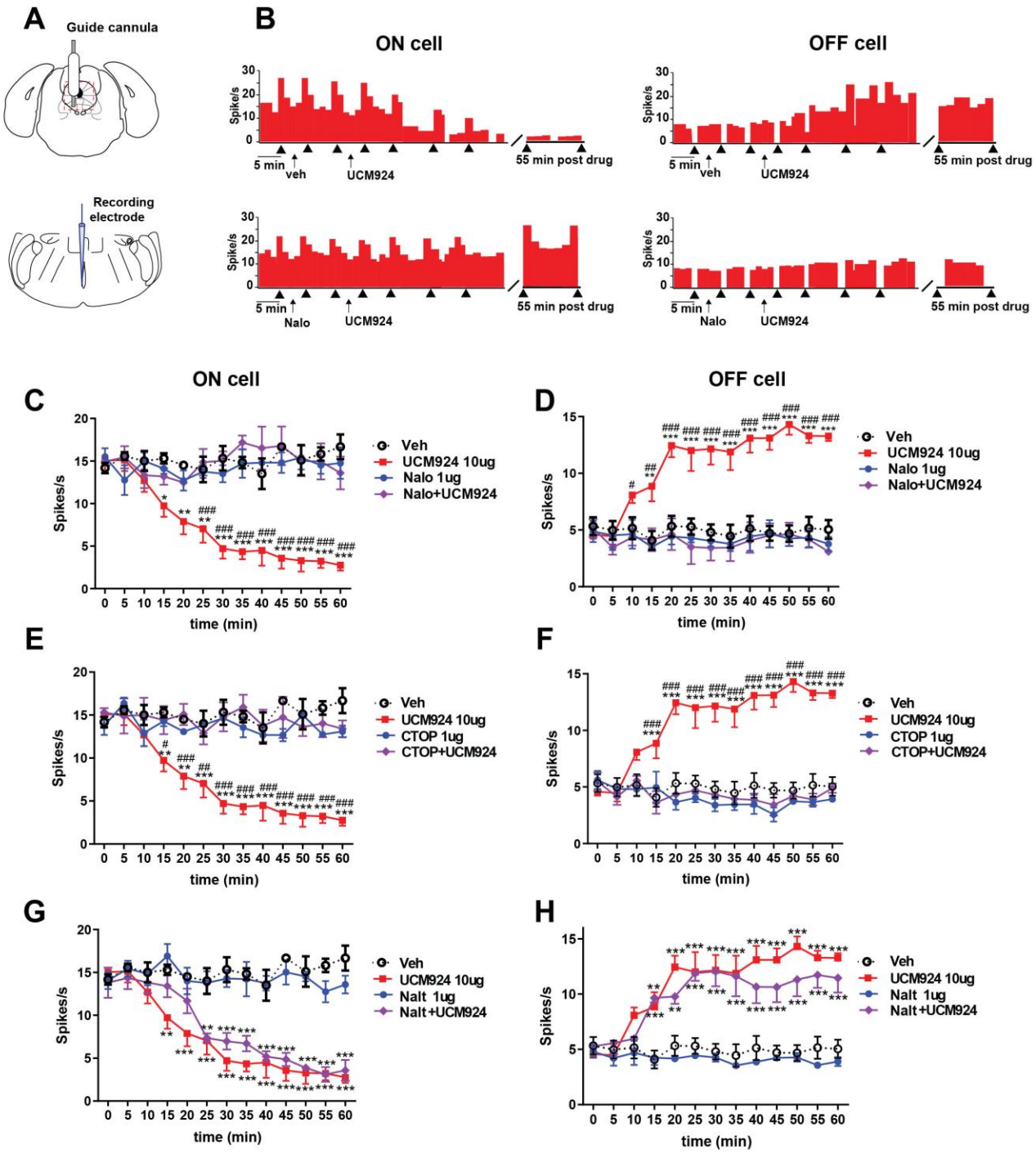

Chapter III - Figure 3. The non-selective naloxone and selective MOR antagonist CTOP block the effects of MT_2 on ON and OFF cells of the PAG-RVM descending antinociceptive pathway.

(A) Schematic illustration of microinjections in the vlPAG site (top) and of site of the electrophysiological recording in the RVM (bottom). **(B)** Firing rate histogram of a single ON (top left) and OFF (top right) neuron of the RVM after Veh followed by UCM924 microinjections; and of a single ON (bottom left) and OFF (bottom right) neuron of the RVM after naloxone followed by UCM924 microinjections. Scale bars indicate 5 minutes for ratemater records, whereas arrowheads indicate the noxious stimulation. UCM924 (10 μg, intra-vlPAG) decreases spontaneous firing rate activity of ON cells (**C**, **E, G**) and increases the firing activity of OFF cells (**D**, **F, H**) across time in neuropathic rats. Pretreatment with 1μg intra-vlPAG of naloxone (**C-D**) and CTOP (**E-F**), but not naltrindole (**G-H**), blocked the UCM924-induced modulation of ON (**C**, **E, G**) and of OFF cells (**D**, **F, H**). Data are expressed as mean ± SEM for n= 4-2 each group (**C-H**). *P < 0.05, **P < 0.01, and ***P < 0.001 vs Veh; ##P < 0.01, and ###P < 0.001 vs naloxone or CTOP + UCM924. Two-way ANOVA followed by Tukey post-hoc test. Detailed data and post hoc analysis are available in Supplementary Table.

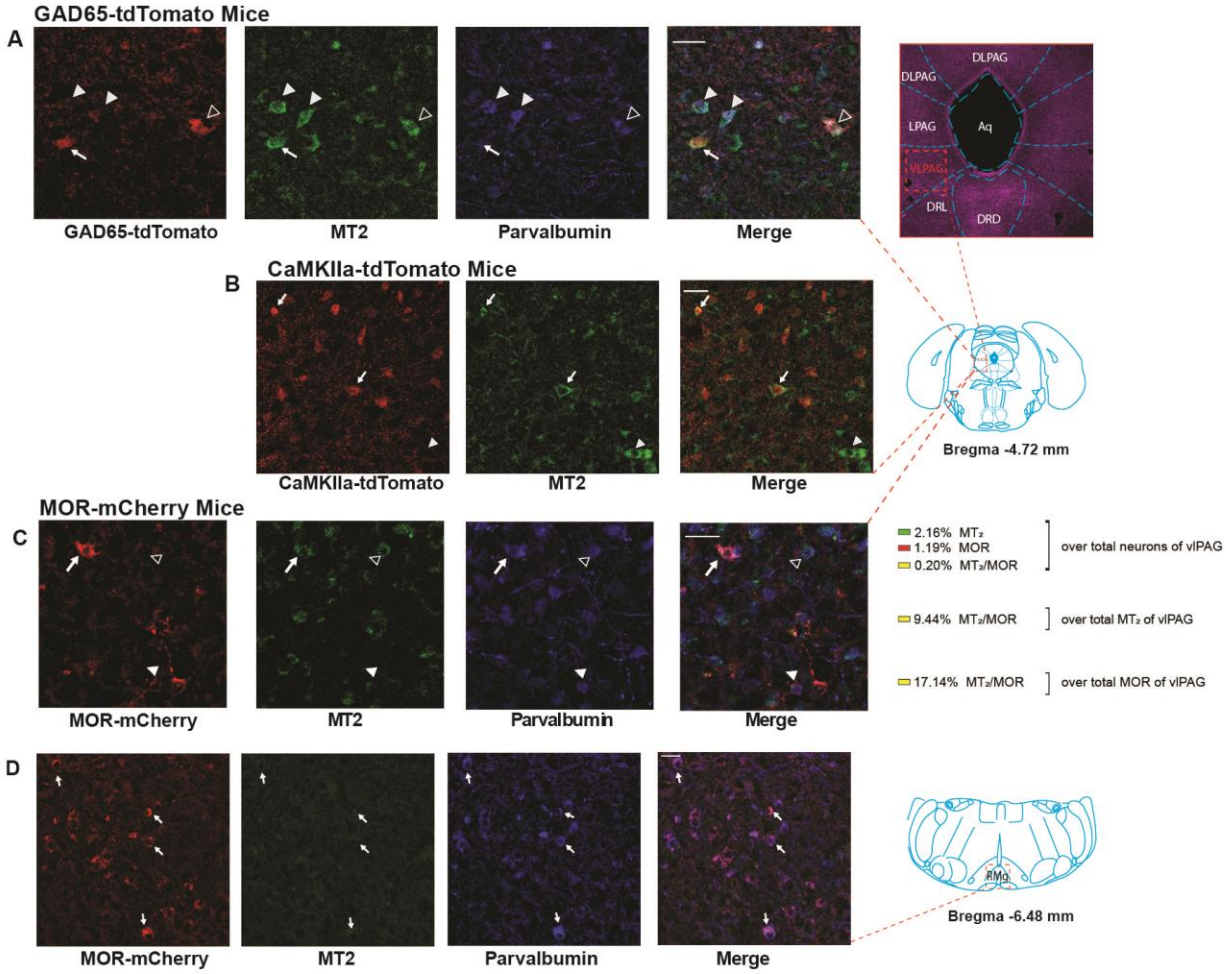

Chapter III - Figure 4. MT_2 receptors and MORs expression in the PAG-RVM descending pathway.

(**A**) MT_2 receptors are expressed in GAD65-tdTomato$^+$ neurons of the vlPAG, and this colocalization was observed particularly in parvalbumin (PV) inhibitory expressing interneurons. (**B**) MT_2 receptors are expressed in CaMKIIα^+ neurons, an excitatory neuronal promoter of the adult forebrain. (**C**) MOR-mCherry, MT_2 receptor and inhibitory PV$^+$ GABAergic neurons are expressed in vlPAG. Both MOR-mCherry (filled arrowhead) and MT_2 (empty arrowhead) colocalize with PV$^+$ GABAergic neurons. Counting: 2.16 ± 0.32% of MT_2 receptor and 1.19 ± 0.18% of MOR-mCherry are expressed in the total neural cell body population of the vlPAG. Colabel MT_2^+/MOR-mCherry$^+$ neurons are 0.20 ± 0.02 % of the total neuronal population (arrow). (**D**) MT_2 receptors are poorly expressed in the RVM, while MORs are abundantly localized in this area. Scale bars: 25 µm.

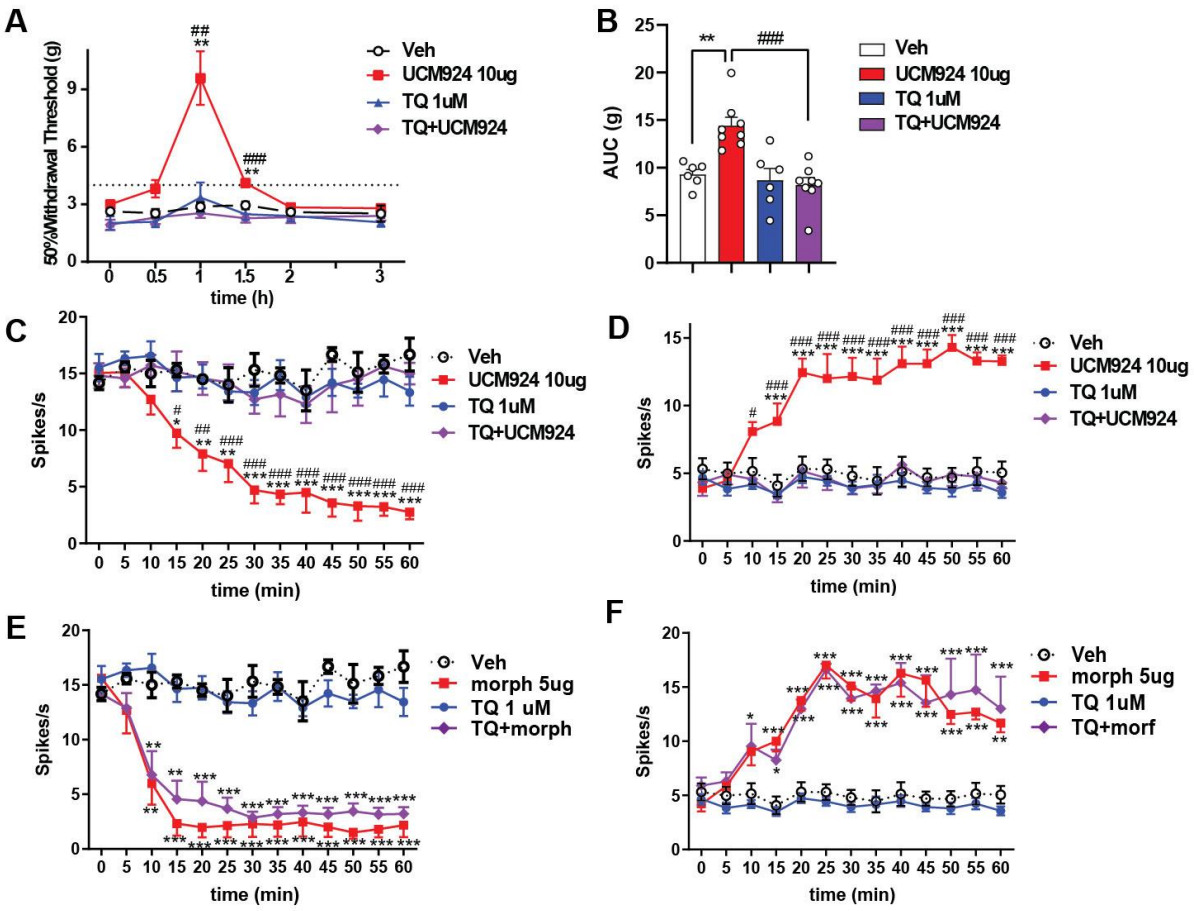

Chapter III - Figure 5. The inwardly-rectifying potassium channels (GIRKs) involvement in the antiallodynic effects and modulation of ON/OFF cells induced by UCM924 and morphine.

Pre-administration of GIRK1/4 blocker tertiapine-Q (T-Q 1 µM intra-vlPAG) prevents the antiallodynic effect of UCM924 (**A-B**), blocked the UCM924-induced modulation of ON (**C**) and OFF (**G**) cells. Morphine (5 µg, intra-vlPAG) decreases spontaneous firing rate of ON cells (**E**) and increases the firing activity of OFF cells (**F**) in neuropathic rats. Pretreatment with GIRK1/4 blocker T-Q (1 µM intra-vlPAG) did not block the morphine-induced modulation of ON (**E**) and OFF (**F**) cells. Intermittent line on the bottom of E represents the threshold cutoff (4 g) for allodynia in SNI rats. Values above this line are considered an antiallodynic effect. Data are expressed as mean ± SEM for n= 8-6 each group (**A, B**) or n= 4-2 each group (**C-F**). *P < 0.05, **P < 0.01, and ***P < 0.001 vs Veh; #P < 0.05 ##P < 0.01, and ###P < 0.001 vs T-Q + UCM924. Two-way (**A, C, D, E, F**) or one-way (**B**) ANOVA

followed by Tukey post-hoc test. Detailed data and post hoc analysis are available in Supplementary Table.

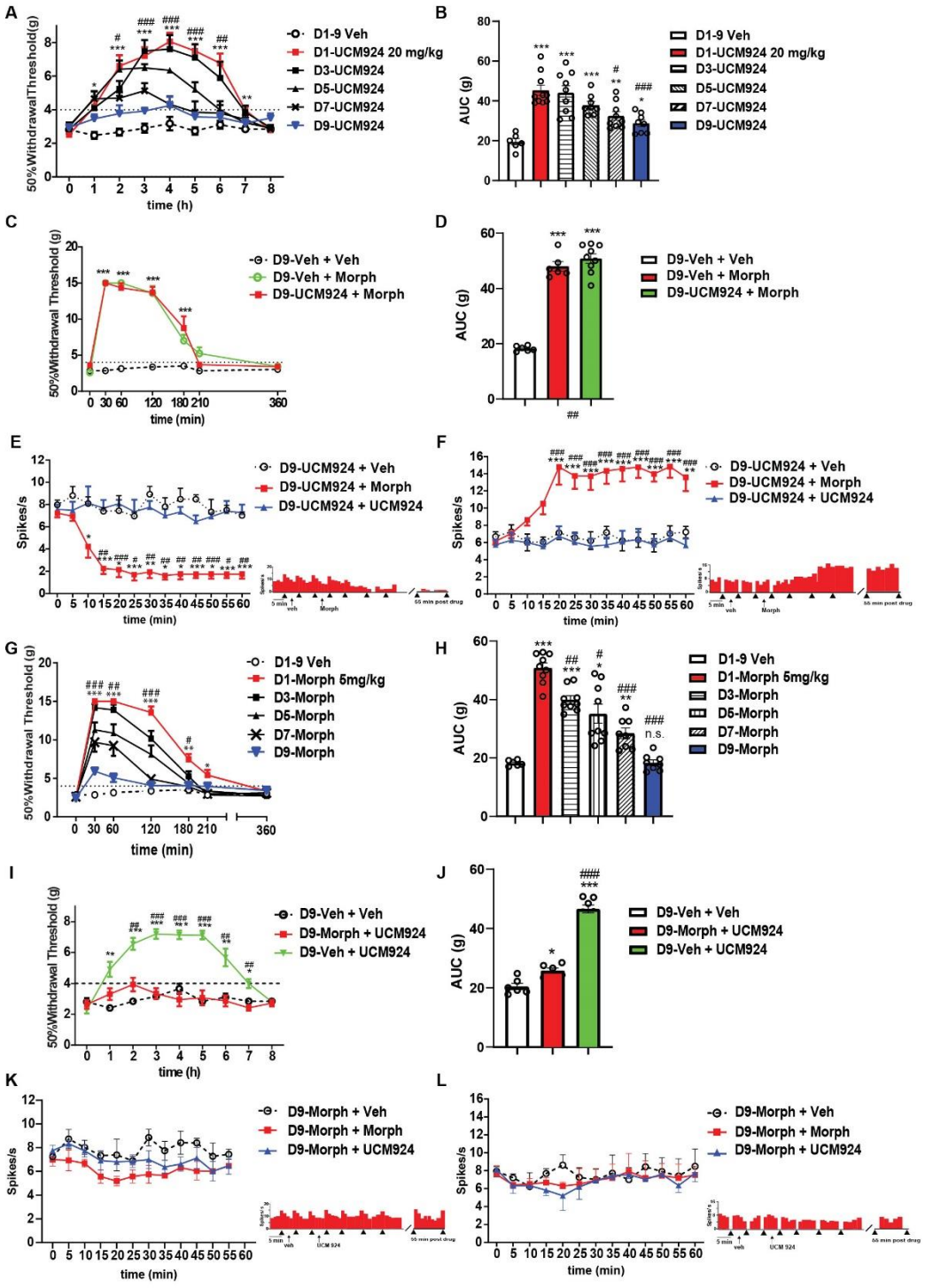

Chapter III - Figure 6. Cross-tolerance after repeated MT_2 and MOR agonists administration.

Repeated UMC924 administration (D1-D9 UCM924, 20 mg/kg, s.c., once daily for 9 days) results in a decrease of antiallodynic effect (**A**: time course; **B**: AUC). Acute morphine injection after repeated administration of UCM924 (D9-UCM924+ Morph, 5 mg/kg, s.c.) increases the paw withdrawal threshold (**C**) and the AUC (**D**) in neuropathic rats treated 9-day with UCM924.

Microinjection of morphine (D9-UCM924+ Morph, 5 μg, intra-vlPAG), but not UCM924 (D9-UCM924+ UCM924 10 μg), decreases spontaneous firing rate of ON cells (**E**) and increases the firing activity of OFF cells (**F**) after 9 day treatment with UCM924.

Repeated morphine administration (D1-D9 Morph, 5 mg/kg, s.c., twice daily for 9 days) resulted in a decrease of antiallodynic property (**G**: time course; **H**: AUC) leading to tolerance. Acute administration of the UCM924 after 9-day treatment with morphine (D9-Morph+UCM924, 20 mg/kg, s.c.) failed to increase the paw withdrawal threshold across time (**I**), but showed a slight increase in the AUC compared to vehicle treated (D9-Veh+Veh, **J**). UCM924 (D9-Morph+UCM924, 10 μg, intra-vlPAG) failed to decrease spontaneous firing rate of ON cells (**K**) as well as to increase the firing activity of OFF cells (**L**) in rats with 9-day morphine treatment. Intermittent line on the bottom of **A, C, G** and **I** represents the threshold cutoff (4 g) for allodynia in SNI rats. Values above this line are considered an antiallodynic effect. Data are expressed as mean ± SEM for n=10-6 (**A, B, C, D, G, H**) and n= 4-3 each group (**E, F, K, L**). *P < 0.05, **P < 0.01, and ***P < 0.001 vs D1-9 Veh (**A, B, G, H**) or vs D9-Veh+Veh (**C, D, I, J**) or D9-UCM924 + Veh (**E, F**); #P < 0.05, ##P < 0.01, and ###P < 0.001 vs D9-UCM924 (**A, B**) or D9-UCM924 + UCM924 (**E, F**) or D9-Morph (**G, H**) or D9-Morph + UCM924 (**I, J**). Two-way (**A, C, D, E, F, G, I, K, L**) or one-way (**B, D, H, J**) ANOVA followed by Tukey (**A, C, E, F, G, I, J, K, L**) or Dunnet (**B, D, H**) post hoc test. Detailed data and post hoc analysis are available in Supplementary Table.

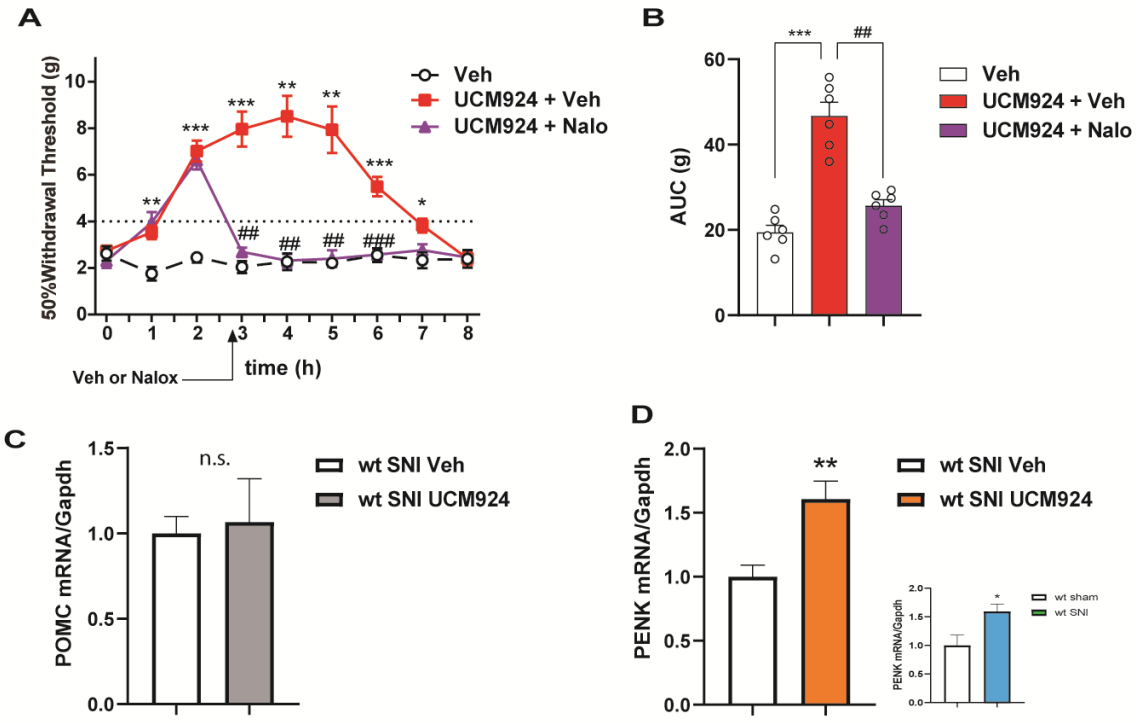

Chapter III - Figure 7. UCM924 antiallodynic effect is reverted post administration of naloxone and increases the PENK gene expression in the PAG of neuropathic mice.

(A) Time course. Naloxone (1 mg/kg, s.c.) administration *post* UCM924 (20 mg/kg, s.c.) reverses the increased paw withdrawal threshold in neuropathic mice. **(B)** AUC. Naloxone administration *post* UCM924 reduces the overall UCM924 antiallodynic effect across time. **(C-D)** UCM924 (20 mg/kg, s.c.) increases the relative PENK, but not POMC, mRNA level in the PAG in SNI mice. **(D indent)** In SNI neuropathic mice the basal level of PENK mRNA is increased compared to sham animals. Data are expressed as mean ± SEM for n= 6-5 each group (**A, B**) or n= 4 each group (**C-D**). *P < 0.05, **P < 0.01, and ***P < 0.001 vs Veh (**A, B**) or vs wt SNI Veh (**D**) or vs wt sham (**D indent**); ##P < 0.01, and ###P < 0.001 vs UCM924 + Veh. Two-way (**A**) or one-way (**B**) ANOVA followed by Tukey post-hoc test or Student's t-test (**C-D**). Detailed data and post hoc analysis are available in Supplementary Table.

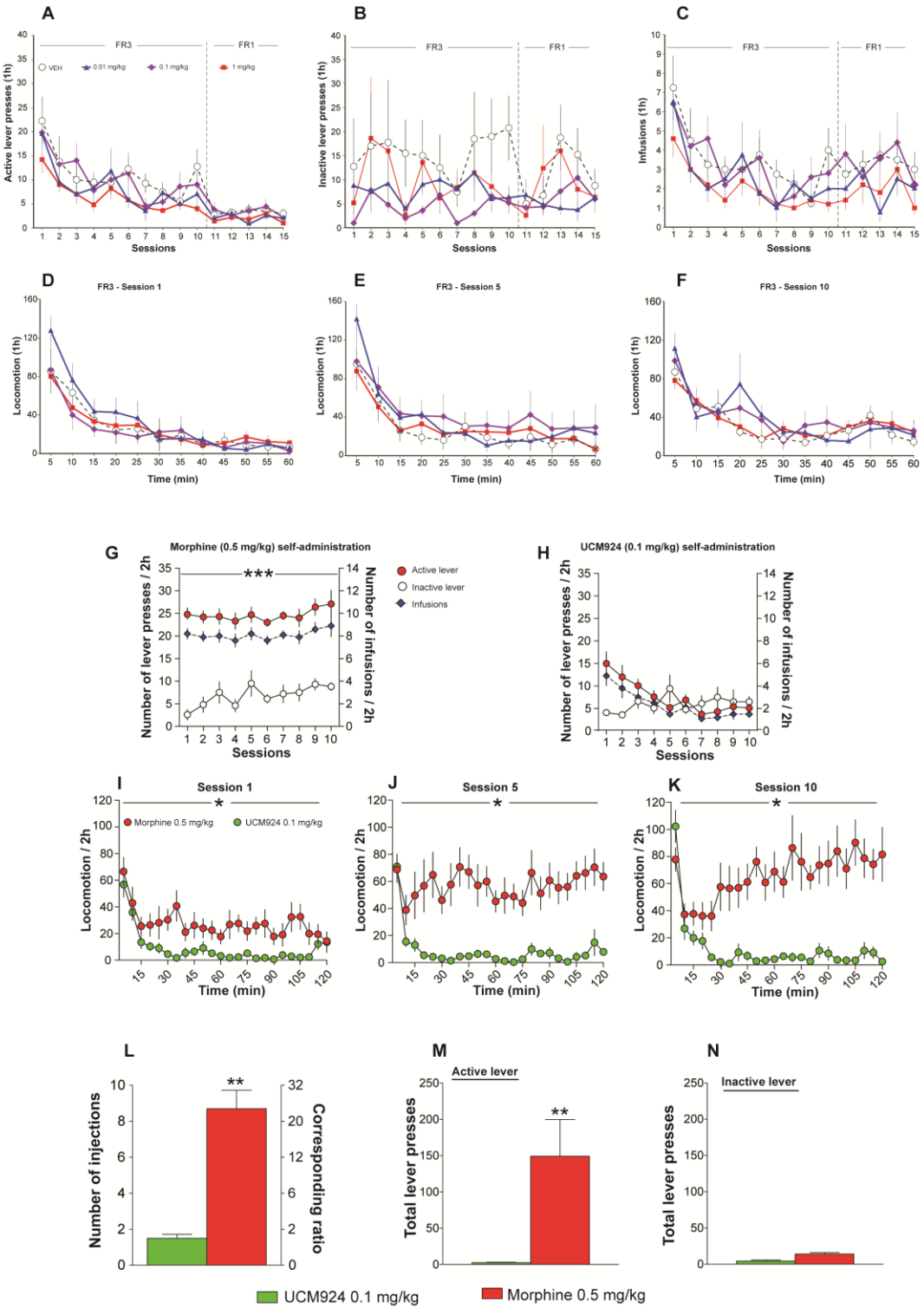

Chapter III - Figure 8. Intravenous self-administration with UCM924 (dose-response) and UCM924 vs Morphine.

Number of active (**A**) and inactive (**B**) lever presses is similar in rats given access to UCM924 compared to vehicle controls. Control and UCM924 rats also earned a similar number of infusions (**C**) and displayed similar locomotor activity on session 1 (**D**), session 5 (**E**) and session 10 (**F**). All data are mean ± SEM. Vehicle, n = 4; UCM924 0.01 mg/kg, n = 4; 0.1 mg/kg, n = 5; and 1 mg/kg, n = 5. Thus, across a range of doses and schedules of reinforcement, rats do not self-administer UCM924 more than vehicle, and UCM924 does not have significant locomotor effects. Rats reliably self-administer morphine (**G**) but not UCM924 (**H**). (**G**) The morphine (0.5 mg/kg/infusion) rats pressed significantly more often on a lever that delivered the drug (active) than on a lever that did not (inactive). (**H**) The UCM924 (0.1 mg/kg/infusion) rats did not press a similar number of times on a lever that delivered UCM924 (active) and on a lever that did not (inactive). (**I-K**) Morphine rats showed greater locomotor activity than UCM924 rats did, and only morphine rats developed psychomotor sensitization over the 10 self-administration sessions. Under a progressive ratio schedule of reinforcement, (**L**) rats self-administering morphine took more drug injections and (**M**) pressed more often on the active lever than rats self-administering UCM924 did. (**N**) There was no group difference in inactive lever presses. Thus, rats show greater incentive motivation for morphine (0.5 mg/kg/infusion) than for UCM924 (0.1 mg/kg/infusion). All data are mean ± SEM. Morphine, n = 10; UCM924, n = 10. *** $P < 0.001$, Active > inactive lever presses. ** $P < 0.05$, Morphine vs UCM924 rats. Detailed data and post hoc analysis are available in Supplementary Table.

3.8 Supplemental Figures:

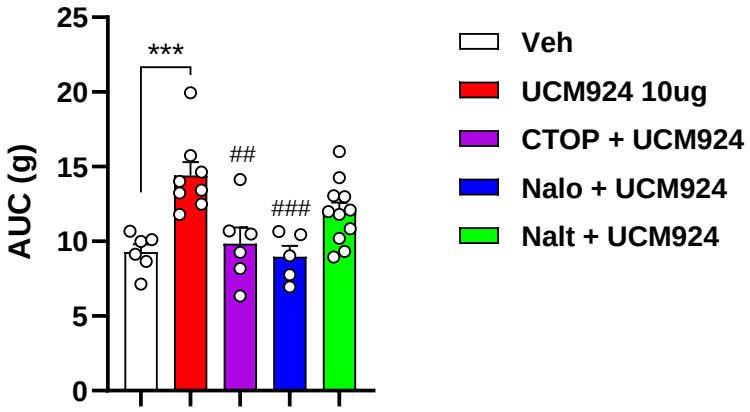

Chapter III - Figure. S1. The non-selective Naloxone and selective MOR antagonist CTOP block the MT_2 receptor-induced mechanical antiallodynia.

AUC. Intra-vlPAG naloxone and CTOP fully block the UCM924 antiallodynic effect in SNI rats, while naltrindole do not. Data are expressed as mean ± SEM (n= 5-11 each group). ***P < 0.001 vs Veh; ##P < 0.01, and ###P < 0.001 vs UCM924. One-way ANOVA followed by Tukey post-hoc test. Detailed data and post hoc analysis are available in Supplementary Table.

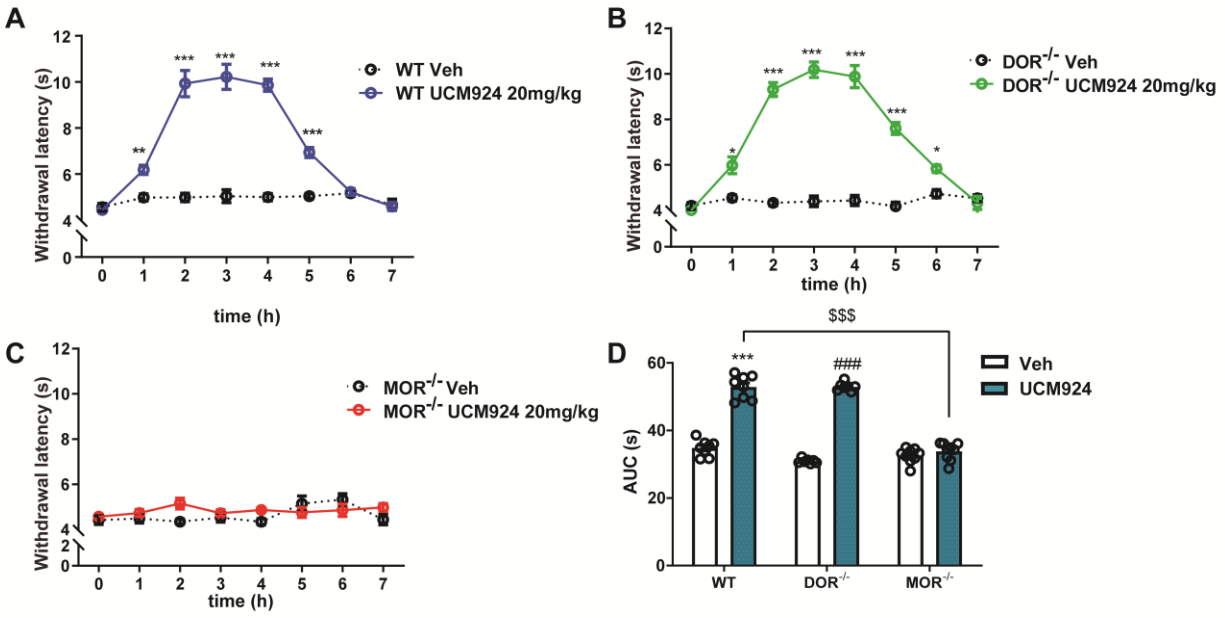

Chapter III - Figure S2. MOR, but nor DOR, genetic deletion prevents the MT_2 agonist-induced cold antiallodynia.

(A-C) Time course. UCM924 (20 mg/kg, s.c.) increases the paw withdrawal latency in WT **(A)** and $DOR^{-/-}$ **(B)**, but not in $MOR^{-/-}$ **(C)** neuropathic mice. **(D)** AUC. UCM924 (20 mg/kg, s.c.) produces a cumulative antiallodynic effect in WT and $DOR^{-/-}$, but not in $MOR^{-/-}$ neuropathic mice. Data are expressed as mean ± SEM (n= 9-7 each group). **P < 0.01, ***P < 0.001 vs WT Veh **(A)** or $DOR^{-/-}$ Veh **(B).** ***P < 0.001 vs WT Veh **(D),** ###P < 0.001 vs $DOR^{-/-}$ Veh **(D)** and $^{\$\$\$}$ P < 0.001 vs WT UCM924. Two-way ANOVA followed by Tukey post-hoc test. Detailed data and post hoc analysis are available in Supplementary Table.

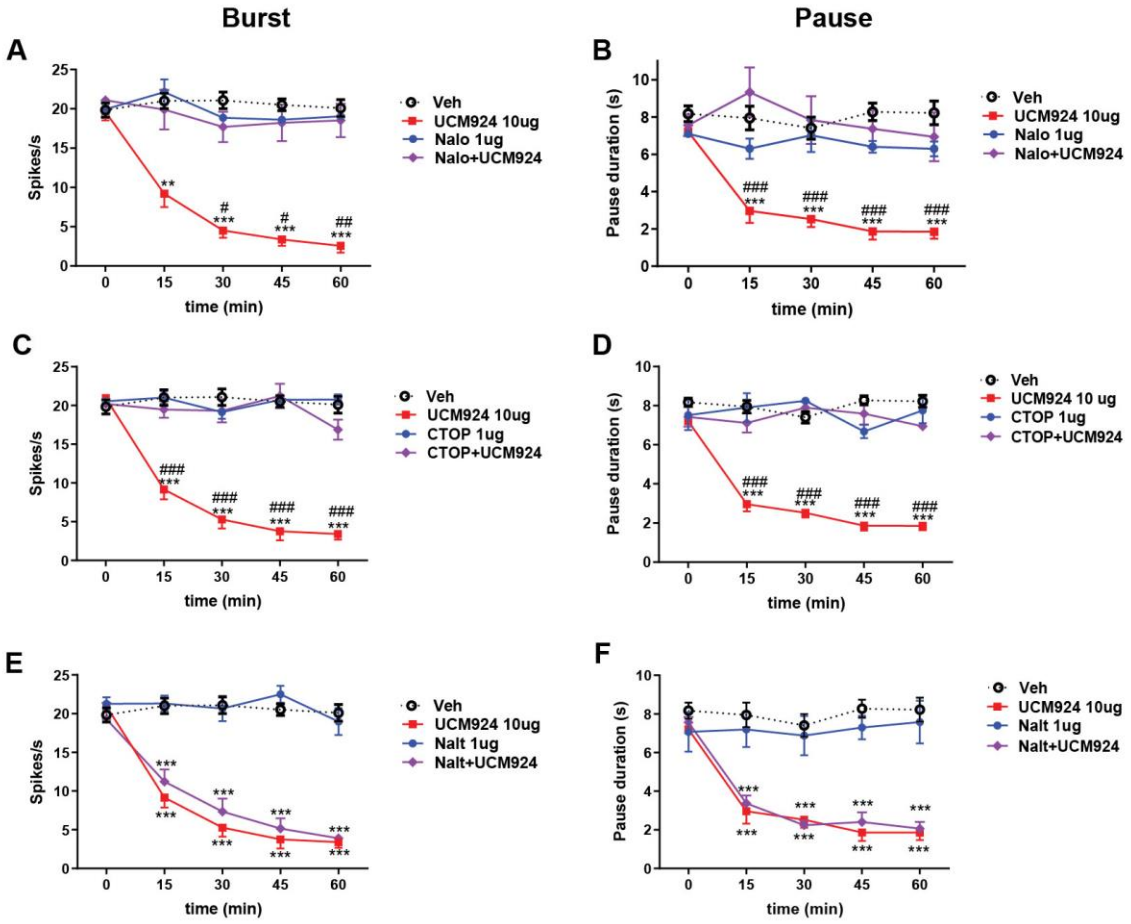

Chapter III - Figure S3. The non-selective naloxone and selective MOR antagonist CTOP block the effects of the MT_2 agonist UCM924 on ON cell burst and OFF cell pause of the PAG-RVM descending antinociceptive pathway.

UCM924 (10 µg, intra-vlPAG) reduces the burst activity of ON cell burst (**A**, **C** and **E**) and the pause of OFF cell pause (**B**, **D** and **F**) across time in neuropathic rats. Pretreatment with 1 µg intra-vlPAG of naloxone (**A-B**) and CTOP (**C-D**), but not naltrindole (**E-F**), blocked the UCM924-induced modulation of ON cells' burst (**A**, **C** and **E**) and of OFF cell's pause (**B**, **D** and **F**) cells. Data are expressed as mean ± SEM for n= 4-2 each group. **P < 0.01, and ***P < 0.001 vs Veh; #P < 0.05, ##P < 0.01, and ###P < 0.001 vs naloxone/CTOP/naltrindole + UCM924. Two-way ANOVA followed by Tukey post-hoc test. Detailed data and post hoc analysis are available in Supplementary Table.

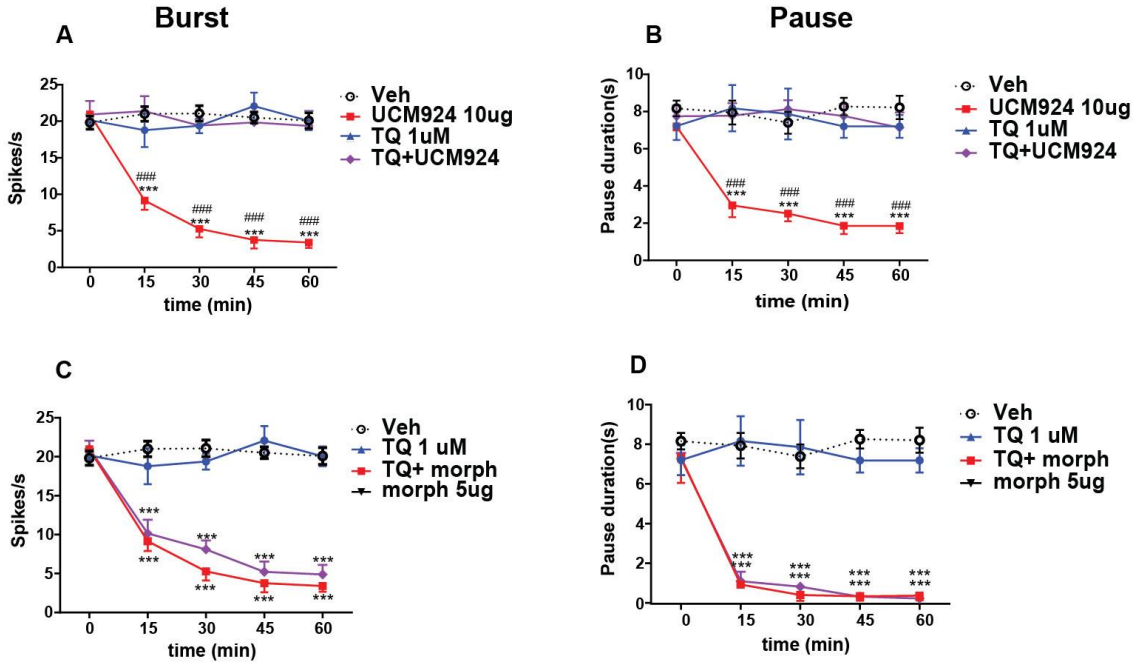

Chapter III - Figure S4. Inwardly-rectifying potassium channels (GIRKs) mediate UCM924-, but not morphine-induced modulation of ON cell burst and OFF cell pause. UCM924 (10 µg, intra-vlPAG) and morphine (5 µg intra-vlPAG) both reduce the burst activity of ON cell (**A, C**) and the pause of OFF cell pause (**B, D**) across time in neuropathic rats. Pretreatment with GIRK1/4 blocker T-Q (1 µM intra-vlPAG) blocks the modulation of the burst and pause produced by UCM924 (**A, B**), but not by morphine (**C, D**). Data are expressed as mean ± SEM for n= 4-2 each group. ***P < 0.001 vs Veh; ###P < 0.001 vs T-Q + UCM924. Two-way ANOVA followed by Tukey post-hoc test. Detailed data and post hoc analysis are available in Supplementary Table.

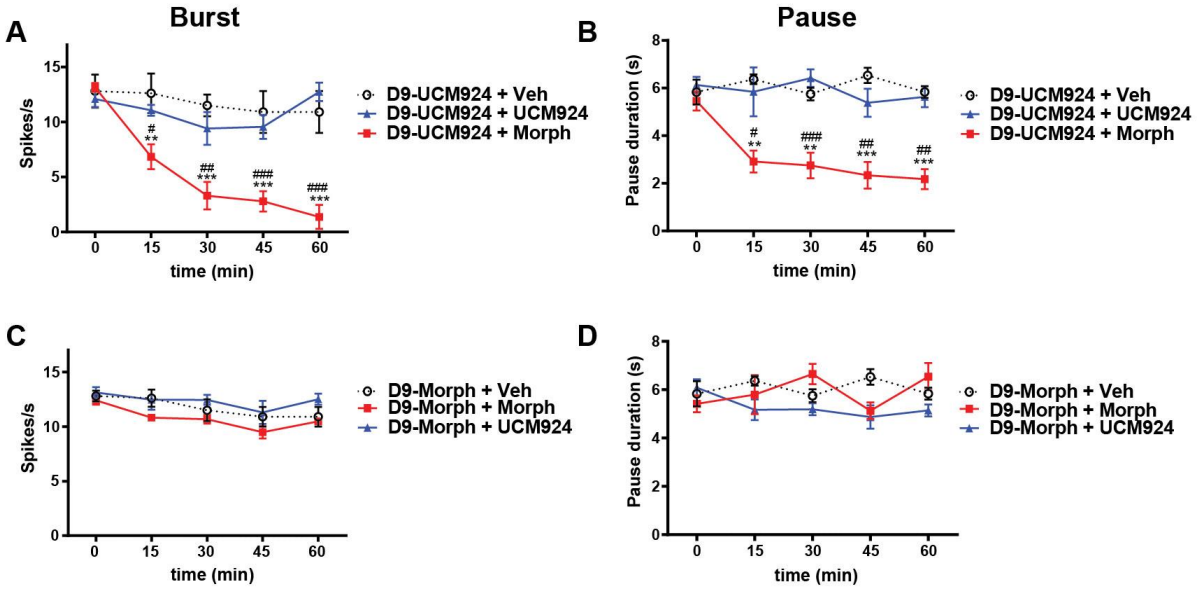

Chapter III - Figure S5. Effects of repeated MT_2 and MOR agonists administration and cross-tolerance analysis of ON cell burst and OFF cell pause modulation.

Morphine (5 µg, intra-vlPAG) decreases the burst activity of ON cells (**A**) and reduces the pause of OFF cells (**B**) after 9 days of treatment with UCM924 (20 mg/kg, s.c.). UCM924 (10 µg, intra-vlPAG) failed to reduce the burst activity of ON cells (**C**) as well as to reduce the pause of OFF cells (**D**) after 9 days of treatment with morphine (5 mg/kg, intra-vlPAG, twice daily). Data are expressed as mean ± SEM for n= 4-3 each group. **P < 0.01, and ***P < 0.001 vs D9-UCM924+Veh; #P < 0.05, ##P < 0.01, and ###P < 0.001 vs D9-UCM924+UCM924. Two-way ANOVA followed by Tukey post-hoc test. Detailed data and post hoc analysis are available in Supplementary Table.

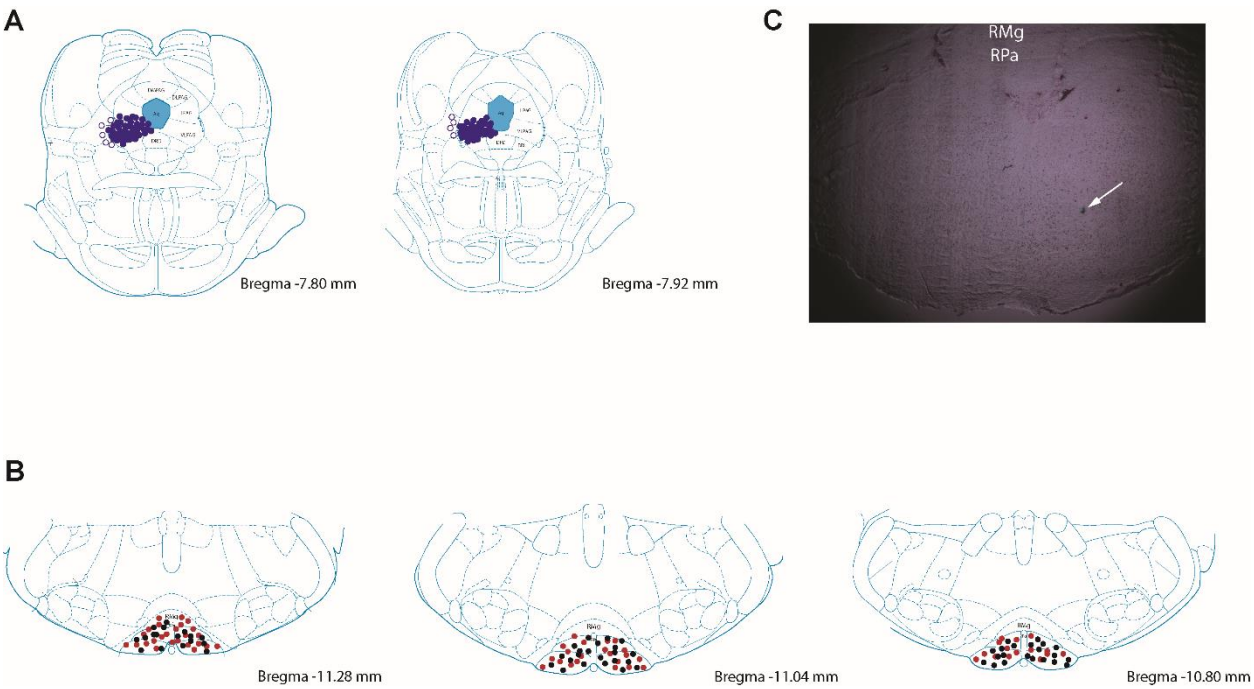

Chapter III - Fig S6. Schematic illustration of the location of vlPAG and RVM microinjection sites.

(**A**) Vehicle or drug(s) microinjections were performed in the left vlPAG (filled blue circle). The open circle indicates microinjections accidentally or intentionally performed outside of vlPAG and were excluded from the analysis. (**B**) Neuronal recordings were performed by lowering a glass electrode into the RVM. ON cells (red circles) or OFF cells (black circles) recording sites are shown. Some sites are not shown because of symbol overlapping. Distances from the bregma are indicated. (**C**) Representation of coronal sections of the rat brain with the photomicrograph of the recording site in the RVM. Raphe magnus nucleus (RMg); raphe pallidus nucleus (RPa). The white arrow indicates the site of the electrode recording labeled with pontamine sky blue dye.

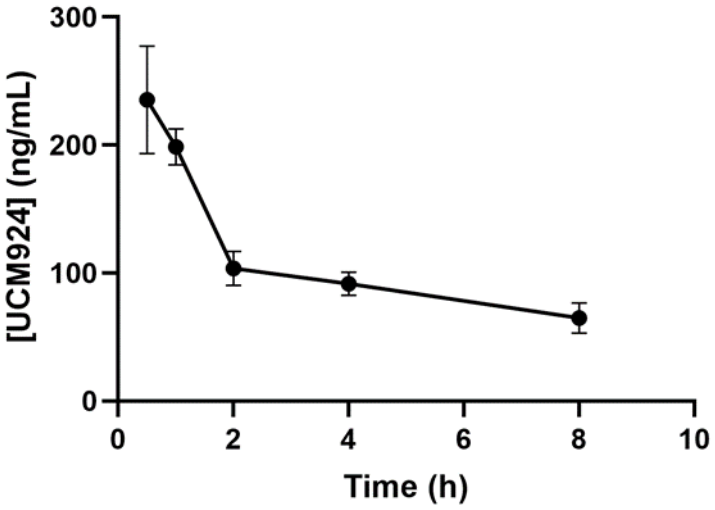

Chapter III - Figure S7. Pharmacokinetic of the MT_2 partial agonist UCM924.

Three SD rats were s.c. injected with 20 mg/kg of UCM924 (diluted in 70% DMSO and 30% saline) and blood was collected after 0.5, 1, 2, 4 and 8 hours after injection.

Appendix to Chapter III

3.9 Introduction

In order to better understand the behavioural self-administration results exposed in chapter III showing the lack of rewarding effects of UCM924, we further investigated the response of the MT_2 receptor stimulation in the reward/motivation circuit.

The neurotransmitter dopamine (DA) is the most widely explored underpinning mechanisms to drug addiction due to reward/motivation mechanisms in the mesocorticolimbic components which include the ventral tegmental area (VTA) and nucleus accumbens (NAc) (Fields and Margolis 2015; Koob and Volkow 2016; Robinson and Berridge 2008). Systemic and local VTA injection of MOR agonists like morphine showed an increased dopamine release in the ventral striatum (Di Chiara and Imperato 1988; Spanagel et al. 1992) and to enhance the firing rate of DA neurons in the VTA (Gysling and Wang 1983; Jalabert et al. 2011). Moreover, MORs are located on GABA neurons within the VTA and opioid-induced disinhibition of adjacent DA neurons (Johnson and North 1992; Margolis et al. 2014).

Based on these considerations, we examined the effects of the MT_2 partial agonist UCM924 administration on DA neurons in the VTA using *in vivo* electrophysiological recordings, and the expression of the MT_2 receptor in the VTA.

3.10 Materials and methods

Animals

Adult male Sprague-Dawley rats (Charles River, Ste. Constant, Quebec, Canada), weighing between 260 g and 330 g were used for in vivo electrophysiology. Rats were housed 2 per cage

under standard laboratory conditions (12 h light : 12 hr dark cycle, lights on at 07:00; temperature approximately 20˚C; 50-60% relative humidity; free access to food and water). All procedures were performed in compliance with the standards and ethical guidelines mandated by the Canadian Institutes for Health Research, the Canadian Council on Animal Care, and the McGill Comparative Medicine and Animal Resources Centre.

Drug delivery

N-{2-[(3-bromophenyl)-(4-fluorophenyl)amino]}ethylacetamide (Rivara et al. 2009) were all dissolved in a vehicle (Veh) composed of 70% dimethylsulfoxide (MP Biochemicals, Solon, OH, USA) and 30% saline. The dose of UCM924 was chosen according to our recent study (Lopez-Canul et al. 2015) and no endothelial damage was revealed at this concentration of DMSO. UCM924 was injected at doses of 10 mg/kg up to a maximum of 40 kg/mg. Intravenous (i.v.) injection of vehicle preceded injections of UCM924. Apomorphine (Sigma-Aldrich, St-Louis, MO), a non-selective dopamine (DA) agonist, was dissolved in 0.9% saline and injected i.v., with injections of 30 µg/kg up to a maximum dose of 120 µg/kg, after UCM924 (apomorphine inhibits spontaneous firing of DA neurons). Haloperidol (Sigma-Aldrich), a D2 receptor antagonist, was also injected, following apomorphine, at doses of 50 µg/kg up to a maximum of 100 µg/kg (haloperidol increases spontaneous firing of DA neurons). Intravenous (i.v.) administration of all drugs was carried out using a catheter inserted into the lateral tail vein. The maximum volume for a single i.v. injection was 0.1 ml (infused in approximately 1 minute).

In vivo Electrophysiological Recording

In vivo extracellular single-unit recordings of presumed dopamine (DA) neurons in the ventral tegmental area (VTA) were performed to study the modulatory effects of acute administration of the novel selective MT_2 partial agonist UCM924 on DA neuronal firing and burst activity in the VTA. The following methods were adapted from (Domínguez-López et al. 2014; Gobbi et al. 2001).

Preparation for electrophysiological experiments

Adult male Sprague-Dawley rats were anesthetized with chloral hydrate (400 mg/kg, i.p.) and mounted in a stereotaxic apparatus (Stoelting Instruments) with the skull positioned horizontally. A full anesthetic state was confirmed by the absence of a nociceptive reflex reaction to a paw or tail pinch and the absence of an eye blink response to applied pressure. Animals were continuously monitored and supplemental chloral hydrate injections (100 mg/kg, i.p.) were administered as needed to maintain an anesthetic state. Rat body temperature was maintained at approximately 37˚C throughout the experiment using a heating pad. Single-barreled glass micropipettes with an internal diameter of 1.5 mm (Harvard Apparatus, St-Laurent, QC, Canada) were pulled to a length of approximately 1 cm in a Narashige PE-2 pipette puller (Tokyo, Japan) and were preloaded with fiberglass strands to promote filling with 2% pontamine sky blue dye in 0.5 M sodium acetate solution (pH 7.5). The electrode tips were broken down under microscopic control to diameters of 1–3 μm with impedances ranging between 4–8 MΩ.

Single-unit extracellular recordings of VTA DA neurons

The VTA is the principal source of DA innervation in the brain. To record from the VTA, an incision was made in the scalp. A burr hole was drilled above the VTA, according to the stereotaxic coordinates in Paxinos and Watson's atlas (2013); A-P: 3.4 to 4.1 mm from the interaural line;

lateral: 0.6 mm to 1.1 mm from the midline. A hydraulic micropositioner (model 650; David Kopf Instruments) was used to lower the electrode into the VTA to a depth between 7.5 to 8.8 mm. The electrode was slowly advanced (approximately 0.15 mm/min) until a clear neuronal signal was isolated. Presumed DA neurons were identified according to well-established electrophysiological properties: low and irregular firing rate (0.5–5 Hz) with a characteristic low burst activity, a triphasic action potential with a marked negative deflection, a long duration (>2.5 ms), and a characteristic notch on the rising phase (Grace and Bunney 1983; Ungless and Grace 2012; Labonte et al. 2012). An inhibitory response to the injection of apomorphine, a DA agonist (injected after UCM924 or vehicle), as well as an excitatory response to the injection of haloperidol, a D2 antagonist (injected after apomorphine), also ensured that recorded neurons were dopaminergic. 2-4 electrode descents were carried out in order to achieve maximum sampling of the VTA DA neurons. Single-unit activity was recorded as discriminated action potentials using a single-barreled glass micropipette. The analog signal was converted into a digital signal using a 1401 Plus interface (CED, Cambridge Electronic Design, Cambridge, UK) and was analyzed off-line using Spike 2 software (CED, Cambridge Electronic Design, Cambridge, UK). Changes in neuronal firing activity and pattern resulting from drug injections were monitored continuously (200s intervals were analyzed) but the first 30s following injections were not considered to minimize artifacts caused by the injection.

DA burst activity

DA burst activity was categorized by a train of at least two spikes with an initial interspike interval of ≤80 ms and the longest interspike interval (ISI) allowed with bursts being ≤160 ms, within a regular low-frequency firing pattern and decreased amplitude from the first to the last spike within the burst (Domínguez-López et al. 2014; Ungless and Grace 2012). Burst parameters studied were:

number of bursts per 200s, percentage of spikes occurring in bursts, number of spikes/burst, burst interspike interval, and bursts length.

Histological Verification

At the end of experiments, the recording site was marked by iontophoretic ejection by passing a positive current of 20 µA for 10 minutes through the recording pipette. To verify that the recorded neurons were in fact dopaminergic, the rat brains were sliced at -22°C into 50µm-thick cross-sections using a cryostat (CM30505, Lieca Microsystems, Wetzlar, Germany) and sections were mounted on glass slides. The slides were studied using an Olympus (Olympus America, Center Valley, PA) digital camera attached to an Olympus CX41 microscope to confirm that the iontophoretic ejection was correctly localized at the VTA.

Tissue preparation and immunohistochemistry

Rats were anesthetized with sodium pentobarbital (100 mg/kg, i.p.) and perfused intracardially with 50 ml of freshly prepared, ice-cold 4% paraformaldehyde in 0.1 M phosphate buffer (PB) pH 7.4 for 15 minutes at 10mL/min using a peristaltic pump. Brains were dissected and post-fixed for 24 h at 4 °C in 4 % PFA solution, cryoprotected at 4 °C in a 30 % sucrose, PB 0.1 M pH 7.4 solution, embedded in OCT (optimal cutting temperature medium, Thermo Scientific), frozen and kept at −80 °C. 30-µm thick brain coronal sections containing the VTA were collected using a cryostat (CM3050, Leica) and kept floating in PB 30-µm thick sections were incubated in blocking solution (BS) of PBST (PB Triton X100 (Sigma, St. Louis, MO, USA) with 10% donkey serum (Abcam, ab7475) for 2 h at room temperature (RT). Sections were then incubated for 48 hours at 4 °C in the blocking solution (BS) with appropriate primary antibodies: rabbit polyclonal anti MT_2 (Alomone, AMR-032, dilution 1:250), and chicken polyclonal anti tyrosine hydroxylase TH (Abcam, ab76442, 1:1000). After 3 washes with PB 0.1 M pH 7.4, 0.5 % Triton X100 buffer,

sections were incubated for 2 hours at RT with appropriate donkey AlexaFluor-conjugated secondary antibodies: anti-rabbit Alexa 555 (Invitrogen, A-31572, dilution 1:200), anti-chicken IgY (H+L) fluorescein (Invitrogen, A-16055, dilution 1:1000). Sections were washed two times with PB 0.1 M pH 7.4, 0.5 % Triton X100, one with PB 0.1 M pH 7.4, and finally were mounted on gelatin-coated glass slides for air-dry, and coverslipped with antifade fluoroshield mounting medium with DAPI (Vectashield, H-1200, 1.5 µg/ml). Next, images of VTA were collected with a confocal microscope (Carl Zeiss, LSM 710). Acquisitions were performed using X10; 0.80 NA dry objective and zoom values 0.6 were used for high magnification and images were acquired with the LCS (Leica) software. Confocal acquisitions in the sequential mode (single excitation beams: 405, 488, and 594 nm) to avoid potential crosstalk between the different fluorescence emissions were also used to validate double colocalization. 3 slices from 2 animals were stained.

Statistical analysis

Data were analyzed using GraphPad Prism (version 8.0.1; Inc., San Diego, CA) and Excel 2010 (Microsoft Office), and were first tested for assumptions of normality and homogeneity of variance. Data were expressed as mean ± S.E.M. Neuronal responses to cumulative administration of drugs were calculated as percentage of change from baseline before drug injections, were reported as mean (% of veh) ± S.E.M., and were computed using one-way analysis of variance (ANOVA) (factor: treatment dose) followed by Tuckey post hoc comparisons to analyze the effect of treatment with UCM924 on spontaneous DA neuron firing, burst activity, percentage of spikes in burst, number of bursts, spikes per burst, burst interspike interval and burst length in the VTA. Statistical significance was taken as probability value of $p \leq 0.05$.

3.11 Results

Dose response effects of the MT_2 partial agonist UCM924 on firing rate and burst activity of DA-VTA neurons

A total of 12 neurons were recorded in the VTA from 7 rats. Of these neurons, one from each rat was selected (the last neuron) in which to test the effects of a range of doses of UCM924. The DA firing rate was found to be 4.18 ± 0.77 Hz, and of the DA neurons recorded (Fig. 2A), all were burst-firing neurons. The effect of acute intravenous administration of UCM924 was tested in 6 neurons. In VTA DA neurons, increasing doses of UCM924 produced a dose-dependent inhibition of DA cell firing $F_{4,25} = 6.93$, P= 0.0007; Fig. 2B). Tuckey post hoc analysis revealed that at 30 mg/kg and 40mg/kg, there was significant decrease in the firing activity as compared to vehicle (P=0.029 and P=0.001, respectively; Fig. 2B). Moreover, at 40mg/kg the decrease in firing activity was even significant as compared to 10 mg/kg (P= 0.004; Fig. 2B). Notably, as illustrated in Figure 2A, the injection of apomorphine at 30µg further decreased the firing as expected.

Figure 2C reports the burst firing activity of VTA DA neurons. The number of bursts in a 200s interval was significantly decreased by the administration of UCM924. Post hoc analysis revealed that UCM924 at the dose of 40 mg/kg significantly decreased the number of bursts compared to Veh (P= 0.025) and to UCM924 10 mg/kg (P= 0.016). No overall effect of UCM924 was observed for spikes in burst, spikes per burst, burst interspike interval and burst length.

MT_2 receptors expression in the ventral tegmental area

Our immunohistochemistry study indicated that MT_2 receptor fluorescent signal was weak in the VTA, as previously reported (Klosen et al. 2019; Lacoste et al. 2015). Conversely, high density of

the tyrosine hydroxylase (TH)-positive cell bodies was revealed in this area. TH is a widely used marker for DA neurons in the central nervous system (Björklund and Dunnett 2007).

3.12 Discussion

As the results presented in this Appendix are intimately connected to the behavioural self-administration findings presented in Chapter III, I will overall discuss them in the Chapter IV - discussion.

3.13 Figures

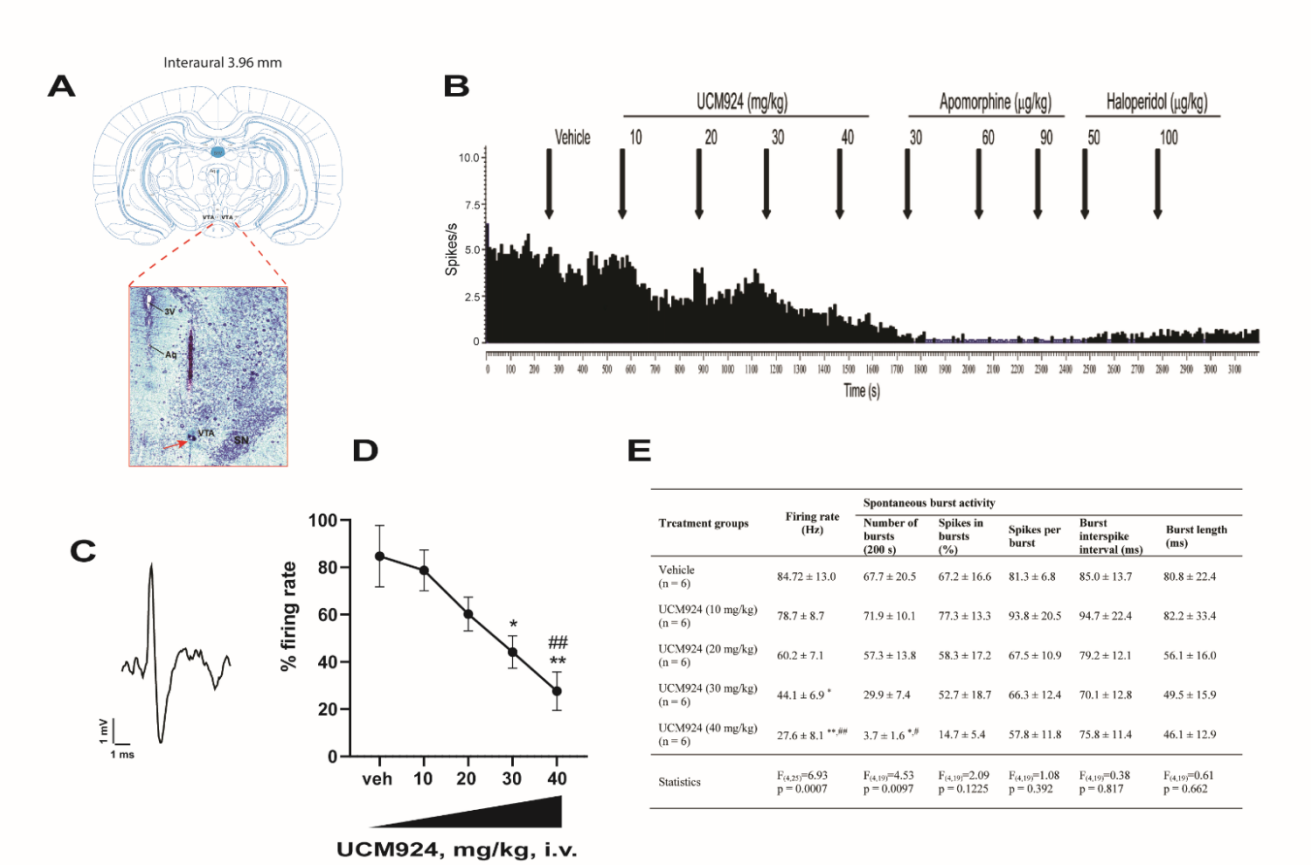

Treatment groups	Firing rate (Hz)	Spontaneous burst activity				
		Number of bursts (200 s)	Spikes in bursts (%)	Spikes per burst	Burst interspike interval (ms)	Burst length (ms)
Vehicle (n = 6)	84.72 ± 13.0	67.7 ± 20.5	67.2 ± 16.6	81.3 ± 6.8	85.0 ± 13.7	80.8 ± 22.4
UCM924 (10 mg/kg) (n = 6)	78.7 ± 8.7	71.9 ± 10.1	77.3 ± 13.3	93.8 ± 20.5	94.7 ± 22.4	82.2 ± 33.4
UCM924 (20 mg/kg) (n = 6)	60.2 ± 7.1	57.3 ± 13.8	58.3 ± 17.2	67.5 ± 10.9	79.2 ± 12.1	56.1 ± 16.0
UCM924 (30 mg/kg) (n = 6)	44.1 ± 6.9 *	29.9 ± 7.4	52.7 ± 18.7	66.3 ± 12.4	70.1 ± 12.8	49.5 ± 15.9
UCM924 (40 mg/kg) (n = 6)	27.6 ± 8.1 **,##	3.7 ± 1.6 *,#	14.7 ± 5.4	57.8 ± 11.8	75.8 ± 11.4	46.1 ± 12.9
Statistics	$F_{(4,25)}$=6.93 p = 0.0007	$F_{(4,19)}$=4.53 p = 0.0097	$F_{(4,19)}$=2.09 p = 0.1225	$F_{(4,19)}$=1.08 p = 0.392	$F_{(4,19)}$=0.38 p = 0.817	$F_{(4,19)}$=0.61 p = 0.662

Appendix chapter III - Figure 1. MT_2 receptor activation of dopaminergic neurons.
(**A**) Rat brain representation with 50 µm coronal section photomicrograph of the recording site in the VTA (approximately 3.7 mm from interaural line). Ventral tegmental area (VTA); substantia nigra (SN); aqueduct (Aq); third ventricle (3V). The red arrow indicates the site of the electrode recording labeled with pontamine sky blue dye. (**B**) Representative firing rate histograms showing the acute response of DA neurons to increasing doses of the MT_2 partial agonist UCM924 followed by apomorphine and haloperidol. UCM924 decreased spontaneous firing rate, apomorphine further inhibited firing and haloperidol increased firing rate in VTA DA neurons. (**C**) The typical spike waveform of DA neuron. (**D**) Acute intravenous (i.v.) increasing UCM924 administration decreases firing rate of VTA DA neurons (n = 6). (**E**) Burst activity parameters of VTA neurons recoded in vivo after administration of veh and increasing doses of the UCM924. Each point of the line (**D**) or data (**E**) represent mean ± SEM expressed

as percentage of baseline before injections of veh and UCM924. *P< 0.05, **P< 0.01 vs veh; #P< 0.05, ##P< 0.01 vs 10; One-way ANOVA followed by Tukey post hoc test.

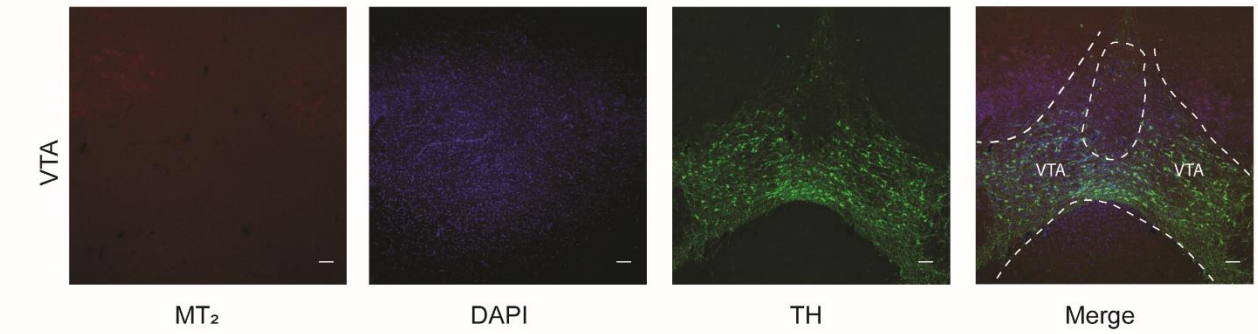

Appendix Chapter III - Figure 2. Immunohistochemical expression of the MT_2 receptor in the VTA.

Immunohistochemical localization of MT_2 receptors in the VTA. MT_2 immunostaining reveals poor immunoreactive neurons in the VTA. TH immunostaining showing high fluorescence in the VTA. Double labeling demonstrates the no colocalization of MT_2 receptors with TH in the VTA. Scale bars: 50 μm.

3.14 References

Björklund, Anders, and Stephen B Dunnett. 2007. 'Dopamine neuron systems in the brain: an update', *Trends in neurosciences*, 30: 194-202.

Di Chiara, Gaetano, and Assunta Imperato. 1988. 'Drugs abused by humans preferentially increase synaptic dopamine concentrations in the mesolimbic system of freely moving rats', *Proceedings of the National Academy of Sciences*, 85: 5274-78.

Domínguez-López, Sergio, Rebecca Dean Howell, Martha Graciela López-Canúl, Marco Leyton, and Gabriella Gobbi. 2014. 'Electrophysiological characterization of dopamine neuronal activity in the ventral tegmental area across the light–dark cycle', *Synapse*, 68: 454-67.

Fields, Howard L, and Elyssa B Margolis. 2015. 'Understanding opioid reward', *Trends in neurosciences*, 38: 217-25.

Gobbi, Gabriella, Anna Muntoni, Gian Gessa, and Marco Diana. 2001. 'Clonidine fails to modify dopaminergic neuronal activity during morphine withdrawal', *Psychopharmacology*, 158: 1-6.

Gysling, Katia, and Rex Y Wang. 1983. 'Morphine-induced activation of A10 dopamine neurons in the rat', *Brain research*, 277: 119-27.

Jalabert, Marion, Romain Bourdy, Julien Courtin, Pierre Veinante, Olivier J Manzoni, Michel Barrot, and François Georges. 2011. 'Neuronal circuits underlying acute morphine action on dopamine neurons', *Proceedings of the National Academy of Sciences*, 108: 16446-50.

Johnson, SW, and RA North. 1992. 'Opioids excite dopamine neurons by hyperpolarization of local interneurons', *Journal of Neuroscience*, 12: 483-88.

Klosen, Paul, Sarawut Lapmanee, Carole Schuster, Beatrice Guardiola, David Hicks, Paul Pevet, and Marie Paule Felder-Schmittbuhl. 2019. 'MT1 and MT2 melatonin receptors are expressed in nonoverlapping neuronal populations', *Journal of Pineal Research*: e12575.

Koob, George F, and Nora D Volkow. 2016. 'Neurobiology of addiction: a neurocircuitry analysis', *The Lancet Psychiatry*, 3: 760-73.

Lacoste, Baptiste, Debora Angeloni, Sergio Dominguez-Lopez, Sara Calderoni, Alessandro Mauro, Franco Fraschini, Laurent Descarries, and Gabriella Gobbi. 2015. 'Anatomical and cellular localization of melatonin MT1 and MT2 receptors in the adult rat brain', *Journal of Pineal Research*, 58: 397-417.

Margolis, Elyssa B, Gregory O Hjelmstad, Wakako Fujita, and Howard L Fields. 2014. 'Direct bidirectional μ-opioid control of midbrain dopamine neurons', *Journal of Neuroscience*, 34: 14707-16.

Robinson, Terry E, and Kent C Berridge. 2008. 'The incentive sensitization theory of addiction: some current issues', *Philosophical Transactions of the Royal Society B: Biological Sciences*, 363: 3137-46.

Spanagel, Rainer, Albert Herz, and Toni S Shippenberg. 1992. 'Opposing tonically active endogenous opioid systems modulate the mesolimbic dopaminergic pathway', *Proceedings of the National Academy of Sciences*, 89: 2046-50.

Ungless, Mark A, and Anthony A Grace. 2012. 'Are you or aren't you? Challenges associated with physiologically identifying dopamine neurons', *Trends in neurosciences*, 35: 422-30.

Chapter IV

4.1 General Discussion

The studies described in this dissertation studied the role of the opioid system in the analgesia induced by the activation of the melatonergic receptors. In order to characterize the possible interaction between these two systems in pain states, we used acute and chronic neuropathic pain models in wild type rats and mice transgenic for MLT and opioid receptors, selective MLT MT_2 partial agonists, behavioural pain tests, *in vivo* electrophysiological recordings, mRNA expression quantification, and immunohistochemistry. The potential rewarding properties of MT_2 partial agonists were also investigated.

4.2 Summary of primary findings

In chapter II, we discovered a key role for the MT_2 receptor in pain control and the functional interaction between melatonergic and opioid systems. In brief, we studied the distinct roles of melatonin MT_1 and MT_2 receptor subtypes in acute (hot plate test, HPT) and tonic (formalin test, FT) pain rodent models. We found that $MT_2^{-/-}$ and $MT_1^{-/-}/MT_2^{-/-}$, but not $MT_1^{-/-}$, mice showed an increased thermal threshold in the HPT and a decrease in the nociceptive overall time in the tonic phase of the FT compared to WT littermate. We also measured the nociceptive threshold across the light-dark cycle in WT and $MT_2^{-/-}$ mice and found that this decreased sensitivity in $MT_2^{-/-}$ mice was more evident in the inactive/light phase. In fact, during the active/dark phase, WT mice nociceptive sensitivity was reduced in both the HTP and FT, while in $MT_2^{-/-}$, nociceptive sensitivity did not change in the HTP and in phase 1 of the FT, but it was increased in phase 2 of the FT. Moreover, antinociceptive effects of the systemically administered

MT_2 partial agonist, UCM924, were measured in the WT, $MT_1^{-/-}$, $MT_2^{-/-}$ and $MT_1^{-/-}/MT_2^{-/-}$ mice. Confirming our previous results (Lopez-Canul, Comai, et al. 2015), UCM924 reduced the temperature to the first paw licking in the HT and the cumulative time the animal spent in nociceptive response to the injected hind paw in both phases of the FT in WT and $MT_1^{-/-}$, but not $MT_2^{-/-}$ and $MT_1^{-/-}/MT_2^{-/-}$, mice.

Later, we tested whether this loss of nociceptive sensitivity in mice lacking the functional MT_2 receptor was linked to a tonic opioid activation. We thus injected $MT_2^{-/-}$ and WT mice with a low dose (2 mg/kg, s.c.) of the non-selective opioid antagonist, naloxone. Interestingly, while in WT mice naloxone did not modify the thresholds in the HPT and FT, it significantly reduced the temperature to the first paw licking (HPT) and the cumulative time spent in nociceptive behaviors in phase 2 of FT in $MT_2^{-/-}$ mice. Finally, we hypothesized that this tonic opioid activation was induced by a hyper-activation of the opioid endogenous system. To evaluate this, we measured the relative gene expression of the endogenous opioid enkephalin, *Penk,* in the periaqueductal gray (PAG) and rostral ventromedial medulla (RVM), two pivotal areas of the descending antinociceptive pathway. *Penk* mRNA levels were increased in the RVM, but not in the PAG, of $MT_2^{-/-}$ mice. In conclusion, we demonstrated for the first time that the genetic inactivation of MT_2, but not MT_1, receptors lead to an increased nociceptive threshold in these transgenic mice. This phenotype is likely due to an increased opioid tone in some brain nuclei, such as the RVM.

In chapter III, we discovered a key role for the mu opioid receptor in MT_2-mediated analgesia. Specifically, we examined the distinct role of mu (MOR) and delta (DOR) opioid receptors as well as their function and location in the descending antinociceptive pathway in MT_2 receptor-mediated antiallodynia. We chose these two opioid receptor subtypes for two reasons: (1) they both share their expression in the vlPAG with MT_2 receptors (Commons, Van Bockstaele,

and Pfaff 1999; Erbs et al. 2014; Le Merrer et al. 2009); (2) MOR agonists (i.e. morphine, oxycodone, buprenorphine) are drugs commonly prescribed in the clinical practice to alleviate chronic pain (Gress et al. 2020; Trescot et al. 2008), and DOR agonists seem to have potential for therapeutic targeting of chronic pain and its related emotional disorders including anxiety and depression (Pradhan et al. 2011). Here, we demonstrated that the MOR plays a fundamental function in MT_2-induced antiallodynic effects. When the MOR was pharmacologically blocked or genetically silenced, the UCM924 antiallodynic effects were nullified, as well as the UCM924-induced modulation of the pronociceptive ON and antinociceptive OFF cell firing in the RVM. Our immunohistochemical findings display that the MT_2 receptors are expressed in inhibitory interneurons and excitatory neuronal somas in the vlPAG, but not in the RVM, while MORs have been revealed in both these structures of the descending antinociceptive pathway. Moreover, we found that MORs and MT_2 receptors poorly colocalize in the neuronal somas in the vlPAG (~ 0.20 %). Of note, while a G protein-coupled inwardly-rectifying potassium (GIRK) channels blocker tertiapin-Q (T-Q) antagonized the antiallodynic effect and the ON/OFF cell modulation both induced by MT_2 partial agonist UCM924 microinjection into the vlPAG, T-Q was ineffective to counteract the descending modulation of ON/OFF cells provoked by the MOR agonist, morphine. We also found that both UCM924 and morphine lost their antiallodynic and ON/OFF modulatory properties after repeated administration over time (9 days), confirming previous findings about morphine-induced tolerance (Mayer et al. 1999; Tortorici, Morgan, and Vanegas 2001). Interestingly, cross-tolerance studies revealed that while the acute s.c. morphine injection after 9-days of UCM924 treatment increased the paw withdrawal threshold in neuropathic rats, the acute UCM924 injection after 9-days of morphine treatment did not. Similarly, *in vivo* electrophysiological recordings showed that morphine microinjections into the vlPAG after 9-days

of UCM924 treatment still modulate the ON/OFF cell firing, while acutely UCM924 microinjections into the vlPAG after 9-days of morphine treatment failed to alter their firing. Preliminary experiments showed that s.c. UCM924 administration increased the endogenous opioid proenkephalin, *Penk*, mRNA level in the PAG. Summarizing, we demonstrated that MT_2-induced antiallodynia requires the presence of functional MOR at the supraspinal level. This mechanism likely occurs through enkephalin release induced by MT_2 receptor activation.

In the last experiment presented in chapter III and its Annex, we did not find evidence that the MT_2 receptor partial agonist, UCM924, induces reward in rats. Our behavioural experiments showed that while rats did not voluntarily self-administer UCM924, they did self-inject morphine. This finding is consistent with our preliminary data showing that UCM924 dose-dependently decreased the neuronal activity of dopaminergic neurons in the VTA - whereas morphine increased it (Jalabert et al. 2011) - and MT_2 receptors are poorly expressed is in this area.

4.3 The Opioid system contribution to MT_2-induced analgesia

We identified critical roles of the opioidergic tone in determining the increased nociceptive threshold in MT_2 knock-out mice (4.3.1) and that of MOR in the anti-allodynic effects induced by MT_2 agonism (4.3.2).

4.3.1 Genetic inactivation of MT_2 receptors leads to a reduced nociceptive sensitivity due to an opioidergic tonic activation

As mentioned in the introduction, some studies suggested the involvement of the opioid system in MLT-induced analgesia, since MLT's analgesic effects are blocked by the non-selective opioid antagonist, naloxone (Lakin et al. 1981; Golombek et al. 1991). However, the specific role of MLT and opioid receptor subtypes in pain conditions was not studied. Consequently, in chapter II, we

turned our attention to the role of each MLT receptor subtype on the regulation of nociception. Our major discovery in chapter II was that the genetic inactivation of MT_2 receptors (but not MT_1) lead to decreased pain sensitivity in the HPT and in the second phase of the FT during the light/inactive phase. We hypothesized that the decreased response to nociceptive stimuli in the mice lacking the MT_2 receptor could be related to hyper-activation of the opioid system as result of a developmental adaptation due to the genetic inactivation of the MT_2 receptor In fact, a recent study by Minett and colleagues (2015) demonstrated that mice lacking sodium channel Nav1.7 displayed a congenital insensitivity to pain and upregulation of the endogenous opioid, *Penk*, mRNA in sensory neurons. We thus injected a low dose of naloxone (2 mg/kg) which reversed the constitutive low pain sensitivity in $MT_2^{-/-}$ in HPT and phase 2 of FT, confirming a tonic activation of the opioidergic system. Later, we investigated whether the opioid tonic activation could be linked to an overexpression of endogenous opioid ligand enkephalin in some brain areas of the descending antinociceptive pathway involved in the modulation of pain (Heinricher et al. 2009). We found that the enkephalin precursor, *Penk*, mRNA was upregulated in RVM of $MT_2^{-/-}$ mice. These findings suggest that $MT_2^{-/-}$ mice may have an adaptive response to pain, as confirmed by the elevated opioid tonic activation, observed here with the naloxone challenge and with the increase of the enkephalin precursor, *Penk*, mRNA in the RVM.

As no difference was found in the pain threshold in the early phase of the FT among the four genotypes, it can be speculated that the MT_2 receptors play a less relevant role in this early phase where C afferent fibers are involved. However, both MLT and MT_2 selective partial agonists reduced the overall time spent engaged in nociceptive behaviors in the early phase both in rats (Lopez-Canul, Comai, et al. 2015) and mice (chapter II). More research is required to fully elucidate the participation of MT_2 receptors in the antinociceptive mechanism of phase 1 of the

FT, as well as the involvement of the MT_2 receptor in mechanical (brush), thermal (cold) sensitivity. Of note, $MT_2^{-/-}$ mice showed an increased threshold in the late phase of the FT. This phase describes a tonic response that combines an increased excitability of neurons in the dorsal horns (sensitization) (Coderre et al. 1993; Coderre and Melzack 1992) and an inflammatory reaction (i.e. prostaglandin synthesis) in the peripheral tissue (Hunskaar and Hole 1987; Wheeler-Aceto, Porreca, and Cowan 1990). Although our finding showing the *Penk* upregulation in the RVM would explain this phenotype, further experiments are needed to rule out a possible role of the inflammatory process in the decreased sensitivity in these animals. Indeed, an anti-inflammatory activity of MLT has been identified (Reiter et al. 2000). MLT's ability to directly scavenge free radicals and reactive oxygen and nitrogen species including the inflammatory mediator, peroxynitrite, (Costantino et al. 1998), the inducible isoform of NO synthase (Cuzzocrea et al. 1997), and prostaglandins (Cuzzocrea et al. 1999), could explain the reduction of edema and inflammation after MLT administration. Notably, some evidence suggests that MLT exerts its anti-inflammatory effects through the activation of the NO-cGMP-protein kinase G–K^+ channels pathway (Hernández-Pacheco et al. 2008)

Our results confirmed that the selective activation of MT_2 receptors by UCM924 (20 mg/kg) during the light/inactive phase produced antinociception in the HPT and during both phases of the FT. Moreover, during the dark/active phase, when endogenous MLT levels are higher (0-2 hours) (Arendt 1988), the nociceptive threshold was increased in the HPT and both phases of the FT, confirming previous findings (Xu et al. 1996; Lakin et al. 1981; Lutsch and Morris 1971). Interestingly, at night, the $MT_2^{-/-}$ mice sensitivity was normalized during the late phase of the FT. This condition might be explained by MOR expression across the light/dark cycle. Takada et al. (2013) demonstrated that the expression of MOR follows a circadian pattern, where MOR is more

expressed during the late light phase (14-20 hours) and less during the dark one (2-8 hours). As said above, MOR is highly expressed in the RVM and modulates both ON and OFF cells projecting into the spinal cord through the dorsolateral funiculus (DLF). DLF issues collateral branches to lamina I-II of the dorsal horn containing most of the nociceptive neurons which receive C afferent fibers (Fields, Malick, and Burstein 1995). As mentioned above, the tonic noxious stimulation (phase 2) is produced by an increase in the excitability of spinal cord neurons (wind up) (Coderre and Melzack 1992) and involves the descending pathway contained in the DLF which acts via lamina II dorsal horn interneurons to reduce nociceptive responses (Abbott, Hong, and Franklin 1996; Kline and Wiley 2008). Thus, the increased sensitivity during the night in $MT_2^{-/-}$ mice might be related to the scarce availability of MOR in these areas of the brainstem descending antinociceptive pathway, despite the upregulation of the MOR endogenous ligand enkephalin in the RVM.

The series of experiments summarized above provided evidence that the lack of functional MT_2 receptors leads to decreased pain sensitivity in an acute (HPT) and a tonic (FT) model of pain during the light phase which likely activates neuronal compensatory mechanisms through an upregulation of the endogenous opioid enkephalin at the central level.

4.3.2 The role of the mu opioid receptor (MOR) in the supraspinal MT_2-induced antiallodynia: behavioural, electrophysiological and immunohistochemical characterization

In chapter III, we investigated the specific role of MOR and DOR in MT_2-induced antiallodynia in a chronic neuropathic pain model. Our results identified a crucial role of the MOR. In fact, the antiallodynia and modulation of ON and OFF cells of the brain descending antinociceptive pathway provoked by MT_2 partial agonist UCM924 were fully nullified when MOR was

genetically inactivated in neuropathic $MOR^{-/-}$ mice or pharmacologically blocked using naloxone or CTOP in neuropathic rats. Although DOR blockage with naltrindole at the dose of 1 µg intra-PAG showed a significant effect at 1h post injection of UCM924 compared to vehicle, the AUC analysis confirmed that the cumulative effect of naltrindole+UCM924 was not different compared to the control group. In keeping with this, UCM924 alleviated mechanical and cold allodynia in neuropathic $DOR^{-/-}$ mice and *in vivo* electrophysiological recordings in the PAG-RVM circuit showed that 1 µg naltrindole was not able to block the modulation of ON and OFF cells induced by UCM924. Consequently, we focused our next experiments on MORs and MT_2 receptors. Next, using the transgenic MOR-mCherry mice line (Erbs et al. 2015; Erbs et al. 2014), we confirmed that, while MOR was expressed in both PAG (Commons, Van Bockstaele, and Pfaff 1999; Kalyuzhny et al. 1996) and RVM (Kalyuzhny et al. 1996) in neuropathic mice, MT_2 receptors were found in the neuronal somas of the vlPAG (~ 2.16 %) (Lacoste et al. 2015; Lopez-Canul, Palazzo, et al. 2015), but they were not revealed in the RVM. Also, the percentage of co-localization between MORs and MT_2 receptors was quite low (~ 0.20 %) of the total vlPAG neurons. We also found that the soma MOR immunoreactivity was not strong (~ 1.19 % over the total vlPAG), as previously reported (Kalyuzhny et al. 1996). Finally, we found that MT_2 receptors were expressed in both excitatory and inhibitory neurons (particularly with inhibitory interneurons) of the vlPAG. Collectively, these finding suggest that MORs and MT_2 receptors are mostly expressed in two different subpopulations of neurons in the vlPAG.

Additionally, the behavioural and electrophysiological analysis of the cross-tolerance challenge between morphine and UCM924 showed that while morphine had an antiallodynic and modulatory effect on ON-OFF cells in UCM924-tolerant neuropathic rats, UCM924 failed to provide any antiallodynic and modulatory effects in morphine-tolerant neuropathic rats. This outcome

confirms that when MORs are desensitized after prolonged exposure to morphine, both antiallodynic and modulatory effects induced by MT_2 agonism are abolished. Conversely, MOR analgesic and modulatory effects are independent of MT_2 receptor availability. Taken together, these findings demonstrated the fundamental role of MORs in MT_2-induced pain modulation, but also corroborated the immunohistochemical findings that the MT_2 receptor is located upstream in the antinociceptive descending pathway.

Finally, in chapter III, we showed that the injection of 20 mg/kg UCM924 increased *Penk,* but not *POMC*, mRNA expression in the PAG of neuropathic mice. This finding suggests an involvement of endogenous opioids in the MT_2-induced antiallodynia. The lack of induction of the *POMC* gene by UCM924 is not astonishing, since it is not constitutively expressed in the PAG despite the presence of POMC peptide in this area (Le Merrer et al. 2009). Indeed, the cycle threshold (Ct) in our PCR assays was more than 35, indicating a very low expression of the *POMC* gene in the PAG. Nevertheless, we showed that *Penk* mRNA levels are increased in SNI neuropathic mice compared to sham. This finding is in keeping with the literature showing an increased enkephalin peptide level in supraspinal brain areas including PAG, RVM and dorsal reticular nucleus in chronic pain conditions (Williams, Mullet, and Beitz 1995; Costa et al. 2019; Hurley and Hammond 2001), and a consequent decrease in the MOR availability (Willoch et al. 2004; Maarrawi et al. 2007).

Based on these findings, we hypothesized that the MT_2-MOR interaction likely occurs at the extracellular rather than intracellular level (e.g., sharing pathway or dimer formation).

A possible explanation for the circuit activation by MLT ligands may be the following. The MT_2 receptor stimulation by MLT or selective partial agonists activates excitatory synapses activating antinociceptive OFF cells (Chapter IV – Figure 1). In parallel, the MT_2-induced inhibition of

glutamatergic cells activated by noxious stimuli directly contributes to the decrease of pronociceptive ON cell firing (Chapter IV – Figure 1). Although inhibition of glutamatergic neuronal activity or activation of GABAergic neuronal activity potentiates nociception (Samineni et al. 2017), previous studies suggested that presynaptic inhibition of glutamatergic transmission onto ON cells in the PAG can contribute to analgesia (Connor et al. 1999); MT_2 receptor activation on glutamatergic neurons may play this role.

Nevertheless, GABA-disinhibition has been proposed as a mechanism underlying opioid analgesia (Fields, Barbaro, and Heinricher 1988; Roychowdhury and Fields 1996). Indeed, opioids activate the PAG–RVM descending pathway by indirectly removing the inhibitory control of local GABAergic interneurons, thereby disinhibiting the antinociceptive transmission via neuronal output to the spinal cord. Based on this evidence, the GABA-disinhibition promoted by MT_2 activation in the vlPAG may stimulate the release of endogenous opioids such as enkephalins at a downstream level in the RVM. Indeed, in chapter III, we found that UCM924 administration increased *Penk* mRNA levels in the PAG. In support of this, previous studies have shown that the MLT system modulates opioid tone by increasing the release of endogenous opioids (Barrett, Kent, and Voudouris 2000; Shavali et al. 2005). Similarly, the expression of the enkephalin precursor gene, *Penk*, is increased in the RVM of MT_2 knockout mice (see chapter II). Here, MT_2 receptors may induce a double effect, activating MORs, which are presynaptically expressed on GABA inhibitory neurons, thus promoting the disinhibition of antinociceptive OFF cells; and/or, in parallel, activating enkephalins, which stimulate postsynaptic MORs localized on the ON cells, thus inhibiting the pronociceptive ON firing (Chapter IV – Figure 1).

4.4 Involvement of G protein-coupled inwardly-rectifying potassium channels 1/4 GIRKs: difference between MT_2 and MOR agonists in the descending antinociceptive pathway

We have investigated the MT_2 receptor and MOR signaling pathway at supraspinal level with a focus on the involvement of GIRK channels in the antiallodynic and modulatory effects on the PAG-RVM circuit.

In chapter III, we tested the hypothesis that UCM924's antiallodynic effect at the supraspinal level and its capability to modulate ON and OFF cells are linked to G protein coupled inwardly-rectifying potassium channels (GIRKs) 1/4 and, consequently, the coupling of MT_2 receptors to Gi/o-coupled GPCRs in the vlPAG. The G protein βγ subunit (Gβγ) binds directly to GIRKs and opens these channels (Lüscher and Slesinger 2010). The administration of GIRK 1/4 blocker tertiapin-Q (T-Q) prior to UCM924 antagonized both UCM924-induced antiallodynic effect and ON-OFF cells modulation. A limitation of this electrophysiological approach is that, while the ligands were microinjected in the vlPAG, the cellular recordings were collected downstream in the RVM. Although this is indirect evidence of the possible involvement of GIRKs in the MT_2 receptor pathway, it is well known that GIRKs contribute to specific cellular responses of the Gi/o.

We also found that, in contrast to UCM924, morphine microinjection into the vlPAG failed to modulate ON-OFF cells. These findings are in line with previous results, showing that supraspinal, but not spinal, morphine analgesia was not directly mediated by GIRKs in a oxaliplatin-induced neuropathic model (Kanbara et al. 2014) and in a bone cancer pain model (Takasu et al. 2015). Moreover, GIRKs have been found to be involved at a postsynaptic but not presynaptic level in the hippocampus (Lüscher et al. 1997). Interestingly, it has been shown that the $GABA_BR$ agonist, baclofen, induces post-synaptic inhibition through GIRK in the vlPAG (Liu et al. 2012), leading

to analgesia (Bonanno et al. 1998; Levy and Proudfit 1979). This effect can stimulate excitatory synapses activating antinociceptive OFF cells (see Chapter IV – Figure 1). In conclusion, our data show that MORs and MT_2 receptors use different signaling pathways. It is likely that MT_2 receptor activation results in the release of endogenous opioids in a GIRK1/4-dependent manner, but that the opioids exert their actions via disinhibition of GABAergic neurotransmission.

4.5 The potential abuse liability of the MT_2 receptor agonist, UCM924, compared to morphine

In the last part of my thesis, we explored the reinforcing properties of the MT_2 partial agonist, UCM924, and its effect on the modulation of mesolimbic dopamine (DA) neurons of the VTA.

In the last set of experiments in chapter III, we assessed the potential behavioral effects of UCM924 in the reward process. As reported, animals self-administrated morphine (Weeks 1962), but they did not spontaneously self-inject UCM924. This finding provides the evidence that UCM924, but not morphine, has no marked reinforcing properties, indirectly suggesting no abuse potential. In the Appendix to chapter III (Fig. 2), we found a sparse MT_2 receptor immunoreactivity in the VTA neurons, confirming data from Lacoste et al. (2015). Drug addiction and reinforcement are associated with activation of mesolimbic and mesocortical systems (Koob and Volkow 2016). The mesolimbic system consists of dopaminergic neurons in the ventral tegmental area (VTA) and their axonal projections to the nucleus accumbens (NAc) and the prefrontal cortex (PFC). Psychotropic drugs including cocaine, morphine, and amphetamine preferentially increase extracellular release of dopamine in the shell of the NAc (Pontieri, Tanda, and Di Chiara 1995). Furthermore, morphine administration increases the firing rates and the burst activity of VTA DA

neurons and these effected were blocked by naloxone (Jalabert et al. 2011; Gysling and Wang 1983).

The lack of rewarding effects of UCM924 could be explained by the absence of MT_2 receptors in the mesolimbic dopaminergic pathways, including the VTA, NAc and PFC (Lacoste et al. 2015). Moreover, UCM924's long half-life (chapter III) and its slow indirect stimulation of MORs through the MT_2-induced release of the endogenous opioids may explain the observed absence of the MT_2 agonist reinforcement. In support of this hypothesis, a recent study showed that morphine and synthetic opioids, but not endogenous opioids, also activate opioid receptors inside cells at the endosome and Golgi apparatus level (Stoeber et al. 2018), since they are able to cross cell membranes without binding receptors or entering endosomes. In this way, they travel directly to the Golgi apparatus, reaching their target much more quickly than endogenous opioids which do not cross the cell membrane and thus require endosomes. This time difference could be important in the development of addiction, because typically drugs that act faster have an enhanced propensity to addiction (Samaha and Robinson 2005).

Nonetheless, using *in vivo* electrophysiological recording, we showed that UCM924 produced a significant dose-response decrease in firing and burst activity of VTA DA neurons (see Appendix Chapter III – Fig. 1), contrary to morphine (Jalabert et al. 2011; Gysling and Wang 1983). Notably, burst-firing activity is related to the release of the neurotransmitter in the synapse (Florin-Lechner et al. 1996). Therefore, UCM924 seems to modulate dopaminergic neural activity despite the absence of MT_2 receptors in the VTA. One hypothesis involves the ventral pallidum (VP), a basal forebrain nucleus involved in reward and motivation processes (Smith et al. 2009). The VP is an area rich in MT_2 receptors (Lacoste et al. 2015) which projects to the VTA (Mahler et al. 2014), and several studies demonstrated that pharmacological inactivation (McFarland et al. 2004;

McFarland and Kalivas 2001), or chemogenetic silencing (Mahler et al. 2014) of the VP prevents different forms of reinstatement to drug seeking. Thus, the MT_2 activation in the VP could play a role in the decrease dopamine neural activity and likely dopamine release. In support of this, it has been demonstrated that through modulation of diurnal rhythms in DA transmission, MLT can also influence cocaine sensitization (Akhisaroglu et al. 2004), reduce the risk of relapse triggered by cues in cocaine-experienced animals (Takahashi, Vengeliene, and Spanagel 2017), and prevent cocaine-induced locomotor sensitization and place preference in rats (Barbosa-Méndez et al. 2020). In conclusion, these observations underscore the need to explore whether the melatonergic neurotransmission in the VP-VTA circuit is implicated in the reward, and whether MLT compounds may have beneficial effects for the treatment and/or prevention of drug addiction.

4.6 Future directions and limitations

4.6.1 The role of the endogenous peptide, enkephalin, in the MT_2-induced antiallodynia: the extracellular pathway

One limitation of our findings is the indirect measurement of the increase of the endogenous opioid precursor, *PENK*, mRNA following MT_2 receptor stimulation. Our findings could be supported by quantifying the release of the endogenous opioid, *enkephalin peptide*, following MT_2 receptor stimulation. *In vivo* microdialysis in freely moving rats coupled to the quantification through capillary liquid chromatography with mass spectrometric detection (LC/MS) could be a valid approach. However, some technical challenges such as the degradation of endogenous peptides, and the low sensitivity of the methodology due to the small quantity of the endogenous peptide (the order of magnitude within fmol/sample (Nieto et al. 2002; Maidment et al. 1989) need to be considered.

Alternatively, a downregulation of enkephalin expression by the delivery of a lentiviral vector expressing shRNA specific to enkephalin mRNA in vlPAG could be a valid and elegant option. This technique would locally knock-down the enkephalin mRNA in the vlPAG using a lentivirus. These methods have been successfully used to knock down enkephalin in the amygdala with an average downregulation between 62-56% enkephalin mRNA (Bérubé et al. 2014; Poulin et al. 2013). After surgery, animals could be tested for the antiallodynic effect of intra-PAG injection of UCM924. Moreover, the effect of the MT_2 receptor stimulation on ON-OFF cells after depletion of enkephalins in the vlPAG could be also tested.

The location of the viral injection could also be a topic of investigation *per se*, since enkephalins may be produced distally and released in the vlPAG at terminals. Thus, there could be the need to characterize the relevant pathway and identify other brain areas, besides vlPAG, which could be involved. For example, the prelimbic and infralimbic cortices project to the vlPAG (Floyd et al. 2000), contain enkephalinergic neurons (Fallon and Leslie 1986) and mediate antinociceptive effects. The central amygdala also projects to the vlPAG (Rizvi et al. 1991) and enkephalinergic neurons are widely distributed in this structure (Fallon and Leslie 1986; Le Merrer et al. 2009), which also accounts for pain-related emotional responses and anxiety-like behaviors (Neugebauer et al. 2004), particularly in chronic persistent pain conditions.

In conclusion, the evaluation of the capability of MT_2 agonists to induce the release of the endogenous opioid, enkephalin, in the vlPAG or testing the efficacy of MT_2 agonists in the absence (or marked reduction) of enkephalins in vlPAG or in other brain structures would corroborate our proposal about the crucial role, not only of MOR, but also of its endogenous ligand enkephalin for the supraspinal pain modulation induced by the melatonin MT_2 agonism.

4.6.2 Intracellular interaction: MT_2-MOR and MT_2/5-HT_{2C} heteromers formation

In order to fully understand the specific role of MT_2 receptors in pain conditions, the further directions for this project would include the investigation and evaluation of the complex receptor dimerization, particularly as heterodimers composed of these two different receptors. Recent work demonstrated that the capacity of MT_1 and MT_2 receptors to form homo- and hetero-dimers (Ayoub et al. 2002) in transfected HEK293 cells, with MT_1/MT_2 heterodimers showing a pharmacological profile distinct from MT_2 homodimers (Ayoub et al. 2004). Furthermore, the MT_2 receptor has been reported to form heteromers with the orphan GPR50 receptor (Levoye et al. 2006). Although our immunohistochemical findings showed a low level of co-localization between MOR and MT_2 receptors (~ 0.2 % in the total neuronal population of the vlPAG), further studies are needed to rule out this hypothesis about a possible receptor interaction (heterodimerization) between the MOR and MT_2 receptor, particularly in *ex vivo* conditions. This approach will remove any bias introduced by the overexpressing receptors in transfected cell culture which may force heterodimerization, leading to inconclusive results, since the rate of physiological colocalization of MOR and MT_2 receptors in the vlPAG has been found to be modest.

A number of experiments were proposed above that would complement the work done in this thesis. In the contest of the intracellular interaction/dimerization hypothesis, it would be of interest to investigate and characterize the MT_2/5-HT_{2C} receptor heteromers. Recent studies demonstrated that MT_2 forms heterodimers with 5-HT_{2C} receptor both in HEK293 cells (Kamal et al. 2015) and in the hypothalamus and cerebellum of mice (Gerbier et al. 2020). MT_2 receptors are expressed in excitatory neurons in the vlPAG (see chapter III and Lopez-Canul, Palazzo, et al. 2015) and the 5-HT_{2C} is also expressed in PAG neurons (Abramowski et al. 1995) and it is has been shown to be frequently co-localized with substance P (SP) that plays an important role in different forms of supraspinal mediated analgesia (Rosén et al. 2004). 5-HT_{2C} is coupled to a Gq/11 and MT_2/5-HT_{2C}

receptor heteromer is also coupled to a stimulatory Gq protein (Kamal et al. 2015; Gerbier et al. 2020). This stimulation might lead to a release of SP promoting a postsynaptic glutamate-mediated excitation in PAG neurons which project to the RVM and thus promote an analgesic effect (Behbehani and Fields 1979; Carstens et al. 1990; Samineni et al. 2017).

4.6.3 The role of the MT_2 receptor and its possible interaction with the opioid system in spinal analgesia

Another area of investigation that would complement the work done in this thesis would be to assess the antinociceptive effect of the melatonergic system at the spinal level.

As discussed in chapter I, systemic MLT administration showed analgesic effects in the tail-flick test which measures the spinal nociceptive reflex (Yu et al. 2000; Wang et al. 2006; Xu et al. 1996; Naguib et al. 2003; Li et al. 2005). Although i.t. MLT anti-hyperalgesic effects remain debated (Zahn et al. 2003), i.t. MLT (Tu, Sun, and Willis 2004) and MT_2 partial agonist UCM764 and UCM871 (unpublished data) administration resulted in decreasing mechanical allodynia in rats and this effect was MT_2-mediated since it was blocked by 4P-PDOT.

Several studies have demonstrated the expression of MLT receptors in laminae I–V and lamina X of chicken and rabbits (Wan and Pang 1994; Wan et al. 1996) and in the dorsal and ventral horns of the spinal cord in rats (Zahn et al. 2003), areas that are involved in nociceptive transmission.

In the spinal cord, MOR is expressed presynaptically on terminals of nociceptive primary afferents and postsynaptically on neurons in laminas I and II of the dorsal horn of spinal cord (Moriwaki et al. 1996). Recently, Corder et al. (2017) demonstrated that genetic deletion of MOR from nociceptors reduced i.t. morphine antinociception, indicating that spinal opioid antinociception primarily results from presynaptic MOR signaling in nociceptors. Of note, some studies showed that i.p. and i.t. MLT administration enhances morphine analgesia (Li et al. 2005; Pang, Tsang, and Yang 2001; Zahn et al. 2003).

On the ground of these findings, the future directions for this project include the investigation of the extracellular cross-talk between the MT_2 and MOR in spinal antinociception.

4.6.4 Sexual dimorphism of pain: what is role of the MT_2 receptor?

Both preclinical and clinical research over the last three decades has implicated sex as a biological variable influencing the modulation of pain (Unruh 1996; Mogil 2012; Sorge et al. 2015). These sex-based differences have also been found in the responsiveness to opiates (Bobeck, McNeal, and Morgan 2009; Craft 2003; Loyd and Murphy 2006; Kepler et al. 1991), showing that morphine is more potent in male than female rats. Interestingly, this evidence seems to be ascribable to the PAG-RVM pathway which is sexually dimorphic in its anatomical organization (Loyd and Murphy 2006). Particularly, the most prominent sex difference in retrograde labeling was observed within the lateral/ventrolateral region of the PAG, where female rats had almost twice the number of retrogradely labeled neurons compared to males (Loyd and Murphy 2006). This sexual difference was also found to be relevant in the PAG-RVM activation during persistent inflammatory pain (Loyd and Murphy 2006).

The results presented here have the limitation to have been collected exclusively in male rodents. Although very little is known about sexual dimorphism in MLT and its receptors, some clinical findings would suggest it. For example, in a clinical study females were found to have a significantly higher MLT amplitude and lower temperature amplitude than males (Cain et al. 2010), and MLT secretion was significantly and inversely associated with diabetes in males, but not in females (Obayashi et al. 2018). Eventually, sleep architecture variation over the years was also found to be different between males and females, with a reductions in the percentage and mean of slow wave activity, an increased stage 2 of NREM sleep, and decreases in time, activity, density and intensity in REM sleep in males (Ehlers and Kupfer 1997).

Based on these findings, some interesting questions arise. In order to fully understand the role of MT_2 receptors in nociception, it will be worthwhile to investigate sex differences in knockout mice for MT_2 receptors and evaluate the efficacy of MT_2 partial agonists in female rodents in chronic pain conditions. This will provide useful information about relevant sex-related differences in the next steps of the clinical trials.

4.7 Clinical relevance

Chronic pain is a major health problem that afflicts a significant number of patients, resulting in personal suffering, reduced productivity, and substantial health care costs. Epidemiological studies demonstrate that chronic pain affects 20.4% of American and 18.9% of Canadian adults (Dahlhamer et al. 2018; Schopflocher, Taenzer, and Jovey 2011). This disease is associated with an annual cost estimated at $560 to $635 billion only in the United States (Simon 2012) and is related to impaired physical and mental functioning and poor quality of life. Particularly, neuropathic pain is a chronic disorder characterized by severe pain that develops following nerve damage, resulting from conditions such as shingles, traumas, injury, amputation, autoimmune inflammation, and cancer. It is a persistent pain that lasts for more than three months (Treede et al. 2015). Therapeutics are scant and there is a need for more effective drugs for reducing pain, offering long-term pain relief with better safety. The Neuropathic Pain Special Interest Group of IASP has developed evidence-based guidelines for its pharmacological treatment. Tricyclic antidepressants, dual reuptake inhibitors of serotonin and norepinephrine, calcium channel α2-δ ligands (i.e., gabapentin and pregabalin), and topical lidocaine are recommended as first-line treatment options based on the results of randomized clinical trials. Opioid analgesics and tramadol are recommended as second-line treatments, but must be considered as first-line use in certain clinical circumstances. Further, 10-30% of patients for whom pregabalin is prescribed experience

adverse side effects; a significant number of patients have no relief from symptoms during the first months of therapy; 79% of patients discontinue this treatment after one year because of side effects (Wettermark et al. 2014) and many patients switch to opioids. The prescription of opioid medications for chronic pain has more than tripled in the last few years (Hoots et al. 2018). Long-term use of prescription opioids presents serious adverse effects including tolerance, physical dependence, the so-called opioid-induced hyperalgesia, and their misuse might lead to addiction. This increase has been accompanied by a marked increase in the prevalence of opioid use disorders and drug overdose mortality (Control and Prevention 2011), producing the so-called "opioid crisis". It is thus mandatory for the scientific community to find alternatives to opioid treatments.

The preclinical work presented here, alongside past research in our laboratory, provide evidence that the MT_2 receptor is a novel target at the CNS level for the treatment of chronic pain. Indeed, MT_2 receptor stimulation by agonists may represent a novel avenue to treat chronic pain conditions by indirectly activating opioid system, all along presenting low abuse liability.

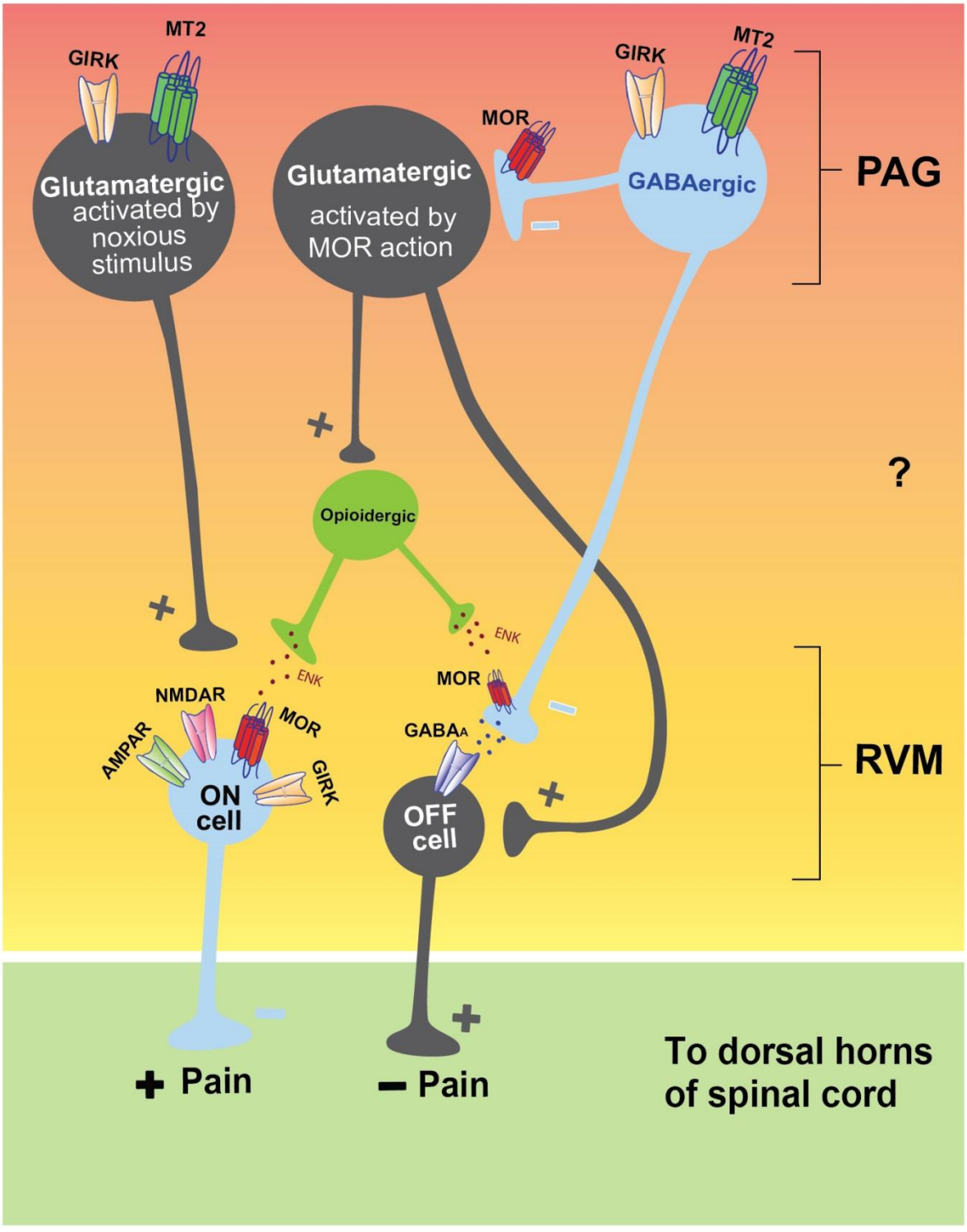

Chapter IV – Figure 1. Schematic model to illustrating the role of MT_2 receptors and MORs in PAG-RVM circuit in nociceptive modulatory state.

MT_2 receptors are located on both somatodendritic regions of GABA- and glutamatergic neurons in the vlPAG, but not in the RVM. The MT_2-mediated disinhibition of GABA-ergic projections positively modulate antinociceptive OFF, while MT_2 receptors silence glutamatergic inputs to pronociceptive ON cells in the RVM. MOR antagonism nullifies MT_2-induced anti-allodynia, but not vice-versa, confirming the upstream localization of MT_2 receptors in the pathway. AMPAR: α-amino-3-hydroxy-5-methyl-4-isoxazolepropionate receptor; ENK: enkephalin; GIRK: inwardly-rectifying potassium channel; MT_2: melatonin MT_2 receptor, MOR: μ-opioid receptor; NMDAR: N-methyl-D-aspartate receptor; From *Fields (2004)*. Adapted with permission from Springer *Nature Reviews Neuroscience*.

4.8 References

Abbott, Frances V, Yanguo Hong, and Keith Franklin. 1996. 'The effect of lesions of the dorsolateral funiculus on formalin pain and morphine analgesia: a dose-response analysis', *Pain*, 65: 17-23.

Abramowski, D, M Rigo, D Duc, D Hoyer, and M Staufenbiel. 1995. 'Localization of the 5-hydroxytryptamine2C receptor protein in human and rat brain using specific antisera', *Neuropharmacology*, 34: 1635-45.

Ahn, Seong-Ki, Roza Khalmuratova, Young-Sool Hah, Sea-Yuong Jeon, Dong Gu Hur, Hung-Soo Kang, and Carey D Balaban. 2012. 'Immunohistochemical and biomolecular identification of melatonin 1a and 1b receptors in rat vestibular nuclei', *Auris Nasus Larynx*, 39: 479-83.

Akhisaroglu, Mustafa, Rehan Ahmed, Murat Kurtuncu, Hari Manev, and Tolga Uz. 2004. 'Diurnal rhythms in cocaine sensitization and in Period1 levels are common across rodent species', *Pharmacology Biochemistry and Behavior*, 79: 37-42.

Akil, Huda, Constance Owens, Howard Gutstein, Larry Taylor, and Eileen Curran. 1998. 'Endogenous opioids: overview and current issues', *Drug and alcohol dependence*, 51: 127-40.

Al-Ghoul, Walid M, Martin D Herman, and Margarita L Dubocovich. 1998. 'Melatonin receptor subtype expression in human cerebellum', *Neuroreport*, 9: 4063-68.

Al-Hasani, Ream, and Michael R Bruchas. 2011. 'Molecular mechanisms of opioid receptor-dependent signaling and behavior', *Anesthesiology: The Journal of the American Society of Anesthesiologists*, 115: 1363-81.

Alhaider, Abdulqader A, Sizheng Z Lei, and George L Wilcox. 1991. 'Spinal 5-HT3 receptor-mediated antinociception: possible release of GABA', *Journal of Neuroscience*, 11: 1881-88.

Allouche, Stéphane, Jocelyne Polastron, and Philippe Jauzac. 1996. 'The δ-Opioid Receptor Regulates Activity of Ryanodine Receptors in the Human Neuroblastoma Cell Line SK-N-BE', *Journal of neurochemistry*, 67: 2461-70.

Alstadhaug, Karl B., Francis Odeh, Rolf Salvesen, and Svein I. Bekkelund. 2010. 'Prophylaxis of migraine with melatonin', *Neurology*, 75: 1527-32.

Ambriz-Tututi, M., S. L. Cruz, H. Urquiza-Marin, and V. Granados-Soto. 2011. 'Formalin-induced long-term secondary allodynia and hyperalgesia are maintained by descending facilitation', *Pharmacology, Biochemistry and Behavior*, 98: 417-24.

Ambriz-Tututi, Monic, and Vinicio Granados-Soto. 2007. 'Oral and spinal melatonin reduces tactile allodynia in rats via activation of MT2 and opioid receptors', *Pain*, 132: 273-80.

Ambriz-Tututi, Mónica, Héctor I Rocha-González, Silvia L Cruz, and Vinicio Granados-Soto. 2009. 'Melatonin: a hormone that modulates pain', *Life sciences*, 84: 489-98.

Andersen, Lars Peter Holst, Bülent Kücükakin, Mads U Werner, Jacob Rosenberg, and Ismail Gögenur. 2014. 'Absence of analgesic effect of intravenous melatonin administration during daytime after laparoscopic cholecystectomy: a randomized trial', *J. Clin. Anesth.*, 26: 545-50.

Andersen, Lars PH, Ismail Gögenur, Andreas Q Fenger, Marian C Petersen, Jacob Rosenberg, and Mads U Werner. 2015. 'Analgesic and antihyperalgesic effects of melatonin in a human inflammatory pain model: a randomized, double-blind, placebo-controlled, three-arm crossover study', *Pain*, 156: 2286-94.

Arendt, J. 1988. 'Melatonin', *Clinical endocrinology*, 29: 205-29.
Arreola-Espino, Rosaura, Héctor Urquiza-Marín, Mónica Ambriz-Tututi, Claudia Ivonne Araiza-Saldaña, Nadia L Caram-Salas, Héctor I Rocha-González, Teresa Mixcoatl-Zecuatl, and Vinicio Granados-Soto. 2007. 'Melatonin reduces formalin-induced nociception and tactile allodynia in diabetic rats', *European journal of pharmacology*, 577: 203-10.
Arvidsson, Ulf, M Riedl, Sumita Chakrabarti, Jang-Hern Lee, Albert H Nakano, RJ Dado, Horace H Loh, Ping-Yee Law, Martin W Wessendorf, and R Elde. 1995. 'Distribution and targeting of a mu-opioid receptor (MOR1) in brain and spinal cord', *Journal of Neuroscience*, 15: 3328-41.
Ayoub, Mohammed A, Cyril Couturier, Estelle Lucas-Meunier, Stephane Angers, Philippe Fossier, Michel Bouvier, and Ralf Jockers. 2002. 'Monitoring of ligand-independent dimerization and ligand-induced conformational changes of melatonin receptors in living cells by bioluminescence resonance energy transfer', *Journal of Biological Chemistry*, 277: 21522-28.
Ayoub, Mohammed A, Angelique Levoye, Philippe Delagrange, and Ralf Jockers. 2004. 'Preferential formation of MT1/MT2 melatonin receptor heterodimers with distinct ligand interaction properties compared with MT2 homodimers', *Molecular pharmacology*, 66: 312-21.
Bagley, Elena E, and Susan L Ingram. 2020. 'Endogenous opioid peptides in the descending pain modulatory circuit', *Neuropharmacology*: 108131.
Bajic, Dusica, and Herbert K Proudfit. 1999. 'Projections of neurons in the periaqueductal gray to pontine and medullary catecholamine cell groups involved in the modulation of nociception', *Journal of Comparative Neurology*, 405: 359-79.
Barajas-López, Carlos, Andrea L Peres, Rosa Espinosa-Luna, Cruz Reyes-Vázquez, and Bertha Prieto-Gómez. 1996. 'Melatonin modulates cholinergic transmission by blocking nicotinic channels in the guinea-pig submucous plexus', *Eur. J. Pharmacol.*, 312: 319-25.
Barbaro, Nicholas M, Donna L Hammond, and Howard L Fields. 1985. 'Effects of intrathecally administered methysergide and yohimbine on microstimulation-produced antinociception in the rat', *Brain research*, 343: 223-29.
Barbosa-Méndez, Susana, Gilberto Pérez-Sánchez, Enrique Becerril-Villanueva, and Alberto Salazar-Juárez. 2020. 'Melatonin decreases cocaine-induced locomotor sensitization and cocaine-conditioned place preference in rats', *Journal of Psychiatric Research*, 132: 97-110.
Barrett, Tracey, Stephen Kent, and Nicholas Voudouris. 2000. 'Does melatonin modulate beta-endorphin, corticosterone, and pain threshold?', *Life sciences*, 66: 467-76.
Basbaum, Allan I, Diana M Bautista, Grégory Scherrer, and David Julius. 2009. 'Cellular and molecular mechanisms of pain', *Cell*, 139: 267-84.
Basbaum, Allan I, and Howard L Fields. 1984. 'Endogenous pain control systems: brainstem spinal pathways and endorphin circuitry', *Annual review of neuroscience*, 7: 309-38.
Bederson, Joshua B, Howard L Fields, and Nicholas M Barbaro. 1990. 'Hyperalgesia during naloxone-precipitated withdrawal from morphine is associated with increased on-cell activity in the rostral ventromedial medulla', *Somatosensory & motor research*, 7: 185-203.
Befort, Katia, Lina Tabbara, Dominique Kling, Bernard Maigret, and Brigitte L Kieffer. 1996. 'Role of aromatic transmembrane residues of the-opioid receptor in ligand recognition', *Journal of Biological Chemistry*, 271: 10161-68.

Behbehani, Michael M, and Howard L Fields. 1979. 'Evidence that an excitatory connection between the periaqueductal gray and nucleus raphe magnus mediates stimulation produced analgesia', *Brain research*, 170: 85-93.

Bennett, G. J. 2001. 'Animal Models of Pain.' in L. Kruger (ed.), *Methods in Pain Research* (CRC Press).

Bennett, Gary J, and Y-K Xie. 1988. 'A peripheral mononeuropathy in rat that produces disorders of pain sensation like those seen in man', *Pain*, 33: 87-107.

Bernstein, Marissa A, and Sandra P Welch. 1998. 'μ-Opioid receptor down-regulation and cAMP-dependent protein kinase phosphorylation in a mouse model of chronic morphine tolerance', *Molecular brain research*, 55: 237-42.

Bérubé, Patrick, Jean-Francois Poulin, Sylvie Laforest, and Guy Drolet. 2014. 'Enkephalin knockdown in the basolateral amygdala reproduces vulnerable anxiety-like responses to chronic unpredictable stress', *Neuropsychopharmacology*, 39: 1159-68.

Bilici, D, E Akpinar, and A Kiziltunc. 2002. 'Protective effect of melatonin in carrageenan-induced acute local inflammation', *Pharmacological research*, 46: 133-39.

Bobeck, Erin N, Amy L McNeal, and Michael M Morgan. 2009. 'Drug dependent sex-differences in periaqueducatal gray mediated antinociception in the rat', *Pain*, 147: 210-16.

Bonanno, Giambattista, Anna Fassio, Roberta Sala, Giovanna Schmid, and Maurizio Raiteri. 1998. 'GABAB receptors as potential targets for drugs able to prevent excessive excitatory amino acid transmission in the spinal cord', *European journal of pharmacology*, 362: 143-48.

Bougea, Anastasia, Nikolaos Spantideas, Vasilis Lyras, Theodoros Avramidis, and Thomas Thomaidis. 2016. 'Melatonin 4 mg as prophylactic therapy for primary headaches: a pilot study', *Funct. neurol.*, 31: 33.

Braz, J. M., and A. I. Basbaum. 2010. 'Differential ATF3 expression in dorsal root ganglion neurons reveals the profile of primary afferents engaged by diverse noxious chemical stimuli', *Pain*, 150: 290-301.

Brenchat, Alex, Luz Romero, Mónica García, Marta Pujol, Javier Burgueño, Antoni Torrens, Michel Hamon, José Manuel Baeyens, Helmut Buschmann, and Daniel Zamanillo. 2009. '5-HT7 receptor activation inhibits mechanical hypersensitivity secondary to capsaicin sensitization in mice', *Pain*, 141: 239-47.

Brydon, Lena, Florian Roka, Laurence Petit, Pierre de Coppet, Michele Tissot, Perry Barrett, Peter J Morgan, Christian Nanoff, A Donny Strosberg, and Ralf Jockers. 1999. 'Dual signaling of human Mel1a melatonin receptors via Gi2, Gi3, and Gq/11 proteins', *Molecular Endocrinology*, 13: 2025-38.

Bubenik, George A, and Savita Dhanvantari. 1989. 'Influence of serotonin and melatonin on some parameters of gastrointestinal activity', *J. Pineal Res.*, 7: 333-44.

Budai, Dénes, Ichiro Harasawa, and Howard L Fields. 1998. 'Midbrain periaqueductal gray (PAG) inhibits nociceptive inputs to sacral dorsal horn nociceptive neurons through α2-adrenergic receptors', *Journal of neurophysiology*, 80: 2244-54.

Burgess, Shannon E, Luis R Gardell, Michael H Ossipov, T Philip Malan, Todd W Vanderah, Josephine Lai, and Frank Porreca. 2002. 'Time-dependent descending facilitation from the rostral ventromedial medulla maintains, but does not initiate, neuropathic pain', *Journal of Neuroscience*, 22: 5129-36.

Cain, Sean W, Christopher F Dennison, Jamie M Zeitzer, Aaron M Guzik, Sat Bir S Khalsa, Nayantara Santhi, Martin W Schoen, Charles A Czeisler, and Jeanne F Duffy. 2010. 'Sex

differences in phase angle of entrainment and melatonin amplitude in humans', *Journal of biological rhythms*, 25: 288-96.
Cameron, Adrian A, Iqbal A Khan, Karin N Westlund, and William D Willis. 1995. 'The efferent projections of the periaqueductal gray in the rat: a Phaseolus vulgaris-leucoagglutinin study. II. Descending projections', *Journal of Comparative Neurology*, 351: 585-601.
Cardinali, Daniel P, and Paul Pévet. 1998. 'Basic aspects of melatonin action', *Sleep medicine reviews*, 2: 175-90.
Carlson, Jonathan D, Jennifer J Maire, Melissa E Martenson, and Mary M Heinricher. 2007. 'Sensitization of pain-modulating neurons in the rostral ventromedial medulla after peripheral nerve injury', *Journal of Neuroscience*, 27: 13222-31.
Carstens, Earl, M Hartung, B Stelzer, and M Zimmermann. 1990. 'Suppression of a hind limb flexion withdrawal reflex by microinjection of glutamate or morphine into the periaqueductal gray in the rat', *Pain*, 43: 105-12.
Caumo, Wolnei, Maria Paz Hidalgo, Andressa Souza, Iraci LS Torres, and Luciana C Antunes. 2019. 'Melatonin is a biomarker of circadian dysregulation and is correlated with major depression and fibromyalgia symptom severity', *Journal of pain research*, 12: 545.
Chakrabarti, Sumita, and Alan R Gintzler. 2007. 'Phosphorylation of Gαs influences its association with the μ-opioid receptor and is modulated by long-term morphine exposure', *Molecular pharmacology*, 72: 753-60.
Chakrabarti, Sumita, Annette Regec, and Alan R Gintzler. 2005. 'Biochemical demonstration of mu-opioid receptor association with Gsα: enhancement following morphine exposure', *Molecular brain research*, 135: 217-24.
Chenaf, Chouki, Eric Chapuy, Frédéric Libert, Fabien Marchand, Christine Courteix, Marianne Bertrand, Cecilia Gabriel, Elisabeth Mocaër, Alain Eschalier, and Nicolas Authier. 2016. 'Agomelatine: a new opportunity to reduce neuropathic pain. Preclinical evidence', *Pain*.
Cheng, Zhen-Feng, Howard L Fields, and Mary M Heinricher. 1986. 'Morphine microinjected into the periaqueductal gray has differential effects on 3 classes of medullary neurons', *Brain research*, 375: 57-65.
Chieng, B, and MJ Christie. 1994a. 'Hyperpolarization by opioids acting on μ-receptors of a sub-population of rat periaqueductal gray neurones in vitro', *British journal of pharmacology*, 113: 121-28.
———. 1994b. 'Inhibition by opioids acting on μ-receptors of GABAergic and glutamatergic postsynaptic potentials in single rat periaqueductal gray neurones in vitro', *British journal of pharmacology*, 113: 303-09.
Chojnacki, Cezary, Ewa Walecka-Kapica, K Lokieć, Monika Pawłowicz, Katarzyna Winczyk, Jan Chojnacki, and Grażyna Klupińska. 2013. 'Influence of melatonin on symptoms of irritable bowel syndrome in postmenopausal women', *Endokrynol Pol*, 64: 114-20.
Cipolla-Neto, José, and Fernanda Gaspar do Amaral. 2018. 'Melatonin as a hormone: new physiological and clinical insights', *Endocrine reviews*, 39: 990-1028.
Citera, G, MA Arias, JA Maldonado-Cocco, MA La, MG Rosemffet, LI Brusco, EJ Scheines, and DP Cardinalli. 2000. 'The effect of melatonin in patients with fibromyalgia: a pilot study', *Clinical rheumatology*, 19: 9-13.
Clark, A. K., P. K. Yip, J. Grist, C. Gentry, A. A. Staniland, F. Marchand, M. Dehvari, G. Wotherspoon, J. Winter, J. Ullah, S. Bevan, and M. Malcangio. 2007. 'Inhibition of spinal microglial cathepsin S for the reversal of neuropathic pain', *Proceedings of the National Academy of Sciences of the United States of America*, 104: 10655-60.

Cleary, Daniel R, Miranda J Neubert, and Mary M Heinricher. 2008. 'Are opioid-sensitive neurons in the rostral ventromedial medulla inhibitory interneurons?', *Neuroscience*, 151: 564-71.

Coderre, Terence J, Joel Katz, Anthony L Vaccarino, and Ronald Melzack. 1993. 'Contribution of central neuroplasticity to pathological pain: review of clinical and experimental evidence', *Pain*, 52: 259-85.

Coderre, Terence J, and Ronald Melzack. 1992. 'The role of NMDA receptor-operated calcium channels in persistent nociception after formalin-induced tissue injury', *Journal of Neuroscience*, 12: 3671-75.

Comai, Stefano, Danilo De Gregorio, Luca Posa, Rafael Ochoa-Sanchez, Annalida Bedini, and Gabriella Gobbi. 2020. 'Dysfunction of serotonergic activity and emotional responses across the light-dark cycle in mice lacking melatonin MT2 receptors', *Journal of Pineal Research*, 00: e12653.

Comai, Stefano, Rafael Ochoa-Sanchez, Sergio Dominguez-Lopez, Francis Rodriguez Bambico, and Gabriella Gobbi. 2015. 'Melancholic-like behaviors and circadian neurobiological abnormalities in melatonin MT1 receptor knockout mice', *International Journal of Neuropsychopharmacology*, 18.

Comai, Stefano, Rafael Ochoa-Sanchez, and Gabriella Gobbi. 2013. 'Sleep–wake characterization of double MT1/MT2 receptor knockout mice and comparison with MT1 and MT2 receptor knockout mice', *Behavioural brain research*, 243: 231-38.

Comb, Michael, Peter H Seeburg, John Adelman, Lee Eiden, and Edward Herbert. 1982. 'Primary structure of the human Met-and Leu-enkephalin precursor and its mRNA', *Nature*, 295: 663-66.

Commons, Kathryn G, Elisabeth J Van Bockstaele, and Donald W Pfaff. 1999. 'Frequent colocalization of mu opioid and NMDA-type glutamate receptors at postsynaptic sites in periaqueductal gray neurons', *Journal of Comparative Neurology*, 408: 549-59.

Connor, Mark, Alwin Schuller, John E Pintar, and MacDonald J Christie. 1999. 'μ-opioid receptor modulation of calcium channel current in periaqueductal grey neurons from C57B16/J mice and mutant mice lacking MOR-1', *British journal of pharmacology*, 126: 1553-58.

Control, Centers for Disease, and Prevention. 2011. 'Vital signs: overdoses of prescription opioid pain relievers---United States, 1999--2008', *MMWR. Morbidity and mortality weekly report*, 60: 1487.

Corder, Gregory, Biafra Ahanonu, Benjamin F Grewe, Dong Wang, Mark J Schnitzer, and Grégory Scherrer. 2019. 'An amygdalar neural ensemble that encodes the unpleasantness of pain', *Science*, 363: 276-81.

Corder, Gregory, Vivianne L Tawfik, Dong Wang, Elizabeth I Sypek, Sarah A Low, Jasmine R Dickinson, Chaudy Sotoudeh, J David Clark, Ben A Barres, and Christopher J Bohlen. 2017. 'Loss of μ opioid receptor signaling in nociceptors, but not microglia, abrogates morphine tolerance without disrupting analgesia', *Nature medicine*, 23: 164.

Costa, Ana Rita, Paulina Carvalho, Gunnar Flik, Steven P Wilson, Carlos Reguenga, Isabel Martins, and Isaura Tavares. 2019. 'Neuropathic pain induced alterations in the opioidergic modulation of a descending pain facilitatory area of the brain', *Frontiers in cellular neuroscience*, 13: 287.

Costantino, Giuseppina, Salvatore Cuzzocrea, Emanuela Mazzon, and Achille P Caputi. 1998. 'Protective effects of melatonin in zymosan-activated plasma-induced paw inflammation', *European journal of pharmacology*, 363: 57-63.

Courteix, C, A Eschalier, and J Lavarenne. 1993. 'Streptozocin-induced diabetic rats: behavioural evidence for a model of chronic pain', *Pain*, 53: 81-88.

Craft, Rebecca M. 2003. 'Sex differences in opioid analgesia:"from mouse to man"', *The Clinical journal of pain*, 19: 175-86.

Cui, M, Y Feng, DJ McAdoo, and WD Willis. 1999. 'Periaqueductal gray stimulation-induced inhibition of nociceptive dorsal horn neurons in rats is associated with the release of norepinephrine, serotonin, and amino acids', *Journal of Pharmacology and Experimental Therapeutics*, 289: 868-76.

Cuzzocrea, Salvatore, Giuseppina Costantino, Emanuela Mazzon, and Achille P Caputi. 1999. 'Regulation of prostaglandin production in carrageenan-induced pleurisy melatonin', *Journal of Pineal Research*, 27: 9-14.

Cuzzocrea, Salvatore, Basilia Zingarelli, Eli Gilad, Paul Hake, Andrew L Salzman, and Csaba Szabo. 1997. 'Protective effect of melatonin in carrageenan-induced models of local inflammation: relationship to its inhibitory effect on nitric oxide production and its peroxynitrite scavenging activity', *Journal of Pineal Research*, 23: 106-16.

Dahlhamer, James, Jacqueline Lucas, Carla Zelaya, Richard Nahin, Sean Mackey, Lynn DeBar, Robert Kerns, Michael Von Korff, Linda Porter, and Charles Helmick. 2018. 'Prevalence of chronic pain and high-impact chronic pain among adults—United States, 2016', *Morbidity and Mortality Weekly Report*, 67: 1001.

de Zanette, Simone Azevedo, Rafael Vercelino, Gabriela Laste, Joanna Ripoll Rozisky, André Schwertner, Caroline Buzzatti Machado, Fernando Xavier, Izabel Cristina Custódio de Souza, Alicia Deitos, and Iraci LS Torres. 2014. 'Melatonin analgesia is associated with improvement of the descending endogenous pain-modulating system in fibromyalgia: a phase II, randomized, double-dummy, controlled trial', *BMC Pharmacology and Toxicology*, 15: 1.

Decosterd, Isabelle, and Clifford J Woolf. 2000. 'Spared nerve injury: an animal model of persistent peripheral neuropathic pain', *Pain*, 87: 149-58.

Del Burgo, Laura Saenz, Roser Cortes, Guadalupe Mengod, Jon Zarate, Enrique Echevarria, and Joan Salles. 2008. 'Distribution and neurochemical characterization of neurons expressing GIRK channels in the rat brain', *Journal of Comparative Neurology*, 510: 581-606.

Deng, Yun-Kun, Ji-Fei Ding, Jin Liu, and Yong-Yao Yang. 2015. 'Analgesic effects of melatonin on post-herpetic neuralgia', *International journal of clinical and experimental medicine*, 8: 5004.

Dhanaraj, Ethiraj, Kumar Venkata Subrahmanya Nemmani, and Poduri Ramarao. 2004. 'Melatonin inhibits the development of tolerance to U-50,488 H analgesia via benzodiazepine–GABA A ergic mechanisms', *Pharmacology Biochemistry and Behavior*, 79: 733-37.

Dogrul, Ahmet, Michael H Ossipov, and Frank Porreca. 2009. 'Differential mediation of descending pain facilitation and inhibition by spinal 5HT-3 and 5HT-7 receptors', *Brain research*, 1280: 52-59.

Doly, Stéphane, Jacqueline Fischer, Marie-Jeanne Brisorgueil, Daniel Vergé, and Marie Conrath. 2005. 'Pre-and postsynaptic localization of the 5-HT7 receptor in rat dorsal spinal cord: immunocytochemical evidence', *Journal of Comparative Neurology*, 490: 256-69.

Doolen, Suzanne, Diana N Krause, Margarita L Dubocovich, and Sue P Duckles. 1998. 'Melatonin mediates two distinct responses in vascular smooth muscle', *European journal of pharmacology*, 345: 67-69.

Dowdall, Tom, Ian Robinson, and Theo F Meert. 2005. 'Comparison of five different rat models of peripheral nerve injury', *Pharmacol. Biochem. Behav.*, 80: 93-108.

Dubocovich, Margarita L, Philippe Delagrange, Diana N Krause, David Sugden, Daniel P Cardinali, and James Olcese. 2010. 'International Union of Basic and Clinical Pharmacology. LXXV. Nomenclature, classification, and pharmacology of G protein-coupled melatonin receptors', *Pharmacological reviews*, 62: 343-80.

Dubocovich, Margarita L, Monica I Masana, Stanca Iacob, and Daniel M Sauri. 1997. 'Melatonin receptor antagonists that differentiate between the human Mel1a and Mel1b recombinant subtypes are used to assess the pharmacological profile of the rabbit retina ML1 presynaptic heteroreceptor', *Naunyn-Schmiedeberg's archives of pharmacology*, 355: 365-75.

Dubocovich, Margarita L, and Joseph S Takahashi. 1987. 'Use of 2-[125I] iodomelatonin to characterize melatonin binding sites in chicken retina', *Proceedings of the National Academy of Sciences*, 84: 3916-20.

Ehlers, Cindy, and David Kupfer. 1997. 'Slow-wave sleep: do young adult men and women age differently?', *Journal of sleep research*, 6: 211-15.

Erbs, Eric, Lauren Faget, Gregory Scherrer, Audrey Matifas, Dominique Filliol, Jean-Luc Vonesch, Marc Koch, Pascal Kessler, Didier Hentsch, and Marie-Christine Birling. 2015. 'A mu–delta opioid receptor brain atlas reveals neuronal co-occurrence in subcortical networks', *Brain Structure and Function*, 220: 677-702.

Erbs, Eric, Lauren Faget, Pierre Veinante, Brigitte L Kieffer, and Dominique Massotte. 2014. 'In vivo neuronal co-expression of mu and delta opioid receptors uncovers new therapeutic perspectives', *Receptors & clinical investigation*, 1: 210.

Esposti, D., G. Esposti, P. Lissoni, L. Parravicini, and F. Fraschini. 1988. 'Action of morphine on melatonin release in the rat', *J. Pineal. Res.*, 5: 35-9.

Fallon, James H, and Frances M Leslie. 1986. 'Distribution of dynorphin and enkephalin peptides in the rat brain', *Journal of Comparative Neurology*, 249: 293-336.

Fan, Theresa, George Varghese, Tuan Nguyen, Roderick Tse, Brian F O'Dowd, and Susan R George. 2005. 'A role for the distal carboxyl tails in generating the novel pharmacology and G protein activation profile of μ and δ opioid receptor hetero-oligomers', *Journal of Biological Chemistry*, 280: 38478-88.

Fang, Fernette G, CM Haws, K Drasner, A Williamson, and Howard L Fields. 1989. 'Opioid peptides (DAGO-enkephalin, dynorphin A (1–13), BAM 22P) microinjected into the rat brainstem: comparison of their antinociceptive effect and their effect on neuronal firing in the rostral ventromedial medulla', *Brain research*, 501: 116-28.

Fernández-Alacid, Laura, Masahiko Watanabe, Elek Molnár, Kevin Wickman, and Rafael Luján. 2011. 'Developmental regulation of G protein-gated inwardly-rectifying K+ (GIRK/Kir3) channel subunits in the brain', *European Journal of Neuroscience*, 34: 1724-36.

Fields, HL, Nicholas M Barbaro, and MM Heinricher. 1988. 'Brain stem neuronal circuitry underlying the antinociceptive action of opiates', *Progress in brain research*, 77: 245-57.

Fields, HL, John Bry, Ian Hentall, and Greg Zorman. 1983. 'The activity of neurons in the rostral medulla of the rat during withdrawal from noxious heat', *Journal of Neuroscience*, 3: 2545-52.

Fields, HL, A Malick, and R Burstein. 1995. 'Dorsal horn projection targets of ON and OFF cells in the rostral ventromedial medulla', *Journal of neurophysiology*, 74: 1742-59.

Fields, Howard. 2004. 'State-dependent opioid control of pain', *Nature Reviews Neuroscience*, 5: 565-75.

Finnegan, Thomas F, De-Pei Li, Shao-Rui Chen, and Hui-Lin Pan. 2004. 'Activation of μ-opioid receptors inhibits synaptic inputs to spinally projecting rostral ventromedial medulla neurons', *Journal of Pharmacology and Experimental Therapeutics*, 309: 476-83.

Florin-Lechner, Sandra M, Jonathan P Druhan, Gary Aston-Jones, and Rita J Valentino. 1996. 'Enhanced norepinephrine release in prefrontal cortex with burst stimulation of the locus coeruleus', *Brain research*, 742: 89-97.

Floyd, Nicole S, Joseph L Price, Amon T Ferry, Kevin A Keay, and Richard Bandler. 2000. 'Orbitomedial prefrontal cortical projections to distinct longitudinal columns of the periaqueductal gray in the rat', *Journal of Comparative Neurology*, 422: 556-78.

Fourtillan, JB, AM Brisson, M Fourtillan, I Ingrand, JPh Decourt, and J Girault. 2001. 'Melatonin secretion occurs at a constant rate in both young and older men and women', *American Journal of Physiology-Endocrinology and Metabolism*, 280: E11-E22.

Fourtillan, JB, AM Brisson, P Gobin, I Ingrand, J Ph Decourt, and J Girault. 2000. 'Bioavailability of melatonin in humans after day-time administration of D7 melatonin', *Biopharmaceutics & drug disposition*, 21: 15-22.

Fricker, Lloyd D, Elyssa B Margolis, Ivone Gomes, and Lakshmi A Devi. 2020. 'Five decades of research on opioid peptides: current knowledge and unanswered questions', *Molecular pharmacology*, 98: 96-108.

Fu, K. Y., A. R. Light, and W. Maixner. 2001. 'Long-lasting inflammation and long-term hyperalgesia after subcutaneous formalin injection into the rat hindpaw', *Journal of Pain*, 2: 2-11.

Fu, K. Y., A. R. Light, G. K. Matsushima, and W. Maixner. 1999. 'Microglial reactions after subcutaneous formalin injection into the rat hind paw', *Brain Research*, 825: 59-67.

Gagnier, Joel J. 2001. 'The therapeutic potential of melatonin in migraines and other headache types', *Altern. Med. Rev.*, 6: 383-83.

Gao, Keming, and Peggy Mason. 2000. 'Serotonergic raphe magnus cells that respond to noxious tail heat are not ON or OFF cells', *Journal of neurophysiology*, 84: 1719-25.

———. 2001. 'Physiological and anatomic evidence for functional subclasses of serotonergic raphe magnus cells', *Journal of Comparative Neurology*, 439: 426-39.

Gardell, LR, M Ibrahim, R Wang, Z Wang, MH Ossipov, TP Malan Jr, Frank Porreca, and J Lai. 2004. 'Mouse strains that lack spinal dynorphin upregulation after peripheral nerve injury do not develop neuropathic pain', *Neuroscience*, 123: 43-52.

Gardell, LR, Todd W Vanderah, SE Gardell, R Wang, MH Ossipov, J Lai, and Frank Porreca. 2003. 'Enhanced evoked excitatory transmitter release in experimental neuropathy requires descending facilitation', *Journal of Neuroscience*, 23: 8370-79.

Gassner, Matthias, Ruth Ruscheweyh, and Jürgen Sandkühler. 2009. 'Direct excitation of spinal GABAergic interneurons by noradrenaline', *Pain*, 145: 204-10.

Geffard, M., O. Gaffori, J. Chauveau, J. P. Muyard, and M. Le Moal. 1981. 'Dramatic increase in pineal melatonin levels in the rat after subcutaneous injection of Des-tyrosine1-gamma-endorphin', *Neurosci. Lett.*, 27: 329-34.

Gerbier, Romain, Delphine Ndiaye-Lobry, Pablo B Martinez de Morentin, Erika Cecon, Lora K Heisler, Philippe Delagrange, Florence Gbahou, and Ralf Jockers. 2020. 'Pharmacological evidence for transactivation within melatonin MT2 and serotonin 5-HT2C receptor heteromers in mouse brain', *The FASEB Journal*.

Ghirardi, Orlando, Pietro Lo Giudice, Claudio Pisano, Mario Vertechy, Augusta Bellucci, Loredana Vesci, Sante Cundari, Mariarosaria Miloso, Laura Maria Rigamonti, and Gabriella Nicolini. 2005. 'Acetyl-L-carnitine prevents and reverts experimental chronic neurotoxicity induced by oxaliplatin, without altering its antitumor properties', *Anticancer Res*, 25: 2681-87.

Gibbs, Finley P, and Jerry Vriend. 1981. 'The half-life of melatonin elimination from rat plasma', *Endocrinology*, 109: 1796-98.

Gilchrist, Hart D, Brandon L Allard, and Donald A Simone. 1996. 'Enhanced withdrawal responses to heat and mechanical stimuli following intraplantar injection of capsaicin in rats', *Pain*, 67: 179-88.

Goldstein, Avram, S Tachibana, LI Lowney, M Hunkapiller, and L Hood. 1979. 'Dynorphin-(1-13), an extraordinarily potent opioid peptide', *Proceedings of the National Academy of Sciences*, 76: 6666-70.

Golombek, Diego A, Esteban Escolar, Leila J Burin, María G De Brito Sánchez, and Daniel P Cardinali. 1991. 'Time-dependent melatonin analgesia in mice: inhibition by opiate or benzodiazepine antagonism', *European journal of pharmacology*, 194: 25-30.

Gonçalves, Leonor, Armando Almeida, and Antti Pertovaara. 2007. 'Pronociceptive changes in response properties of rostroventromedial medullary neurons in a rat model of peripheral neuropathy', *European Journal of Neuroscience*, 26: 2188-95.

Gress, Kyle, Karina Charipova, Jai Won Jung, Alan D Kaye, Antonella Paladini, Giustino Varrassi, Omar Viswanath, and Ivan Urits. 2020. 'A comprehensive review of partial opioid agonists for the treatment of chronic pain', *Best Practice & Research Clinical Anaesthesiology*, 34: 449-61.

Gysling, Katia, and Rex Y Wang. 1983. 'Morphine-induced activation of A10 dopamine neurons in the rat', *Brain research*, 277: 119-27.

Harlow, Henry J, and Bruce L Weekley. 1986. 'Effect of melatonin on the force of spontaneous contractions of in vitro rat small and large intestine', *J. Pineal Res.*, 3: 277-84.

Heinricher, M. M., M. M. Morgan, V. Tortorici, and H. L. Fields. 1994. 'Disinhibition of off-cells and antinociception produced by an opioid action within the rostral ventromedial medulla', *Neuroscience*, 63: 279-88.

Heinricher, Mary M, Zhen-feng Cheng, and Howard L Fields. 1987. 'Evidence for two classes of nociceptive modulating neurons in the periaqueductal gray', *Journal of Neuroscience*, 7: 271-78.

Heinricher, Mary M, and Howard L Fields. 2013. 'Central nervous system mechanisms of pain modulation.' in Elsevier (ed.), *Wall & Melzack's Textbook of Pain* (London).

Heinricher, Mary M, and Miranda J Neubert. 2004. 'Neural basis for the hyperalgesic action of cholecystokinin in the rostral ventromedial medulla', *Journal of neurophysiology*, 92: 1982-89.

Heinricher, MM, and S McGaraughty. 1998. 'Analysis of excitatory amino acid transmission within the rostral ventromedial medulla: implications for circuitry', *Pain*, 75: 247-55.

Heinricher, MM, S McGaraughty, and V Tortorici. 2001. 'Circuitry underlying antiopioid actions of cholecystokinin within the rostral ventromedial medulla', *Journal of neurophysiology*, 85: 280-86.

Heinricher, MM, MM Morgan, and HL Fields. 1992. 'Direct and indirect actions of morphine on medullary neurons that modulate nociception', *Neuroscience*, 48: 533-43.

Heinricher, MM, I Tavares, JL Leith, and BM Lumb. 2009. 'Descending control of nociception: specificity, recruitment and plasticity', *Brain research reviews*, 60: 214-25.

Heinricher, MM, and V Tortorici. 1994. 'Interference with GABA transmission in the rostral ventromedial medulla: disinhibition of off-cells as a central mechanism in nociceptive modulation', *Neuroscience*, 63: 533-46.

Hernández-Pacheco, Alfonso, Claudia Ivonne Araiza-Saldaña, Vinicio Granados-Soto, and Teresa Mixcoatl-Zecuatl. 2008. 'Possible participation of the nitric oxide-cyclic GMP-protein kinase GK+ channels pathway in the peripheral antinociception of melatonin', *European journal of pharmacology*, 596: 70-76.

Holden, JE, and HK Proudfit. 1998. 'Enkephalin neurons that project to the A7 catecholamine cell group are located in nuclei that modulate nociception: ventromedial medulla', *Neuroscience*, 83: 929-47.

Hoots, Brooke E, Likang Xu, Mbabazi Kariisa, Nana Otoo Wilson, Rose A Rudd, Lawrence Scholl, Lyna Schieber, and Puja Seth. 2018. '2018 Annual surveillance report of drug-related risks and outcomes - United States'.

Howe, R James, Jia-Yi Wang, and L Tony Yaksh. 1983. 'Selective antagonism of the antinociceptive effect of intrathecally applied alpha adrenergic agonists by intrathecal prazosin and intrathecal yohimbine', *Journal of Pharmacology and Experimental Therapeutics*, 224: 552-58.

Huang, Chun-Ta, Seu-Hwa Chen, Chi-Fen Chang, Shih-Chang Lin, June-Horng Lue, and Yi-Ju Tsai. 2020. 'Melatonin Reduces Neuropathic Pain Behavior and Glial Activation through MT2 Melatonin Receptor Modulation in a Rat Model of Lysophosphatidylcholine-Induced Demyelination Neuropathy', *Neurochemistry International*: 104827.

Huang, Junting, Vinicius M Gadotti, Lina Chen, Ivana A Souza, Shuo Huang, Decheng Wang, Charu Ramakrishnan, Karl Deisseroth, Zizhen Zhang, and Gerald W Zamponi. 2019. 'A neuronal circuit for activating descending modulation of neuropathic pain', *Nature neuroscience*: 1-10.

Hunskaar, Steinar, Odd-Geir Berge, and Kjell Hole. 1986. 'A modified hot-plate test sensitivie to mild analgesics', *Behavioural brain research*, 21: 101-08.

Hunskaar, Steinar, and Kjell Hole. 1987. 'The formalin test in mice: dissociation between inflammatory and non-inflammatory pain', *Pain*, 30: 103-14.

Hurley, Robert W, and Donna L Hammond. 2001. 'Contribution of endogenous enkephalins to the enhanced analgesic effects of supraspinal μ opioid receptor agonists after inflammatory injury', *Journal of Neuroscience*, 21: 2536-45.

Hussain, Saad Abdul-Rehman, Ihab Ibrahim Al-Khalifa, Nizar Abdullatif Jasim, and Faiq Isho Gorial. 2011. 'Adjuvant use of melatonin for treatment of fibromyalgia', *Journal of Pineal Research*, 50: 267-71.

Jalabert, Marion, Romain Bourdy, Julien Courtin, Pierre Veinante, Olivier J Manzoni, Michel Barrot, and François Georges. 2011. 'Neuronal circuits underlying acute morphine action on dopamine neurons', *Proceedings of the National Academy of Sciences*, 108: 16446-50.

Janak, Patricia H, and Kay M Tye. 2015. 'From circuits to behaviour in the amygdala', *Nature*, 517: 284-92.

Jensen, Troels S, and Tony L Yaksh. 1984. 'Spinal monoamine and opiate systems partly mediate the antinociceptive effects produced by glutamate at brainstem sites', *Brain research*, 321: 287-97.

———. 1989. 'Comparison of the antinociceptive effect of morphine and glutamate at coincidental sites in the periaqueductal gray and medial medulla in rats', *Brain research*, 476: 1-9.

Jiao, Jian, Yaner Ma, Sha Chen, Chonghuai Liu, Yuyang Song, Yi Qin, Chunlong Yuan, and Yanlin Liu. 2016. 'Melatonin-producing endophytic bacteria from grapevine roots promote the abiotic stress-induced production of endogenous melatonin in their hosts', *Frontiers in Plant Science*, 7: 1387.

Kalyuzhny, Alexander E, Ulf Arvidsson, Wei Wu, and Martin W Wessendorf. 1996. 'μ-Opioid and δ-opioid receptors are expressed in brainstem antinociceptive circuits: studies using immunocytochemistry and retrograde tract-tracing', *Journal of Neuroscience*, 16: 6490-503.

Kamal, Maud, Florence Gbahou, Jean-Luc Guillaume, Avais M Daulat, Abla Benleulmi-Chaachoua, Marine Luka, Patty Chen, Dina Kalbasi Anaraki, Marc Baroncini, and Clotilde Mannoury la Cour. 2015. 'Convergence of melatonin and serotonin (5-HT) signaling at MT2/5-HT2C receptor heteromers', *Journal of Biological Chemistry*, 290: 11537-46.

Kanbara, Tomoe, Atsushi Nakamura, Masahiro Shibasaki, Tomohisa Mori, Tsutomu Suzuki, Gaku Sakaguchi, and Toshiyuki Kanemasa. 2014. 'Morphine and oxycodone, but not fentanyl, exhibit antinociceptive effects mediated by G-protein inwardly rectifying potassium (GIRK) channels in an oxaliplatin-induced neuropathy rat model', *Neuroscience letters*, 580: 119-24.

Kaplan, Hilary, and Howard L Fields. 1991. 'Hyperalgesia during acute opioid abstinence: evidence for a nociceptive facilitating function of the rostral ventromedial medulla', *Journal of Neuroscience*, 11: 1433-39.

Kasap, Merve, and Özgür Devrim Can. 2016. 'Opioid System Mediated Anti-Nociceptive Effect of Agomelatine in Mice', *Life Sci.*

Kawasaki, Yasuhiko, Eiichi Kumamoto, Hidemasa Furue, and Megumu Yoshimura. 2003. 'α2Adrenoceptor–mediated Presynaptic Inhibition of Primary Afferent Glutamatergic Transmission in Rat Substantia Gelatinosa Neurons', *Anesthesiology: The Journal of the American Society of Anesthesiologists*, 98: 682-89.

Kepler, Karen L, Kelly M Standifer, Dennis Paul, Benjamin Kest, Gavril W Pasternak, and Richard J Bodnar. 1991. 'Gender effects and central opioid analgesia', *Pain*, 45: 87-94.

Khezri, Marzieh-Beigom, Mohammad-Reza Oladi, and Ali Atlasbaf. 2013. 'Effect of melatonin and gabapentin on anxiety and pain associated with retrobulbar eye block for cataract surgery: A randomized double-blind study', *Indian J. Pharmacol.*, 45: 581.

Kieffer, Brigitte L, and Claire Gavériaux-Ruff. 2002. 'Exploring the opioid system by gene knockout', *Progress in neurobiology*, 66: 285-306.

Kim, Dong H, Howard L Fields, and Nicholas M Barbaro. 1990. 'Morphine analgesia and acute physical dependence: rapid onset of two opposing, dose-related processes', *Brain research*, 516: 37-40.

Kim, Sun Ho, and Jin Mo Chung. 1992. 'An experimental model for peripheral neuropathy produced by segmental spinal nerve ligation in the rat', *Pain*, 50: 355-63.

Kincaid, Wendy, Miranda J Neubert, Mei Xu, Chang Jae Kim, and Mary M Heinricher. 2006. 'Role for medullary pain facilitating neurons in secondary thermal hyperalgesia', *Journal of neurophysiology*, 95: 33-41.

King, Tamara, Louis Vera-Portocarrero, Tannia Gutierrez, Todd W Vanderah, Gregory Dussor, Josephine Lai, Howard L Fields, and Frank Porreca. 2009. 'Unmasking the tonic-aversive state in neuropathic pain', *Nature neuroscience*, 12: 1364.

Kirchhoff, C, S Jung, PW Reeh, and HO Handwerker. 1990. 'Carrageenan inflammation increases bradykinin sensitivity of rat cutaneous nociceptors', *Neurosci. Lett.*, 111: 206-10.

Kirksey, Meghan A, Daniel Yoo, Thomas Danninger, Ottokar Stundner, Yan Ma, and Stavros G Memtsoudis. 2015. 'Impact of Melatonin on Sleep and Pain After Total Knee Arthroplasty Under Regional Anesthesia With Sedation: A Double-Blind, Randomized, Placebo-Controlled Pilot Study', *J. Arthroplasty*, 30: 2370-75.

Kitchen, Ian, Susan J Slowe, Hans WD Matthes, and Brigitte Kieffer. 1997. 'Quantitative autoradiographic mapping of μ-, δ-and κ-opioid receptors in knockout mice lacking the μ-opioid receptor gene', *Brain research*, 778: 73-88.

Klerman, Elizabeth B, Don L Goldenberg, Emery N Brown, Anne M Maliszewski, and Gail K Adler. 2001. 'Circadian Rhythms of Women with Fibromyalgia', *J. Clin. Endocrinol. Metab.*, 86: 1034-39.

Kline, Robert H, and Ronald G Wiley. 2008. 'Spinal μ-opioid receptor-expressing dorsal horn neurons: role in nociception and morphine antinociception', *Journal of Neuroscience*, 28: 904-13.

Klosen, Paul, Sarawut Lapmanee, Carole Schuster, Beatrice Guardiola, David Hicks, Paul Pevet, and Marie Paule Felder-Schmittbuhl. 2019. 'MT1 and MT2 melatonin receptors are expressed in nonoverlapping neuronal populations', *Journal of Pineal Research*: e12575.

Koob, George F, and Nora D Volkow. 2016. 'Neurobiology of addiction: a neurocircuitry analysis', *The Lancet Psychiatry*, 3: 760-73.

Kopin, Irwly J, C Pare, Julius Axelrod, and Herbert Weissbach. 1961. 'The fate of melatonin in animals', *J Biol Chem*, 236: 1961-3075.

Kovelowski, CJ, MH Ossipov, H Sun, J Lai, TP Malan Jr, and Frank Porreca. 2000. 'Supraspinal cholecystokinin may drive tonic descending facilitation mechanisms to maintain neuropathic pain in the rat', *Pain*, 87: 265-73.

Kurganova, Yu M, and AB Danilov. 2016. 'The Role of Melatonin in the Treatment of Chronic Back Pain', *Neuroscience and Behavioral Physiology*, 46: 737-42.

Kwiat, Geoffrey C, and Allan I Basbaum. 1992. 'The origin of brainstem noradrenergic and serotonergic projections to the spinal cord dorsal horn in the rat', *Somatosensory & motor research*, 9: 157-73.

Lacoste, Baptiste, Debora Angeloni, Sergio Dominguez-Lopez, Sara Calderoni, Alessandro Mauro, Franco Fraschini, Laurent Descarries, and Gabriella Gobbi. 2015. 'Anatomical and cellular localization of melatonin MT1 and MT2 receptors in the adult rat brain', *Journal of Pineal Research*, 58: 397-417.

Lai, Josephine, Miaw-Chyi Luo, Qingmin Chen, Shouwu Ma, Luis R Gardell, Michael H Ossipov, and Frank Porreca. 2006. 'Dynorphin A activates bradykinin receptors to maintain neuropathic pain', *Nature neuroscience*, 9: 1534-40.

Lakin, ML, CH Miller, ML Stott, and WD Winters. 1981. 'Involvement of the pineal gland and melatonin in murine analgesia', *Life sciences*, 29: 2543-51.

Laurido, Claudio, Teresa Pelissier, Rubén Soto-Moyano, Luis Valladares, Francisco Flores, and Alejandro Hernández. 2002. 'Effect of melatonin on rat spinal cord nociceptive transmission', *Neuroreport*, 13: 89-91.

Le Merrer, Julie, Jérôme AJ Becker, Katia Befort, and Brigitte L Kieffer. 2009. 'Reward processing by the opioid system in the brain', *Physiological reviews*, 89: 1379-412.

Levoye, Angélique, Julie Dam, Mohammed A Ayoub, Jean-Luc Guillaume, Cyril Couturier, Philippe Delagrange, and Ralf Jockers. 2006. 'The orphan GPR50 receptor specifically

inhibits MT1 melatonin receptor function through heterodimerization', *The EMBO journal*, 25: 3012-23.

Levy, Richard A, and Herbert K Proudfit. 1979. 'Analgesia produced by microinjection of baclofen and morphine at brain stem sites', *European journal of pharmacology*, 57: 43-55.

Li, Shi-rong, Ting Wang, Rui Wang, Xu Dai, and Qiang Chen. 2005. 'Melatonin enhances antinociceptive effects of δ-, but not μ-opioid agonist in mice', *Brain research*, 1043: 132-38.

Lin, Jia-Ji, Ye Lin, Tian-Zhi Zhao, Chun-Kui Zhang, Ting Zhang, Xiao-Li Chen, Jia-Qi Ding, Ting Chang, Zhuo Zhang, and Chao Sun. 2017. 'Melatonin suppresses neuropathic pain via MT2-dependent and-independent pathways in dorsal root ganglia neurons of mice', *Theranostics*, 7: 2015.

Lin, Tzer-Bin, Ming-Chun Hsieh, Cheng-Yuan Lai, Jen-Kun Cheng, Hsueh-Hsiao Wang, Yat-Pang Chau, Gin-Den Chen, and Hsien-Yu Peng. 2016. 'Melatonin relieves neuropathic allodynia through spinal MT 2-enhanced PP 2Ac and downstream HDAC 4 shuttling-dependent epigenetic modification of hmgb1 transcription', *Journal of Pineal Research*, 60: 263-76.

Ling, Bing, Nicolas Authier, David Balayssac, Alain Eschalier, and François Coudore. 2007. 'Behavioral and pharmacological description of oxaliplatin-induced painful neuropathy in rat', *Pain*, 128: 225-34.

Ling, Bing, Marie-Ange Coudoré-Civiale, David Balayssac, Alain Eschalier, François Coudoré, and Nicolas Authier. 2007. 'Behavioral and immunohistological assessment of painful neuropathy induced by a single oxaliplatin injection in the rat', *Toxicology*, 234: 176-84.

Liu, Zhi-Liang, Hongyu Ma, Ru-Xiang Xu, Yi-Wu Dai, Hong-Tian Zhang, Xue-Qin Yao, and Kun Yang. 2012. 'Potassium channels underlie postsynaptic but not presynaptic GABAB receptor-mediated inhibition on ventrolateral periaqueductal gray neurons', *Brain Research Bulletin*, 88: 529-33.

Longatti, Pierluigi, Alessandro Perin, Vittoria Rizzo, Stefano Comai, Pietro Giusti, and Carlo Virgilio Luigi Costa. 2007. 'Ventricular cerebrospinal fluid melatonin concentrations investigated with an endoscopic technique', *Journal of Pineal Research*, 42: 113-18.

Lopez-Canul, Martha, Stefano Comai, Sergio Domínguez-López, Vinicio Granados-Soto, and Gabriella Gobbi. 2015. 'Antinociceptive properties of selective MT2 melatonin receptor partial agonists', *European journal of pharmacology*, 764: 424-32.

Lopez-Canul, Martha, Seung Hyun Min, Luca Posa, Danilo De Gregorio, Annalida Bedini, Gilberto Spadoni, Gabriella Gobbi, and Stefano Comai. 2019. 'Melatonin MT1 and MT2 receptors exhibit distinct effects in the modulation of body temperature across the light/dark cycle', *International Journal of Molecular Sciences*, 20: 2452.

Lopez-Canul, Martha, Enza Palazzo, Sergio Dominguez-Lopez, Livio Luongo, Baptiste Lacoste, Stefano Comai, Debora Angeloni, Franco Fraschini, Serena Boccella, and Gilberto Spadoni. 2015. 'Selective melatonin MT2 receptor ligands relieve neuropathic pain through modulation of brainstem descending antinociceptive pathways', *Pain*, 156: 305-17.

Loyd, Dayna R, and Anne Z Murphy. 2006. 'Sex differences in the anatomical and functional organization of the periaqueductal gray-rostral ventromedial medullary pathway in the rat: A potential circuit mediating the sexually dimorphic actions of morphine', *Journal of Comparative Neurology*, 496: 723-38.

Lu, WZ, KA Gwee, S Moochhalla, and KY Ho. 2005. 'Melatonin improves bowel symptoms in female patients with irritable bowel syndrome: a double-blind placebo-controlled study', *Aliment. Pharmacol. Ther.*, 22: 927-34.

Luongo, L., F. Guida, S. Boccella, G. Bellini, L. Gatta, F. Rossi, V. de Novellis, and S. Maione. 2013. 'Palmitoylethanolamide reduces formalin-induced neuropathic-like behaviour through spinal glial/microglial phenotypical changes in mice', *CNS & Neurological Disorders Drug Targets*, 12: 45-54.

Lüscher, Christian, Lily Y Jan, Markus Stoffel, Robert C Malenka, and Roger A Nicoll. 1997. 'G protein-coupled inwardly rectifying K+ channels (GIRKs) mediate postsynaptic but not presynaptic transmitter actions in hippocampal neurons', *Neuron*, 19: 687-95.

Lüscher, Christian, and Paul A Slesinger. 2010. 'Emerging roles for G protein-gated inwardly rectifying potassium (GIRK) channels in health and disease', *Nature Reviews Neuroscience*, 11: 301-15.

Lutsch, EF, and RW Morris. 1971. 'Light reversal of a morphine-induced analgesia susceptibility rhythm in mice', *Cellular and Molecular Life Sciences*, 27: 420-21.

Maarrawi, Joseph, Roland Peyron, Patrick Mertens, Nicolas Costes, Michel Magnin, Marc Sindou, Bernard Laurent, and Luis Garcia-Larrea. 2007. 'Differential brain opioid receptor availability in central and peripheral neuropathic pain', *Pain*, 127: 183-94.

Mahler, Stephen V, Elena M Vazey, Jacob T Beckley, Colby R Keistler, Ellen M McGlinchey, Jennifer Kaufling, Steven P Wilson, Karl Deisseroth, John J Woodward, and Gary Aston-Jones. 2014. 'Designer receptors show role for ventral pallidum input to ventral tegmental area in cocaine seeking', *Nature neuroscience*, 17: 577-85.

Maidment, NT, DR Brumbaugh, VD Rudolph, E Erdelyi, and CJ Evans. 1989. 'Microdialysis of extracellular endogenous opioid peptides from rat brain in vivo', *Neuroscience*, 33: 549-57.

Mailliet, François, Gilles Ferry, Fanny Vella, Sylvie Berger, Francis Cogé, Pascale Chomarat, Catherine Mallet, Sophie-Pénélope Guénin, Gérald Guillaumet, and Marie-Claude Viaud-Massuard. 2005. 'Characterization of the melatoninergic MT 3 binding site on the NRH: quinone oxidoreductase 2 enzyme', *Biochemical pharmacology*, 71: 74-88.

Mannelli, Lorenzo Di Cesare, Matteo Zanardelli, Paola Failli, and Carla Ghelardini. 2012. 'Oxaliplatin-induced neuropathy: oxidative stress as pathological mechanism. Protective effect of silibinin', *The Journal of Pain*, 13: 276-84.

Mansour, Alfred, Charles A Fox, Sharon Burke, Fan Meng, Robert C Thompson, Huda Akil, and Stanley J Watson. 1994. 'Mu, delta, and kappa opioid receptor mRNA expression in the rat CNS: an in situ hybridization study', *Journal of Comparative Neurology*, 350: 412-38.

Mansour, Alfred, Henry Khachaturian, Michael E Lewis, Huda Akil, and Stanley J Watson. 1988. 'Anatomy of CNS opioid receptors', *Trends in neurosciences*, 11: 308-14.

Mantovani, Michela, Roberto Pértile, Joao B Calixto, Adair RS Santos, and Ana Lúcia S Rodrigues. 2003. 'Melatonin exerts an antidepressant-like effect in the tail suspension test in mice: evidence for involvement of N-methyl-D-aspartate receptors and the L-arginine-nitric oxide pathway', *Neurosci. Lett.*, 343: 1-4.

Marinelli, Silvia, Christopher W Vaughan, Stephen A Schnell, Martin W Wessendorf, and MacDonald J Christie. 2002. 'Rostral ventromedial medulla neurons that project to the spinal cord express multiple opioid receptor phenotypes', *Journal of Neuroscience*, 22: 10847-55.

Marker, Cheryl L, Stephanie C Cintora, Maria I Roman, Markus Stoffel, and Kevin Wickman. 2002. 'Hyperalgesia and blunted morphine analgesia in G protein-gated potassium channel subunit knockout mice', *Neuroreport*, 13: 2509-13.

Marker, Cheryl L, Rafael Luján, José Colón, and Kevin Wickman. 2006. 'Distinct populations of spinal cord lamina II interneurons expressing G-protein-gated potassium channels', *Journal of Neuroscience*, 26: 12251-59.

Marker, Cheryl L, Rafael Luján, Horace H Loh, and Kevin Wickman. 2005. 'Spinal G-protein-gated potassium channels contribute in a dose-dependent manner to the analgesic effect of μ-and δ-but not κ-opioids', *The Journal of neuroscience*, 25: 3551-59.

Marker, Cheryl L, Markus Stoffel, and Kevin Wickman. 2004. 'Spinal G-protein-gated K+ channels formed by GIRK1 and GIRK2 subunits modulate thermal nociception and contribute to morphine analgesia', *Journal of Neuroscience*, 24: 2806-12.

Marseglia, L, S Manti, G D'Angelo, T Arrigo, C Cuppari, C Salpietro, and E Gitto. 2015. 'Potential use of melatonin in procedural anxiety and pain in children undergoing blood withdrawal', *J Biol Regul Homeost Agents*, 29: 509-14.

Masana, Monica I, and Margarita L Dubocovich. 2001. 'Melatonin receptor signaling: finding the path through the dark', *Science's STKE*, 2001: pe39-pe39.

Mason, Peggy. 2001. 'Contributions of the medullary raphe and ventromedial reticular region to pain modulation and other homeostatic functions', *Annual review of neuroscience*, 24: 737-77.

Mayer, David J, Jianren Mao, Jason Holt, and Donald D Price. 1999. 'Cellular mechanisms of neuropathic pain, morphine tolerance, and their interactions', *Proceedings of the National Academy of Sciences*, 96: 7731-36.

Mazzucchelli, Cristina, Marilou Pannacci, Romolo Nonno, Valeria Lucini, Franco Fraschini, and Bojidar Michaylov Stankov. 1996. 'The melatonin receptor in the human brain: cloning experiments and distribution studies', *Molecular brain research*, 39: 117-26.

McArthur, Angela J, Amanda E Hunt, and Martha U Gillette. 1997. 'Melatonin Action and Signal Transduction in the Rat Suprachiasmatic Circadian Clock: Activation of Protein Kinase C at Dusk and Dawn 1', *Endocrinology*, 138: 627-34.

McFarland, Krista, Susan B Davidge, Christopher C Lapish, and Peter W Kalivas. 2004. 'Limbic and motor circuitry underlying footshock-induced reinstatement of cocaine-seeking behavior', *Journal of Neuroscience*, 24: 1551-60.

McFarland, Krista, and Peter W Kalivas. 2001. 'The circuitry mediating cocaine-induced reinstatement of drug-seeking behavior', *Journal of Neuroscience*, 21: 8655-63.

McNamara, Colleen R, Josh Mandel-Brehm, Diana M Bautista, Jan Siemens, Kari L Deranian, Michael Zhao, Neil J Hayward, Jayhong A Chong, David Julius, and Magdalene M Moran. 2007. 'TRPA1 mediates formalin-induced pain', *Proceedings of the National Academy of Sciences*, 104: 13525-30.

Meng, Ian D, Barton H Manning, William J Martin, and Howard L Fields. 1998. 'An analgesia circuit activated by cannabinoids', *Nature*, 395: 381-83.

Meyer, Richard A, M Ringkamp, J N Campbell, and S N Raja. 2006. 'Peripheral mechanisms of cutaneous nociception.' in Elsevier (ed.), *Wall and Melzack's textbook of pain*.

Miano, Silvia, Pasquale Parisi, Andrea Pelliccia, Anna Luchetti, Maria Chiara Paolino, and Maria Pia Villa. 2008. 'Melatonin to prevent migraine or tension-type headache in children', *Neurol. Sci.*, 29: 285-87.

Miki, Kenji, Q-Q Zhou, W Guo, Yun Guan, R Terayama, R Dubner, and K Ren. 2002. 'Changes in gene expression and neuronal phenotype in brain stem pain modulatory circuitry after inflammation', *Journal of neurophysiology*, 87: 750-60.

Minett, Michael S, Vanessa Pereira, Shafaq Sikandar, Ayako Matsuyama, Stéphane Lolignier, Alexandros H Kanellopoulos, Flavia Mancini, Gian D Iannetti, Yury D Bogdanov, and Sonia Santana-Varela. 2015. 'Endogenous opioids contribute to insensitivity to pain in humans and mice lacking sodium channel Na v 1.7', *Nature communications*, 6: 8967.

Mitrovic, Igor, Marta Margeta-Mitrovic, Semon Bader, Markus Stoffel, Lily Y Jan, and Allan I Basbaum. 2003. 'Contribution of GIRK2-mediated postsynaptic signaling to opiate and α2-adrenergic analgesia and analgesic sex differences', *Proceedings of the National Academy of Sciences*, 100: 271-76.

Mogil, Jeffrey S. 2009. 'Animal models of pain: progress and challenges', *Nature Reviews Neuroscience*, 10: 283-94.

———. 2012. 'Sex differences in pain and pain inhibition: multiple explanations of a controversial phenomenon', *Nature Reviews Neuroscience*, 13: 859-66.

Moore, RY. 1981. 'The anatomy of central serotonin neuron systems in the rat brain', *Serotonin neurotransmission and behavior*: 35-71.

Moreau, Jean-Luc, and Howard L Fields. 1986. 'Evidence for GABA involvement in midbrain control of medullary neurons that modulate nociceptive transmission', *Brain research*, 397: 37-46.

Morgan, Michael M, Kelsey L Whittier, Deborah M Hegarty, and Sue A Aicher. 2008. 'Periaqueductal gray neurons project to spinally projecting GABAergic neurons in the rostral ventromedial medulla', *Pain*, 140: 376-86.

Moriwaki, Akiyoshi, Jia-Bei Wang, Adena Svingos, Elizabeth Van Bockstaele, Peter Cheng, Virginia Pickel, and George R Uhl. 1996. 'μ Opiate receptor immunoreactivity in rat central nervous system', *Neurochemical research*, 21: 1315-31.

Morris, Ralph W, and Edward F Lutsch. 1969. 'Daily susceptibility rhythm to morphine analgesia', *J. Pharm. Sci.*, 58: 374-76.

Musshoff, Ulrich, Daniel Riewenherm, Eva Berger, Jan-Dirk Fauteck, and Erwin-Josef Speckmann. 2002. 'Melatonin receptors in rat hippocampus: molecular and functional investigations', *Hippocampus*, 12: 165-73.

Naguib, M, DL Hammond, PG Schmid III, MT Baker, J Cutkomp, L Queral, and T Smith. 2003. 'Pharmacological effects of intravenous melatonin: comparative studies with thiopental and propofol', *British journal of anaesthesia*, 90: 504-07.

Nakanishi, Shigetada, Akira Inoue, Toru Kita, Masahiro Nakamura, Annie CY Chang, Stanley N Cohen, and Shosaku Numa. 1979. 'Nucleotide sequence of cloned cDNA for bovine corticotropin-β-lipotropin precursor', *Nature*, 278: 423-27.

Nelson, Cole S, Jennifer L Marino, and Charles N Allen. 1996. 'Melatonin receptors activate heteromeric G-protein coupled Kir3 channels', *Neuroreport*, 7: 717-20.

Neubert, Miranda J, Wendy Kincaid, and Mary M Heinricher. 2004. 'Nociceptive facilitating neurons in the rostral ventromedial medulla', *Pain*, 110: 158-65.

Neugebauer, Volker, Weidong Li, Gary C Bird, and Jeong S Han. 2004. 'The amygdala and persistent pain', *The Neuroscientist*, 10: 221-34.

Nieh, Edward H, Sung-Yon Kim, Praneeth Namburi, and Kay M Tye. 2013. 'Optogenetic dissection of neural circuits underlying emotional valence and motivated behaviors', *Brain research*, 1511: 73-92.

Nieto, Magdalena Mas, Jodie Wilson, Annie Cupo, Bernard P Roques, and Florence Noble. 2002. 'Chronic morphine treatment modulates the extracellular levels of endogenous enkephalins in rat brain structures involved in opiate dependence: a microdialysis study', *Journal of Neuroscience*, 22: 1034-41.

Noseda, Rodrigo, Alejandro Hernández, Luis Valladares, Mauricio Mondaca, Claudio Laurido, and Rubén Soto-Moyano. 2004. 'Melatonin-induced inhibition of spinal cord synaptic potentiation in rats is MT 2 receptor-dependent', *Neurosci. Lett.*, 360: 41-44.

Nosjean, Olivier, Myriam Ferro, Francis Cogé, Philippe Beauverger, Jean-Michel Henlin, François Lefoulon, Jean-Luc Fauchère, Philippe Delagrange, Emmanuel Canet, and Jean A Boutin. 2000. 'Identification of the Melatonin-binding SiteMT 3 as the Quinone Reductase 2', *Journal of Biological Chemistry*, 275: 31311-17.

Obayashi, Kenji, Yuki Yamagami, Junko Iwamoto, Norio Kurumatani, and Keigo Saeki. 2018. 'Gender differences in the association between melatonin secretion and diabetes in elderly: The HEIJO-KYO cohort', *Clinical endocrinology*, 89: 750-56.

Ochoa-Sanchez, Rafael, Stefano Comai, Baptiste Lacoste, Francis Rodriguez Bambico, Sergio Dominguez-Lopez, Gilberto Spadoni, Silvia Rivara, Annalida Bedini, Debora Angeloni, and Franco Fraschini. 2011. 'Promotion of non-rapid eye movement sleep and activation of reticular thalamic neurons by a novel MT2 melatonin receptor ligand', *The Journal of Neuroscience*, 31: 18439-52.

Ochoa-Sanchez, Rafael, Quentin Rainer, Stefano Comai, Gilberto Spadoni, Annalida Bedini, Silvia Rivara, Franco Fraschini, Marco Mor, Giorgio Tarzia, and Gabriella Gobbi. 2012. 'Anxiolytic effects of the melatonin MT 2 receptor partial agonist UCM765: Comparison with melatonin and diazepam', *Progress in Neuro-Psychopharmacology and Biological Psychiatry*, 39: 318-25.

Oliveira-Abreu, Klausen, Francisco Walber Ferreira-da-Silva, Kerly Shamyra da Silva-Alves, Nathalia Maria Silva-dos-Santos, Ana Carolina Cardoso-Teixeira, Fernanda Gaspar do Amaral, Jose Cipolla-Neto, and José Henrique Leal-Cardoso. 2018. 'Melatonin decreases neuronal excitability in a sub-population of dorsal root ganglion neurons', *Brain research*, 1692: 1-8.

Osborne, PB, CW Vaughan, HI Wilson, and MJ Christie. 1996. 'Opioid inhibition of rat periaqueductal grey neurones with identified projections to rostral ventromedial medulla in vitro', *The Journal of Physiology*, 490: 383-89.

Ossipov, Michael H, Phil Malan Jr, Josephine Lai, and Frank Porreca. 2000. 'Mediation of spinal nerve injury induced tactile allodynia by descending facilitatory pathways in the dorsolateral funiculus in rats', *Neuroscience letters*, 290: 129-32.

Palazzo, Enza, Francesca Guida, Luisa Gatta, Livio Luongo, Serena Boccella, Giulia Bellini, Ida Marabese, Vito de Novellis, Francesca Rossi, and Sabatino Maione. 2011. 'EPI Receptor within the Ventrolateral Periaqueductal Grey Controls Thermonociception and Rostral Ventromedial Medulla Cell Activity in Healthy and Neuropathic Rat', *Molecular pain*, 7: 1744-8069-7-82.

Palazzo, Enza, Livio Luongo, Vito de Novellis, Liberato Berrino, Francesco Rossi, and Sabatino Maione. 2010. 'Moving towards supraspinal TRPV1 receptors for chronic pain relief', *Mol. pain*, 6: 1.

Pan, Yu-Zhen, De-Pei Li, and Hui-Lin Pan. 2002. 'Inhibition of glutamatergic synaptic input to spinal lamina IIo neurons by presynaptic α2-adrenergic receptors', *Journal of neurophysiology*, 87: 1938-47.

Pan, Zhizhong Z, JT Williams, and PB Osborne. 1990. 'Opioid actions on single nucleus raphe magnus neurons from rat and guinea-pig in vitro', *The Journal of Physiology*, 427: 519-32.
Pang, CS, SF Tsang, and JC Yang. 2001. 'Effects of melatonin, morphine and diazepam on formalin-induced nociception in mice', *Life Sci*, 68: 943-51.
Park, Cheongdahm, Jong-Hyun Kim, Bo-Eun Yoon, Eui-Ju Choi, C Justin Lee, and Hee-Sup Shin. 2010. 'T-type channels control the opioidergic descending analgesia at the low threshold-spiking GABAergic neurons in the periaqueductal gray', *Proceedings of the National Academy of Sciences*, 107: 14857-62.
Patil, Nila, David R Cox, Deepti Bhat, Malek Faham, Richard M Myers, and Andrew S Peterson. 1995. 'A potassium channel mutation in weaver mice implicates membrane excitability in granule cell differentiation', *Nature genetics*, 11: 126-29.
Peres, M. F. 2005. 'Melatonin, the pineal gland and their implications for headache disorders', *Cephalalgia*, 25: 403-11.
Peres, M. F.P., E. Zukerman, F. da Cunha Tanuri, F. R. Moreira, and J. Cipolla-Neto. 2004. 'Melatonin, 3 mg, is effective for migraine prevention', *Neurology*, 63: 757.
Peres, Mario FP, Marcelo R Masruha, Eliova Zukerman, Carlos Alberto Moreira-Filho, and Esper A Cavalheiro. 2006. 'Potential therapeutic use of melatonin in migraine and other headache disorders', *Expert. Opin. Investig. Drugs*, 15: 367-75.
Pert, Candace B, Gavril Pasternak, and Solomon H Snyder. 1973. 'Opiate agonists and antagonists discriminated by receptor binding in brain', *Science*, 182: 1359-61.
Pert, Candace B, and Solomon H Snyder. 1973. 'Opiate receptor: demonstration in nervous tissue', *Science*, 179: 1011-14.
Pertovaara, Antti. 2006. 'Noradrenergic pain modulation', *Progress in neurobiology*, 80: 53-83.
Pertovaara, Antti, Hong Wei, and Minna M Hämäläinen. 1996. 'Lidocaine in the rostroventromedial medulla and the periaqueductal gray attenuates allodynia in neuropathic rats', *Neuroscience letters*, 218: 127-30.
Petit, Laurence, Isabelle Lacroix, Pierre de Coppet, A Donny Strosberg, and Ralf Jockers. 1999. 'Differential signaling of human Mel1a and Mel1b melatonin receptors through the cyclic guanosine 3′-5′-monophosphate pathway', *Biochemical pharmacology*, 58: 633-39.
Pinto-Ribeiro, Filipa, Osei B Ansah, Armando Almeida, and Antti Pertovaara. 2008. 'Influence of arthritis on descending modulation of nociception from the paraventricular nucleus of the hypothalamus', *Brain research*, 1197: 63-75.
Pinto, M, D Lima, and I Tavares. 2007. 'Neuronal activation at the spinal cord and medullary pain control centers after joint stimulation: a c-fos study in acute and chronic articular inflammation', *Neuroscience*, 147: 1076-89.
Pontieri, FE, G Tanda, and GAETANO Di Chiara. 1995. 'Intravenous cocaine, morphine, and amphetamine preferentially increase extracellular dopamine in the" shell" as compared with the" core" of the rat nucleus accumbens', *Proceedings of the National Academy of Sciences*, 92: 12304-08.
Porreca, Frank, Shannon E Burgess, Luis R Gardell, Todd W Vanderah, T Philip Malan, Michael H Ossipov, Douglas A Lappi, and Josephine Lai. 2001. 'Inhibition of neuropathic pain by selective ablation of brainstem medullary cells expressing the μ-opioid receptor', *Journal of Neuroscience*, 21: 5281-88.
Posa, Luca, Alison Accarie, Florence Noble, and Nicolas Marie. 2015. 'Methadone reverses analgesic tolerance induced by morphine pretreatment', *Int. J. Neuropsychopharmacol.*: pyv108.

Posa, Luca, Danilo De Gregorio, Gabriella Gobbi, and Stefano Comai. 2018. 'Targeting melatonin MT2 receptors: A novel pharmacological avenue for inflammatory and neuropathic pain', *Current medicinal chemistry*, 25: 3866-82.

Potrebic, SB, HL Fields, and P Mason. 1994. 'Serotonin immunoreactivity is contained in one physiological cell class in the rat rostral ventromedial medulla', *Journal of Neuroscience*, 14: 1655-65.

Poulin, Jean-François, Patrick Bérubé, Sylvie Laforest, and Guy Drolet. 2013. 'Enkephalin knockdown in the central amygdala nucleus reduces unconditioned fear and anxiety', *European Journal of Neuroscience*, 37: 1357-67.

Pradhan, Amynah A, Katia Befort, Chihiro Nozaki, Claire Gavériaux-Ruff, and Brigitte L Kieffer. 2011. 'The delta opioid receptor: an evolving target for the treatment of brain disorders', *Trends in pharmacological sciences*, 32: 581-90.

Radwan, K, M Youssef, A El-Tawdy, M Zeidan, and N Kamal. 2010. 'Melatonin versus Gabapentin. A comparative study of preemptive medications', *Internet J. Anaesth.*, 23: 1.

Raghavendra, Vasudeva, Javed N Agrewala, and Shrinivas K Kulkarni. 2000. 'Melatonin reversal of lipopolysacharides-induced thermal and behavioral hyperalgesia in mice', *Eur. J. Pharmacol.*, 395: 15-21.

Raja, Srinivasa N, Daniel B Carr, Milton Cohen, Nanna B Finnerup, Herta Flor, Stephen Gibson, Francis J Keefe, Jeffrey S Mogil, Matthias Ringkamp, and Kathleen A Sluka. 2020. 'The revised International Association for the Study of Pain definition of pain: concepts, challenges, and compromises', *Pain*, 161: 1976-82.

Raveh, Adi, Inbal Riven, and Eitan Reuveny. 2009. 'Elucidation of the gating of the GIRK channel using a spectroscopic approach', *The Journal of Physiology*, 587: 5331-35.

Ray, M, Pramod K Mediratta, P Mahajan, and KK Sharma. 2004. 'Evaluation of the role of melatonin in formalin-induced pain response in mice'.

Recio, Joaquín, Paul Pévet, Berthe Vivien-Roels, Jesús M Míguez, and Mireille Masson-Pévet. 1996. 'Daily and photoperiodic melatonin binding changes in the suprachiasmatic nuclei, paraventricular thalamic nuclei, and pars tuberalis of the female Siberian hamster (Phodopus sungorus)', *Journal of biological rhythms*, 11: 325-32.

Reiter, Russel J, Juan R Calvo, Malgorzata Karbownik, Wenbo Qi, and Dun Xian Tan. 2000. 'Melatonin and its relation to the immune system and inflammation', *Annals of the New York Academy of Sciences*, 917: 376-86.

Reiter, Russel J, Dun-Xian Tan, and Lorena Fuentes-Broto. 2010. 'Melatonin: a multitasking molecule.' in, *Progress in brain research* (Elsevier).

Reppert, S M, C Godson, C D Mahle, D R Weaver, S A Slaugenhaupt, and J F Gusella. 1995. 'Molecular characterization of a second melatonin receptor expressed in human retina and brain: the Mel1b melatonin receptor', *Proceedings of the National Academy of Sciences*, 92: 8734-38.

Reppert, Steven M, David R Weaver, and Takashi Ebisawa. 1994. 'Cloning and characterization of a mammalian melatonin receptor that mediates reproductive and circadian responses', *Neuron*, 13: 1177-85.

Rivara, Silvia, Alessio Lodola, Marco Mor, Annalida Bedini, Gilberto Spadoni, Valeria Lucini, Marilou Pannacci, Franco Fraschini, Francesco Scaglione, and Rafael Ochoa Sanchez. 2007. 'N-(substituted-anilinoethyl) amides: design, synthesis, and pharmacological characterization of a new class of melatonin receptor ligands', *J. Med. Chem.*, 50: 6618-26.

Rizvi, Tilat A, Matthew Ennis, Michael M Behbehani, and Michael T Shipley. 1991. 'Connections between the central nucleus of the amygdala and the midbrain periaqueductal gray: topography and reciprocity', *Journal of Comparative Neurology*, 303: 121-31.

Rosén, Annika, Yu-Xuan Zhang, Irene Lund, Thomas Lundeberg, and Long-Chuan Yu. 2004. 'Substance P microinjected into the periaqueductal gray matter induces antinociception and is released following morphine administration', *Brain research*, 1001: 87-94.

Roychowdhury, SM, and HL Fields. 1996. 'Endogenous opioids acting at a medullary μ-opioid receptor contribute to the behavioral antinociception produced by GABA antagonism in the midbrain periaqueductal gray', *Neuroscience*, 74: 863-72.

Rozisky, Joanna Ripoll, Vanessa Leal Scarabelot, Carla de Oliveira, Isabel Cristina de Macedo, Alícia Deitos, Gabriela Laste, Wolnei Caumo, and Iraci LS Torres. 2016. 'Melatonin as a potential counter-effect of hyperalgesia induced by neonatal morphine exposure', *Neurosci. Lett.*

Saha, Lekha, Samir Malhotra, Surinder Rana, Deepak Bhasin, and Promila Pandhi. 2007. 'A preliminary study of melatonin in irritable bowel syndrome', *J. Clin. Gastroenterol.*, 41: 29-32.

Salinas-Abarca, A. B., S. H. Avila-Rojas, P. Barragan-Iglesias, J. B. Pineda-Farias, and V. Granados-Soto. 2017. 'Formalin injection produces long-lasting hypersensitivity with characteristics of neuropathic pain', *European Journal of Pharmacology*.

Sallinen, Pirkko, Seppo Saarela, Mika Ilves, Olli Vakkuri, and Juhani Leppäluoto. 2005. 'The expression of MT1 and MT2 melatonin receptor mRNA in several rat tissues', *Life sciences*, 76: 1123-34.

Samaha, Anne-Noel, and Terry E Robinson. 2005. 'Why does the rapid delivery of drugs to the brain promote addiction?', *Trends in pharmacological sciences*, 26: 82-87.

Samineni, Vijay K, Jose G Grajales-Reyes, Bryan A Copits, Daniel E O'Brien, Sarah L Trigg, Adrian M Gomez, Michael R Bruchas, and Robert W Gereau IV. 2017. 'Divergent modulation of nociception by glutamatergic and GABAergic neuronal subpopulations in the periaqueductal gray', *eneuro*, 4: e0129-16.2017.

Scarabelot, Vanessa Leal, Liciane Fernandes Medeiros, Carla de Oliveira, Lauren Naomi Spezia Adachi, Isabel Cristina de Macedo, Stefania Giotti Cioato, Joice S de Freitas, Andressa de Souza, Alexandre Quevedo, and Wolnei Caumo. 2016. 'Melatonin Alters the Mechanical and Thermal Hyperalgesia Induced by Orofacial Pain Model in Rats', *Inflammation*: 1-11.

Schopflocher, Donald, Paul Taenzer, and Roman Jovey. 2011. 'The prevalence of chronic pain in Canada', *Pain research and management*, 16: 445-50.

Schwertner, André, Claudia C Conceição Dos Santos, Gislene Dalferth Costa, Alícia Deitos, Andressa de Souza, Izabel Cristina Custodio de Souza, Iraci LS Torres, João Sabino L da Cunha Filho, and Wolnei Caumo. 2013. 'Efficacy of melatonin in the treatment of endometriosis: a phase II, randomized, double-blind, placebo-controlled trial', *Pain*, 154: 874-81.

Seet, Edwin, Chen Mei Liaw, Sylvia Tay, and Chang Su. 2015. 'Melatonin premedication versus placebo in wisdom teeth extraction: a randomised controlled trial', *Singapore Med. J.*, 56: 666.

Semak, Igor, Elena Korik, Maria Antonova, Jacobo Wortsman, and Andrzej Slominski. 2008. 'Metabolism of melatonin by cytochrome P450s in rat liver mitochondria and microsomes', *Journal of Pineal Research*, 45: 515-23.

Sharkey, James T, Roopashri Puttaramu, R Ann Word, and James Olcese. 2009. 'Melatonin synergizes with oxytocin to enhance contractility of human myometrial smooth muscle cells', *The Journal of Clinical Endocrinology & Metabolism*, 94: 421-27.

Shavali, Shaik, Begonia Ho, Piyarat Govitrapong, Saiphon Sawlom, Amornpan Ajjimaporn, Sirirat Klongpanichapak, and Manuchair Ebadi. 2005. 'Melatonin exerts its analgesic actions not by binding to opioid receptor subtypes but by increasing the release of β-endorphin an endogenous opioid', *Brain Research Bulletin*, 64: 471-79.

Simon, Eric J, Jacob M Hiller, and Irit Edelman. 1973. 'Stereospecific binding of the potent narcotic analgesic [3H] etorphine to rat-brain homogenate', *Proceedings of the National Academy of Sciences*, 70: 1947-49.

Simon, Lee S. 2012. 'Relieving pain in America: A blueprint for transforming prevention, care, education, and research', *Journal of pain & palliative care pharmacotherapy*, 26: 197-98.

Smith, Kyle S, Amy J Tindell, J Wayne Aldridge, and Kent C Berridge. 2009. 'Ventral pallidum roles in reward and motivation', *Behavioural brain research*, 196: 155-67.

Song, Guang Hui, Poh Hock Leng, Kok Ann Gwee, Shabbir M Moochhala, and Khek Yu Ho. 2005. 'Melatonin improves abdominal pain in irritable bowel syndrome patients who have sleep disturbances: a randomised, double blind, placebo controlled study', *Gut*, 54: 1402-07.

Song, Li, Chaoran Wu, and Yunxia Zuo. 2015. 'Melatonin prevents morphine-induced hyperalgesia and tolerance in rats: role of protein kinase C and N-methyl-D-aspartate receptors', *BMC Anesthesiol.*, 15: 1.

Sorge, Robert E, Josiane CS Mapplebeck, Sarah Rosen, Simon Beggs, Sarah Taves, Jessica K Alexander, Loren J Martin, Jean-Sebastien Austin, Susana G Sotocinal, and Di Chen. 2015. 'Different immune cells mediate mechanical pain hypersensitivity in male and female mice', *Nature neuroscience*, 18: 1081-83.

Spetea, Mariana, Muhammad Faheem Asim, Gerhard Wolber, and Helmut Schmidhammer. 2013. 'The μ opioid receptor and ligands acting at the μ opioid receptor, as therapeutics and potential therapeutics', *Current Pharmaceutical Design*, 19: 7415-34.

Stefani, Luciana Cadore, Suzana Muller, Iraci LS Torres, Bruna Razzolini, Joanna R Rozisky, Felipe Fregni, Regina Markus, and Wolnei Caumo. 2013. 'A phase II, randomized, double-blind, placebo controlled, dose-response trial of the melatonin effect on the pain threshold of healthy subjects', *PloS one*, 8: e74107.

Stein, C, MJ Millan, and A Herz. 1988. 'Unilateral inflammation of the hindpaw in rats as a model of prolonged noxious stimulation: alterations in behavior and nociceptive thresholds', *Pharmacol. Biochem. Behav.*, 31: 445-51.

Stoeber, Miriam, Damien Jullié, Braden T Lobingier, Toon Laeremans, Jan Steyaert, Peter W Schiller, Aashish Manglik, and Mark von Zastrow. 2018. 'A genetically encoded biosensor reveals location bias of opioid drug action', *Neuron*, 98: 963-76. e5.

Storr, M, V Schusdziarra, and H-D Allescher. 2000. 'Inhibition of small conductance K+-channels attenuated melatonin-induced relaxation of serotonin-contracted rat gastric fundus', *Can. J. Physiol. Pharmacol.*, 78: 799-806.

Sufka, Kenneth J, G Stennis Watson, Rebeccah E Nothdurft, and Jeffrey S Mogil. 1998. 'Scoring the mouse formalin test: validation study', *European Journal of Pain*, 2: 351-58.

Tabeeva, GR, AV Sergeev, and SA Gromova. 2011. 'Possibilities of preventive treatment of migraine with the MT1-and MT2 agonist and 5-HT2c receptor antagonist agomelatin (valdoxan)', *Zh. Nevrol. Psikhiatr. Im S. S. Korsakova.*, 111: 32-36.

Takada, Tomohiko, Akira Yamashita, Akitoshi Date, Makoto Yanase, Yuki Suhara, Asami Hamada, Hiroyasu Sakai, Daigo Ikegami, Masako Iseki, and Eiichi Inada. 2013. 'Changes in the circadian rhythm of mRNA expression for μ-opioid receptors in the periaqueductal gray under a neuropathic pain-like state', *Synapse*, 67: 216-23.

Takahashi, Tatiane T, Valentina Vengeliene, and Rainer Spanagel. 2017. 'Melatonin reduces motivation for cocaine self-administration and prevents relapse-like behavior in rats', *Psychopharmacology*, 234: 1741-48.

Takasu, Keiko, Koichi Ogawa, Atsushi Nakamura, Tomoe Kanbara, Hiroko Ono, Takako Tomii, Yasuhide Morioka, Minoru Hasegawa, Masahiro Shibasaki, and Tomohisa Mori. 2015. 'Enhanced GABA ergic synaptic transmission at VLPAG neurons and potent modulation by oxycodone in a bone cancer pain model', *British journal of pharmacology*, 172: 2148-64.

Terayama, Ryuji, Yun Guan, Ronald Dubner, and Ke Ren. 2000. 'Activity-induced plasticity in brain stem pain modulatory circuitry after inflammation', *Neuroreport*, 11: 1915-19.

Tortorici, V, and MM Morgan. 2002. 'Comparison of morphine and kainic acid microinjections into identical PAG sites on the activity of RVM neurons', *Journal of neurophysiology*, 88: 1707-15.

Tortorici, Víctor, Michael M Morgan, and Horacio Vanegas. 2001. 'Tolerance to repeated microinjection of morphine into the periaqueductal gray is associated with changes in the behavior of off-and on-cells in the rostral ventromedial medulla of rats', *J Pain*, 89: 237-44.

Treede, Rolf-Detlef, Winfried Rief, Antonia Barke, Qasim Aziz, Michael I Bennett, Rafael Benoliel, Milton Cohen, Stefan Evers, Nanna B Finnerup, and Michael B First. 2015. 'A classification of chronic pain for ICD-11', *Pain*, 156: 1003.

Trescot, Andrea M, Standiford Helm, Hans Hansen, Ramsin Benyamin, Scott E Glaser, Rajive Adlaka, Samir Patel, and Laxmaiah Manchikanti. 2008. 'Opioids in the management of chronic non-cancer pain: an update of American Society of the Interventional Pain Physicians'(ASIPP) Guidelines', *Pain physician*, 11: S5-S62.

Tsujino, H., E. Kondo, T. Fukuoka, Y. Dai, A. Tokunaga, K. Miki, K. Yonenobu, T. Ochi, and K. Noguchi. 2000. 'Activating transcription factor 3 (ATF3) induction by axotomy in sensory and motoneurons: A novel neuronal marker of nerve injury', *Molecular and Cellular Neurosciences*, 15: 170-82.

Tu, Yijun, Rui-Qing Sun, and William D Willis. 2004. 'Effects of intrathecal injections of melatonin analogs on capsaicin-induced secondary mechanical allodynia and hyperalgesia in rats', *Pain*, 109: 340-50.

Ulugol, A, D Dokmeci, G Guray, N Sapolyo, F Ozyigit, and M Tamer. 2006. 'Antihyperalgesic, but not antiallodynic, effect of melatonin in nerve-injured neuropathic mice: Possible involvements of the L-arginine-NO pathway and opioid system', *Life Sci*, 78: 1592-7.

Unruh, Anita M. 1996. 'Gender variations in clinical pain experience', *Pain*, 65: 123-67.

Urban, MO, and GF Gebhart. 1999. 'Supraspinal contributions to hyperalgesia', *Proceedings of the National Academy of Sciences*, 96: 7687-92.

Vanegas, Horacio, Nicholas M Barbaro, and Howard L Fields. 1984. 'Tail-flick related activity in medullospinal neurons', *Brain research*, 321: 135-41.

Vaughan, Christopher W, Elena E Bagley, Geoffrey M Drew, Alwin Schuller, John E Pintar, Stephen P Hack, and MacDonald J Christie. 2003. 'Cellular actions of opioids on

periaqueductal grey neurons from C57B16/J mice and mutant mice lacking MOR-1', *British journal of pharmacology*, 139: 362-67.

Vaughan, CW, and MJ Christie. 1997. 'Presynaptic inhibitory action of opioids on synaptic transmission in the rat periaqueductal grey in vitro', *The Journal of Physiology*, 498: 463-72.

Vaughan, CW, SL Ingram, MA Connor, and MJ Christie. 1997. 'How opioids inhibit GABA-mediated neurotransmission', *Nature*, 390: 611-14.

Vogler, Barbara, Alan M Rapoport, Stewart J Tepper, Fred Sheftell, and Marcelo E Bigal. 2006. 'Role of melatonin in the pathophysiology of migraine', *CNS drugs*, 20: 343-50.

Volpe, Donna A, Grainne A McMahon Tobin, R Daniel Mellon, Aspandiar G Katki, Robert J Parker, Thomas Colatsky, Timothy J Kropp, and S Leigh Verbois. 2011. 'Uniform assessment and ranking of opioid mu receptor binding constants for selected opioid drugs', *Regulatory Toxicology and Pharmacology*, 59: 385-90.

Wan, QI, Mingxia Liao, Gregory M Brown, and Shiu Fun Pang. 1996. 'Localization and characterization of melatonin receptors in the rabbit spinal cord', *Neuroscience letters*, 204: 77-80.

Wan, Qi, Heng-Ye Man, Fang Liu, Jodi Braunton, Hyman B Niznik, Shiu Fun Pang, Gregory M Brown, and Yu Tian Wang. 1999. 'Differential modulation of GABA A receptor function by Mel 1a and Mel 1b receptors', *Nature neuroscience*, 2: 401-03.

Wan, QI, and Shiu Fun Pang. 1994. 'Segmental, coronal and subcellular distribution of 2-[125I] iodomelatonin binding sites in the chicken spinal cord', *Neuroscience letters*, 180: 253-56.

Wang, Ting, Shi-rong Li, Xu Dai, Ya-li Peng, Qiang Chen, and Rui Wang. 2006. 'Effects of melatonin on orphanin FQ/nociceptin-induced hyperalgesia in mice', *Brain research*, 1085: 43-48.

Wang, Zaijie, Luis R Gardell, Michael H Ossipov, Todd W Vanderah, Miles B Brennan, Ute Hochgeschwender, Victor J Hruby, T Phil Malan, Josephine Lai, and Frank Porreca. 2001. 'Pronociceptive actions of dynorphin maintain chronic neuropathic pain', *Journal of Neuroscience*, 21: 1779-86.

Weaver, David R, Scott A Rivkees, and Steven M Reppert. 1989. 'Localization and characterization of melatonin receptors in rodent brain by in vitro autoradiography', *The Journal of neuroscience*, 9: 2581-90.

Weaver, DR, JH Stehle, EG Stopa, and SM Reppert. 1993. 'Melatonin receptors in human hypothalamus and pituitary: implications for circadian and reproductive responses to melatonin', *The Journal of Clinical Endocrinology & Metabolism*, 76: 295-301.

Weeks, James R. 1962. 'Experimental morphine addiction: method for automatic intravenous injections in unrestrained rats', *Science*, 138: 143-44.

Wei, Feng, Ronald Dubner, Shiping Zou, Ke Ren, Guang Bai, Dong Wei, and Wei Guo. 2010. 'Molecular depletion of descending serotonin unmasks its novel facilitatory role in the development of persistent pain', *Journal of Neuroscience*, 30: 8624-36.

Wettermark, B., L. Brandt, H. Kieler, and R. Boden. 2014. 'Pregabalin is increasingly prescribed for neuropathic pain, generalised anxiety disorder and epilepsy but many patients discontinue treatment', *Int J Clin Pract*, 68: 104-10.

Wheeler-Aceto, Helen, Frank Porreca, and Alan Cowan. 1990. 'The rat paw formalin test: comparison of noxious agents', *Pain*, 40: 229-38.

Wickman, Kevin D, Jorge A Iñiguez-Lluhi, Philip A Davenport, Ronald Taussig, Grigory B Krapivinsky, Maurine E Linder, Alfred G Gilman, and David E Clapham. 1994.

'Recombinant G-protein βγ-subunits activate the muscarinic-gated atrial potassium channel', *Nature*, 368: 255-57.

Wigdor, Seth, and George L Wilcox. 1987. 'Central and systemic morphine-induced antinociception in mice: contribution of descending serotonergic and noradrenergic pathways', *Journal of Pharmacology and Experimental Therapeutics*, 242: 90-95.

Wiklund, Leif, Gila Behzadi, Peter Kalén, P Max Headley, Lina S Nicolopoulos, Chris G Parsons, and David C West. 1988. 'Autoradiographic and electrophysiological evidence for excitatory amino acid transmission in the periaqueductal gray projection to nucleus raphe magnus in the rat', *Neuroscience letters*, 93: 158-63.

Wikner, Johan, Ulf Hirsch, Lennart Wetterberg, and Sven Röjdmark. 1998. 'Fibromyalgia—a syndrome associated with decreased nocturnal melatonin secretion', *Clinical endocrinology*, 49: 179-83.

Williams, Frank G, Mary A Mullet, and Alvin J Beitz. 1995. 'Basal release of Met-enkephalin and neurotensin in the ventrolateral periaqueductal gray matter of the rat: a microdialysis study of antinociceptive circuits', *Brain research*, 690: 207-16.

Williams, John T, MacDonald J Christie, and Olivier Manzoni. 2001. 'Cellular and synaptic adaptations mediating opioid dependence', *Physiological reviews*, 81: 299-343.

Willoch, Frode, Florian Schindler, Hans Jürgen Wester, Monika Empl, Andreas Straube, Markus Schwaiger, Bastian Conrad, and Thomas Rudolf Tölle. 2004. 'Central poststroke pain and reduced opioid receptor binding within pain processing circuitries: a [11C] diprenorphine PET study', *Pain*, 108: 213-20.

Winkler, Clayton W, Sam M Hermes, Charles I Chavkin, Carrie T Drake, Shaun F Morrison, and Sue A Aicher. 2006. 'Kappa opioid receptor (KOR) and GAD67 immunoreactivity are found in OFF and NEUTRAL cells in the rostral ventromedial medulla', *Journal of neurophysiology*, 96: 3465-73.

Witt-Enderby, Paula A, Jennifer Bennett, Michael J Jarzynka, Steven Firestine, and Melissa A Melan. 2003. 'Melatonin receptors and their regulation: biochemical and structural mechanisms', *Life sciences*, 72: 2183-98.

Wittert, G, P Hope, and D Pyle. 1996. 'Tissue distribution of opioid receptor gene expression in the rat', *Biochemical and biophysical research communications*, 218: 877-81.

Xie, Jennifer Y, David S Herman, Carl-Olav Stiller, Luis R Gardell, Michael H Ossipov, Josephine Lai, Frank Porreca, and Todd W Vanderah. 2005. 'Cholecystokinin in the rostral ventromedial medulla mediates opioid-induced hyperalgesia and antinociceptive tolerance', *Journal of Neuroscience*, 25: 409-16.

Xu, Mei, Chang Jae Kim, Miranda J Neubert, and Mary M Heinricher. 2007. 'NMDA receptor-mediated activation of medullary pro-nociceptive neurons is required for secondary thermal hyperalgesia', *Pain*, 127: 253-62.

Xu, Mei, Michael Petraschka, Jay P McLaughlin, Ruth E Westenbroek, Marc G Caron, Robert J Lefkowitz, Traci A Czyzyk, John E Pintar, Gregory W Terman, and Charles Chavkin. 2004. 'Neuropathic pain activates the endogenous κ opioid system in mouse spinal cord and induces opioid receptor tolerance', *Journal of Neuroscience*, 24: 4576-84.

Xu, Shuyun, Wei Wei, Yuxian Shen, Jieqing Hao, and Changhai Ding. 1996. 'Studies on the antiinflammatory, immunoregulatory, and analgesic actions of melatonin', *Drug development research*, 39: 167-73.

Yaksh, Tony L, and PR Wilson. 1979. 'Spinal serotonin terminal system mediates antinociception', *Journal of Pharmacology and Experimental Therapeutics*, 208(3): 446-53.

Yeomans, DC, and HK Proudfit. 1990. 'Projections of substance P-immunoreactive neurons located in the ventromedial medulla to the A7 noradrenergic nucleus of the rat demonstrated using retrograde tracing combined with immunocytochemistry', *Brain research*, 532: 329-32.

Yerer, Mükerrem Betül, MDPA Delgado, and Sami Aydogan. 2010. 'Regulation of MT1 and MT2 receptors in pineal gland with light/dark cycle: a novel approach', *Turk J Biochem*, 35: 256-61.

Yeung, Joseph C, Tony L Yaksh, and Thomas A Rudy. 1977. 'Concurrent mapping of brain sites for sensitivity to the direct application of morphine and focal electrical stimulation in the production of antinociception in the rat', *Pain*, 4: 23-40.

Ying, SW, and ZQ Huang. 1990. 'Effects of the pineal body and melatonin on sensitivity to pain in mice', *Acta Pharmacol. Sin.*, 11: 411-14.

Yoon, Myung Ha, Heon Chang Park, Woong Mo Kim, Hyung Gon Lee, Yeo Ok Kim, and Lan Ji Huang. 2008. 'Evaluation for the interaction between intrathecal melatonin and clonidine or neostigmine on formalin-induced nociception', *Life sciences*, 83: 845-50.

Yu, Chang-Xi, Chong-Bin Zhu, Shao-Fen Xu, Xiao-Ding Cao, and Gen-Cheng Wu. 2000. 'Selective MT2 melatonin receptor antagonist blocks melatonin-induced antinociception in rats', *Neuroscience letters*, 282: 161-64.

Zahn, Peter K, Tanja Lansmann, Eva Berger, Erwin-Josef Speckmann, and Ulrich Musshoff. 2003. 'Gene expression and functional characterization of melatonin receptors in the spinal cord of the rat: implications for pain modulation', *Journal of Pineal Research*, 35: 24-31.

Zeng, Q, S Wang, G Lim, L Yang, J Mao, B Sung, Y Chang, JA Lim, and G Guo. 2008. 'Exacerbated mechanical allodynia in rats with depression-like behavior', *Brain Res*, 1200: 27-38.

Zhang, Wenjun, Shannon Gardell, Dongqin Zhang, Jennifer Y Xie, Richard S Agnes, Hamid Badghisi, Victor J Hruby, Naomi Rance, Michael H Ossipov, and Todd W Vanderah. 2009. 'Neuropathic pain is maintained by brainstem neurons co-expressing opioid and cholecystokinin receptors', *Brain*, 132: 778-87.

Zhao, Dake, Yang Yu, Yong Shen, Qin Liu, Zhiwei Zhao, Ramaswamy Sharma, and Russel J Reiter. 2019. 'Melatonin synthesis and function: evolutionary history in animals and plants', *Frontiers in endocrinology*, 10: 249.

Supplementary Table - Statistical analysis Chapter III

Figure	Panel	Test	Group-size	Statistic	P value	Pair-wise comparison	Statistic 2		
							Test details	Summary	Adjusted P Value
1	A	Repeated measures 2-way ANOVA (treatment x time)	Veh = 6 UCM924 = 9 Nalox = 5 Nalox+UCM924 = 7	Time x treatment : F (27, 207) = 12.36 Time : F (2.494, 57.37) = 16.07 Treatment : F (3, 23) = 25.87	P<0.0001 P<0.0001 P<0.0001	Tuckey post hoc comparison	0		
							Veh vs. UCM924	ns	0.2837
							Veh vs. Nalo	ns	0.9973
							Veh vs. Nalo + UCM924	ns	0.9944
							UCM924 vs. Nalo	ns	0.5976
							UCM924 vs. Nalo + UCM924	ns	0.4413
							Nalo vs. Nalo + UCM924	ns	>0.9999
							0.5		
							Veh vs. UCM924	ns	0.2951
							Veh vs. Nalo	ns	0.9721
							Veh vs. Nalo + UCM924	ns	0.7992
							UCM924 vs. Nalo	ns	0.3035
							UCM924 vs. Nalo + UCM924	ns	0.5152
							Nalo vs. Nalo + UCM924	ns	0.8505
							1		
							Veh vs. UCM924	***	0.0006
							Veh vs. Nalo	ns	0.2329
							Veh vs. Nalo + UCM924	ns	0.9989
							UCM924 vs. Nalo	***	0.0001
							UCM924 vs. Nalo + UCM924	**	0.0014
							Nalo vs. Nalo + UCM924	ns	0.3453
							2		
							Veh vs. UCM924	***	0.0002
							Veh vs. Nalo	ns	0.8654
							Veh vs. Nalo + UCM924	ns	0.2438
							UCM924 vs. Nalo	***	0.0005
							UCM924 vs. Nalo + UCM924	*	0.0162
							Nalo vs. Nalo + UCM924	ns	0.3541
							3		
							Veh vs. UCM924	****	<0.0001
							Veh vs. Nalo	ns	0.8759
							Veh vs. Nalo + UCM924	ns	0.2991
							UCM924 vs. Nalo	****	<0.0001
							UCM924 vs. Nalo + UCM924	***	0.0002
							Nalo vs. Nalo + UCM924	ns	0.1347
							4		
							Veh vs. UCM924	****	<0.0001
							Veh vs. Nalo	ns	0.9943
							Veh vs. Nalo + UCM924	ns	0.5456
							UCM924 vs. Nalo	*	0.0157
							UCM924 vs. Nalo + UCM924	**	0.0065
							Nalo vs. Nalo + UCM924	ns	0.8851
							5		
							Veh vs. UCM924	****	<0.0001
							Veh vs. Nalo	ns	0.8169
							Veh vs. Nalo + UCM924	ns	0.5011
							UCM924 vs. Nalo	****	<0.0001
							UCM924 vs. Nalo + UCM924	***	0.0004
							Nalo vs. Nalo + UCM924	ns	0.2913
							6		
							Veh vs. UCM924	**	0.0013
							Veh vs. Nalo	ns	0.9779
							Veh vs. Nalo + UCM924	ns	0.258
							UCM924 vs. Nalo	**	0.0019
							UCM924 vs. Nalo + UCM924	**	0.009
							Nalo vs. Nalo + UCM924	ns	0.3977
							7		
							Veh vs. UCM924	**	0.0019
							Veh vs. Nalo	ns	0.9991
							Veh vs. Nalo + UCM924	ns	0.1471
							UCM924 vs. Nalo	*	0.0138
							UCM924 vs. Nalo + UCM924	ns	0.3013
							Nalo vs. Nalo + UCM924	ns	0.2287
							8		
							Veh vs. UCM924	ns	0.9841
							Veh vs. Nalo	ns	0.9687
							Veh vs. Nalo + UCM924	ns	0.7975
							UCM924 vs. Nalo	ns	0.8208
							UCM924 vs. Nalo + UCM924	ns	0.8243
							Nalo vs. Nalo + UCM924	ns	0.5642
1	B	1-way ANOVA	Veh = 6 UCM924 = 9 Nalox = 5 Nalox+UCM924 = 7	F (3, 23) = 28.28	P<0.0001	Tuckey post hoc comparison	Test details	Summary	Adjusted P Value
							Veh vs. UCM924	****	<0.0001
							Veh vs. Nalo	ns	>0.9999
							Veh vs. Nalo + UCM924	ns	0.5536
							UCM924 vs. Nalo	****	<0.0001
							UCM924 vs. Nalo + UCM924	****	<0.0001
							Nalo vs. Nalo + UCM924	ns	0.5161
1	C	Repeated measures 2-way ANOVA (treatment x time)	Veh = 6 UCM924 = 8 Nalox = 3 Nalox+UCM924 = 5	Time x treatment : F (15, 90) = 8.361 Time : F (1.634, 29.41) = 7.957 Treatment : F (3, 18) = 16.47	P<0.0001 P=0.0030 P<0.0001	Tuckey post hoc comparison	Test details	Summary	Adjusted P Value
							0		
							Veh vs. UCM924	ns	0.3193
							Veh vs. Nalo	ns	0.7595
							Veh vs. Nalo + UCM924	ns	0.9986
							UCM924 vs. Nalo	ns	0.4718
							UCM924 vs. Nalo + UCM924	ns	0.1891
							Nalo vs. Nalo + UCM924	ns	0.7255

							0.5		
							Veh vs. UCM924	ns	0.1152
							Veh vs. Nalo	ns	0.9985
							Veh vs. Nalo + UCM924	ns	0.3272
							UCM924 vs. Nalo	ns	0.1625
							UCM924 vs. Nalo + UCM924	*	0.0184
							Nalo vs. Nalo + UCM924	ns	0.3432
							1		
							Veh vs. UCM924	**	0.0078
							Veh vs. Nalo	ns	0.765
							Veh vs. Nalo + UCM924	ns	0.9429
							UCM924 vs. Nalo	**	0.0056
							UCM924 vs. Nalo + UCM924	**	0.0092
							Nalo vs. Nalo + UCM924	ns	0.5876
							1.5		
							Veh vs. UCM924	**	0.0079
							Veh vs. Nalo	ns	0.6262
							Veh vs. Nalo + UCM924	ns	0.4065
							UCM924 vs. Nalo	ns	0.3466
							UCM924 vs. Nalo + UCM924	*	0.0128
							Nalo vs. Nalo + UCM924	ns	0.1707
							2		
							Veh vs. UCM924	ns	0.7834
							Veh vs. Nalo	ns	0.8755
							Veh vs. Nalo + UCM924	ns	0.9975
							UCM924 vs. Nalo	ns	>0.9999
							UCM924 vs. Nalo + UCM924	ns	0.7622
							Nalo vs. Nalo + UCM924	ns	0.8448
							3		
							Veh vs. UCM924	ns	0.9241
							Veh vs. Nalo	ns	0.4724
							Veh vs. Nalo + UCM924	ns	>0.9999
							UCM924 vs. Nalo	ns	0.4875
							UCM924 vs. Nalo + UCM924	ns	0.709
							Nalo vs. Nalo + UCM924	ns	0.2231
1	D	1-way ANOVA	Veh = 6 UCM924 = 8 Nalox = 3 Nalox+UCM924 = 5	F (3, 18) = 12.36	P=0.0001	Tuckey post hoc comparison	Test details	Summary	Adjusted P Value
							Veh vs. UCM924	***	0.0005
							Veh vs. Nalo	ns	0.9136
							Veh vs. Nalo + UCM924	ns	0.9923
							UCM924 vs. Nalo	*	0.0181
							UCM924 vs. Nalo + UCM924	***	0.0004
							Nalo vs. Nalo + UCM924	ns	0.8248
1	E	Repeated measures 2-way ANOVA (treatment x time)	Veh = 6 UCM924 = 8 CTOP = 3 CTOP+UCM924 = 6	Time x treatment : F (15, 95) = 9.096 Time : F (1.718, 32.63) = 8.531 Treatment : F (3, 19) = 16.03	P<0.0001 P=0.0017 P<0.0001	Tuckey post hoc comparison	Test details	Summary	Adjusted P Value
							0		
							Veh vs. UCM924	ns	0.3193
							Veh vs. CTOP	ns	0.4336
							Veh vs. CTOP + UCM924	ns	0.7383
							UCM924 vs. CTOP	ns	0.2259
							UCM924 vs. CTOP + UCM924	ns	0.1562
							CTOP vs. CTOP + UCM924	ns	0.7625
							0.5		
							Veh vs. UCM924	ns	0.1152
							Veh vs. CTOP	ns	0.7522
							Veh vs. CTOP + UCM924	ns	0.9772
							UCM924 vs. CTOP	*	0.049
							UCM924 vs. CTOP + UCM924	ns	0.0736
							CTOP vs. CTOP + UCM924	ns	0.9067
							1		
							Veh vs. UCM924	**	0.0078
							Veh vs. CTOP	ns	>0.9999
							Veh vs. CTOP + UCM924	ns	0.4895
							UCM924 vs. CTOP	**	0.0081
							UCM924 vs. CTOP + UCM924	**	0.0051
							CTOP vs. CTOP + UCM924	ns	0.3594
							1.5		
							Veh vs. UCM924	**	0.0079
							Veh vs. CTOP	ns	0.8828
							Veh vs. CTOP + UCM924	ns	0.7557
							UCM924 vs. CTOP	**	0.0017
							UCM924 vs. CTOP + UCM924	*	0.0112
							CTOP vs. CTOP + UCM924	ns	0.8867
							2		
							Veh vs. UCM924	ns	0.7834
							Veh vs. CTOP	ns	0.8304
							Veh vs. CTOP + UCM924	ns	0.9461
							UCM924 vs. CTOP	ns	0.9566
							UCM924 vs. CTOP + UCM924	ns	0.6928
							CTOP vs. CTOP + UCM924	ns	0.7634
							3		
							Veh vs. UCM924	ns	0.9241
							Veh vs. CTOP	ns	0.9965
							Veh vs. CTOP + UCM924	ns	0.9995
							UCM924 vs. CTOP	ns	0.9927
							UCM924 vs. CTOP + UCM924	ns	0.9666
							CTOP vs. CTOP + UCM924	ns	0.9995
1	F	1-way ANOVA	Veh = 6	F (3, 19) = 9.026	P=0.0006	Tuckey post hoc	Test details	Summary	Adjusted P Value

			UCM924 = 8 CTOP = 3 CTOP+UCM924 = 6			comparison	Veh vs. UCM924 Veh vs. CTOP Veh vs. CTOP + UCM924 UCM924 vs. CTOP UCM924 vs. CTOP + UCM924 CTOP vs. CTOP + UCM924	** ns ns * ** ns	0.0017 0.9998 0.9684 0.0101 0.0051 0.9686
1	G	Repeated measures 2-way ANOVA (treatment x time)	Veh = 6 UCM924 = 8 Nalt = 3 Nalt+UCM924 = 8	Time x treatment : F (15, 105) = 5.548 Time : F (1.439, 30.22) = 12.70 Treatment : F (3, 21) = 9.023	P<0.0001 P=0.0004 P=0.0005	Tuckey post hoc comparison	Test details 0 Veh vs. UCM924 Veh vs. Nalt Veh vs. Nalt + UCM924 UCM924 vs. Nalt UCM924 vs. Nalt + UCM924 Nalt vs. Nalt + UCM924 0.5 Veh vs. UCM924 Veh vs. Nalt Veh vs. Nalt + UCM924 UCM924 vs. Nalt UCM924 vs. Nalt + UCM924 Nalt vs. Nalt + UCM924 1 Veh vs. UCM924 Veh vs. Nalt Veh vs. Nalt + UCM924 UCM924 vs. Nalt UCM924 vs. Nalt + UCM924 Nalt vs. Nalt + UCM924 1.5 Veh vs. UCM924 Veh vs. Nalt Veh vs. Nalt + UCM924 UCM924 vs. Nalt UCM924 vs. Nalt + UCM924 Nalt vs. Nalt + UCM924 2 Veh vs. UCM924 Veh vs. Nalt Veh vs. Nalt + UCM924 UCM924 vs. Nalt UCM924 vs. Nalt + UCM924 Nalt vs. Nalt + UCM924 3 Veh vs. UCM924 Veh vs. Nalt Veh vs. Nalt + UCM924 UCM924 vs. Nalt UCM924 vs. Nalt + UCM924 Nalt vs. Nalt + UCM924	Summary ns ns ns ns ns ns ns ns * ns ns * ** ns ns ** ns ns ** ns ns * ** ns ns ns ns ns ns ns ns ns ns ns ns ns	Adjusted P Value 0.3193 0.9134 0.9134 0.9964 0.8921 0.9959 0.1152 0.9861 0.0167 0.1429 0.9998 0.0251 0.0078 0.8952 0.0766 0.0057 0.3621 0.0565 0.0079 0.9995 0.9215 0.0151 0.0024 0.8653 0.7834 0.9605 0.8657 0.9851 >0.9999 0.9926 0.9241 0.9895 0.7275 0.5563 0.859 0.3268
1	H	1-way ANOVA	Veh = 6 UCM924 = 8 Nalt = 3 Nalt+UCM924 = 8	F (3, 24) = 9.056	P=0.0003	Tuckey post hoc comparison	Test details Veh vs. UCM924 10ug Veh vs. Nalt 1ug Veh vs. Nalt + UCM924 UCM924 10ug vs. Nalt 1ug UCM924 10ug vs. Nalt + UCM924 Nalt 1ug vs. Nalt + UCM924	Summary *** ns ns ** ns ns	Adjusted P Value 0.0005 >0.9999 0.0717 0.0049 0.0715 0.1916

Figure	Panel	Test	Group-size	Statistic	P value	Pair-wise comparison	Statistic 2		
							Test details	Summary	Adjusted P Value
2	A	Repeated measures 2-way ANOVA (treatment x time)	WT Veh = 7 WT UCM924 = 11	Time x treatment : F (7, 119) = 13.40 Time : F (4.080, 69.36) = 12.91 Treatment : F (1, 17) = 70.56	<0.0001 <0.0001 <0.0001	Tuckey post hoc comparison	WT Veh - WT UCM924 20mg/kg		
							0	ns	>0.9999
							1	ns	>0.9999
							2	***	0.0001
							3	****	<0.0001
							4	****	<0.0001
							5	****	<0.0001
							6	ns	0.2862
							7	ns	>0.9999
2	B	Repeated measures 2-way ANOVA (treatment x time)	DOR-/- Veh = 7 DOR-/- UCM924 = 9	Time x treatment : F (7, 98) = 31.78 Time : F (7, 98) = 33.75 Treatment : F (1, 14) = 193.1	P<0.0001 P<0.0001 P<0.0001	Tuckey post hoc comparison	$DOR^{-/-}$ Veh - $DOR^{-/-}$ UCM924 20mg/kg		
							0	ns	>0.9999
							1	ns	>0.9999
							2	****	<0.0001
							3	****	<0.0001
							4	****	<0.0001
							5	****	<0.0001
							6	ns	0.2737
							7	ns	>0.9999
2	C	Repeated measures 2-way ANOVA (treatment x time)	MOR-/- Veh = 7 MOR-/- UCM924 = 9	Time x treatment : F (7, 98) = 0.8017 Time : F (7, 98) = 0.9032 Treatment : F (1, 14) = 3.158	P=0.5878 P=0.5073 P=0.0973	Tuckey post hoc comparison	$MOR^{-/-}$ Veh - $MOR^{-/-}$ UCM924 20mg/kg		
							0	ns	>0.9999
							1	ns	>0.9999
							2	ns	>0.9999
							3	ns	>0.9999
							4	ns	>0.9999
							5	ns	>0.9999
							6	ns	0.0781
							7	ns	>0.9999
2	D	2-way ANOVA (treatment x genotype)	WT Veh = 7 WT UCM924 = 11 DOR-/- Veh = 7 DOR-/- UCM924 = 9 MOR-/- Veh = 7 MOR-/- UCM924 = 9	treatment x genotype : F (2, 45) = 97.26 treatment : F (2, 45) = 202.2 genotype : F (1, 45) = 356.6	P<0.0001 P<0.0001 P<0.0001	Tuckey post hoc comparison	WT:Veh vs. WT:UCM924	****	<0.0001
							WT:Veh vs. DOR-/-:Veh	ns	0.2013
							WT:Veh vs. DOR-/-:UCM924	****	<0.0001
							WT:Veh vs. MOR-/-:Veh	**	0.0013
							WT:Veh vs. MOR-/-:UCM924	***	0.0001
							WT:UCM924 vs. DOR-/-:Veh	****	<0.0001
							WT:UCM924 vs. DOR-/-:UCM924	****	<0.0001
							WT:UCM924 vs. MOR-/-:Veh	****	<0.0001
							WT:UCM924 vs. MOR-/-:UCM924	****	<0.0001
							DOR-/-:Veh vs. DOR-/-:UCM924	****	<0.0001
							DOR-/-:Veh vs. MOR-/-:Veh	ns	0.3994
							DOR-/-:Veh vs. MOR-/-:UCM924	ns	0.1603
							DOR-/-:UCM924 vs. MOR-/-:Veh	****	<0.0001
							DOR-/-:UCM924 vs. MOR-/-:UCM924	****	<0.0001
							MOR-/-:Veh vs. MOR-/-:UCM924	ns	0.9991

Figure	Panel	Test	Group-size	Statistic	P value	Pair-wise comparison	Statistic 2		
							Test details	Summary	Adjusted P Value
3	C	2-Way Mixed ANOVA (treatment x time)	Veh = 3 UCM924 = 4 Nalox = 2 Nalox+UCM924 = 4	Time x treatment : F (36, 117) = 3.717 Time : F (12, 117) = 1.934 Treatment : F (3, 117) = 105.2	P<0.0001 P=0.0369 P<0.0001	Tuckey post hoc comparison	0		
							VEH vs. Nalo	ns	0.9416
							VEH vs. UCM924	ns	0.9698
							VEH vs. Nalo+UCM924	ns	0.9785
							Nalo vs. UCM924	ns	0.997
							Nalo vs. Nalo+UCM924	ns	0.9947
							UCM924 vs. Nalo+UCM924	ns	>0.9999
							5		
							VEH vs. Nalo	ns	0.6291
							VEH vs. UCM924	ns	0.9961
							VEH vs. Nalo+UCM924	ns	>0.9999
							Nalo vs. UCM924	ns	0.7102
							Nalo vs. Nalo+UCM924	ns	0.6214
							UCM924 vs. Nalo+UCM924	ns	0.9981
							10		
							VEH vs. Nalo	ns	>0.9999
							VEH vs. UCM924	ns	0.6503
							VEH vs. Nalo+UCM924	ns	0.828
							Nalo vs. UCM924	ns	0.734
							Nalo vs. Nalo+UCM924	ns	0.8749
							UCM924 vs. Nalo+UCM924	ns	0.987
							15		
							VEH vs. Nalo	ns	0.9564
							VEH vs. UCM924	*	0.0274
							VEH vs. Nalo+UCM924	ns	0.7079
							Nalo vs. UCM924	ns	0.2085
							Nalo vs. Nalo+UCM924	ns	0.9772
							UCM924 vs. Nalo+UCM924	ns	0.2316
							20		
							VEH vs. Nalo	ns	0.8697
							VEH vs. UCM924	**	0.0057
							VEH vs. Nalo+UCM924	ns	0.731
							Nalo vs. UCM924	ns	0.1415
							Nalo vs. Nalo+UCM924	ns	0.9996
							UCM924 vs. Nalo+UCM924	ns	0.0627
							25		
							VEH vs. Nalo	ns	0.9996
							VEH vs. UCM924	**	0.0032
							VEH vs. Nalo+UCM924	ns	0.972
							Nalo vs. UCM924	*	0.0166
							Nalo vs. Nalo+UCM924	ns	0.9596
							UCM924 vs. Nalo+UCM924	***	0.0002
							30		
							VEH vs. Nalo	ns	0.8634
							VEH vs. UCM924	****	<0.0001
							VEH vs. Nalo+UCM924	ns	0.9989
							Nalo vs. UCM924	***	0.0008
							Nalo vs. Nalo+UCM924	ns	0.8997
							UCM924 vs. Nalo+UCM924	****	<0.0001
							35		
							VEH vs. Nalo	ns	>0.9999
							VEH vs. UCM924	****	<0.0001
							VEH vs. Nalo+UCM924	ns	0.6362
							Nalo vs. UCM924	****	<0.0001
							Nalo vs. Nalo+UCM924	ns	0.6862
							UCM924 vs. Nalo+UCM924	****	<0.0001
							40		
							VEH vs. Nalo	ns	0.9455
							VEH vs. UCM924	****	<0.0001
							VEH vs. Nalo+UCM924	ns	0.4158
							Nalo vs. UCM924	****	<0.0001
							Nalo vs. Nalo+UCM924	ns	0.8647
							UCM924 vs. Nalo+UCM924	****	<0.0001
							45		
							VEH vs. Nalo	ns	0.857
							VEH vs. UCM924	****	<0.0001
							VEH vs. Nalo+UCM924	ns	>0.9999
							Nalo vs. UCM924	****	<0.0001
							Nalo vs. Nalo+UCM924	ns	0.808
							UCM924 vs. Nalo+UCM924	****	<0.0001
							50		
							VEH vs. Nalo	ns	0.9993
							VEH vs. UCM924	****	<0.0001
							VEH vs. Nalo+UCM924	ns	>0.9999
							Nalo vs. UCM924	****	<0.0001
							Nalo vs. Nalo+UCM924	ns	0.9982
							UCM924 vs. Nalo+UCM924	****	<0.0001
							55		
							VEH vs. Nalo	ns	0.9436
							VEH vs. UCM924	****	<0.0001
							VEH vs. Nalo+UCM924	ns	0.9718
							Nalo vs. UCM924	****	<0.0001
							Nalo vs. Nalo+UCM924	ns	0.997

							UCM924 vs. Nalo+UCM924	****	<0.0001
							60		
							VEH vs. Nalo	ns	0.8471
							VEH vs. UCM924	****	<0.0001
							VEH vs. Nalo+UCM924	ns	0.4051
							Nalo vs. UCM924	****	<0.0001
							Nalo vs. Nalo+UCM924	ns	0.9549
							UCM924 vs. Nalo+UCM924	****	<0.0001
3	D	2-Way Mixed ANOVA (treatment x time)	Veh = 4 UCM924 = 3 Nalox = 3 Nalox+UCM924 = 3	Time x treatment : F (36, 117) = 3.102 Time : F (12, 117) = 2.779 Treatment : F (3, 117) = 139.3	P<0.0001 P=0.0023 P<0.0001	Tuckey post hoc comparison	Test details		
							0		
							VEH vs. Nalo	ns	0.9855
							VEH vs. UCM924	ns	0.9409
							VEH vs. Nalo+UCM924	ns	0.9992
							Nalo vs. UCM924	ns	0.9968
							Nalo vs. Nalo+UCM924	ns	0.997
							UCM924 vs. Nalo+UCM924	ns	0.9764
							5		
							VEH vs. Nalo	ns	0.9864
							VEH vs. UCM924	ns	0.9791
							VEH vs. Nalo+UCM924	ns	0.661
							Nalo vs. UCM924	ns	>0.9999
							Nalo vs. Nalo+UCM924	ns	0.8741
							UCM924 vs. Nalo+UCM924	ns	0.8951
							10		
							VEH vs. Nalo	ns	0.9794
							VEH vs. UCM924	ns	0.1245
							VEH vs. Nalo+UCM924	ns	0.932
							Nalo vs. UCM924	ns	0.075
							Nalo vs. Nalo+UCM924	ns	0.9974
							UCM924 vs. Nalo+UCM924	*	0.0465
							15		
							VEH vs. Nalo	ns	0.9718
							VEH vs. UCM924	**	0.0026
							VEH vs. Nalo+UCM924	ns	>0.9999
							Nalo vs. UCM924	**	0.0014
							Nalo vs. Nalo+UCM924	ns	0.9694
							UCM924 vs. Nalo+UCM924	**	0.0063
							20		
							VEH vs. Nalo	ns	0.9047
							VEH vs. UCM924	****	<0.0001
							VEH vs. Nalo+UCM924	ns	0.9494
							Nalo vs. UCM924	****	<0.0001
							Nalo vs. Nalo+UCM924	ns	0.9992
							UCM924 vs. Nalo+UCM924	****	<0.0001
							25		
							VEH vs. Nalo	ns	0.8743
							VEH vs. UCM924	****	<0.0001
							VEH vs. Nalo+UCM924	ns	0.5289
							Nalo vs. UCM924	****	<0.0001
							Nalo vs. Nalo+UCM924	ns	0.9428
							UCM924 vs. Nalo+UCM924	****	<0.0001
							30		
							VEH vs. Nalo	ns	0.9375
							VEH vs. UCM924	****	<0.0001
							VEH vs. Nalo+UCM924	ns	0.7233
							Nalo vs. UCM924	****	<0.0001
							Nalo vs. Nalo+UCM924	ns	0.9725
							UCM924 vs. Nalo+UCM924	****	<0.0001
							35		
							VEH vs. Nalo	ns	0.9557
							VEH vs. UCM924	****	<0.0001
							VEH vs. Nalo+UCM924	ns	0.8717
							Nalo vs. UCM924	****	<0.0001
							Nalo vs. Nalo+UCM924	ns	0.9956
							UCM924 vs. Nalo+UCM924	****	<0.0001
							40		
							VEH vs. Nalo	ns	0.952
							VEH vs. UCM924	****	<0.0001
							VEH vs. Nalo+UCM924	ns	0.8527
							Nalo vs. UCM924	****	<0.0001
							Nalo vs. Nalo+UCM924	ns	0.994
							UCM924 vs. Nalo+UCM924	****	<0.0001
							45		
							VEH vs. Nalo	ns	>0.9999
							VEH vs. UCM924	****	<0.0001
							VEH vs. Nalo+UCM924	ns	0.9991
							Nalo vs. UCM924	****	<0.0001
							Nalo vs. Nalo+UCM924	ns	0.9996
							UCM924 vs. Nalo+UCM924	****	<0.0001
							50		
							VEH vs. Nalo	ns	0.9873
							VEH vs. UCM924	****	<0.0001
							VEH vs. Nalo+UCM924	ns	>0.9999
							Nalo vs. UCM924	****	<0.0001
							Nalo vs. Nalo+UCM924	ns	0.9932

							UCM924 vs. Nalo+UCM924	****	<0.0001
							55		
							VEH vs. Nalo	ns	0.9258
							VEH vs. UCM924	****	<0.0001
							VEH vs. Nalo+UCM924	ns	0.8815
							Nalo vs. UCM924	****	<0.0001
							Nalo vs. Nalo+UCM924	ns	0.9995
							UCM924 vs. Nalo+UCM924	****	<0.0001
							60		
							VEH vs. Nalo	ns	0.7687
							VEH vs. UCM924	****	<0.0001
							VEH vs. Nalo+UCM924	ns	0.453
							Nalo vs. UCM924	****	<0.0001
							Nalo vs. Nalo+UCM924	ns	0.9633
							UCM924 vs. Nalo+UCM924	****	<0.0001
3	E	2-Way Mixed ANOVA (treatment x time)	Veh = 3 UCM924 = 4 CTOP = 3 CTOP+UCM924 = 3	Time x treatment : F (36, 117) = 3.874 Time : F (12, 117) = 4.461 Treatment : F (3, 117) = 125.0	P<0.0001 P<0.0001 P<0.0001	Tuckey post hoc comparison	Test details	Summary	Adjusted P Value
							0		
							VEH vs. CTOP	ns	0.9955
							VEH vs. UCM924	ns	0.9561
							VEH vs. CTOP+UCM924	ns	0.9248
							CTOP vs. UCM924	ns	0.8714
							CTOP vs. CTOP+UCM924	ns	0.8274
							UCM924 vs. CTOP+UCM924	ns	0.9987
							5		
							VEH vs. CTOP	ns	0.9735
							VEH vs. UCM924	ns	0.9942
							VEH vs. CTOP+UCM924	ns	0.9834
							CTOP vs. UCM924	ns	0.8922
							CTOP vs. CTOP+UCM924	ns	0.8575
							UCM924 vs. CTOP+UCM924	ns	0.9991
							10		
							VEH vs. CTOP	ns	0.6761
							VEH vs. UCM924	ns	0.5461
							VEH vs. CTOP+UCM924	ns	>0.9999
							CTOP vs. UCM924	ns	0.9992
							CTOP vs. CTOP+UCM924	ns	0.6706
							UCM924 vs. CTOP+UCM924	ns	0.5401
							15		
							VEH vs. CTOP	ns	0.9478
							VEH vs. UCM924	**	0.0085
							VEH vs. CTOP+UCM924	ns	0.9629
							CTOP vs. UCM924	*	0.0443
							CTOP vs. CTOP+UCM924	ns	>0.9999
							UCM924 vs. CTOP+UCM924	*	0.0372
							20		
							VEH vs. CTOP	ns	0.8678
							VEH vs. UCM924	**	0.0011
							VEH vs. CTOP+UCM924	ns	0.9897
							CTOP vs. UCM924	*	0.0165
							CTOP vs. CTOP+UCM924	ns	0.7028
							UCM924 vs. CTOP+UCM924	***	0.0003
							25		
							VEH vs. CTOP	ns	0.9999
							VEH vs. UCM924	***	0.0005
							VEH vs. CTOP+UCM924	ns	0.9308
							CTOP vs. UCM924	***	0.0007
							CTOP vs. CTOP+UCM924	ns	0.9515
							UCM924 vs. CTOP+UCM924	**	0.0051
							30		
							VEH vs. CTOP	ns	0.9824
							VEH vs. UCM924	****	<0.0001
							VEH vs. CTOP+UCM924	ns	0.9913
							CTOP vs. UCM924	****	<0.0001
							CTOP vs. CTOP+UCM924	ns	0.9998
							UCM924 vs. CTOP+UCM924	****	<0.0001
							35		
							VEH vs. CTOP	ns	0.8992
							VEH vs. UCM924	****	<0.0001
							VEH vs. CTOP+UCM924	ns	0.9372
							CTOP vs. UCM924	****	<0.0001
							CTOP vs. CTOP+UCM924	ns	0.5798
							UCM924 vs. CTOP+UCM924	****	<0.0001
							40		
							VEH vs. CTOP	ns	0.9691
							VEH vs. UCM924	****	<0.0001
							VEH vs. CTOP+UCM924	ns	0.9989
							CTOP vs. UCM924	****	<0.0001
							CTOP vs. CTOP+UCM924	ns	0.9331
							UCM924 vs. CTOP+UCM924	****	<0.0001
							45		
							VEH vs. CTOP	ns	0.1396
							VEH vs. UCM924	****	<0.0001
							VEH vs. CTOP+UCM924	ns	0.7159
							CTOP vs. UCM924	****	<0.0001
							CTOP vs. CTOP+UCM924	ns	0.6864

							UCM924 vs. CTOP+UCM924	****	<0.0001
							50		
							VEH vs. CTOP	ns	>0.9999
							VEH vs. UCM924	****	<0.0001
							VEH vs. CTOP+UCM924	ns	0.8517
							CTOP vs. UCM924	****	<0.0001
							CTOP vs. CTOP+UCM924	ns	0.876
							UCM924 vs. CTOP+UCM924	****	<0.0001
							55		
							VEH vs. CTOP	ns	0.3453
							VEH vs. UCM924	****	<0.0001
							VEH vs. CTOP+UCM924	ns	0.7637
							CTOP vs. UCM924	****	<0.0001
							CTOP vs. CTOP+UCM924	ns	0.8998
							UCM924 vs. CTOP+UCM924	****	<0.0001
							60		
							VEH vs. CTOP	ns	0.218
							VEH vs. UCM924	****	<0.0001
							VEH vs. CTOP+UCM924	ns	0.2948
							CTOP vs. UCM924	****	<0.0001
							CTOP vs. CTOP+UCM924	ns	0.9982
							UCM924 vs. CTOP+UCM924	****	<0.0001
3	F	2-Way Mixed ANOVA (treatment x time)	Veh = 4 UCM924 = 3 CTOP = 3 CTOP+UCM924 = 3	Time x treatment : F (36, 117) = 4.674 Time : F (12, 117) = 2.279 Treatment : F (3, 117) = 181.0	P<0.0001 P=0.0122 P<0.0001	Tuckey post hoc comparison	Test details	Summary	Adjusted P Value
							0		
							VEH vs. CTOP	ns	0.9947
							VEH vs. UCM924	ns	0.9153
							VEH vs. CTOP+UCM924	ns	0.9992
							CTOP vs. UCM924	ns	0.8359
							CTOP vs. CTOP+UCM924	ns	0.9996
							UCM924 vs. CTOP+UCM924	ns	0.8839
							5		
							VEH vs. CTOP	ns	0.9993
							VEH vs. UCM924	ns	0.9695
							VEH vs. CTOP+UCM924	ns	0.8837
							CTOP vs. UCM924	ns	0.9901
							CTOP vs. CTOP+UCM924	ns	0.9409
							UCM924 vs. CTOP+UCM924	ns	0.9935
							10		
							VEH vs. CTOP	ns	0.9897
							VEH vs. UCM924	ns	0.0605
							VEH vs. CTOP+UCM924	ns	0.9849
							CTOP vs. UCM924	*	0.044
							CTOP vs. CTOP+UCM924	ns	0.9258
							UCM924 vs. CTOP+UCM924	ns	0.1804
							15		
							VEH vs. CTOP	ns	0.8757
							VEH vs. UCM924	***	0.0004
							VEH vs. CTOP+UCM924	ns	0.9785
							CTOP vs. UCM924	*	0.0113
							CTOP vs. CTOP+UCM924	ns	0.7047
							UCM924 vs. CTOP+UCM924	***	0.0003
							20		
							VEH vs. CTOP	ns	0.476
							VEH vs. UCM924	****	<0.0001
							VEH vs. CTOP+UCM924	ns	0.8322
							CTOP vs. UCM924	****	<0.0001
							CTOP vs. CTOP+UCM924	ns	0.9444
							UCM924 vs. CTOP+UCM924	****	<0.0001
							25		
							VEH vs. CTOP	ns	0.6944
							VEH vs. UCM924	****	<0.0001
							VEH vs. CTOP+UCM924	ns	0.9531
							CTOP vs. UCM924	****	<0.0001
							CTOP vs. CTOP+UCM924	ns	0.9511
							UCM924 vs. CTOP+UCM924	****	<0.0001
							30		
							VEH vs. CTOP	ns	0.6198
							VEH vs. UCM924	****	<0.0001
							VEH vs. CTOP+UCM924	ns	0.9734
							CTOP vs. UCM924	****	<0.0001
							CTOP vs. CTOP+UCM924	ns	0.8834
							UCM924 vs. CTOP+UCM924	****	<0.0001
							35		
							VEH vs. CTOP	ns	0.8266
							VEH vs. UCM924	****	<0.0001
							VEH vs. CTOP+UCM924	ns	0.9712
							CTOP vs. UCM924	****	<0.0001
							CTOP vs. CTOP+UCM924	ns	0.9799
							UCM924 vs. CTOP+UCM924	****	<0.0001
							40		
							VEH vs. CTOP	ns	0.4779
							VEH vs. UCM924	****	<0.0001
							VEH vs. CTOP+UCM924	ns	0.6926
							CTOP vs. UCM924	****	<0.0001
							CTOP vs. CTOP+UCM924	ns	0.9886

							UCM924 vs. CTOP+UCM924	****	<0.0001
							45		
							VEH vs. CTOP	ns	0.2604
							VEH vs. UCM924	****	<0.0001
							VEH vs. CTOP+UCM924	ns	0.6859
							CTOP vs. UCM924	****	<0.0001
							CTOP vs. CTOP+UCM924	ns	0.9028
							UCM924 vs. CTOP+UCM924	****	<0.0001
							50		
							VEH vs. CTOP	ns	0.8441
							VEH vs. UCM924	****	<0.0001
							VEH vs. CTOP+UCM924	ns	0.9771
							CTOP vs. UCM924	****	<0.0001
							CTOP vs. CTOP+UCM924	ns	0.9801
							UCM924 vs. CTOP+UCM924	****	<0.0001
							55		
							VEH vs. CTOP	ns	0.5711
							VEH vs. UCM924	****	<0.0001
							VEH vs. CTOP+UCM924	ns	0.6991
							CTOP vs. UCM924	****	<0.0001
							CTOP vs. CTOP+UCM924	ns	0.9975
							UCM924 vs. CTOP+UCM924	****	<0.0001
							60		
							VEH vs. CTOP	ns	0.7633
							VEH vs. UCM924	****	<0.0001
							VEH vs. CTOP+UCM924	ns	0.9991
							CTOP vs. UCM924	****	<0.0001
							CTOP vs. CTOP+UCM924	ns	0.8597
							UCM924 vs. CTOP+UCM924	****	<0.0001
3	G	2-Way Mixed ANOVA (treatment x time)	Veh = 3 UCM924 = 4 Nalt = 3 Nalt+UCM924 = 3	Time x treatment : F (36, 117) = 4.656 Time : F (12, 117) = 13.83 Treatment : F (3, 117) = 145.8	P<0.0001 P<0.0001 P<0.0001	Tuckey post hoc comparison	Test details	Summary	Adjusted P Value
							0		
							Veh vs. Nalt	ns	>0.9999
							Veh vs. UCM924	ns	0.9531
							Veh vs. Nalt+UCM924	ns	0.9973
							Nalt vs. UCM924	ns	0.9348
							Nalt vs. Nalt+UCM924	ns	0.9991
							UCM924 vs. Nalt+UCM924	ns	0.8831
							5		
							Veh vs. Nalt	ns	0.9999
							Veh vs. UCM924	ns	0.9938
							Veh vs. Nalt+UCM924	ns	0.909
							Nalt vs. UCM924	ns	0.9977
							Nalt vs. Nalt+UCM924	ns	0.932
							UCM924 vs. Nalt+UCM924	ns	0.9687
							10		
							Veh vs. Nalt	ns	0.9998
							Veh vs. UCM924	ns	0.5259
							Veh vs. Nalt+UCM924	ns	0.9143
							Nalt vs. UCM924	ns	0.5857
							Nalt vs. Nalt+UCM924	ns	0.9424
							UCM924 vs. Nalt+UCM924	ns	0.9106
							15		
							Veh vs. Nalt	ns	0.806
							Veh vs. UCM924	**	0.0066
							Veh vs. Nalt+UCM924	ns	0.7171
							Nalt vs. UCM924	***	0.0002
							Nalt vs. Nalt+UCM924	ns	0.2118
							UCM924 vs. Nalt+UCM924	ns	0.1333
							20		
							Veh vs. Nalt	ns	0.993
							Veh vs. UCM924	***	0.0008
							Veh vs. Nalt+UCM924	ns	0.3986
							Nalt vs. UCM924	**	0.0023
							Nalt vs. Nalt+UCM924	ns	0.5639
							UCM924 vs. Nalt+UCM924	ns	0.1162
							25		
							Veh vs. Nalt	ns	0.9994
							Veh vs. UCM924	***	0.0004
							Veh vs. Nalt+UCM924	**	0.0019
							Nalt vs. UCM924	***	0.0006
							Nalt vs. Nalt+UCM924	**	0.0029
							UCM924 vs. Nalt+UCM924	ns	0.9974
							30		
							Veh vs. Nalt	ns	0.9371
							Veh vs. UCM924	****	<0.0001
							Veh vs. Nalt+UCM924	****	<0.0001
							Nalt vs. UCM924	****	<0.0001
							Nalt vs. Nalt+UCM924	***	0.0005
							UCM924 vs. Nalt+UCM924	ns	0.5346
							35		
							Veh vs. Nalt	ns	0.9869
							Veh vs. UCM924	****	<0.0001
							Veh vs. Nalt+UCM924	****	<0.0001
							Nalt vs. UCM924	****	<0.0001
							Nalt vs. Nalt+UCM924	***	0.0003

							UCM924 vs. Nalt+UCM924	ns	0.4965
							40		
							Veh vs. Nalt	ns	0.9992
							Veh vs. UCM924	****	<0.0001
							Veh vs. Nalt+UCM924	****	<0.0001
							Nalt vs. UCM924	****	<0.0001
							Nalt vs. Nalt+UCM924	****	<0.0001
							UCM924 vs. Nalt+UCM924	ns	0.9756
							45		
							Veh vs. Nalt	ns	0.7975
							Veh vs. UCM924	****	<0.0001
							Veh vs. Nalt+UCM924	****	<0.0001
							Nalt vs. UCM924	****	<0.0001
							Nalt vs. Nalt+UCM924	****	<0.0001
							UCM924 vs. Nalt+UCM924	ns	0.8685
							50		
							Veh vs. Nalt	ns	0.9886
							Veh vs. UCM924	****	<0.0001
							Veh vs. Nalt+UCM924	****	<0.0001
							Nalt vs. UCM924	****	<0.0001
							Nalt vs. Nalt+UCM924	****	<0.0001
							UCM924 vs. Nalt+UCM924	ns	0.9852
							55		
							Veh vs. Nalt	ns	0.3301
							Veh vs. UCM924	****	<0.0001
							Veh vs. Nalt+UCM924	****	<0.0001
							Nalt vs. UCM924	****	<0.0001
							Nalt vs. Nalt+UCM924	****	<0.0001
							UCM924 vs. Nalt+UCM924	ns	0.9999
							60		
							Veh vs. Nalt	ns	0.3226
							Veh vs. UCM924	****	<0.0001
							Veh vs. Nalt+UCM924	****	<0.0001
							Nalt vs. UCM924	****	<0.0001
							Nalt vs. Nalt+UCM924	****	<0.0001
							UCM924 vs. Nalt+UCM924	ns	0.9632
3	H	2-Way Mixed ANOVA (treatment x time)	Veh = 4 UCM924 = 3 Nalt = 3 Nalt+UCM924 = 3	Time x treatment : F (36, 117) = 3.815 Time : F (12, 117) = 8.312 Treatment : F (3, 117) = 166.0	P<0.0001 P<0.0001 P<0.0001	Tuckey post hoc comparison	Test details	Summary	Adjusted P Value
							0		
							Veh vs. Nalt	ns	0.9765
							Veh vs. UCM924	ns	0.9365
							Veh vs. Nalt+UCM924	ns	>0.9999
							Nalt vs. UCM924	ns	0.9985
							Nalt vs. Nalt+UCM924	ns	0.9866
							UCM924 vs. Nalt+UCM924	ns	0.9587
							5		
							Veh vs. Nalt	ns	0.933
							Veh vs. UCM924	ns	0.9775
							Veh vs. Nalt+UCM924	ns	0.9689
							Nalt vs. UCM924	ns	0.9979
							Nalt vs. Nalt+UCM924	ns	0.7602
							UCM924 vs. Nalt+UCM924	ns	0.8532
							10		
							Veh vs. Nalt	ns	0.9843
							Veh vs. UCM924	ns	0.1097
							Veh vs. Nalt+UCM924	ns	0.9209
							Nalt vs. UCM924	ns	0.0713
							Nalt vs. Nalt+UCM924	ns	0.7906
							UCM924 vs. Nalt+UCM924	ns	0.4195
							15		
							Veh vs. Nalt	ns	0.9993
							Veh vs. UCM924	**	0.0019
							Veh vs. Nalt+UCM924	***	0.0002
							Nalt vs. UCM924	**	0.0061
							Nalt vs. Nalt+UCM924	***	0.0008
							UCM924 vs. Nalt+UCM924	ns	0.9357
							20		
							Veh vs. Nalt	ns	0.8066
							Veh vs. UCM924	****	<0.0001
							Veh vs. Nalt+UCM924	**	0.0043
							Nalt vs. UCM924	****	<0.0001
							Nalt vs. Nalt+UCM924	***	0.0005
							UCM924 vs. Nalt+UCM924	ns	0.2209
							25		
							Veh vs. Nalt	ns	0.9103
							Veh vs. UCM924	****	<0.0001
							Veh vs. Nalt+UCM924	****	<0.0001
							Nalt vs. UCM924	****	<0.0001
							Nalt vs. Nalt+UCM924	****	<0.0001
							UCM924 vs. Nalt+UCM924	ns	0.9997
							30		
							Veh vs. Nalt	ns	0.9756
							Veh vs. UCM924	****	<0.0001
							Veh vs. Nalt+UCM924	****	<0.0001
							Nalt vs. UCM924	****	<0.0001
							Nalt vs. Nalt+UCM924	****	<0.0001

							UCM924 vs. Nalt+UCM924	ns	0.9999
							35		
							Veh vs. Nalt	ns	0.8951
							Veh vs. UCM924	****	<0.0001
							Veh vs. Nalt+UCM924	****	<0.0001
							Nalt vs. UCM924	****	<0.0001
							Nalt vs. Nalt+UCM924	****	<0.0001
							UCM924 vs. Nalt+UCM924	ns	0.9977
							40		
							Veh vs. Nalt	ns	0.7642
							Veh vs. UCM924	****	<0.0001
							Veh vs. Nalt+UCM924	***	0.0002
							Nalt vs. UCM924	****	<0.0001
							Nalt vs. Nalt+UCM924	****	<0.0001
							UCM924 vs. Nalt+UCM924	ns	0.2967
							45		
							Veh vs. Nalt	ns	0.9832
							Veh vs. UCM924	****	<0.0001
							Veh vs. Nalt+UCM924	****	<0.0001
							Nalt vs. UCM924	****	<0.0001
							Nalt vs. Nalt+UCM924	****	<0.0001
							UCM924 vs. Nalt+UCM924	ns	0.2841
							50		
							Veh vs. Nalt	ns	0.9889
							Veh vs. UCM924	****	<0.0001
							Veh vs. Nalt+UCM924	****	<0.0001
							Nalt vs. UCM924	****	<0.0001
							Nalt vs. Nalt+UCM924	****	<0.0001
							UCM924 vs. Nalt+UCM924	ns	0.136
							55		
							Veh vs. Nalt	ns	0.6084
							Veh vs. UCM924	****	<0.0001
							Veh vs. Nalt+UCM924	****	<0.0001
							Nalt vs. UCM924	****	<0.0001
							Nalt vs. Nalt+UCM924	****	<0.0001
							UCM924 vs. Nalt+UCM924	ns	0.6624
							60		
							Veh vs. Nalt	ns	0.8095
							Veh vs. UCM924	****	<0.0001
							Veh vs. Nalt+UCM924	****	<0.0001
							Nalt vs. UCM924	****	<0.0001
							Nalt vs. Nalt+UCM924	****	<0.0001
							UCM924 vs. Nalt+UCM924	ns	0.5523

Figure	Panel	Test	Group-size	Statistic	P value	Pair-wise comparison	Statistic 2		
							Test details	Summary	Adjusted P Value
5	A	Repeated measures 2-way ANOVA (treatment x time)	Veh = 6 UCM924 = 8 TQ = 6 TQ+UCM924 = 8	Time x treatment : F (15, 120) = 9.893 Time : F (1.727, 41.44) = 16.93 Treatment : F (3, 24) = 16.91	P<0.0001 P<0.0001 P<0.0001	Tuckey post hoc comparison	0		
							Veh vs. UCM924 10ug	ns	0.3193
							Veh vs. TQ 1 uM	ns	0.4497
							Veh vs. TQ + UCM924	ns	0.1656
							UCM924 10ug vs. TQ 1 uM	ns	0.1374
							UCM924 10ug vs. TQ + UCM924	*	0.022
							TQ 1 uM vs. TQ + UCM924	ns	0.9961
							0.5		
							Veh vs. UCM924 10ug	ns	0.1152
							Veh vs. TQ 1 uM	ns	0.6132
							Veh vs. TQ + UCM924	ns	0.9437
							UCM924 10ug vs. TQ 1 uM	*	0.0336
							UCM924 10ug vs. TQ + UCM924	ns	0.0822
							TQ 1 uM vs. TQ + UCM924	ns	0.9569
							1		
							Veh vs. UCM924 10ug	**	0.0078
							Veh vs. TQ 1 uM	ns	0.9362
							Veh vs. TQ + UCM924	ns	0.7616
							UCM924 10ug vs. TQ 1 uM	*	0.0122
							UCM924 10ug vs. TQ + UCM924	**	0.0059
							TQ 1 uM vs. TQ + UCM924	ns	0.7625
							1.5		
							Veh vs. UCM924 10ug	**	0.0079
							Veh vs. TQ 1 uM	ns	0.6004
							Veh vs. TQ + UCM924	ns	0.1712
							UCM924 10ug vs. TQ 1 uM	**	0.0072
							UCM924 10ug vs. TQ + UCM924	***	0.0002
							TQ 1 uM vs. TQ + UCM924	ns	0.9441
							2		
							Veh vs. UCM924 10ug	ns	0.7834
							Veh vs. TQ 1 uM	ns	0.9362
							Veh vs. TQ + UCM924	ns	0.8756
							UCM924 10ug vs. TQ 1 uM	ns	0.6165
							UCM924 10ug vs. TQ + UCM924	ns	0.5263
							TQ 1 uM vs. TQ + UCM924	ns	0.9987
							3		
							Veh vs. UCM924 10ug	ns	0.9241
							Veh vs. TQ 1 uM	ns	0.7847
							Veh vs. TQ + UCM924	ns	0.9946
							UCM924 10ug vs. TQ 1 uM	ns	0.1117
							UCM924 10ug vs. TQ + UCM924	ns	0.5427
							TQ 1 uM vs. TQ + UCM924	ns	0.7456
5	B	1-way ANOVA	Veh = 6 UCM924 = 8 TQ = 6 TQ+UCM924 = 8	F (3, 24) = 11.62	<0.0001	Tuckey post hoc comparison	Test details	Summary	Adjusted P Value
							Veh vs. UCM924 10ug	**	0.0026
							Veh vs. TQ 1 uM	ns	0.9708
							Veh vs. TQ + UCM924	ns	0.819
							UCM924 10ug vs. TQ 1 uM	***	0.0008
							UCM924 10ug vs. TQ + UCM924	***	0.0001
							TQ 1 uM vs. TQ + UCM924	ns	0.9776
5	C	Repeated measures 2-way ANOVA (treatment x time)	Veh = 3 UCM924 = 4 TQ = 3 TQ+UCM924 = 4	Time x treatment : F (36, 130) = 2.983 Time : F (12, 130) = 4.834 Treatment : F (3, 130) = 107.7	P<0.0001 P<0.0001 P<0.0001	Tuckey post hoc comparison	Test details	Summary	Adjusted P Value
							0		
							Veh vs. TQ	ns	0.982
							Veh vs. UCM924	ns	0.9958
							Veh vs. TQ+UCM924	ns	0.956
							TQ vs. UCM924	ns	0.9228
							TQ vs. TQ+UCM924	ns	0.7979
							UCM924 vs. TQ +UCM924	ns	0.9899
							5		
							Veh vs. TQ	ns	0.8738
							Veh vs. UCM924	ns	0.6321
							Veh vs. TQ+UCM924	ns	0.9818
							TQ vs. UCM924	ns	0.1925
							TQ vs. TQ+UCM924	ns	0.9728
							UCM924 vs. TQ +UCM924	ns	0.3302
							10		
							Veh vs. TQ	ns	0.9889
							Veh vs. UCM924	ns	0.5344
							Veh vs. TQ+UCM924	ns	>0.9999
							TQ vs. UCM924	ns	0.0549
							TQ vs. TQ+UCM924	ns	0.9922
							UCM924 vs. TQ +UCM924	ns	0.2843
							15		
							Veh vs. TQ	ns	0.9889
							Veh vs. UCM924	*	0.0222
							Veh vs. TQ+UCM924	ns	>0.9999
							TQ vs. UCM924	ns	0.0549

							TQ vs. TQ+UCM924	ns	0.9922
							UCM924 vs. TQ +UCM924	*	0.0135
							20		
							Veh vs. TQ	ns	0.9994
							Veh vs. UCM924	**	0.0042
							Veh vs. TQ+UCM924	ns	>0.9999
							TQ vs. UCM924	**	0.0028
							TQ vs. TQ+UCM924	ns	0.9997
							UCM924 vs. TQ +UCM924	**	0.0015
							25		
							Veh vs. TQ	ns	0.9921
							Veh vs. UCM924	**	0.0023
							Veh vs. TQ+UCM924	ns	0.9995
							TQ vs. UCM924	**	0.0062
							TQ vs. TQ+UCM924	ns	0.9756
							UCM924 vs. TQ +UCM924	***	0.0005
							30		
							Veh vs. TQ	ns	0.7601
							Veh vs. UCM924	****	<0.0001
							Veh vs. TQ+UCM924	ns	0.5271
							TQ vs. UCM924	****	<0.0001
							TQ vs. TQ+UCM924	ns	0.9896
							UCM924 vs. TQ +UCM924	****	<0.0001
							35		
							Veh vs. TQ	ns	>0.9999
							Veh vs. UCM924	****	<0.0001
							Veh vs. TQ+UCM924	ns	0.8206
							TQ vs. UCM924	****	<0.0001
							TQ vs. TQ+UCM924	ns	0.8138
							UCM924 vs. TQ +UCM924	****	<0.0001
							40		
							Veh vs. TQ	ns	0.9922
							Veh vs. UCM924	****	<0.0001
							Veh vs. TQ+UCM924	ns	0.9177
							TQ vs. UCM924	***	0.0001
							TQ vs. TQ+UCM924	ns	0.9861
							UCM924 vs. TQ +UCM924	***	0.0001
							45		
							Veh vs. TQ	ns	0.634
							Veh vs. UCM924	****	<0.0001
							Veh vs. TQ+UCM924	ns	0.5001
							TQ vs. UCM924	****	<0.0001
							TQ vs. TQ+UCM924	ns	0.9992
							UCM924 vs. TQ +UCM924	****	<0.0001
							50		
							Veh vs. TQ	ns	0.8606
							Veh vs. UCM924	****	<0.0001
							Veh vs. TQ+UCM924	ns	0.9904
							TQ vs. UCM924	****	<0.0001
							TQ vs. TQ+UCM924	ns	0.9494
							UCM924 vs. TQ +UCM924	****	<0.0001
							55		
							Veh vs. TQ	ns	0.9314
							Veh vs. UCM924	****	<0.0001
							Veh vs. TQ+UCM924	ns	0.9997
							TQ vs. UCM924	****	<0.0001
							TQ vs. TQ+UCM924	ns	0.9459
							UCM924 vs. TQ +UCM924	****	<0.0001
							60		
							Veh vs. TQ	ns	0.3971
							Veh vs. UCM924	****	<0.0001
							Veh vs. TQ+UCM924	ns	0.8202
							TQ vs. UCM924	****	<0.0001
							TQ vs. TQ+UCM924	ns	0.8486
							UCM924 vs. TQ +UCM924	****	<0.0001
5	D	Repeated measures 2-way ANOVA (treatment x time)	Veh = 4 UCM924 = 3 TQ = 3 TQ+UCM924 = 4	Time x treatment : F (36, 132) = 3.953 Time : F (4.350, 47.85) = 2.828 Treatment : F (3, 11) = 74.01	P<0.0001 P=0.0312 P<0.0001	Tuckey post hoc comparison	Test details	Summary	Adjusted P Value
							0		
							Veh vs. UCM924 10ug	ns	0.9991
							Veh vs. TQ 1 uM	ns	0.9797
							Veh vs. TQ+UCM924	ns	0.9545
							UCM924 10ug vs. TQ 1 uM	ns	0.9573
							UCM924 10ug vs. TQ+UCM924	ns	0.9279
							TQ 1 uM vs. TQ+UCM924	ns	0.9524
							5		
							Veh vs. UCM924 10ug	ns	0.9948
							Veh vs. TQ 1 uM	ns	0.9964

Veh vs. TQ+UCM924	ns	0.9965
UCM924 10ug vs. TQ 1 uM	ns	0.9487
UCM924 10ug vs. TQ+UCM924	ns	0.9992
TQ 1 uM vs. TQ+UCM924	ns	0.6514
10		
Veh vs. UCM924 10ug	ns	0.5092
Veh vs. TQ 1 uM	ns	0.7737
Veh vs. TQ+UCM924	*	0.0224
UCM924 10ug vs. TQ 1 uM	ns	0.6508
UCM924 10ug vs. TQ+UCM924	ns	0.7289
TQ 1 uM vs. TQ+UCM924	ns	0.5741
15		
Veh vs. UCM924 10ug	***	0.0066
Veh vs. TQ 1 uM	ns	0.9157
Veh vs. TQ+UCM924	ns	0.9791
UCM924 10ug vs. TQ 1 uM	**	0.001
UCM924 10ug vs. TQ+UCM924	***	0.0008
TQ 1 uM vs. TQ+UCM924	ns	0.458
20		
Veh vs. UCM924 10ug	****	<0.0001
Veh vs. TQ 1 uM	ns	0.9988
Veh vs. TQ+UCM924	ns	0.9994
UCM924 10ug vs. TQ 1 uM	*	0.0239
UCM924 10ug vs. TQ+UCM924	****	<0.0001
TQ 1 uM vs. TQ+UCM924	ns	0.9865
25		
Veh vs. UCM924 10ug	***	0.0009
Veh vs. TQ 1 uM	ns	0.9908
Veh vs. TQ+UCM924	ns	0.9817
UCM924 10ug vs. TQ 1 uM	**	0.0033
UCM924 10ug vs. TQ+UCM924	***	0.001
TQ 1 uM vs. TQ+UCM924	ns	0.9969
30		
Veh vs. UCM924 10ug	****	<0.0001
Veh vs. TQ 1 uM	ns	0.9826
Veh vs. TQ+UCM924	ns	0.998
UCM924 10ug vs. TQ 1 uM	*	0.0265
UCM924 10ug vs. TQ+UCM924	****	<0.0001
TQ 1 uM vs. TQ+UCM924	ns	0.9387
35		
Veh vs. UCM924 10ug	****	<0.0001
Veh vs. TQ 1 uM	ns	0.9925
Veh vs. TQ+UCM924	ns	0.9648
UCM924 10ug vs. TQ 1 uM	**	0.0021
UCM924 10ug vs. TQ+UCM924	****	<0.0001
TQ 1 uM vs. TQ+UCM924	ns	0.7769
40		
Veh vs. UCM924 10ug	****	<0.0001
Veh vs. TQ 1 uM	ns	0.9981
Veh vs. TQ+UCM924	ns	0.947
UCM924 10ug vs. TQ 1 uM	***	0.0002
UCM924 10ug vs. TQ+UCM924	****	<0.0001
TQ 1 uM vs. TQ+UCM924	ns	0.7146
45		
Veh vs. UCM924 10ug	****	<0.0001
Veh vs. TQ 1 uM	ns	0.9854
Veh vs. TQ+UCM924	ns	0.927
UCM924 10ug vs. TQ 1 uM	***	0.0003
UCM924 10ug vs. TQ+UCM924	****	<0.0001
TQ 1 uM vs. TQ+UCM924	ns	0.4878
50		
Veh vs. UCM924 10ug	****	<0.0001
Veh vs. TQ 1 uM	ns	0.8063
Veh vs. TQ+UCM924	ns	0.61
UCM924 10ug vs. TQ 1 uM	**	0.0091
UCM924 10ug vs. TQ+UCM924	****	<0.0001
TQ 1 uM vs. TQ+UCM924	ns	0.2823
55		
Veh vs. UCM924 10ug	****	<0.0001
Veh vs. TQ 1 uM	ns	0.5489
Veh vs. TQ+UCM924	ns	0.9243
UCM924 10ug vs. TQ 1 uM	**	0.0043
UCM924 10ug vs. TQ+UCM924	****	<0.0001
TQ 1 uM vs. TQ+UCM924	ns	0.6301
60		

							Veh vs. UCM924 10ug	****	<0.0001
							Veh vs. TQ 1 uM	ns	0.9164
							Veh vs. TQ+UCM924	ns	0.9943
							UCM924 10ug vs. TQ 1 uM	**	0.0093
							UCM924 10ug vs. TQ+UCM924	****	<0.0001
							TQ 1 uM vs. TQ+UCM924	ns	0.9745
5	E	Repeated measures 2-way ANOVA (treatment x time)	Veh = 3 morph = 3 TQ = 3 TQ+morph = 4	Time x treatment : F (36, 132) = 6.767 Time : F (4.710, 51.81) = 26.48 Treatment : F (3, 11) = 53.15	P<0.0001 P<0.0001 P<0.0001	Tuckey post hoc comparison	Test details	Summary	Adjusted P Value
							0		
							TQ 1 uM vs. TQ+ morph 5ug	ns	>0.9999
							TQ 1 uM vs. Veh	ns	>0.9999
							TQ 1 uM vs. morph 5ug	ns	>0.9999
							TQ+ morph 5ug vs. Veh	ns	>0.9999
							TQ+ morph 5ug vs. morph 5ug	ns	>0.9999
							Veh vs. morph 5ug	ns	>0.9999
							5		
							TQ 1 uM vs. TQ+ morph 5ug	ns	0.8852
							TQ 1 uM vs. Veh	ns	>0.9999
							TQ 1 uM vs. morph 5ug	ns	0.9117
							TQ+ morph 5ug vs. Veh	ns	>0.9999
							TQ+ morph 5ug vs. morph 5ug	ns	>0.9999
							Veh vs. morph 5ug	ns	>0.9999
							10		
							TQ 1 uM vs. TQ+ morph 5ug	**	0.0018
							TQ 1 uM vs. Veh	ns	>0.9999
							TQ 1 uM vs. morph 5ug	**	0.0014
							TQ+ morph 5ug vs. Veh	**	0.0044
							TQ+ morph 5ug vs. morph 5ug	ns	>0.9999
							Veh vs. morph 5ug	**	0.0033
							15		
							TQ 1 uM vs. TQ+ morph 5ug	****	<0.0001
							TQ 1 uM vs. Veh	ns	>0.9999
							TQ 1 uM vs. morph 5ug	****	<0.0001
							TQ+ morph 5ug vs. Veh	**	0.0078
							TQ+ morph 5ug vs. morph 5ug	ns	>0.9999
							Veh vs. morph 5ug	***	0.0003
							20		
							TQ 1 uM vs. TQ+ morph 5ug	***	0.0002
							TQ 1 uM vs. Veh	ns	>0.9999
							TQ 1 uM vs. morph 5ug	****	<0.0001
							TQ+ morph 5ug vs. Veh	**	0.0026
							TQ+ morph 5ug vs. morph 5ug	ns	>0.9999
							Veh vs. morph 5ug	****	<0.0001
							25		
							TQ 1 uM vs. TQ+ morph 5ug	****	<0.0001
							TQ 1 uM vs. Veh	ns	>0.9999
							TQ 1 uM vs. morph 5ug	****	<0.0001
							TQ+ morph 5ug vs. Veh	****	<0.0001
							TQ+ morph 5ug vs. morph 5ug	ns	>0.9999
							Veh vs. morph 5ug	****	<0.0001
							30		
							TQ 1 uM vs. TQ+ morph 5ug	****	<0.0001
							TQ 1 uM vs. Veh	ns	>0.9999
							TQ 1 uM vs. morph 5ug	****	<0.0001
							TQ+ morph 5ug vs. Veh	****	<0.0001
							TQ+ morph 5ug vs. morph 5ug	ns	>0.9999
							Veh vs. morph 5ug	****	<0.0001
							35		
							TQ 1 uM vs. TQ+ morph 5ug	***	0.0004
							TQ 1 uM vs. Veh	ns	>0.9999
							TQ 1 uM vs. morph 5ug	***	0.0002
							TQ+ morph 5ug vs. Veh	****	<0.0001
							TQ+ morph 5ug vs. morph 5ug	ns	>0.9999
							Veh vs. morph 5ug	****	<0.0001
							40		
							TQ 1 uM vs. TQ+ morph 5ug	****	<0.0001
							TQ 1 uM vs. Veh	ns	>0.9999
							TQ 1 uM vs. morph 5ug	****	<0.0001
							TQ+ morph 5ug vs. Veh	****	<0.0001
							TQ+ morph 5ug vs. morph 5ug	ns	>0.9999
							Veh vs. morph 5ug	****	<0.0001
							45		
							TQ 1 uM vs. TQ+ morph 5ug	***	0.0002
							TQ 1 uM vs. Veh	ns	>0.9999
							TQ 1 uM vs. morph 5ug	****	<0.0001
							TQ+ morph 5ug vs. Veh	****	<0.0001
							TQ+ morph 5ug vs. morph 5ug	ns	>0.9999
							Veh vs. morph 5ug	****	<0.0001

							50		
							TQ 1 uM vs. TQ+ morph 5ug	***	0.0006
							TQ 1 uM vs. Veh	ns	>0.9999
							TQ 1 uM vs. morph 5ug	****	<0.0001
							TQ+ morph 5ug vs. Veh	****	<0.0001
							TQ+ morph 5ug vs. morph 5ug	ns	>0.9999
							Veh vs. morph 5ug	****	<0.0001
							55		
							TQ 1 uM vs. TQ+ morph 5ug	****	<0.0001
							TQ 1 uM vs. Veh	ns	>0.9999
							TQ 1 uM vs. morph 5ug	****	<0.0001
							TQ+ morph 5ug vs. Veh	****	<0.0001
							TQ+ morph 5ug vs. morph 5ug	ns	>0.9999
							Veh vs. morph 5ug	****	<0.0001
							60		
							TQ 1 uM vs. TQ+ morph 5ug	***	0.0004
							TQ 1 uM vs. Veh	ns	>0.9999
							TQ 1 uM vs. morph 5ug	***	0.0002
							TQ+ morph 5ug vs. Veh	****	<0.0001
							TQ+ morph 5ug vs. morph 5ug	ns	>0.9999
							Veh vs. morph 5ug	****	<0.0001
5	F	Repeated measures 2-way ANOVA (treatment x time)	Veh = 3 morph = 2 TQ = 3 TQ+morph = 2	Time x treatment : F (36, 72) = 9.097 Time : F (2.517, 15.10) = 26.44 Treatment : F (3, 6) = 38.27	P<0.0001 P<0.0001 P=0.0003	Tuckey post hoc comparison	Test details	Summary	Adjusted P Value
							0		
							TQ 1uM vs. TQ+morf	ns	0.9791
							TQ 1uM vs. Veh	ns	>0.9999
							TQ 1uM vs. morph 5ug	ns	0.9944
							TQ+morf vs. Veh	ns	0.9806
							TQ+morf vs. morph 5ug	ns	>0.9999
							Veh vs. morph 5ug	ns	>0.9999
							5		
							TQ 1uM vs. TQ+morf	ns	0.7632
							TQ 1uM vs. Veh	ns	>0.9999
							TQ 1uM vs. morph 5ug	ns	0.5898
							TQ+morf vs. Veh	ns	0.7373
							TQ+morf vs. morph 5ug	ns	>0.9999
							Veh vs. morph 5ug	ns	0.5925
							10		
							TQ 1uM vs. TQ+morf	*	0.0113
							TQ 1uM vs. Veh	ns	0.8863
							TQ 1uM vs. morph 5ug	ns	0.675
							TQ+morf vs. Veh	*	0.0372
							TQ+morf vs. morph 5ug	ns	>0.9999
							Veh vs. morph 5ug	ns	0.779
							15		
							TQ 1uM vs. TQ+morf	*	0.0359
							TQ 1uM vs. Veh	ns	0.9998
							TQ 1uM vs. morph 5ug	***	0.0004
							TQ+morf vs. Veh	*	0.0182
							TQ+morf vs. morph 5ug	ns	0.8936
							Veh vs. morph 5ug	***	0.0002
							20		
							TQ 1uM vs. TQ+morf	****	<0.0001
							TQ 1uM vs. Veh	ns	>0.9999
							TQ 1uM vs. morph 5ug	****	<0.0001
							TQ+morf vs. Veh	***	0.0002
							TQ+morf vs. morph 5ug	ns	>0.9999
							Veh vs. morph 5ug	****	<0.0001
							25		
							TQ 1uM vs. TQ+morf	****	<0.0001
							TQ 1uM vs. Veh	ns	>0.9999
							TQ 1uM vs. morph 5ug	****	<0.0001
							TQ+morf vs. Veh	****	<0.0001
							TQ+morf vs. morph 5ug	ns	>0.9999
							Veh vs. morph 5ug	****	<0.0001
							30		
							TQ 1uM vs. TQ+morf	****	<0.0001
							TQ 1uM vs. Veh	ns	>0.9999
							TQ 1uM vs. morph 5ug	****	<0.0001
							TQ+morf vs. Veh	****	<0.0001
							TQ+morf vs. morph 5ug	ns	>0.9999
							Veh vs. morph 5ug	****	<0.0001
							35		
							TQ 1uM vs. TQ+morf	****	<0.0001
							TQ 1uM vs. Veh	ns	>0.9999
							TQ 1uM vs. morph 5ug	****	<0.0001
							TQ+morf vs. Veh	****	<0.0001

							TQ+morf vs. morph 5ug	ns	>0.9999
							Veh vs. morph 5ug	****	<0.0001
							40		
							TQ 1uM vs. TQ+morf	****	<0.0001
							TQ 1uM vs. Veh	ns	>0.9999
							TQ 1uM vs. morph 5ug	****	<0.0001
							TQ+morf vs. Veh	****	<0.0001
							TQ+morf vs. morph 5ug	ns	>0.9999
							Veh vs. morph 5ug	****	<0.0001
							45		
							TQ 1uM vs. TQ+morf	****	<0.0001
							TQ 1uM vs. Veh	ns	>0.9999
							TQ 1uM vs. morph 5ug	****	<0.0001
							TQ+morf vs. Veh	****	<0.0001
							TQ+morf vs. morph 5ug	ns	>0.9999
							Veh vs. morph 5ug	****	<0.0001
							50		
							TQ 1uM vs. TQ+morf	****	<0.0001
							TQ 1uM vs. Veh	ns	>0.9999
							TQ 1uM vs. morph 5ug	****	<0.0001
							TQ+morf vs. Veh	****	<0.0001
							TQ+morf vs. morph 5ug	ns	>0.9999
							Veh vs. morph 5ug	***	0.0008
							55		
							TQ 1uM vs. TQ+morf	****	<0.0001
							TQ 1uM vs. Veh	ns	>0.9999
							TQ 1uM vs. morph 5ug	****	<0.0001
							TQ+morf vs. Veh	****	<0.0001
							TQ+morf vs. morph 5ug	ns	>0.9999
							Veh vs. morph 5ug	***	0.0006
							60		
							TQ 1uM vs. TQ+morf	****	<0.0001
							TQ 1uM vs. Veh	ns	>0.9999
							TQ 1uM vs. morph 5ug	***	0.0007
							TQ+morf vs. Veh	****	<0.0001
							TQ+morf vs. morph 5ug	ns	>0.9999
							Veh vs. morph 5ug	**	0.0024

Figure	Panel	Test	Group-size	Statistic	P value	Pair-wise comparison	Statistic 2		
6	A	Repeated measures 2-way ANOVA (treatment x time)	D1-9 Veh = 6 D1 UCM924 = 10 D3 = 9 D5 = 9 D7 = 9 D9 = 8	Time x treatment : F (40, 376) = 6.237 Time : F (5.442, 255.8) = 45.95 Treatment : F (5, 47) = 12.50	P<0.0001 P<0.0001 P<0.0001	Tuckey post hoc comparison	Test details	Summary	Adjusted P Value
							0	ns	0.8756
							D1-9 Veh vs. D1 UCM924	ns	>0.9999
							D1-9 Veh vs. D3	ns	0.9819
							D1-9 Veh vs. D5	ns	0.9716
							D1-9 Veh vs. D7	ns	0.9951
							D1-9 Veh vs. D9	ns	0.8825
							D1 UCM924 vs. D3	ns	0.1875
							D1 UCM924 vs. D5	ns	0.3515
							D1 UCM924 vs. D7	ns	0.3479
							D1 UCM924 vs. D9	ns	0.9959
							D3 vs. D5	ns	0.9894
							D3 vs. D7	ns	0.9992
							D3 vs. D9	ns	0.9997
							D5 vs. D7	ns	>0.9999
							D5 vs. D9	ns	0.9984
							D7 vs. D9		
							1	**	0.0087
							D1-9 Veh vs. D1 UCM924	***	0.0002
							D1-9 Veh vs. D3	**	0.0035
							D1-9 Veh vs. D5	**	0.0072
							D1-9 Veh vs. D7	ns	0.0554
							D1-9 Veh vs. D9	ns	>0.9999
							D1 UCM924 vs. D3	ns	0.9393
							D1 UCM924 vs. D5	ns	0.9658
							D1 UCM924 vs. D7	ns	0.6639
							D1 UCM924 vs. D9	ns	0.7233
							D3 vs. D5	ns	0.827
							D3 vs. D7	ns	0.3213
							D3 vs. D9	ns	>0.9999
							D5 vs. D7	ns	0.1801
							D5 vs. D9	ns	0.2593
							D7 vs. D9		
							2	***	0.0009
							D1-9 Veh vs. D1 UCM924	**	0.0083
							D1-9 Veh vs. D3	**	0.0012
							D1-9 Veh vs. D5	**	0.0076
							D1-9 Veh vs. D7	ns	0.4988
							D1-9 Veh vs. D9	ns	0.5475
							D1 UCM924 vs. D3	ns	0.9999
							D1 UCM924 vs. D5	ns	0.1525
							D1 UCM924 vs. D7	*	0.0262
							D1 UCM924 vs. D9	ns	0.576
							D3 vs. D5	ns	0.9351
							D3 vs. D7	ns	0.3206
							D3 vs. D9	ns	0.1353
							D5 vs. D7	*	0.0232
							D5 vs. D9	ns	0.672
							D7 vs. D9		
							3	****	<0.0001
							D1-9 Veh vs. D1 UCM924	**	0.0011
							D1-9 Veh vs. D3	****	<0.0001
							D1-9 Veh vs. D5	*	0.019
							D1-9 Veh vs. D7	ns	0.0994
							D1-9 Veh vs. D9	ns	0.9991
							D1 UCM924 vs. D3	ns	0.811
							D1 UCM924 vs. D5	ns	0.0688
							D1 UCM924 vs. D7	***	0.0004
							D1 UCM924 vs. D9	ns	0.6912
							D3 vs. D5	ns	0.0819
							D3 vs. D7	**	0.0041
							D3 vs. D9	ns	0.1456
							D5 vs. D7	****	<0.0001
							D5 vs. D9	ns	0.2164
							D7 vs. D9		
							4	****	<0.0001
							D1-9 Veh vs. D1 UCM924	*	0.0108
							D1-9 Veh vs. D3	**	0.0026
							D1-9 Veh vs. D5	ns	0.8388
							D1-9 Veh vs. D7	ns	0.9182
							D1-9 Veh vs. D9	ns	0.9968
							D1 UCM924 vs. D3	ns	0.0586
							D1 UCM924 vs. D5	***	0.0004
							D1 UCM924 vs. D7	***	0.0008
							D1 UCM924 vs. D9	ns	0.6692
							D3 vs. D5	*	0.0394
							D3 vs. D7	*	0.039
							D3 vs. D9	*	0.0199
							D5 vs. D7	*	0.0363
							D5 vs. D9	ns	>0.9999
							D7 vs. D9		
							5	****	<0.0001
							D1-9 Veh vs. D1 UCM924	**	0.0053
							D1-9 Veh vs. D3	**	0.0047
							D1-9 Veh vs. D5	ns	0.6486
							D1-9 Veh vs. D7	ns	0.1502
							D1-9 Veh vs. D9	ns	0.9974
							D1 UCM924 vs. D3	*	0.0119
							D1 UCM924 vs. D5	**	0.0031
							D1 UCM924 vs. D7	****	<0.0001
							D1 UCM924 vs. D9	ns	0.3295
							D3 vs. D5	ns	0.0518
							D3 vs. D7	*	0.0153
							D3 vs. D9	ns	0.523
							D5 vs. D7	ns	0.0525
							D5 vs. D9	ns	0.9982
							D7 vs. D9		
							6	***	0.0005
							D1-9 Veh vs. D1 UCM924	ns	0.1456
							D1-9 Veh vs. D3	ns	0.665
							D1-9 Veh vs. D5	ns	0.7875
							D1-9 Veh vs. D7	ns	0.8503
							D1-9 Veh vs. D9	ns	0.9676
							D1 UCM924 vs. D3	*	0.0225
							D1 UCM924 vs. D5	*	0.01
							D1 UCM924 vs. D7	**	0.0016
							D1 UCM924 vs. D9	ns	0.5325
							D3 vs. D5	ns	0.4258
							D3 vs. D7	ns	0.271
							D3 vs. D9	ns	0.9998

							D5 vs. D7	ns	0.9752
							D5 vs. D9	ns	0.9971
							D7 vs. D9		
							7	**	0.002
							D1-9 Veh vs. D1 UCM924	ns	0.2074
							D1-9 Veh vs. D3	ns	0.5942
							D1-9 Veh vs. D5	ns	0.3336
							D1-9 Veh vs. D7	ns	0.7073
							D1-9 Veh vs. D9	ns	0.9997
							D1 UCM924 vs. D3	ns	0.1827
							D1 UCM924 vs. D5	ns	0.5787
							D1 UCM924 vs. D7	ns	0.1898
							D1 UCM924 vs. D9	ns	0.7167
							D3 vs. D5	ns	0.9344
							D3 vs. D7	ns	0.6977
							D3 vs. D9	ns	0.9895
							D5 vs. D7	ns	>0.9999
							D5 vs. D9	ns	0.9841
							D7 vs. D9		
							8	ns	0.9904
							D1-9 Veh vs. D1 UCM924	ns	0.9933
							D1-9 Veh vs. D3	ns	0.9846
							D1-9 Veh vs. D5	ns	>0.9999
							D1-9 Veh vs. D7	ns	0.2968
							D1-9 Veh vs. D9	ns	0.9267
							D1 UCM924 vs. D3	ns	0.8159
							D1 UCM924 vs. D5	ns	>0.9999
							D1 UCM924 vs. D7	ns	0.2278
							D1 UCM924 vs. D9	ns	>0.9999
							D3 vs. D5	ns	0.9995
							D3 vs. D7	ns	0.4606
							D3 vs. D9	ns	0.9996
							D5 vs. D7	ns	0.3938
							D5 vs. D9	ns	0.5197
							D7 vs. D9		
6	B	Welch's ANOVA test	D1-9 Veh = 6 D1 UCM924 = 10 D3 = 9 D5 = 9 D7 = 9 D9 = 8	W (5.000, 20.54) = 20.75	<0.0001	Dunnett post hoc comparison	Test details	Summary	Adjusted P Value
							D1-9 Veh vs. D1 UCM924 20 mg/kg	****	<0.0001
							D1-9 Veh vs. D3	***	0.0007
							D1-9 Veh vs. D5	****	<0.0001
							D1-9 Veh vs. D7	**	0.0051
							D1-9 Veh vs. D9	*	0.0252
							D1 UCM924 20 mg/kg vs. D3	ns	>0.9999
							D1 UCM924 20 mg/kg vs. D5	ns	0.2682
							D1 UCM924 20 mg/kg vs. D7	*	0.0175
							D1 UCM924 20 mg/kg vs. D9	***	0.001
							D3 vs. D5	ns	0.7896
							D3 vs. D7	ns	0.1611
							D3 vs. D9	*	0.0249
							D5 vs. D7	ns	0.5225
							D5 vs. D9	*	0.0181
							D7 vs. D9	ns	0.9286
6	C	Repeated measures 2-way ANOVA (treatment x time)	D9-Veh+Veh = 6 D9-Veh + Morph = 7 D9-UCM924 + Morph = 6	Time x treatment : F (12, 96) = 38.97 Time : F (6, 96) = 161.7 Treatment : F (2, 16) = 155.3	P<0.0001 P<0.0001 P<0.0001	Tuckey post hoc comparison	Test details	Summary	Adjusted P Value
							0		
							D9-UCM924 + Morph vs. D9-Veh + Morph	ns	0.541
							D9-Veh+Veh vs. D9-Veh + Morph	ns	0.9338
							D9-Veh+Veh vs. D9-UCM924 + Morph	ns	0.7748
							30		
							D9-UCM924 + Morph vs. D9-Veh + Morph	ns	>0.9999
							D9-Veh+Veh vs. D9-Veh + Morph	****	<0.0001
							D9-Veh+Veh vs. D9-UCM924 + Morph	****	<0.0001
							60		
							D9-UCM924 + Morph vs. D9-Veh + Morph	ns	0.7388
							D9-Veh+Veh vs. D9-Veh + Morph	****	<0.0001
							D9-Veh+Veh vs. D9-UCM924 + Morph	****	<0.0001
							120		
							D9-UCM924 + Morph vs. D9-Veh + Morph	ns	0.9311
							D9-Veh+Veh vs. D9-Veh + Morph	****	<0.0001
							D9-Veh+Veh vs. D9-UCM924 + Morph	****	<0.0001
							180		
							D9-UCM924 + Morph vs. D9-Veh + Morph	ns	0.1452
							D9-Veh+Veh vs. D9-Veh + Morph	****	<0.0001
							D9-Veh+Veh vs. D9-UCM924 + Morph	****	<0.0001
							210		
							D9-UCM924 + Morph vs. D9-Veh + Morph	ns	0.0981
							D9-Veh+Veh vs. D9-Veh + Morph	**	0.0046
							D9-Veh+Veh vs. D9-UCM924 + Morph	ns	0.5106
							360		
							D9-UCM924 + Morph vs. D9-Veh + Morph	ns	0.9811
							D9-Veh+Veh vs. D9-Veh + Morph	ns	0.8502
							D9-Veh+Veh vs. D9-UCM924 + Morph	ns	0.9368
6	D	Welch's ANOVA test	D9-Veh+Veh = 6 D9-Veh + Morph = 7 D9-UCM924 + Morph = 6	W (2.000, 7.862) = 217.9	P<0.0001	Dunnett post hoc comparison	Test details	Summary	Adjusted P Value
							D9-Veh+Veh vs. D9-UCM924 + Morph	****	<0.0001
							D9-Veh+Veh vs. D9-Veh + Morph	****	<0.0001
							D9-UCM924 + Morph vs. D9-Veh + Morph	ns	0.7697
6	E	Repeated measures 2-way ANOVA (treatment x time)	D9-UCM924+Veh = 3 D9-UCM924+Morph = 4 D9-UCM924+UCM924 = 3	Time x treatment : F (24, 84) = 5.670 Time : F (2.990, 20.93) = 10.50 Treatment : F (2, 7) = 56.34	P<0.0001 P=0.0002 P<0.0001	Tuckey post hoc comparison	Test details	Summary	Adjusted P Value
							0		
							D9-UCM924+Veh vs. D9-UCM924+Morph	ns	0.5693
							D9-UCM924+Veh vs. D9-UCM924+UCM924	ns	0.8197
							D9-UCM924+Morph vs. D9-UCM924+UCM924	ns	0.9095
							5		
							D9-UCM924+Veh vs. D9-UCM924+Morph	ns	0.3325
							D9-UCM924+Veh vs. D9-UCM924+UCM924	ns	0.5207
							D9-UCM924+Morph vs. D9-UCM924+UCM924	ns	0.9918
							10		
							D9-UCM924+Veh vs. D9-UCM924+Morph	*	0.0382
							D9-UCM924+Veh vs. D9-UCM924+UCM924	ns	0.5972
							D9-UCM924+Morph vs. D9-UCM924+UCM924	ns	0.072
							15		
							D9-UCM924+Veh vs. D9-UCM924+Morph	***	0.0002
							D9-UCM924+Veh vs. D9-UCM924+UCM924	ns	0.9511
							D9-UCM924+Morph vs. D9-UCM924+UCM924	**	0.01
							20		
							D9-UCM924+Veh vs. D9-UCM924+Morph	*	0.0103
							D9-UCM924+Veh vs. D9-UCM924+UCM924	ns	0.9467
							D9-UCM924+Morph vs. D9-UCM924+UCM924	***	0.0007

							25		
							D9-UCM924+Veh vs. D9-UCM924+Morph	***	0.0002
							D9-UCM924+Veh vs. D9-UCM924+UCM924	ns	0.9573
							D9-UCM924+Morph vs. D9-UCM924+UCM924	*	0.0315
							30		
							D9-UCM924+Veh vs. D9-UCM924+Morph	**	0.0022
							D9-UCM924+Veh vs. D9-UCM924+UCM924	ns	0.3701
							D9-UCM924+Morph vs. D9-UCM924+UCM924	**	0.0017
							35		
							D9-UCM924+Veh vs. D9-UCM924+Morph	*	0.012
							D9-UCM924+Veh vs. D9-UCM924+UCM924	ns	0.2451
							D9-UCM924+Morph vs. D9-UCM924+UCM924	**	0.0014
							40		
							D9-UCM924+Veh vs. D9-UCM924+Morph	*	0.015
							D9-UCM924+Veh vs. D9-UCM924+UCM924	ns	0.4369
							D9-UCM924+Morph vs. D9-UCM924+UCM924	**	0.0011
							45		
							D9-UCM924+Veh vs. D9-UCM924+Morph	***	0.0002
							D9-UCM924+Veh vs. D9-UCM924+UCM924	ns	0.1304
							D9-UCM924+Morph vs. D9-UCM924+UCM924	**	0.0051
							50		
							D9-UCM924+Veh vs. D9-UCM924+Morph	*	0.0428
							D9-UCM924+Veh vs. D9-UCM924+UCM924	ns	0.6326
							D9-UCM924+Morph vs. D9-UCM924+UCM924	***	0.0008
							55		
							D9-UCM924+Veh vs. D9-UCM924+Morph	***	0.0007
							D9-UCM924+Veh vs. D9-UCM924+UCM924	ns	0.1754
							D9-UCM924+Morph vs. D9-UCM924+UCM924	*	0.0428
							60		
							D9-UCM924+Veh vs. D9-UCM924+Morph	***	0.0003
							D9-UCM924+Veh vs. D9-UCM924+UCM924	ns	0.8436
							D9-UCM924+Morph vs. D9-UCM924+UCM924	**	0.0051
6	F	2-Way Mixed ANOVA (treatment x time)	D9-UCM924+Veh = 3 D9-UCM924+Morph = 4 D9-UCM924+UCM924 = 3	Time x treatment : F (24, 91) = 1.675 Time : F (12, 91) = 3.327 Treatment : F (2, 91) = 94.36	P=0.0426 P=0.0005 P<0.0001	Tuckey post hoc comparison	Test details	Summary	Adjusted P Value
							0		
							D9-UCM924+Morph vs. D9-UCM924+Veh	ns	>0.9999
							D9-UCM924+UCM924 vs. D9-UCM924+Veh	ns	>0.9999
							D9-UCM924+UCM924 vs. D9-UCM924+Morph	ns	>0.9999
							5		
							D9-UCM924+Morph vs. D9-UCM924+Veh	ns	>0.9999
							D9-UCM924+UCM924 vs. D9-UCM924+Veh	ns	>0.9999
							D9-UCM924+UCM924 vs. D9-UCM924+Morph	ns	>0.9999
							10		
							D9-UCM924+Morph vs. D9-UCM924+Veh	ns	>0.9999
							D9-UCM924+UCM924 vs. D9-UCM924+Veh	ns	>0.9999
							D9-UCM924+UCM924 vs. D9-UCM924+Morph	ns	>0.9999
							15		
							D9-UCM924+Morph vs. D9-UCM924+Veh	****	<0.0001
							D9-UCM924+UCM924 vs. D9-UCM924+Veh	ns	>0.9999
							D9-UCM924+UCM924 vs. D9-UCM924+Morph	***	0.0004
							20		
							D9-UCM924+Morph vs. D9-UCM924+Veh	****	<0.0001
							D9-UCM924+UCM924 vs. D9-UCM924+Veh	ns	>0.9999
							D9-UCM924+UCM924 vs. D9-UCM924+Morph	****	<0.0001
							25		
							D9-UCM924+Morph vs. D9-UCM924+Veh	***	0.001
							D9-UCM924+UCM924 vs. D9-UCM924+Veh	ns	>0.9999
							D9-UCM924+UCM924 vs. D9-UCM924+Morph	***	0.0003
							30		
							D9-UCM924+Morph vs. D9-UCM924+Veh	**	0.006
							D9-UCM924+UCM924 vs. D9-UCM924+Veh	ns	>0.9999
							D9-UCM924+UCM924 vs. D9-UCM924+Morph	*	0.019
							35		
							D9-UCM924+Morph vs. D9-UCM924+Veh	****	<0.0001
							D9-UCM924+UCM924 vs. D9-UCM924+Veh	ns	>0.9999
							D9-UCM924+UCM924 vs. D9-UCM924+Morph	***	0.0001
							40		
							D9-UCM924+Morph vs. D9-UCM924+Veh	****	<0.0001
							D9-UCM924+UCM924 vs. D9-UCM924+Veh	ns	>0.9999
							D9-UCM924+UCM924 vs. D9-UCM924+Morph	****	<0.0001
							45		
							D9-UCM924+Morph vs. D9-UCM924+Veh	****	<0.0001
							D9-UCM924+UCM924 vs. D9-UCM924+Veh	ns	>0.9999
							D9-UCM924+UCM924 vs. D9-UCM924+Morph	****	<0.0001
							50		
							D9-UCM924+Morph vs. D9-UCM924+Veh	****	<0.0001
							D9-UCM924+UCM924 vs. D9-UCM924+Veh	ns	>0.9999
							D9-UCM924+UCM924 vs. D9-UCM924+Morph	****	<0.0001
							55		
							D9-UCM924+Morph vs. D9-UCM924+Veh	****	<0.0001
							D9-UCM924+UCM924 vs. D9-UCM924+Veh	ns	>0.9999
							D9-UCM924+UCM924 vs. D9-UCM924+Morph	****	<0.0001
							60		
							D9-UCM924+Morph vs. D9-UCM924+Veh	****	<0.0001
							D9-UCM924+UCM924 vs. D9-UCM924+Veh	ns	>0.9999
							D9-UCM924+UCM924 vs. D9-UCM924+Morph	****	<0.0001
6	G	2-Way Mixed ANOVA (treatment x time)	D1-9 Veh = 6 D1 morph = 9 D3 =9 D5 = 9 D7 =8 D9 = 8	Time x treatment : F (30, 234) = 14.43 Time : F (3.168, 123.6) = 161.3 Treatment : F (5, 45) = 34.65	<0.0001 <0.0001 <0.0001	Tuckey post hoc comparison	Test details	Summary	Adjusted P Value
							0		
							D1 morph vs. D3	ns	0.9977
							D1 morph vs. D5	ns	0.9989
							D1 morph vs. D7	ns	>0.9999
							D1 morph vs. D9	ns	0.9182
							D1 morph vs. D1-9 Veh	ns	0.8904
							D3 vs. D5	ns	>0.9999
							D3 vs. D7	ns	0.9998
							D3 vs. D9	ns	0.9719
							D3 vs. D1-9 Veh	ns	0.795
							D5 vs. D7	ns	>0.9999
							D5 vs. D9	ns	0.9773
							D5 vs. D1-9 Veh	ns	0.8237

							D7 vs. D9	ns	0.9439
							D7 vs. D1-9 Veh	ns	0.8509
							D9 vs. D1-9 Veh	ns	0.676
							30		
							D1 morph vs. D3	ns	0.5568
							D1 morph vs. D5	*	0.0381
							D1 morph vs. D7	*	0.0208
							D1 morph vs. D9	****	<0.0001
							D1 morph vs. D1-9 Veh	****	<0.0001
							D3 vs. D5	ns	0.1508
							D3 vs. D7	ns	0.053
							D3 vs. D9	****	<0.0001
							D3 vs. D1-9 Veh	****	<0.0001
							D5 vs. D7	ns	0.8969
							D5 vs. D9	**	0.0032
							D5 vs. D1-9 Veh	***	0.0001
							D7 vs. D9	ns	0.1237
							D7 vs. D1-9 Veh	**	0.0043
							D9 vs. D1-9 Veh	**	0.0016
							60		
							D1 morph vs. D3	ns	0.6298
							D1 morph vs. D5	ns	0.0547
							D1 morph vs. D7	*	0.0226
							D1 morph vs. D9	**	0.0019
							D1 morph vs. D1-9 Veh	****	<0.0001
							D3 vs. D5	ns	0.2841
							D3 vs. D7	ns	0.074
							D3 vs. D9	****	<0.0001
							D3 vs. D1-9 Veh	****	<0.0001
							D5 vs. D7	ns	0.927
							D5 vs. D9	**	0.0089
							D5 vs. D1-9 Veh	**	0.0012
							D7 vs. D9	ns	0.1155
							D7 vs. D1-9 Veh	*	0.0165
							D9 vs. D1-9 Veh	ns	0.1588
							120		
							D1 morph vs. D3	ns	0.1411
							D1 morph vs. D5	*	0.0176
							D1 morph vs. D7	****	<0.0001
							D1 morph vs. D9	****	<0.0001
							D1 morph vs. D1-9 Veh	****	<0.0001
							D3 vs. D5	ns	0.7661
							D3 vs. D7	**	0.006
							D3 vs. D9	**	0.0022
							D3 vs. D1-9 Veh	**	0.001
							D5 vs. D7	ns	0.1816
							D5 vs. D9	ns	0.0746
							D5 vs. D1-9 Veh	*	0.03
							D7 vs. D9	ns	0.6285
							D7 vs. D1-9 Veh	*	0.015
							D9 vs. D1-9 Veh	ns	0.713
							180		
							D1 morph vs. D3	ns	0.2479
							D1 morph vs. D5	ns	0.0863
							D1 morph vs. D7	*	0.0409
							D1 morph vs. D9	*	0.016
							D1 morph vs. D1-9 Veh	**	0.0033
							D3 vs. D5	ns	0.9414
							D3 vs. D7	ns	0.7678
							D3 vs. D9	ns	0.6564
							D3 vs. D1-9 Veh	ns	0.2182
							D5 vs. D7	ns	0.9988
							D5 vs. D9	ns	0.9996
							D5 vs. D1-9 Veh	ns	0.9193
							D7 vs. D9	ns	>0.9999
							D7 vs. D1-9 Veh	ns	0.9956
							D9 vs. D1-9 Veh	ns	0.8765
							210		
							D1 morph vs. D3	*	0.0387
							D1 morph vs. D5	ns	0.1127
							D1 morph vs. D7	ns	0.0513
							D1 morph vs. D9	ns	0.5145
							D1 morph vs. D1-9 Veh	*	0.0374
							D3 vs. D5	ns	0.4935
							D3 vs. D7	ns	0.9849
							D3 vs. D9	ns	0.4179
							D3 vs. D1-9 Veh	ns	>0.9999
							D5 vs. D7	ns	0.7989
							D5 vs. D9	ns	0.8523
							D5 vs. D1-9 Veh	ns	0.3571
							D7 vs. D9	ns	0.5206
							D7 vs. D1-9 Veh	ns	0.9312
							D9 vs. D1-9 Veh	ns	0.398
							360		
							D1 morph vs. D3	ns	0.071
							D1 morph vs. D5	ns	0.1422
							D1 morph vs. D7	ns	0.9563
							D1 morph vs. D9	ns	>0.9999
							D1 morph vs. D1-9 Veh	ns	0.8767
							D3 vs. D5	ns	0.9698
							D3 vs. D7	ns	0.567
							D3 vs. D9	ns	0.7454
							D3 vs. D1-9 Veh	ns	0.7207
							D5 vs. D7	ns	0.7722
							D5 vs. D9	ns	0.8178
							D5 vs. D1-9 Veh	ns	0.8936
							D7 vs. D9	ns	0.9869
							D7 vs. D1-9 Veh	ns	0.9999
							D9 vs. D1-9 Veh	ns	0.9709
6	H	Welch's ANOVA test	D1-9 Veh = 6 D1 morph = 9 D3 =9 D5 = 9 D7 =8 D9 = 8	W (5.000, 19.25) = 102.6	<0.0001	Dunnett post hoc comparison	Test details	Summary	Adjusted P Value
							D1-9 Veh vs. D1 morph	****	<0.0001
							D1-9 Veh vs. D3	****	<0.0001
							D1-9 Veh vs. D5	*	0.0108
							D1-9 Veh vs. D7	**	0.0087
							D1-9 Veh vs. D9	ns	>0.9999
							D1 morph vs. D3	**	0.0023
							D1 morph vs. D5	*	0.0149
							D1 morph vs. D7	****	<0.0001
							D1 morph vs. D9	****	<0.0001
							D3 vs. D5	ns	0.9119
							D3 vs. D7	**	0.0036
							D3 vs. D9	****	<0.0001

							D5 vs. D7	ns	0.6925
							D5 vs. D9	*	0.0103
							D7 vs. D9	**	0.0096
6	I	2-Way Mixed ANOVA (treatment x time)	D9-Veh+Veh = 5 D9-Veh + UCM924 = 6 D9-Veh + UCM924 = 7	Time x treatment : F (16, 120) = 10.34 Time : F (4.715, 70.73) = 17.29 Treatment : F (2, 15) = 138.7	P<0.0001 P<0.0001 P<0.0001	Tuckey post hoc comparison	Test details	Summary	Adjusted P Value
							0		
							D9-Veh + Veh vs. D9-Morph + UCM924	ns	0.8812
							D9-Veh + Veh vs. D9-Veh + UCM924	ns	0.2631
							D9-Morph + UCM924 vs. D9-Veh + UCM924	ns	0.597
							1		
							D9-Veh + Veh vs. D9-Morph + UCM924	ns	0.1481
							D9-Veh + Veh vs. D9-Veh + UCM924	**	0.0042
							D9-Morph + UCM924 vs. D9-Veh + UCM924	ns	0.0629
							2		
							D9-Veh + Veh vs. D9-Morph + UCM924	ns	0.1159
							D9-Veh + Veh vs. D9-Veh + UCM924	***	0.0001
							D9-Morph + UCM924 vs. D9-Veh + UCM924	**	0.0027
							3		
							D9-Veh + Veh vs. D9-Morph + UCM924	ns	0.8859
							D9-Veh + Veh vs. D9-Veh + UCM924	****	<0.0001
							D9-Morph + UCM924 vs. D9-Veh + UCM924	****	<0.0001
							4		
							D9-Veh + Veh vs. D9-Morph + UCM924	ns	0.4237
							D9-Veh + Veh vs. D9-Veh + UCM924	****	<0.0001
							D9-Morph + UCM924 vs. D9-Veh + UCM924	****	<0.0001
							5		
							D9-Veh + Veh vs. D9-Morph + UCM924	ns	0.8904
							D9-Veh + Veh vs. D9-Veh + UCM924	****	<0.0001
							D9-Morph + UCM924 vs. D9-Veh + UCM924	***	0.0002
							6		
							D9-Veh + Veh vs. D9-Morph + UCM924	ns	0.8512
							D9-Veh + Veh vs. D9-Veh + UCM924	**	0.0079
							D9-Morph + UCM924 vs. D9-Veh + UCM924	**	0.005
							7		
							D9-Veh + Veh vs. D9-Morph + UCM924	ns	0.1401
							D9-Veh + Veh vs. D9-Veh + UCM924	*	0.0154
							D9-Morph + UCM924 vs. D9-Veh + UCM924	**	0.0024
							8		
							D9-Veh + Veh vs. D9-Morph + UCM924	ns	0.8486
							D9-Veh + Veh vs. D9-Veh + UCM924	ns	0.9752
							D9-Morph + UCM924 vs. D9-Veh + UCM924	ns	0.9386
6	J	1-way ANOVA	D9-Veh+Veh = 5 D9-Morph + UCM924 = 6 D9-Veh + UCM924	F (2, 16) = 157.3	P<0.0001	Tuckey post hoc comparison	Test details	Summary	Adjusted P Value
							D9-Veh+Veh vs. D9-Morph + UCM924	*	0.0127
							D9-Veh+Veh vs. D9-Veh + UCM924	****	<0.0001
							D9-Morph + UCM924 vs. D9-Veh + UCM924	****	<0.0001
6	K	2-Way Mixed ANOVA (treatment x time)	D9-Morph+Veh = 3 D9-Morph+Morph = 3 D9-Veh + UCM924 = 4	Time x treatment : F (24, 84) = 0.8946 Time : F (3.532, 24.72) = 2.969 Treatment : F (2, 7) = 3.934	P=0.6080 P=0.0443 P=0.0716	Tuckey post hoc comparison	Test details	Summary	Adjusted P Value
							0		
							D9-Morph+UCM924 vs. D9-Morph+Veh	ns	>0.9999
							D9-Morph+UCM924 vs. D9-Morph+Morph	ns	>0.9999
							D9-Morph+Veh vs. D9-Morph+Morph	ns	0.9977
							5		
							D9-Morph+UCM924 vs. D9-Morph+Veh	ns	>0.9999
							D9-Morph+UCM924 vs. D9-Morph+Morph	ns	0.9763
							D9-Morph+Veh vs. D9-Morph+Morph	ns	0.9892
							10		
							D9-Morph+UCM924 vs. D9-Morph+Veh	ns	>0.9999
							D9-Morph+UCM924 vs. D9-Morph+Morph	ns	0.9693
							D9-Morph+Veh vs. D9-Morph+Morph	ns	0.9073
							15		
							D9-Morph+UCM924 vs. D9-Morph+Veh	ns	>0.9999
							D9-Morph+UCM924 vs. D9-Morph+Morph	ns	0.9954
							D9-Morph+Veh vs. D9-Morph+Morph	ns	0.8632
							20		
							D9-Morph+UCM924 vs. D9-Morph+Veh	ns	>0.9999
							D9-Morph+UCM924 vs. D9-Morph+Morph	ns	0.4157
							D9-Morph+Veh vs. D9-Morph+Morph	ns	0.9674
							25		
							D9-Morph+UCM924 vs. D9-Morph+Veh	ns	>0.9999
							D9-Morph+UCM924 vs. D9-Morph+Morph	ns	0.9792
							D9-Morph+Veh vs. D9-Morph+Morph	ns	0.9079
							30		
							D9-Morph+UCM924 vs. D9-Morph+Veh	ns	0.9586
							D9-Morph+UCM924 vs. D9-Morph+Morph	ns	0.9995
							D9-Morph+Veh vs. D9-Morph+Morph	ns	0.5898
							35		
							D9-Morph+UCM924 vs. D9-Morph+Veh	ns	0.9947
							D9-Morph+UCM924 vs. D9-Morph+Morph	ns	0.9987
							D9-Morph+Veh vs. D9-Morph+Morph	ns	0.7398
							40		
							D9-Morph+UCM924 vs. D9-Morph+Veh	ns	0.9808
							D9-Morph+UCM924 vs. D9-Morph+Morph	ns	>0.9999
							D9-Morph+Veh vs. D9-Morph+Morph	ns	0.855
							45		
							D9-Morph+UCM924 vs. D9-Morph+Veh	ns	0.9973
							D9-Morph+UCM924 vs. D9-Morph+Morph	ns	>0.9999
							D9-Morph+Veh vs. D9-Morph+Morph	ns	0.6779
							50		
							D9-Morph+UCM924 vs. D9-Morph+Veh	ns	>0.9999
							D9-Morph+UCM924 vs. D9-Morph+Morph	ns	>0.9999
							D9-Morph+Veh vs. D9-Morph+Morph	ns	0.9972
							55		
							D9-Morph+UCM924 vs. D9-Morph+Veh	ns	0.9996
							D9-Morph+UCM924 vs. D9-Morph+Morph	ns	>0.9999
							D9-Morph+Veh vs. D9-Morph+Morph	ns	0.8781
							60		
							D9-Morph+UCM924 vs. D9-Morph+Veh	ns	>0.9999
							D9-Morph+UCM924 vs. D9-Morph+Morph	ns	>0.9999
							D9-Morph+Veh vs. D9-Morph+Morph	ns	0.869
6	L	2-Way Mixed ANOVA	D9-Morph+Veh = 3	Time x treatment : F (24, 117) = 0.1450	P>0.9999	Tuckey post hoc comparison	Test details	Summary	Adjusted P Value

		(treatment x time)	D9-Morph+Morph = 4 D9-Veh + UCM924 = 4	Time : F (12, 117) = 1.060 Treatment : F (2, 117) = 2.075	P=0.4004 P=0.1301		0		
							D9-Morph+Morph vs. D9-Morph+Veh	ns	>0.9999
							D9-Veh + UCM924 vs. D9-Morph+Veh	ns	>0.9999
							D9-Veh + UCM924 vs. D9-Morph+Morph	ns	>0.9999
							5		
							D9-Morph+Morph vs. D9-Morph+Veh	ns	>0.9999
							D9-Veh + UCM924 vs. D9-Morph+Veh	ns	>0.9999
							D9-Veh + UCM924 vs. D9-Morph+Morph	ns	>0.9999
							10		
							D9-Morph+Morph vs. D9-Morph+Veh	ns	>0.9999
							D9-Veh + UCM924 vs. D9-Morph+Veh	ns	>0.9999
							D9-Veh + UCM924 vs. D9-Morph+Morph	ns	>0.9999
							15		
							D9-Morph+Morph vs. D9-Morph+Veh	ns	>0.9999
							D9-Veh + UCM924 vs. D9-Morph+Veh	ns	>0.9999
							D9-Veh + UCM924 vs. D9-Morph+Morph	ns	>0.9999
							20		
							D9-Morph+Morph vs. D9-Morph+Veh	ns	>0.9999
							D9-Veh + UCM924 vs. D9-Morph+Veh	ns	>0.9999
							D9-Veh + UCM924 vs. D9-Morph+Morph	ns	>0.9999
							25		
							D9-Morph+Morph vs. D9-Morph+Veh	ns	>0.9999
							D9-Veh + UCM924 vs. D9-Morph+Veh	ns	>0.9999
							D9-Veh + UCM924 vs. D9-Morph+Morph	ns	>0.9999
							30		
							D9-Morph+Morph vs. D9-Morph+Veh	ns	>0.9999
							D9-Veh + UCM924 vs. D9-Morph+Veh	ns	>0.9999
							D9-Veh + UCM924 vs. D9-Morph+Morph	ns	>0.9999
							35		
							D9-Morph+Morph vs. D9-Morph+Veh	ns	>0.9999
							D9-Veh + UCM924 vs. D9-Morph+Veh	ns	>0.9999
							D9-Veh + UCM924 vs. D9-Morph+Morph	ns	>0.9999
							40		
							D9-Morph+Morph vs. D9-Morph+Veh	ns	>0.9999
							D9-Veh + UCM924 vs. D9-Morph+Veh	ns	>0.9999
							D9-Veh + UCM924 vs. D9-Morph+Morph	ns	>0.9999
							45		
							D9-Morph+Morph vs. D9-Morph+Veh	ns	>0.9999
							D9-Veh + UCM924 vs. D9-Morph+Veh	ns	>0.9999
							D9-Veh + UCM924 vs. D9-Morph+Morph	ns	>0.9999
							50		
							D9-Morph+Morph vs. D9-Morph+Veh	ns	>0.9999
							D9-Veh + UCM924 vs. D9-Morph+Veh	ns	>0.9999
							D9-Veh + UCM924 vs. D9-Morph+Morph	ns	>0.9999
							55		
							D9-Morph+Morph vs. D9-Morph+Veh	ns	>0.9999
							D9-Veh + UCM924 vs. D9-Morph+Veh	ns	>0.9999
							D9-Veh + UCM924 vs. D9-Morph+Morph	ns	>0.9999
							60		
							D9-Morph+Morph vs. D9-Morph+Veh	ns	>0.9999
							D9-Veh + UCM924 vs. D9-Morph+Veh	ns	>0.9999
							D9-Veh + UCM924 vs. D9-Morph+Morph	ns	>0.9999

Figure	Panel	Test	Group-size	Statistic	P value	Pair-wise comparison	Statistic 2		
							Test details	Summary	Adjusted P Value
7	A-B (FR3)	Repeated measures 3-Way ANOVA (Group x Session x Lever type)	Veh = 4 0.01 = 4 0.1 = 5 1 = 5	Group x Session x Lever type F((27, 126) = 0.67 Group x Session F(27, 126) = 0.73 Session x Lever type F(9, 126) = 5.10 Group x Lever type F(3, 14) = 2.08 Session F(9, 126) = 3.70 Lever type F(1, 14) = 0.01 Group F(3, 14) = 1.10	P=0.88 P=0.82 P<0.001 P=0.15 P<0.001 P=0.91 P=0.38	Tuckey post hoc comparison	session 1: Active Lever		
							Veh vs 0.01	ns	>0.9999
							Veh vs 0.1	ns	>0.9999
							Veh vs 1	ns	>0.9999
							0.01 vs 0.1	ns	>0.9999
							0.01 vs 1	ns	>0.9999
							0.1 vs 1	ns	>0.9999
							session 2: Active Lever		
							Veh vs 0.01	ns	>0.9999
							Veh vs 0.1	ns	>0.9999
							Veh vs 1	ns	>0.9999
							0.01 vs 0.1	ns	>0.9999
							0.01 vs 1	ns	>0.9999
							0.1 vs 1	ns	>0.9999
							session 3: Active Lever		
							Veh vs 0.01	ns	>0.9999
							Veh vs 0.1	ns	>0.9999
							Veh vs 1	ns	>0.9999
							0.01 vs 0.1	ns	>0.9999
							0.01 vs 1	ns	>0.9999
							0.1 vs 1	ns	>0.9999
							session 4: Active Lever		
							Veh vs 0.01	ns	>0.9999
							Veh vs 0.1	ns	>0.9999
							Veh vs 1	ns	>0.9999
							0.01 vs 0.1	ns	>0.9999
							0.01 vs 1	ns	>0.9999
							0.1 vs 1	ns	>0.9999
							session 5: Active Lever		
							Veh vs 0.01	ns	>0.9999
							Veh vs 0.1	ns	>0.9999
							Veh vs 1	ns	>0.9999
							0.01 vs 0.1	ns	>0.9999
							0.01 vs 1	ns	>0.9999
							0.1 vs 1	ns	>0.9999
							session 6: Active Lever		
							Veh vs 0.01	ns	>0.9999
							Veh vs 0.1	ns	>0.9999
							Veh vs 1	ns	>0.9999
							0.01 vs 0.1	ns	>0.9999
							0.01 vs 1	ns	>0.9999
							0.1 vs 1	ns	>0.9999
							session 7: Active Lever		
							Veh vs 0.01	ns	>0.9999
							Veh vs 0.1	ns	>0.9999
							Veh vs 1	ns	>0.9999
							0.01 vs 0.1	ns	>0.9999
							0.01 vs 1	ns	>0.9999
							0.1 vs 1	ns	>0.9999
							session 8: Active Lever		
							Veh vs 0.01	ns	>0.9999
							Veh vs 0.1	ns	>0.9999
							Veh vs 1	ns	>0.9999
							0.01 vs 0.1	ns	>0.9999
							0.01 vs 1	ns	>0.9999
							0.1 vs 1	ns	>0.9999
							session 9: Active Lever		
							Veh vs 0.01	ns	>0.9999
							Veh vs 0.1	ns	>0.9999
							Veh vs 1	ns	>0.9999
							0.01 vs 0.1	ns	>0.9999
							0.01 vs 1	ns	>0.9999
							0.1 vs 1	ns	>0.9999
							session 10: Active Lever		
							Veh vs 0.01	ns	>0.9999
							Veh vs 0.1	ns	>0.9999
							Veh vs 1	ns	>0.9999
							0.01 vs 0.1	ns	>0.9999
							0.01 vs 1	ns	>0.9999
							0.1 vs 1	ns	>0.9999
							session 1: Inactive Lever		
							Veh vs 0.01	ns	>0.9999
							Veh vs 0.1	ns	>0.9999
							Veh vs 1	ns	>0.9999
							0.01 vs 0.1	ns	>0.9999
							0.01 vs 1	ns	>0.9999
							0.1 vs 1	ns	>0.9999
							session 2: Inactive Lever		
							Veh vs 0.01	ns	>0.9999
							Veh vs 0.1	ns	>0.9999
							Veh vs 1	ns	>0.9999
							0.01 vs 0.1	ns	>0.9999
							0.01 vs 1	ns	>0.9999
							0.1 vs 1	ns	>0.9999
							session 3: Inactive Lever		
							Veh vs 0.01	ns	>0.9999
							Veh vs 0.1	ns	>0.9999
							Veh vs 1	ns	>0.9999
							0.01 vs 0.1	ns	>0.9999
							0.01 vs 1	ns	>0.9999
							0.1 vs 1	ns	>0.9999
							session 4: Inactive Lever		
							Veh vs 0.01	ns	>0.9999
							Veh vs 0.1	ns	>0.9999
							Veh vs 1	ns	>0.9999
							0.01 vs 0.1	ns	>0.9999
							0.01 vs 1	ns	>0.9999

							0.1 vs 1	ns	>0.9999
							session 5: Inactive Lever		
							Veh vs 0.01	ns	>0.9999
							Veh vs 0.1	ns	>0.9999
							Veh vs 1	ns	>0.9999
							0.01 vs 0.1	ns	>0.9999
							0.01 vs 1	ns	>0.9999
							0.1 vs 1	ns	>0.9999
							session 6: Inactive Lever		
							Veh vs 0.01	ns	>0.9999
							Veh vs 0.1	ns	>0.9999
							Veh vs 1	ns	>0.9999
							0.01 vs 0.1	ns	>0.9999
							0.01 vs 1	ns	>0.9999
							0.1 vs 1	ns	>0.9999
							session 7: Inactive Lever		
							Veh vs 0.01	ns	>0.9999
							Veh vs 0.1	ns	>0.9999
							Veh vs 1	ns	>0.9999
							0.01 vs 0.1	ns	>0.9999
							0.01 vs 1	ns	>0.9999
							0.1 vs 1	ns	>0.9999
							session 8: Inactive Lever		
							Veh vs 0.01	ns	>0.9999
							Veh vs 0.1	ns	>0.9999
							Veh vs 1	ns	>0.9999
							0.01 vs 0.1	ns	>0.9999
							0.01 vs 1	ns	>0.9999
							0.1 vs 1	ns	>0.9999
							session 9: Inactive Lever		
							Veh vs 0.01	ns	>0.9999
							Veh vs 0.1	ns	>0.9999
							Veh vs 1	ns	>0.9999
							0.01 vs 0.1	ns	>0.9999
							0.01 vs 1	ns	>0.9999
							0.1 vs 1	ns	>0.9999
							session 10: Inactive Lever		
							Veh vs 0.01	ns	>0.9999
							Veh vs 0.1	ns	0.9854
							Veh vs 1	ns	0.9881
							0.01 vs 0.1	ns	>0.9999
							0.01 vs 1	ns	>0.9999
							0.1 vs 1	ns	>0.9999
7	A-B (FR1)	Repeated measures 3-Way ANOVA (Group x Session x Lever type)	Veh = 4 0.01 = 4 0.1 = 5 1 = 5	Group x Session x Lever type F(12, 56) = 1.15 Group x Session F(12, 56) = 1.26 Session x Lever type F(4, 56) = 2.54 Group x Lever type F(3, 14) = 0.74 Session F(4, 56) = 2.47 Lever type F(1, 14) = 12.41 Group F(3, 14) = 0.55	P=0.34 P=0.27 P<0.05 P=0.55 p=0.06 P<0.01 P=0.66	Tuckey post hoc comparison	session 11: Active Lever		
							Veh vs 0.01	ns	>0.9999
							Veh vs 0.1	ns	>0.9999
							Veh vs 1	ns	>0.9999
							0.01 vs 0.1	ns	>0.9999
							0.01 vs 1	ns	>0.9999
							0.1 vs 1	ns	>0.9999
							session 12: Active Lever		
							Veh vs 0.01	ns	>0.9999
							Veh vs 0.1	ns	>0.9999
							Veh vs 1	ns	>0.9999
							0.01 vs 0.1	ns	>0.9999
							0.01 vs 1	ns	>0.9999
							0.1 vs 1	ns	>0.9999
							session 13: Active Lever		
							Veh vs 0.01	ns	>0.9999
							Veh vs 0.1	ns	>0.9999
							Veh vs 1	ns	>0.9999
							0.01 vs 0.1	ns	>0.9999
							0.01 vs 1	ns	>0.9999
							0.1 vs 1	ns	>0.9999
							session 14: Active Lever		
							Veh vs 0.01	ns	>0.9999
							Veh vs 0.1	ns	>0.9999
							Veh vs 1	ns	>0.9999
							0.01 vs 0.1	ns	>0.9999
							0.01 vs 1	ns	>0.9999
							0.1 vs 1	ns	>0.9999
							session 15: Active Lever		
							Veh vs 0.01	ns	>0.9999
							Veh vs 0.1	ns	>0.9999
							Veh vs 1	ns	>0.9999
							0.01 vs 0.1	ns	>0.9999
							0.01 vs 1	ns	>0.9999
							0.1 vs 1	ns	>0.9999
							session 11: Inactive Lever		
							Veh vs 0.01	ns	>0.9999
							Veh vs 0.1	ns	>0.9999
							Veh vs 1	ns	>0.9999
							0.01 vs 0.1	ns	>0.9999
							0.01 vs 1	ns	>0.9999
							0.1 vs 1	ns	>0.9999
							session 12: Inactive Lever		
							Veh vs 0.01	ns	>0.9999
							Veh vs 0.1	ns	>0.9999
							Veh vs 1	ns	>0.9999
							0.01 vs 0.1	ns	>0.9999
							0.01 vs 1	ns	>0.9999
							0.1 vs 1	ns	>0.9999
							session 13: Inactive Lever		
							Veh vs 0.01	ns	0.57
							Veh vs 0.1	ns	0.91
							Veh vs 1	ns	>0.9999
							0.01 vs 0.1	ns	>0.9999
							0.01 vs 1	ns	0.83

							0.1 vs 1	ns	>0.9999
							session 14: Inactive Lever		
							Veh vs 0.01	ns	0.92
							Veh vs 0.1	ns	>0.9999
							Veh vs 1	ns	>0.9999
							0.01 vs 0.1	ns	>0.9999
							0.01 vs 1	ns	>0.9999
							0.1 vs 1	ns	>0.9999
							session 15: Inactive Lever		
							Veh vs 0.01	ns	>0.9999
							Veh vs 0.1	ns	>0.9999
							Veh vs 1	ns	>0.9999
							0.01 vs 0.1	ns	>0.9999
							0.01 vs 1	ns	>0.9999
							0.1 vs 1	ns	>0.9999
7	C (FR3)	Repeated measures 2-Way ANOVA (Group x Session)	Veh = 4 0.01 = 4 0.1 = 5 1 = 5	Group x Session F(27, 126) = 0.66 Session F(9, 126) = 11.77 Group F(3, 14) = 1.80	P=0.89 P<0.001 p=0.19	Tuckey post hoc comparison	session 1		
							Veh vs 0.01	ns	>0.9999
							Veh vs 0.1	ns	>0.9999
							Veh vs 1	ns	0.98
							0.01 vs 0.1	ns	>0.9999
							0.01 vs 1	ns	>0.9999
							0.1 vs 1	ns	>0.9999
							session 2		
							Veh vs 0.01	ns	>0.9999
							Veh vs 0.1	ns	>0.9999
							Veh vs 1	ns	>0.9999
							0.01 vs 0.1	ns	>0.9999
							0.01 vs 1	ns	>0.9999
							0.1 vs 1	ns	>0.9999
							session 3		
							Veh vs 0.01	ns	>0.9999
							Veh vs 0.1	ns	>0.9999
							Veh vs 1	ns	>0.9999
							0.01 vs 0.1	ns	>0.9999
							0.01 vs 1	ns	>0.9999
							0.1 vs 1	ns	>0.9999
							session 4		
							Veh vs 0.01	ns	>0.9999
							Veh vs 0.1	ns	>0.9999
							Veh vs 1	ns	>0.9999
							0.01 vs 0.1	ns	>0.9999
							0.01 vs 1	ns	>0.9999
							0.1 vs 1	ns	>0.9999
							session 5		
							Veh vs 0.01	ns	>0.9999
							Veh vs 0.1	ns	>0.9999
							Veh vs 1	ns	>0.9999
							0.01 vs 0.1	ns	>0.9999
							0.01 vs 1	ns	>0.9999
							0.1 vs 1	ns	>0.9999
							session 6		
							Veh vs 0.01	ns	>0.9999
							Veh vs 0.1	ns	>0.9999
							Veh vs 1	ns	>0.9999
							0.01 vs 0.1	ns	>0.9999
							0.01 vs 1	ns	>0.9999
							0.1 vs 1	ns	>0.9999
							session 7		
							Veh vs 0.01	ns	>0.9999
							Veh vs 0.1	ns	>0.9999
							Veh vs 1	ns	>0.9999
							0.01 vs 0.1	ns	>0.9999
							0.01 vs 1	ns	>0.9999
							0.1 vs 1	ns	>0.9999
							session 8		
							Veh vs 0.01	ns	>0.9999
							Veh vs 0.1	ns	>0.9999
							Veh vs 1	ns	>0.9999
							0.01 vs 0.1	ns	>0.9999
							0.01 vs 1	ns	>0.9999
							0.1 vs 1	ns	>0.9999
							session 9		
							Veh vs 0.01	ns	>0.9999
							Veh vs 0.1	ns	>0.9999
							Veh vs 1	ns	>0.9999
							0.01 vs 0.1	ns	>0.9999
							0.01 vs 1	ns	>0.9999
							0.1 vs 1	ns	>0.9999
							session 10		
							Veh vs 0.01	ns	>0.9999
							Veh vs 0.1	ns	>0.9999
							Veh vs 1	ns	0.97
							0.01 vs 0.1	ns	>0.9999
							0.01 vs 1	ns	>0.9999
							0.1 vs 1	ns	>0.9999
7	C (FR1)	Repeated measures 2-Way ANOVA (Group x Session)	Veh = 4 0.01 = 4 0.1 = 5 1 = 5	Group x Session F(12, 56) = 1.08 Session F(4, 56) = 2.25 Group F(3, 14) = 0.96	P=0.39 p=0.08 p=0.44	Tuckey post hoc comparison	session 11		
							Veh vs 0.01	ns	>0.9999
							Veh vs 0.1	ns	>0.9999
							Veh vs 1	ns	0.98
							0.01 vs 0.1	ns	>0.9999
							0.01 vs 1	ns	>0.9999
							0.1 vs 1	ns	>0.9999
							session 12		
							Veh vs 0.01	ns	>0.9999
							Veh vs 0.1	ns	>0.9999
							Veh vs 1	ns	>0.9999
							0.01 vs 0.1	ns	>0.9999

							0.01 vs 1	ns	>0.9999
							0.1 vs 1	ns	>0.9999
							session 13		
							Veh vs 0.01	ns	0.85
							Veh vs 0.1	ns	>0.9999
							Veh vs 1	ns	>0.9999
							0.01 vs 0.1	ns	>0.9999
							0.01 vs 1	ns	>0.9999
							0.1 vs 1	ns	>0.9999
							session 14		
							Veh vs 0.01	ns	>0.9999
							Veh vs 0.1	ns	>0.9999
							Veh vs 1	ns	>0.9999
							0.01 vs 0.1	ns	>0.9999
							0.01 vs 1	ns	>0.9999
							0.1 vs 1	ns	>0.9999
							session 15		
							Veh vs 0.01	ns	>0.9999
							Veh vs 0.1	ns	>0.9999
							Veh vs 1	ns	>0.9999
							0.01 vs 0.1	ns	>0.9999
							0.01 vs 1	ns	>0.9999
							0.1 vs 1	ns	>0.9999
7	D (FR3)	Repeated measures 2-Way ANOVA (Group x Time)	Veh = 4 0.01 = 4 0.1 = 5 1 = 5	Group x Time F(33, 154) = 1.11 Group F(3, 14) = 0.33 Time F(11, 154) = 39.49	P=0.33 p=0.80 P<0.001	Tuckey post hoc comparison	5 min		
							Veh vs 0.01	ns	0.84
							Veh vs 0.1	ns	>0.9999
							Veh vs 1	ns	>0.9999
							0.01 vs 0.1	ns	0.80
							0.01 vs 1	ns	0.48
							0.1 vs 1	ns	>0.9999
							10 min		
							Veh vs 0.01	ns	>0.9999
							Veh vs 0.1	ns	>0.9999
							Veh vs 1	ns	>0.9999
							0.01 vs 0.1	ns	0.94
							0.01 vs 1	ns	>0.9999
							0.1 vs 1	ns	>0.9999
							15 min		
							Veh vs 0.01	ns	>0.9999
							Veh vs 0.1	ns	>0.9999
							Veh vs 1	ns	>0.9999
							0.01 vs 0.1	ns	>0.9999
							0.01 vs 1	ns	>0.9999
							0.1 vs 1	ns	>0.9999
							20 min		
							Veh vs 0.01	ns	>0.9999
							Veh vs 0.1	ns	>0.9999
							Veh vs 1	ns	>0.9999
							0.01 vs 0.1	ns	>0.9999
							0.01 vs 1	ns	>0.9999
							0.1 vs 1	ns	>0.9999
							25 min		
							Veh vs 0.01	ns	>0.9999
							Veh vs 0.1	ns	>0.9999
							Veh vs 1	ns	>0.9999
							0.01 vs 0.1	ns	>0.9999
							0.01 vs 1	ns	>0.9999
							0.1 vs 1	ns	>0.9999
							30 min		
							Veh vs 0.01	ns	>0.9999
							Veh vs 0.1	ns	>0.9999
							Veh vs 1	ns	>0.9999
							0.01 vs 0.1	ns	>0.9999
							0.01 vs 1	ns	>0.9999
							0.1 vs 1	ns	>0.9999
							35 min		
							Veh vs 0.01	ns	>0.9999
							Veh vs 0.1	ns	>0.9999
							Veh vs 1	ns	>0.9999
							0.01 vs 0.1	ns	>0.9999
							0.01 vs 1	ns	>0.9999
							0.1 vs 1	ns	>0.9999
							40 min		
							Veh vs 0.01	ns	>0.9999
							Veh vs 0.1	ns	>0.9999
							Veh vs 1	ns	>0.9999
							0.01 vs 0.1	ns	>0.9999
							0.01 vs 1	ns	>0.9999
							0.1 vs 1	ns	>0.9999
							45 min		
							Veh vs 0.01	ns	>0.9999
							Veh vs 0.1	ns	>0.9999
							Veh vs 1	ns	>0.9999
							0.01 vs 0.1	ns	>0.9999
							0.01 vs 1	ns	>0.9999
							0.1 vs 1	ns	>0.9999
							50 min		
							Veh vs 0.01	ns	>0.9999
							Veh vs 0.1	ns	>0.9999
							Veh vs 1	ns	>0.9999
							0.01 vs 0.1	ns	>0.9999
							0.01 vs 1	ns	>0.9999
							0.1 vs 1	ns	>0.9999
							55 min		
							Veh vs 0.01	ns	>0.9999
							Veh vs 0.1	ns	>0.9999
							Veh vs 1	ns	>0.9999
							0.01 vs 0.1	ns	>0.9999

							0.01 vs 1	ns	>0.9999
							0.1 vs 1	ns	>0.9999
							60 min		
							Veh vs 0.01	ns	>0.9999
							Veh vs 0.1	ns	>0.9999
							Veh vs 1	ns	>0.9999
							0.01 vs 0.1	ns	>0.9999
							0.01 vs 1	ns	>0.9999
							0.1 vs 1	ns	>0.9999
7	E (FR3)	Repeated measures 2-Way ANOVA (Group x Time)	Veh = 4 0.01 = 4 0.1 = 5 1 = 5	Group x Time F(33, 154) = 1.02 Group F(3, 14) = 0.32 Time F(11, 154) = 32.23	P=0.44 p=0.81 P<0.001	Tuckey post hoc comparison	5 min		
							Veh vs 0.01	ns	>0.9999
							Veh vs 0.1	ns	>0.9999
							Veh vs 1	ns	>0.9999
							0.01 vs 0.1	ns	>0.9999
							0.01 vs 1	ns	0.88
							0.1 vs 1	ns	>0.9999
							10 min		
							Veh vs 0.01	ns	>0.9999
							Veh vs 0.1	ns	>0.9999
							Veh vs 1	ns	>0.9999
							0.01 vs 0.1	ns	0.94
							0.01 vs 1	ns	>0.9999
							0.1 vs 1	ns	>0.9999
							15 min		
							Veh vs 0.01	ns	>0.9999
							Veh vs 0.1	ns	>0.9999
							Veh vs 1	ns	>0.9999
							0.01 vs 0.1	ns	>0.9999
							0.01 vs 1	ns	>0.9999
							0.1 vs 1	ns	>0.9999
							20 min		
							Veh vs 0.01	ns	>0.9999
							Veh vs 0.1	ns	>0.9999
							Veh vs 1	ns	>0.9999
							0.01 vs 0.1	ns	>0.9999
							0.01 vs 1	ns	>0.9999
							0.1 vs 1	ns	>0.9999
							25 min		
							Veh vs 0.01	ns	>0.9999
							Veh vs 0.1	ns	>0.9999
							Veh vs 1	ns	>0.9999
							0.01 vs 0.1	ns	>0.9999
							0.01 vs 1	ns	>0.9999
							0.1 vs 1	ns	>0.9999
							30 min		
							Veh vs 0.01	ns	>0.9999
							Veh vs 0.1	ns	>0.9999
							Veh vs 1	ns	>0.9999
							0.01 vs 0.1	ns	>0.9999
							0.01 vs 1	ns	>0.9999
							0.1 vs 1	ns	>0.9999
							35 min		
							Veh vs 0.01	ns	>0.9999
							Veh vs 0.1	ns	>0.9999
							Veh vs 1	ns	>0.9999
							0.01 vs 0.1	ns	>0.9999
							0.01 vs 1	ns	>0.9999
							0.1 vs 1	ns	>0.9999
							40 min		
							Veh vs 0.01	ns	>0.9999
							Veh vs 0.1	ns	>0.9999
							Veh vs 1	ns	>0.9999
							0.01 vs 0.1	ns	>0.9999
							0.01 vs 1	ns	>0.9999
							0.1 vs 1	ns	>0.9999
							45 min		
							Veh vs 0.01	ns	>0.9999
							Veh vs 0.1	ns	>0.9999
							Veh vs 1	ns	>0.9999
							0.01 vs 0.1	ns	>0.9999
							0.01 vs 1	ns	>0.9999
							0.1 vs 1	ns	>0.9999
							50 min		
							Veh vs 0.01	ns	>0.9999
							Veh vs 0.1	ns	>0.9999
							Veh vs 1	ns	>0.9999
							0.01 vs 0.1	ns	>0.9999
							0.01 vs 1	ns	>0.9999
							0.1 vs 1	ns	>0.9999
							55 min		
							Veh vs 0.01	ns	>0.9999
							Veh vs 0.1	ns	>0.9999
							Veh vs 1	ns	>0.9999
							0.01 vs 0.1	ns	>0.9999
							0.01 vs 1	ns	>0.9999
							0.1 vs 1	ns	>0.9999
							60 min		
							Veh vs 0.01	ns	>0.9999
							Veh vs 0.1	ns	>0.9999
							Veh vs 1	ns	>0.9999
							0.01 vs 0.1	ns	>0.9999
							0.01 vs 1	ns	>0.9999
							0.1 vs 1	ns	>0.9999
7	F (FR3)	Repeated measures 2-Way ANOVA (Group x Time)	Veh = 4 0.01 = 4 0.1 = 5 1 = 5	Group x Time F(33, 154) = 0.96 Group F(3, 14) = 0.21 Time F(11, 154) = 17.49	P=0.53 p=0.89 P<0.001	Tuckey post hoc comparison	5 min		
							Veh vs 0.01	ns	>0.9999
							Veh vs 0.1	ns	>0.9999
							Veh vs 1	ns	>0.9999

							0.01 vs 0.1	ns	>0.9999
							0.01 vs 1	ns	>0.9999
							0.1 vs 1	ns	>0.9999
							10 min		
							Veh vs 0.01	ns	>0.9999
							Veh vs 0.1	ns	>0.9999
							Veh vs 1	ns	>0.9999
							0.01 vs 0.1	ns	>0.9999
							0.01 vs 1	ns	>0.9999
							0.1 vs 1	ns	>0.9999
							15 min		
							Veh vs 0.01	ns	>0.9999
							Veh vs 0.1	ns	>0.9999
							Veh vs 1	ns	>0.9999
							0.01 vs 0.1	ns	>0.9999
							0.01 vs 1	ns	>0.9999
							0.1 vs 1	ns	>0.9999
							20 min		
							Veh vs 0.01	ns	0.85
							Veh vs 0.1	ns	>0.9999
							Veh vs 1	ns	>0.9999
							0.01 vs 0.1	ns	>0.9999
							0.01 vs 1	ns	0.92
							0.1 vs 1	ns	>0.9999
							25 min		
							Veh vs 0.01	ns	>0.9999
							Veh vs 0.1	ns	>0.9999
							Veh vs 1	ns	>0.9999
							0.01 vs 0.1	ns	>0.9999
							0.01 vs 1	ns	>0.9999
							0.1 vs 1	ns	>0.9999
							30 min		
							Veh vs 0.01	ns	>0.9999
							Veh vs 0.1	ns	>0.9999
							Veh vs 1	ns	>0.9999
							0.01 vs 0.1	ns	>0.9999
							0.01 vs 1	ns	>0.9999
							0.1 vs 1	ns	>0.9999
							35 min		
							Veh vs 0.01	ns	>0.9999
							Veh vs 0.1	ns	>0.9999
							Veh vs 1	ns	>0.9999
							0.01 vs 0.1	ns	>0.9999
							0.01 vs 1	ns	>0.9999
							0.1 vs 1	ns	>0.9999
							40 min		
							Veh vs 0.01	ns	>0.9999
							Veh vs 0.1	ns	>0.9999
							Veh vs 1	ns	>0.9999
							0.01 vs 0.1	ns	>0.9999
							0.01 vs 1	ns	>0.9999
							0.1 vs 1	ns	>0.9999
							45 min		
							Veh vs 0.01	ns	>0.9999
							Veh vs 0.1	ns	>0.9999
							Veh vs 1	ns	>0.9999
							0.01 vs 0.1	ns	>0.9999
							0.01 vs 1	ns	>0.9999
							0.1 vs 1	ns	>0.9999
							50 min		
							Veh vs 0.01	ns	>0.9999
							Veh vs 0.1	ns	>0.9999
							Veh vs 1	ns	>0.9999
							0.01 vs 0.1	ns	>0.9999
							0.01 vs 1	ns	>0.9999
							0.1 vs 1	ns	>0.9999
							55 min		
							Veh vs 0.01	ns	>0.9999
							Veh vs 0.1	ns	>0.9999
							Veh vs 1	ns	>0.9999
							0.01 vs 0.1	ns	>0.9999
							0.01 vs 1	ns	>0.9999
							0.1 vs 1	ns	>0.9999
							60 min		
							Veh vs 0.01	ns	>0.9999
							Veh vs 0.1	ns	>0.9999
							Veh vs 1	ns	>0.9999
							0.01 vs 0.1	ns	>0.9999
							0.01 vs 1	ns	>0.9999
							0.1 vs 1	ns	>0.9999
7	G-H (Levers)	Repeated measures 3-Way ANOVA (Group x Session x Lever type)	UCM924 = 10 Morphine = 10	Group x Session x Lever type F(9, 162) = 0.97 Group x Session F(9, 162) = 3.19 Session x Lever type F(9, 162) = 4.54 Group x Lever type F(1, 18) = 41.98 Session F(9, 162) = 1.53 Lever type F(1, 18) = 60.01 Group F(1, 18) = 56.92	P=0.47 P<0.01 P<0.001 P<0.001 P=0.14 P<0.001 P<0.001	Tuckey post hoc comparison	Active vs Inactive Lever: UCM924	ns	0.81
							Active vs Inactive Lever: Morphine	***	0.0001
							Morphine vs UCM924: Active Lever	***	0.001
							Morphine vs UCM924: Inactive Lever	ns	0.77
							Session 1: Morphine vs UCM924 - Total lever presses	ns	0.91
							Session 2: Morphine vs UCM924 - Total lever presses	ns	0.17
							Session 3: Morphine vs UCM924 - Total lever presses	ns	0.06
							Session 4: Morphine vs UCM924 - Total lever presses	ns	0.06
							Session 5: Morphine vs UCM924 - Total lever presses	**	0.002
							Session 6: Morphine vs UCM924 - Total lever presses	*	0.011
							Session 7: Morphine vs UCM924 - Total lever presses	***	0.0003
							Session 8: Morphine vs UCM924 - Total lever presses	***	0.002
							Session 9: Morphine vs UCM924 - Total lever presses	***	0.0002
							Session 10: Morphine vs UCM924 - Total lever presses	***	0.0002
7	G-H (injections)	Repeated measures 2-way ANOVA (Group x Session x Lever type)	UCM924 = 10 Morphine = 10	Group x Session F(9, 162) = 3.82 Group F(1, 18) = 88.46 Session F(9, 162) = 2.94	P<0.001 P<0.001 P<0.01	Tuckey post hoc comparison	Morphine vs UCM924 injections intake per session		
							session 1	ns	0.06
							session 2	**	0.004
							session 3	***	0.0002
							session 4	***	0.0002
							session 5	***	0.0002

							session 6	***	0.0002
							session 7	***	0.0002
							session 8	***	0.0002
							session 9	***	0.0002
							session 10	***	0.0002
							Morphine vs UCM924: Total injection intake	***	0.0001
7	I	Repeated measures 2-Way ANOVA (Group x Time)	UCM924 = 10 Morphine = 10	Group x Time F(23, 414) = 1.29 Group F(1, 18) = 8,82 Time F(23, 414) = 8,45	P=0.17 p=0.008 P<0.001	Tuckey post hoc comparison	Locomotion on session 1 Morphine vs UCM924	 **	 0.008
7	J	Repeated measures 2-Way ANOVA (Group x Time)	UCM924 = 10 Morphine = 10	Group x Time F(23, 414) = 1.97 Group F(1, 18) = 29.76 Time F(23, 414) = 3.32	P=0.005 p=0.00004 P=000001	Tuckey post hoc comparison	Locomotion on session 5 all time Morphine vs UCM924 Morphine vs UCM924 5 min 10 min 15 min 20 min 25 min 30 min 35 min 40 min 45 min 50 min 55 min 60 min 65 min 70 min 75 min 80 min 85 min 90 min 95 min 100 min 105 min 110 min 115 min 120 min	 ** ns ns ns ns * ns * ** * ns ns ns ns ns * ns ns ns * * ns ns	 0.008 >0.9999 >0.9999 0.81 0.12 0.016 0.46 0.04 0.004 0.010 0.14 0.07 0.49 0.21 0.21 0.55 0.04 0.39 0.08 0.10 0.052 0.018 0.014 0.0503 0.0503
7	K	Repeated measures 2-Way ANOVA (Group x Time)	UCM924 = 10 Morphine = 10	Group x Time F(23, 414) = 4.60 Group F(1, 18) = 32.27 Time F(23, 414) = 4,38	P=0.00001 p=0.00002 p=0.00005 p=00001	Tuckey post hoc comparison	Locomotion on session 10 all time Morphine vs UCM924 Morphine vs UCM924 5 min 10 min 15 min 20 min 25 min 30 min 35 min 40 min 45 min 50 min 55 min 60 min 65 min 70 min 75 min 80 min 85 min 90 min 95 min 100 min 105 min 110 min 115 min 120 min	 *** ns ns ns ns ns ns * ** * ns ns ns ns ns * ns ns ns * * ns ns	 0.0002 >0.9999 >0.9999 >0.9999 >0.9999 >0.9999 0.19 0.19 0.53 0.22 0.005 0.14 0.04 0.21 0.008 0.009 0.06 0.049 0.024 0.0009 0.018 0.0003 0.016 0.031 0.0012
7	L	Two-tailed unpaired t-test	UCM924 = 10 Morphine = 10	t(18) = 3.46	P=0.0028		Breaking Point Morphine vs UCM924	 **	 0.003
7	L	Two-tailed unpaired t-test	UCM924 = 10 Morphine = 10	t(18) = 6.88	P=0.000002		Number of injections Morphine vs UCM924	 ***	 0.000002
7	M-N	Repeated measures 2-Way ANOVA (Group x Lever)	UCM924 = 10 Morphine = 10	Group x Lever F(1, 18) = 7.69 Group F(1, 18) = 9,03 Lever F(1, 18) = 7.29	P=0.012 p=0.008 p=0.015	Tuckey post hoc comparison	Active vs Inactive Lever: UCM924 Active vs Inactive Lever: Morphine Morphine vs UCM924: Active Lever Morphine vs UCM924: Inactive Lever	ns ** ** ns	>0.9999 0.006 0.0013 0.993

Figure	Panel	Test	Group-size	Statistic	P value	Pair-wise comparison	Statistic 2		
							Test details	Summary	Adjusted P Value
S1	S1	1-way ANOVA	Veh = 6 UCM924 = 8 Nalox+UCM924 = 5 CTOP+UCM924 = 6 Nalt+UCM924 = 11	F (4, 31) = 7.904	P=0.0002	Tuckey post hoc comparison	Veh vs. UCM924 10ug	**	0.001
							Veh vs. Nalo + UCM924	ns	0.9992
							Veh vs. CTOP + UCM924	ns	0.9906
							Veh vs. Nalt + UCM924	ns	0.1289
							UCM924 10ug vs. Nalo + UCM924	***	0.0009
							UCM924 10ug vs. CTOP + UCM924	**	0.0038
							UCM924 10ug vs. Nalt + UCM924	ns	0.1285
							Nalo + UCM924 vs. CTOP + UCM924	ns	0.9595
							Nalo + UCM924 vs. Nalt + UCM924	ns	0.0994
							CTOP + UCM924 vs. Nalt + UCM924	ns	0.3233
S2	A	2-Way Mixed ANOVA (treatment x time)	WT Veh= 8 WT UCM924 = 8	Time x treatment : F (7, 98) = 48.06 Time : F (3.699, 51.79) = 56.90 Treatment : F (1, 14) = 127.0	P<0.0001 P<0.0001 P<0.0001	Tuckey post hoc comparison	Test details	Summary	Adjusted P Value
							WT Veh - WT UCM924 20mg/kg		
							0	ns	>0.9999
							1	**	0.0031
							2	***	0.0002
							3	****	<0.0001
							4	****	<0.0001
							5	****	<0.0001
							6	ns	>0.9999
							7	ns	>0.9999
S2	B	2-Way Mixed ANOVA (treatment x time)	DOR-/- Veh = 7 DOR-/- UCM924 = 7	Time x treatment : F (7, 84) = 44.75 Time : F (7, 84) = 42.63 Treatment : F (1, 12) = 1240	P<0.0001 P<0.0001 P<0.0001	Tuckey post hoc comparison	Test details	Summary	Adjusted P Value
							DOR-/- Veh - DOR-/- UCM924 20mg/kg		
							0	ns	>0.9999
							1	***	0.001
							2	****	<0.0001
							3	****	<0.0001
							4	****	<0.0001
							5	****	<0.0001
							6	*	0.0226
							7	ns	>0.9999
S2	C	2-Way Mixed ANOVA (treatment x time)	MOR-/- Veh = 9 MOR-/- UCM924 = 9	Time x treatment : F (7, 112) = 2.074 Time : F (4.685, 74.95) = 2.371 Treatment : F (1, 16) = 1.362	P=0.0520 P=0.0508 P=0.2602	Tuckey post hoc comparison	Test details	Summary	Adjusted P Value
							$MOR^{-/-}$Veh - $MOR^{-/-}$ UCM924 20mg/kg		
							0	ns	>0.9999
							1	ns	>0.9999
							2	ns	0.0809
							3	ns	>0.9999
							4	ns	0.5251
							5	ns	>0.9999
							6	ns	>0.9999
							7	ns	>0.9999
S2	D	2-way ANOVA (treatment x genotype)	WT Veh = 8 WT UCM924 = 8 DOR-/- Veh = 7 DOR-/- UCM924 = 7 MOR-/- Veh = 9 MOR-/- UCM924 = 9	treatment x genotype: F (2, 42) = 86.39 treatment: F (1, 42) = 410.3 genotype: F (2, 42) = 93.57	P<0.0001 P<0.0001 P<0.0001	Tuckey post hoc comparison	Test details	Summary	Adjusted P Value
							veh:wt vs. veh:MOR-ko	ns	0.4306
							veh:wt vs. veh:DOR-ko	*	0.027
							veh:wt vs. UCM924:wt	****	<0.0001
							veh:wt vs. UCM924:MOR-ko	ns	0.9968
							veh:wt vs. UCM924:DOR-ko	****	<0.0001
							veh:MOR-ko vs. veh:DOR-ko	ns	0.6594
							veh:MOR-ko vs. UCM924:wt	****	<0.0001
							veh:MOR-ko vs. UCM924:MOR-ko	ns	0.7006
							veh:MOR-ko vs. UCM924:DOR-ko	****	<0.0001
							veh:DOR-ko vs. UCM924:wt	****	<0.0001
							veh:DOR-ko vs. UCM924:MOR-ko	ns	0.067
							veh:DOR-ko vs. UCM924:DOR-ko	****	<0.0001
							UCM924:wt vs. UCM924:MOR-ko	****	<0.0001
							UCM924:wt vs. UCM924:DOR-ko	ns	0.9981
							UCM924:MOR-ko vs. UCM924:DOR-ko	****	<0.0001
S3	A	2-Way Mixed ANOVA (treatment x time)	Veh = 3 UCM924 = 4 Nalox = 2 Nalox+UCM924 = 4	Time x treatment : F (12, 36) = 13.41 Time : F (2.618, 23.56) = 19.65 Treatment : F (3, 9) = 24.11	P<0.0001 P<0.0001 P=0.0001	Tuckey post hoc comparison	Test details	Summary	Adjusted P Value
							0		
							VEH vs. Nalo	ns	0.9995
							VEH vs. UCM924	ns	0.9985
							VEH vs. Nalo+UCM924	ns	0.6243
							Nalo vs. UCM924	ns	0.9924
							Nalo vs. Nalo+UCM924	ns	0.5571
							UCM924 vs. Nalo+UCM924	ns	0.6002
							15		
							VEH vs. Nalo	ns	0.9262
							VEH vs. UCM924	**	0.0088
							VEH vs. Nalo+UCM924	ns	0.9748
							Nalo vs. UCM924	*	0.0322
							Nalo vs. Nalo+UCM924	ns	0.8763
							UCM924 vs. Nalo+UCM924	ns	0.0553
							30		
							VEH vs. Nalo	ns	0.3853
							VEH vs. UCM924	***	0.0006
							VEH vs. Nalo+UCM924	ns	0.499
							Nalo vs. UCM924	**	0.0014
							Nalo vs. Nalo+UCM924	ns	0.9278
							UCM924 vs. Nalo+UCM924	*	0.0102
							45		
							VEH vs. Nalo	ns	0.3085
							VEH vs. UCM924	****	<0.0001
							VEH vs. Nalo+UCM924	ns	0.7943
							Nalo vs. UCM924	***	0.0003
							Nalo vs. Nalo+UCM924	ns	0.9981
							UCM924 vs. Nalo+UCM924	*	0.016
							60		
							VEH vs. Nalo	ns	0.8043
							VEH vs. UCM924	***	0.0006
							VEH vs. Nalo+UCM924	ns	0.9097
							Nalo vs. UCM924	***	0.0004
							Nalo vs. Nalo+UCM924	ns	0.9943
							UCM924 vs. Nalo+UCM924	**	0.0079
S3	B	2-Way Mixed ANOVA (treatment x time)	Veh = 4 UCM924 = 3 Nalox = 3	Time x treatment : F (12, 45) = 2.835 Time : F (4, 45) = 3.702 Treatment : F (3, 45) = 47.54	P=0.0056 P=0.0109 P<0.0001	Tuckey post hoc comparison	Test details	Summary	Adjusted P Value
							0		
							VEH vs. Nalo	ns	0.6834

			Nalox+UCM924 = 3				VEH vs. UCM924	ns	0.7488
							VEH vs. Nalo+UCM924	ns	0.9191
							Nalo vs. UCM924	ns	0.9996
							Nalo vs. Nalo+UCM924	ns	0.9704
							UCM924 vs. Nalo+UCM924	ns	0.9862
							15		
							VEH vs. Nalo	ns	0.3285
							VEH vs. UCM924	****	<0.0001
							VEH vs. Nalo+UCM924	ns	0.4838
							Nalo vs. UCM924	*	0.0115
							Nalo vs. Nalo+UCM924	*	0.0252
							UCM924 vs. Nalo+UCM924	****	<0.0001
							30		
							VEH vs. Nalo	ns	0.977
							VEH vs. UCM924	****	<0.0001
							VEH vs. Nalo+UCM924	ns	0.9711
							Nalo vs. UCM924	***	0.0004
							Nalo vs. Nalo+UCM924	ns	0.8575
							UCM924 vs. Nalo+UCM924	****	<0.0001
							45		
							VEH vs. Nalo	ns	0.2248
							VEH vs. UCM924	****	<0.0001
							VEH vs. Nalo+UCM924	ns	0.7793
							Nalo vs. UCM924	***	0.0004
							Nalo vs. Nalo+UCM924	ns	0.7882
							UCM924 vs. Nalo+UCM924	****	<0.0001
							60		
							VEH vs. Nalo	ns	0.2027
							VEH vs. UCM924	****	<0.0001
							VEH vs. Nalo+UCM924	ns	0.5473
							Nalo vs. UCM924	***	0.0005
							Nalo vs. Nalo+UCM924	ns	0.9234
							UCM924 vs. Nalo+UCM924	****	<0.0001
S3	C	2-Way Mixed ANOVA (treatment x time)	Veh = 3 UCM924 = 4 CTOP = 3 CTOP+UCM924 = 3	Time x treatment : F (12, 45) = 51.30 Time : F (4, 45) = 50.07 Treatment : F (3, 45) = 633.7	P<0.0001 P<0.0001 P<0.0001	Tuckey post hoc comparison	Test details	Summary	Adjusted P Value
							0		
							VEH vs. CTOP	ns	0.8205
							VEH vs. UCM924	ns	0.4627
							VEH vs. CTOP+UCM924	ns	0.9704
							CTOP vs. UCM924	ns	0.9482
							CTOP vs. CTOP+UCM924	ns	0.9738
							UCM924 vs. CTOP+UCM924	ns	0.7519
							15		
							VEH vs. CTOP	ns	>0.9999
							VEH vs. UCM924	****	<0.0001
							VEH vs. CTOP+UCM924	ns	0.2468
							CTOP vs. UCM924	****	<0.0001
							CTOP vs. CTOP+UCM924	ns	0.2383
							UCM924 vs. CTOP+UCM924	****	<0.0001
							30		
							VEH vs. CTOP	ns	0.0952
							VEH vs. UCM924	****	<0.0001
							VEH vs. CTOP+UCM924	ns	0.1461
							CTOP vs. UCM924	****	<0.0001
							CTOP vs. CTOP+UCM924	ns	0.9968
							UCM924 vs. CTOP+UCM924	****	<0.0001
							45		
							VEH vs. CTOP	ns	0.9939
							VEH vs. UCM924	****	<0.0001
							VEH vs. CTOP+UCM924	ns	0.8176
							CTOP vs. UCM924	****	<0.0001
							CTOP vs. CTOP+UCM924	ns	0.9262
							UCM924 vs. CTOP+UCM924	****	<0.0001
							60		
							VEH vs. CTOP	ns	0.8458
							VEH vs. UCM924	****	<0.0001
							VEH vs. CTOP+UCM924	**	0.0013
							CTOP vs. UCM924	****	<0.0001
							CTOP vs. CTOP+UCM924	****	<0.0001
							UCM924 vs. CTOP+UCM924	****	<0.0001
S3	D	2-Way Mixed ANOVA (treatment x time)	Veh = 4 UCM924 = 3 CTOP = 3 CTOP+UCM924 = 3	Time x treatment : F (12, 50) = 8.463 Time : F (4, 50) = 9.135 Treatment : F (3, 50) = 109.4	P<0.0001 P<0.0001 P<0.0001	Tuckey post hoc comparison	Test details	Summary	Adjusted P Value
							0		
							Veh vs. CTOP 1ug	ns	0.5945
							Veh vs. UCM924 10 ug	ns	0.9739
							Veh vs. CTOP+UCM924	ns	0.1099
							CTOP 1ug vs. UCM924 10 ug	ns	0.824
							CTOP 1ug vs. CTOP+UCM924	ns	0.7594
							UCM924 10 ug vs. CTOP+UCM924	ns	0.2352
							15		
							Veh vs. CTOP 1ug	**	0.0044
							Veh vs. UCM924 10 ug	****	<0.0001
							Veh vs. CTOP+UCM924	ns	0.0793
							CTOP 1ug vs. UCM924 10 ug	****	<0.0001
							CTOP 1ug vs. CTOP+UCM924	ns	0.7325
							UCM924 10 ug vs. CTOP+UCM924	****	<0.0001
							30		
							Veh vs. CTOP 1ug	ns	0.6538
							Veh vs. UCM924 10 ug	****	<0.0001
							Veh vs. CTOP+UCM924	ns	0.0727
							CTOP 1ug vs. UCM924 10 ug	****	<0.0001
							CTOP 1ug vs. CTOP+UCM924	ns	0.5989
							UCM924 10 ug vs. CTOP+UCM924	****	<0.0001

							45		
							Veh vs. CTOP 1ug	ns	0.7981
							Veh vs. UCM924 10 ug	****	<0.0001
							Veh vs. CTOP+UCM924	ns	0.1676
							CTOP 1ug vs. UCM924 10 ug	****	<0.0001
							CTOP 1ug vs. CTOP+UCM924	ns	0.6855
							UCM924 10 ug vs. CTOP+UCM924	****	<0.0001
							60		
							Veh vs. CTOP 1ug	ns	0.1726
							Veh vs. UCM924 10 ug	****	<0.0001
							Veh vs. CTOP+UCM924	ns	0.1478
							CTOP 1ug vs. UCM924 10 ug	****	<0.0001
							CTOP 1ug vs. CTOP+UCM924	ns	0.9999
							UCM924 10 ug vs. CTOP+UCM924	****	<0.0001
S3	E	2-Way Mixed ANOVA (treatment x time)	Veh = 3 UCM924 = 4 Nalt = 3 Nalt+UCM924 = 3	Time x treatment : F (12, 45) = 36.29 Time : F (4, 45) = 102.8 Treatment : F (3, 45) = 524.5	P<0.0001 P<0.0001 P<0.0001	Tuckey post hoc comparison	Test details	Summary	Adjusted P Value
							0		
							Veh vs. Nalt 1ug	ns	0.475
							Veh vs. UCM924	ns	0.6194
							Veh vs. Nalt+UCM924	ns	0.9395
							Nalt 1ug vs. UCM924	ns	0.987
							Nalt 1ug vs. Nalt+UCM924	ns	0.1943
							UCM924 vs. Nalt+UCM924	ns	0.2729
							15		
							Veh vs. Nalt 1ug	ns	0.9903
							Veh vs. UCM924	****	<0.0001
							Veh vs. Nalt+UCM924	****	<0.0001
							Nalt 1ug vs. UCM924	****	<0.0001
							Nalt 1ug vs. Nalt+UCM924	****	<0.0001
							UCM924 vs. Nalt+UCM924	ns	0.123
							30		
							Veh vs. Nalt 1ug	ns	0.9742
							Veh vs. UCM924	****	<0.0001
							Veh vs. Nalt+UCM924	****	<0.0001
							Nalt 1ug vs. UCM924	****	<0.0001
							Nalt 1ug vs. Nalt+UCM924	****	<0.0001
							UCM924 vs. Nalt+UCM924	ns	0.1234
							45		
							Veh vs. Nalt 1ug	ns	0.1896
							Veh vs. UCM924	****	<0.0001
							Veh vs. Nalt+UCM924	****	<0.0001
							Nalt 1ug vs. UCM924	****	<0.0001
							Nalt 1ug vs. Nalt+UCM924	****	<0.0001
							UCM924 vs. Nalt+UCM924	ns	0.4402
							60		
							Veh vs. Nalt 1ug	ns	0.6569
							Veh vs. UCM924	****	<0.0001
							Veh vs. Nalt+UCM924	****	<0.0001
							Nalt 1ug vs. UCM924	****	<0.0001
							Nalt 1ug vs. Nalt+UCM924	****	<0.0001
							UCM924 vs. Nalt+UCM924	ns	0.9439
S3	F	2-Way Mixed ANOVA (treatment x time)	Veh = 4 UCM924 = 3 Nalt = 3 Nalt+UCM924 = 3	Time x treatment : F (12, 45) = 15.19 Time : F (4, 45) = 43.90 Treatment : F (3, 45) = 263.3	P<0.0001 P<0.0001 P<0.0001	Tuckey post hoc comparison	Test details	Summary	Adjusted P Value
							0		
							Veh vs. Nalt 1ug	ns	0.1029
							Veh vs. UCM924	ns	0.1845
							Veh vs. Nalt+UCM924	ns	0.5661
							Nalt 1ug vs. UCM924	ns	0.9927
							Nalt 1ug vs. Nalt+UCM924	ns	0.7639
							UCM924 vs. Nalt+UCM924	ns	0.896
							15		
							Veh vs. Nalt 1ug	ns	0.3906
							Veh vs. UCM924	****	<0.0001
							Veh vs. Nalt+UCM924	****	<0.0001
							Nalt 1ug vs. UCM924	****	<0.0001
							Nalt 1ug vs. Nalt+UCM924	****	<0.0001
							UCM924 vs. Nalt+UCM924	ns	0.8466
							30		
							Veh vs. Nalt 1ug	ns	0.6825
							Veh vs. UCM924	****	<0.0001
							Veh vs. Nalt+UCM924	****	<0.0001
							Nalt 1ug vs. UCM924	****	<0.0001
							Nalt 1ug vs. Nalt+UCM924	****	<0.0001
							UCM924 vs. Nalt+UCM924	ns	0.9422
							45		
							Veh vs. Nalt 1ug	ns	0.1765
							Veh vs. UCM924	****	<0.0001
							Veh vs. Nalt+UCM924	****	<0.0001
							Nalt 1ug vs. UCM924	****	<0.0001
							Nalt 1ug vs. Nalt+UCM924	****	<0.0001
							UCM924 vs. Nalt+UCM924	ns	0.7081
							60		
							Veh vs. Nalt 1ug	ns	0.531
							Veh vs. UCM924	****	<0.0001
							Veh vs. Nalt+UCM924	****	<0.0001
							Nalt 1ug vs. UCM924	****	<0.0001
							Nalt 1ug vs. Nalt+UCM924	****	<0.0001
							UCM924 vs. Nalt+UCM924	ns	0.9758
S4	A	2-Way Mixed ANOVA (treatment x time)	Veh = 3 UCM924 = 4 TQ = 3 TQ+UCM924 = 4	Time x treatment : F (12, 50) = 26.29 Time : F (4, 50) = 24.42 Treatment : F (3, 50) = 330.6	<0.0001 <0.0001 <0.0001	Tuckey post hoc comparison	Test details	Summary	Adjusted P Value
							0		
							Veh vs. TQ 1 uM	ns	0.9926
							Veh vs. UCM924 10ug	ns	0.7286
							Veh vs. TQ+UCM924	ns	0.7439

							TQ 1 uM vs. UCM924 10ug	ns	0.8791
							TQ+UCM924 vs. TQ 1 uM	ns	0.89
							TQ+UCM924 vs. UCM924 10ug	ns	>0.9999
							15		
							Veh vs. TQ 1 uM	ns	0.2265
							Veh vs. UCM924 10ug	****	<0.0001
							Veh vs. TQ+UCM924	ns	0.9829
							TQ 1 uM vs. UCM924 10ug	****	<0.0001
							TQ+UCM924 vs. TQ 1 uM	ns	0.0833
							TQ+UCM924 vs. UCM924 10ug	****	<0.0001
							30		
							Veh vs. TQ 1 uM	ns	0.4724
							Veh vs. UCM924 10ug	****	<0.0001
							Veh vs. TQ+UCM924	ns	0.4194
							TQ 1 uM vs. UCM924 10ug	****	<0.0001
							TQ+UCM924 vs. TQ 1 uM	ns	>0.9999
							TQ+UCM924 vs. UCM924 10ug	****	<0.0001
							45		
							Veh vs. TQ 1 uM	ns	0.5281
							Veh vs. UCM924 10ug	****	<0.0001
							Veh vs. TQ+UCM924	ns	0.9266
							TQ 1 uM vs. UCM924 10ug	****	<0.0001
							TQ+UCM924 vs. TQ 1 uM	ns	0.1761
							TQ+UCM924 vs. UCM924 10ug	****	<0.0001
							60		
							Veh vs. TQ 1 uM	ns	>0.9999
							Veh vs. UCM924 10ug	****	<0.0001
							Veh vs. TQ+UCM924	ns	0.9023
							TQ 1 uM vs. UCM924 10ug	****	<0.0001
							TQ+UCM924 vs. TQ 1 uM	ns	0.918
							TQ+UCM924 vs. UCM924 10ug	****	<0.0001
S4	B	2-Way Mixed ANOVA (treatment x time)	Veh = 3 UCM924 = 4 TQ = 3 TQ+UCM924 = 4	Time x treatment : F (12, 50) = 9.808 Time : F (4, 50) = 10.33 Treatment : F (3, 50) = 178.3	P<0.0001 P<0.0001 P=0.0002	Tuckey post hoc comparison	Test details	Summary	Adjusted P Value
							0		
							Veh vs. TQ 1 uM	ns	0.2559
							Veh vs. UCM924 10ug	ns	0.2468
							Veh vs. TQ+UCM924	ns	0.8097
							TQ 1 uM vs. UCM924 10ug	ns	>0.9999
							TQ+UCM924 vs. TQ 1 uM	ns	0.7265
							TQ+UCM924 vs. UCM924 10ug	ns	0.714
							15		
							Veh vs. TQ 1 uM	ns	0.9685
							Veh vs. UCM924 10ug	****	<0.0001
							Veh vs. TQ+UCM924	ns	0.9838
							TQ 1 uM vs. UCM924 10ug	****	<0.0001
							TQ+UCM924 vs. TQ 1 uM	ns	0.8596
							TQ+UCM924 vs. UCM924 10ug	****	<0.0001
							30		
							Veh vs. TQ 1 uM	ns	0.7985
							Veh vs. UCM924 10ug	****	<0.0001
							Veh vs. TQ+UCM924	ns	0.4262
							TQ 1 uM vs. UCM924 10ug	****	<0.0001
							TQ+UCM924 vs. TQ 1 uM	ns	0.9571
							TQ+UCM924 vs. UCM924 10ug	****	<0.0001
							45		
							Veh vs. TQ 1 uM	ns	0.1686
							Veh vs. UCM924 10ug	****	<0.0001
							Veh vs. TQ+UCM924	ns	0.7036
							TQ 1 uM vs. UCM924 10ug	****	<0.0001
							TQ+UCM924 vs. TQ 1 uM	ns	0.6935
							TQ+UCM924 vs. UCM924 10ug	****	<0.0001
							60		
							Veh vs. TQ 1 uM	ns	0.2063
							Veh vs. UCM924 10ug	****	<0.0001
							Veh vs. TQ+UCM924	ns	0.1139
							TQ 1 uM vs. UCM924 10ug	****	<0.0001
							TQ+UCM924 vs. TQ 1 uM	ns	0.9992
							TQ+UCM924 vs. UCM924 10ug	****	<0.0001
S4	C	2-Way Mixed ANOVA (treatment x time)	Veh = 3 morph = 3 TQ = 3 TQ+morph = 4	Time x treatment : F (12, 45) = 37.06 Time : F (4, 45) = 93.43 Treatment : F (3, 45) = 425.8	P<0.0001 P<0.0001 P<0.0001	Tuckey post hoc comparison	Test details	Summary	Adjusted P Value
							0		
							Veh vs. TQ 1 uM	ns	0.9893
							Veh vs. morph 5ug	ns	0.6911
							Veh vs. TQ+morph	ns	0.5839
							TQ 1 vs. morph 5u	ns	0.8593
							TQ vs. TQ+ morph 5u	ns	0.7832
							TQ+ morph vs. morph	ns	0.9997
							15		
							Veh vs. TQ 1 uM	ns	0.14
							Veh vs. morph 5ug	****	<0.0001
							Veh vs. TQ+morph	****	<0.0001
							TQ 1 vs. morph 5u	****	<0.0001
							TQ vs. TQ+ morph 5u	****	<0.0001
							TQ+ morph vs. morph	ns	0.7164
							30		
							Veh vs. TQ 1 uM	ns	0.362
							Veh vs. morph 5ug	****	<0.0001
							Veh vs. TQ+morph	****	<0.0001
							TQ 1 vs. morph 5u	****	<0.0001
							TQ vs. TQ+ morph 5u	****	<0.0001
							TQ+ morph vs. morph	*	0.0238
							45		

							Veh vs. TQ 1 uM	ns	0.4193
							Veh vs. morph 5ug	****	<0.0001
							Veh vs. TQ+morph	****	<0.0001
							TQ 1 vs. morph 5u	****	<0.0001
							TQ vs. TQ+ morph 5u	****	<0.0001
							TQ+ morph vs. morph	ns	0.4331
							60		
							Veh vs. TQ 1 uM	ns	>0.9999
							Veh vs. morph 5ug	****	<0.0001
							Veh vs. TQ+morph	****	<0.0001
							TQ 1 vs. morph 5u	****	<0.0001
							TQ vs. TQ+ morph 5u	****	<0.0001
							TQ+ morph vs. morph	ns	0.4035
S4	D	2-Way Mixed ANOVA (treatment x time)	Veh = 3 morph = 2 TQ = 3 TQ+morph = 2	Time x treatment : F (12, 35) = 22.40 Time : F (4, 35) = 59.12 Treatment : F (3, 35) = 415.0	P<0.0001 P<0.0001 P<0.0001	Tuckey post hoc comparison	Test details	Summary	Adjusted P Value
							0		
							Veh vs. TQ 1 uM	ns	0.3009
							Veh vs. morph 5ug	ns	0.3345
							Veh vs. TQ+morph	ns	0.3661
							TQ 1 vs. morph 5u	ns	0.994
							TQ vs. TQ+ morph 5u	ns	0.9995
							TQ+ morph vs. morph	ns	0.9991
							15		
							Veh vs. TQ 1 uM	ns	0.9724
							Veh vs. morph 5ug	****	<0.0001
							Veh vs. TQ+morph	****	<0.0001
							TQ 1 vs. morph 5u	****	<0.0001
							TQ vs. TQ+ morph 5u	****	<0.0001
							TQ+ morph vs. morph	ns	0.9912
							30		
							Veh vs. TQ 1 uM	ns	0.8207
							Veh vs. morph 5ug	****	<0.0001
							Veh vs. TQ+morph	****	<0.0001
							TQ 1 vs. morph 5u	****	<0.0001
							TQ vs. TQ+ morph 5u	****	<0.0001
							TQ+ morph vs. morph	ns	0.8825
							45		
							Veh vs. TQ 1 uM	ns	0.2086
							Veh vs. morph 5ug	****	<0.0001
							Veh vs. TQ+morph	****	<0.0001
							TQ 1 vs. morph 5u	****	<0.0001
							TQ vs. TQ+ morph 5u	****	<0.0001
							TQ+ morph vs. morph	ns	>0.9999
							60		
							Veh vs. TQ 1 uM	ns	0.2489
							Veh vs. morph 5ug	****	<0.0001
							Veh vs. TQ+morph	****	<0.0001
							TQ 1 vs. morph 5u	****	<0.0001
							TQ vs. TQ+ morph 5u	****	<0.0001
							TQ+ morph vs. morph	ns	0.9949
S5	A	2-Way Mixed ANOVA (treatment x time)	D9-UCM924+Veh = 3 D9-UCM924+Morph = 4 D9-UCM924+UCM924 = 3	Time x treatment : F (8, 35) = 4.569 Time : F (4, 35) = 8.444 Treatment : F (2, 35) = 42.32	P=0.0007 P<0.0001 P<0.0001	Tuckey post hoc comparison	Test details	Summary	Adjusted P Value
							0		
							D9-UCM924+Veh vs. D9-UCM924+Morph	ns	0.9774
							D9-UCM924+Veh vs. D9-UCM924+UCM924	ns	0.9158
							D9-UCM924+Morph vs. D9-UCM924+UCM924	ns	0.8042
							15		
							D9-UCM924+Veh vs. D9-UCM924+Morph	**	0.0048
							D9-UCM924+Veh vs. D9-UCM924+UCM924	ns	0.6722
							D9-UCM924+Morph vs. D9-UCM924+UCM924	*	0.0464
							30		
							D9-UCM924+Veh vs. D9-UCM924+Morph	****	<0.0001
							D9-UCM924+Veh vs. D9-UCM924+UCM924	ns	0.4852
							D9-UCM924+Morph vs. D9-UCM924+UCM924	**	0.0027
							45		
							D9-UCM924+Veh vs. D9-UCM924+Morph	****	<0.0001
							D9-UCM924+Veh vs. D9-UCM924+UCM924	ns	0.7394
							D9-UCM924+Morph vs. D9-UCM924+UCM924	***	0.0009
							60		
							D9-UCM924+Veh vs. D9-UCM924+Morph	****	<0.0001
							D9-UCM924+Veh vs. D9-UCM924+UCM924	ns	0.5756
							D9-UCM924+Morph vs. D9-UCM924+UCM924	****	<0.0001
S5	B	2-Way Mixed ANOVA (treatment x time)	D9-UCM924+Veh = 3 D9-UCM924+Morph = 4 D9-UCM924+UCM924 = 3	Time x treatment : F (8, 35) = 3.018 Time : F (4, 35) = 2.800 Treatment : F (2, 35) = 60.48	P=0.0110 P=0.0407 P<0.0001	Tuckey post hoc comparison	Test details	Summary	Adjusted P Value
							0		
							D9-UCM924+Morph vs. D9-UCM924+Veh	ns	>0.9999
							D9-UCM924+UCM924 vs. D9-UCM924+Veh	ns	>0.9999
							D9-UCM924+UCM924 vs. D9-UCM924+Morph	ns	0.9994
							15		
							D9-UCM924+Morph vs. D9-UCM924+Veh	**	0.0012
							D9-UCM924+UCM924 vs. D9-UCM924+Veh	ns	>0.9999
							D9-UCM924+UCM924 vs. D9-UCM924+Morph	*	0.0101
							30		
							D9-UCM924+Morph vs. D9-UCM924+Veh	**	0.0075
							D9-UCM924+UCM924 vs. D9-UCM924+Veh	ns	0.9998
							D9-UCM924+UCM924 vs. D9-UCM924+Morph	***	0.0005
							45		
							D9-UCM924+Morph vs. D9-UCM924+Veh	****	<0.0001
							D9-UCM924+UCM924 vs. D9-UCM924+Veh	ns	0.9557
							D9-UCM924+UCM924 vs. D9-UCM924+Morph	**	0.0061
							60		

							D9-UCM924+Morph vs. D9-UCM924+Veh	***	0.0005
							D9-UCM924+UCM924 vs. D9-UCM924+Veh	ns	>0.9999
							D9-UCM924+UCM924 vs. D9-UCM924+Morph	**	0.0011
S5	C	2-Way Mixed ANOVA (treatment x time)	D9-Morph+Veh = 3 D9-Morph+Morph = 3 D9-Morph+UCM924 = 4	Time x treatment : F (8, 35) = 0.3567 Time : F (4, 35) = 3.948 Treatment : F (2, 35) = 6.555	P=0.9361 P=0.0095 P=0.0038	Tuckey post hoc comparison	Test details	Summary	Adjusted P Value
							0		
							D9-Morph+UCM924 vs. D9-Morph+Veh	ns	>0.9999
							D9-Morph+Morph vs. D9-Morph+Veh	ns	>0.9999
							D9-Morph+Morph vs. D9-Morph+UCM924	ns	>0.9999
							15		
							D9-Morph+UCM924 vs. D9-Morph+Veh	ns	>0.9999
							D9-Morph+Morph vs. D9-Morph+Veh	ns	0.9188
							D9-Morph+Morph vs. D9-Morph+UCM924	ns	0.928
							30		
							D9-Morph+UCM924 vs. D9-Morph+Veh	ns	0.9996
							D9-Morph+Morph vs. D9-Morph+Veh	ns	>0.9999
							D9-Morph+Morph vs. D9-Morph+UCM924	ns	0.8847
							45		
							D9-Morph+UCM924 vs. D9-Morph+Veh	ns	>0.9999
							D9-Morph+Morph vs. D9-Morph+Veh	ns	0.9878
							D9-Morph+Morph vs. D9-Morph+UCM924	ns	0.8681
							60		
							D9-Morph+UCM924 vs. D9-Morph+Veh	ns	0.9412
							D9-Morph+Morph vs. D9-Morph+Veh	ns	>0.9999
							D9-Morph+Morph vs. D9-Morph+UCM924	ns	0.7513
S5	D	2-Way Mixed ANOVA (treatment x time)	D9-Morph+Veh = 3 D9-Morph+Morph = 4 D9-Veh + UCM924 = 4	Time x treatment : F (8, 40) = 1.923 Time : F (4, 40) = 0.3137 Treatment : F (2, 40) = 4.417	P=0.0831 P=0.8671 P=0.0185	Tuckey post hoc comparison	Test details	Summary	Adjusted P Value
							0		
							D9-Morph+Morph vs. D9-Morph+Veh	ns	>0.9999
							D9-Morph+UCM924 vs. D9-Morph+Veh	ns	>0.9999
							D9-Morph+UCM924 vs. D9-Morph+Morph	ns	0.9978
							15		
							D9-Morph+Morph vs. D9-Morph+Veh	ns	0.9998
							D9-Morph+UCM924 vs. D9-Morph+Veh	ns	0.8492
							D9-Morph+UCM924 vs. D9-Morph+Morph	ns	0.9988
							30		
							D9-Morph+Morph vs. D9-Morph+Veh	ns	0.9812
							D9-Morph+UCM924 vs. D9-Morph+Veh	ns	0.9999
							D9-Morph+UCM924 vs. D9-Morph+Morph	ns	0.4804
							45		
							D9-Morph+Morph vs. D9-Morph+Veh	ns	0.6662
							D9-Morph+UCM924 vs. D9-Morph+Veh	ns	0.3946
							D9-Morph+UCM924 vs. D9-Morph+Morph	ns	>0.9999
							60		
							D9-Morph+Morph vs. D9-Morph+Veh	ns	0.9982
							D9-Morph+UCM924 vs. D9-Morph+Veh	ns	0.9984
							D9-Morph+UCM924 vs. D9-Morph+Morph	ns	0.5514